INSTITUTO DE FÍSICA
Universidade Federal Fluminense

Clebson dos Santos Cruz

Characterization of Quantum Correlations in Low-Dimensional Molecular Magnetic Systems

Niterói

July 2018

Clebson dos Santos Cruz

Characterization of Quantum Correlations in Low-Dimensional Molecular Magnetic Systems

Tese de Doutorado submetida ao Programa de Pós-Graduação do Instituto de Física da Universidade Federal Fluminense como requisito parcial para a obtenção do Título de Doutor em Física.

Orientador: Mario de Souza Reis Junior

Co-orientador: Diogo Oliveira Soares-Pinto

Niterói

July 2018

Ficha catalográfica automática - SDC/BIF

Ata dos trabalhos finais da Comissão Examinadora da tese apresentada por **Clebson dos Santos Cruz**. No vigésimo dia do mês de julho de dois mil e dezoito, às nove horas, reuniram-se no Instituto de Física da Universidade Federal Fluminense os membros da Comissão Examinadora constituída pelos professores doutores Mario de Souza Reis Junior – IF/UFF; Diogo Oliveira Soares Pinto - USP/SC; Roberto Silva Sarthour Junior- CBPF; Andre Luiz Saraiva de Oliveira – IF/UFRJ; Thiago Rodrigues de Oliveira – IF/UFF; Daniel Schneider Tasca - IF/UFF, sob a presidência do primeiro, para prova pública de apresentação da tese intitulada *"Characterization of Quantum Correlations in Low-Dimensional Molecular Magnetic Systems"*, tendo em vista as exigências do Regulamento Específico do curso de Física relacionadas com a conclusão do Doutorado em Física pela Universidade Federal Fluminense. A tese foi elaborada sob a orientação do professor Mario de Souza Reis Junior e co-orientação do professor Diogo Oliveira Soares Pinto . Após a exposição do trabalho, o aluno respondeu às questões formuladas pelos integrantes da Comissão Examinadora, que apresentou parecer no sentido de aprová-lo. Para constar, foi lavrada a presente ata, que vai assinada pelos membros da Comissão Examinadora e pelo doutorando.

Niterói, vinte de julho de dois mil e dezoito.

Dr. Mario de Souza Reis Junior
Dr. Diogo Oliveira Soares Pinto
Dr. Roberto Silva Sarthour Junior

Dr. Andre Luiz Saraiva de Oliveira

Dr. Thiago Rodrigues de Oliveira

Dr. Daniel Schneider Tasca

Clebson dos Santos Cruz
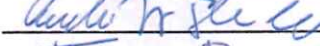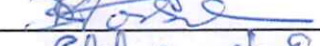
"I don't know where I'm goin'

But I sure know where I've been

Hanging on the promises in songs of yesterday

An' I've made up my mind, I ain't wasting no more time

Here I go again

Tho' I keep searching for an answer

I never seem to find what I'm looking for

Oh Lord, I pray you give me strength to carry on

'Cause I know what it means to walk along the lonely street of dreams

Here I go again on my own

Goin' down the only road I've ever known

Like a drifter I was born to walk alone

An' I've made up my mind, I ain't wasting no more time

Here I go again..."

David Coverdale and Bernie Marsden - Whitesnake.

Agradecimentos

Primeiramente, agradeço a Deus por ter me concedido a oportunidade de alcançar mais uma importante etapa em minha vida, e pela aprovação no concurso de provas e títulos para o provimento de um cargo de professor do magistério superior no Centro das Ciências Exatas e das Tecnologias (CCET) da Universidade Federal do Oeste da Bahia (UFOB).

Agradeço aos meus familiares pelo apoio em meus estudos, especialmete ao meu pai Edinho e minha mãe Istragilda que, mesmo à distância, sempre me apoiaram em todos os momentos, me dando força para continuar minha caminhada. Um agradecimento especial para minha querida avó Maria Ricardina, que infelizmente faleceu antes que eu cumprisse minha promessa de terminar o Doutorado. Agradeço a minha esposa Elisama Lima que com muito carinho esteve sempre a meu lado. Um agradecimento especial a minha sogra Marizete pelas suas orações que me fizeram cada vez mais fortalecido para chegar até aqui. Obrigado por tudo que fizeram por mim.

No âmbito acadêmico, agradeço a todos os professores que me acompanharam durante a graduação, mestrado e doutorado, pelas suas importantes contribuições dadas para minha formação pessoal e profissional, em especial agradeço ao Professores Dr. Mario de Souza Reis Júnior e Dr. Diogo Oliveira Soares Pinto pela excelente orientação e boa vontade comigo. Peço desculpas por qualquer inconveniente nesses últimos 3 anos e por ter que defender nessa correria.

Agradeço ao Dr. Stéphane Soriano (IF-UFF), pela ajuda com o software DAVE-MagProp, à Dra. Paula Brandão do Departamento de Química da Universidade de Aveiro (Portugal) e o Dr. Antonio dos Santos do Oak Ridge National Laboratory, pelas amostras desta tese, e ao Dr. Álvaro Santos Alves (UEFS) e Dr. Jailton Almeida (UFBA) pela colaboração nos cálculos de DFT.

Agradeço também aos meus grandes amigos e amigas que conquistei durante minha trajetória acadêmica, pela convivência e os momentos de diversão, não posso citar todos aqui para não ser injusto com nenhum deles. Agradeço a todos os funcionários do IF UFF que sempre se empenharam em me ofercer um serviço de qualidade, obrigado

pela atenção e dedicação.

Uma agradecimento epecial ao Dr. Angelo Maniero, Dr. Antônio César e Dr. Wanisson Santana da UFOB pela compreenssão e flexibilidade com a nomeação do concurso.

Resumo

Progressos recentes em informação quântica têm demonstrado nossa capacidade de detectar e controlar as propriedades quânticas em materiais magnéticos moleculares. Nos últimos anos, foi demonstrado que estes materiais possuem correlações quânticas altamente estáveis contra perturbações externas como temperatura e pressão. Assim, o estudo desses sistemas abre as portas para o controle total de suas propriedades quânticas, proporcionando perspectivas de pesquisa fascinantes e inovadoras, preparando o caminho para aplicações promissoras em tecnologias quânticas emergentes. Neste contexto, esta tese explora o potencial de sistemas magnéticos moleculares como protótipos de materiais para a tecnologia da informação quântica, abordando três questões principais: (i) projeto e síntese de novos materiais, (ii) caracterização de seu comportamento magnético e quântico e (iii) a detecção e manipulação de quantificadores de informação quântica, como emaranhamento de formação, discórdia quântica entrópica e geométrica em magnetos moleculares pela medição de propriedades termodinâmicas de sólidos, tais como suscetibilidade magnética, energia interna, calor específico e até mesmo propriedades de espalhamento de nêutrons. Os resultados apresentados nessa tese reforçam o fato de que os sistemas magnéticos moleculares podem ser imunes ao mecanismo de decoerência térmica, permitindo a sobrevivência de seus efeitos quânticos acima da temperatura ambiente.

Palavras-chave: Correlação Quântica; Emaranhamento; Magnetismo Molecular; Informação Quântica.

Abstract

Recent progress in quantum information theory has demonstrated our ability to detect and control quantum properties in customized molecular magnetic materials. In recent years, it was demonstrated that engineered molecular magnetic materials has a high stability of its quantum correlations against external perturbations. As a result, the study of these systems provides opportunities to achieve full control of its quantum properties, providing fascinating and innovative research perspectives and paving the way for promising applications in emerging quantum technologies. In this context, this thesis explores the potential of molecular magnets to be prototype materials for quantum information technology by addressing three principal issues: (i) design and synthesis of novel materials, (ii) characterization of their magnetic and quantum behavior, and (iii) detection and manipulation of quantum information quantifiers, such as entanglement of formation and entropic and geometric quantum discord in molecular magnets by the measurement of the thermodynamic properties of solids, such as magnetic susceptibility, internal energy, specific heat, and even neutron scattering properties. The results presented in this thesis strengthen the fact that molecular magnets may be somewhat immune to decoherence mechanisms, allowing survival of quantum effects above room temperature.

Keywords: Quantum Correlations; Entanglement; Molecular Magnetism; Quantum Information.

Contents

List of Figures

List of Tables

List of Papers

Associated with this thesis

1 **Cruz, C. S.**; Soares-Pinto, D. O. ; Brandão, P. ; dos Santos, A. M. ; REIS, M.S. . Carboxylate-based molecular magnet: One path toward achieving stable quantum correlations at room temperature. Europhysics Letters (Print), v. 113, p. 40004, 2016.

2 **Cruz, C**; Alves, Á. S. ; dos Santos, R. N. ; Soares-Pinto, D. O. ; de Jesus, J. C. O. ; de Almeida, J. S. ; Reis, M.S. . Influence of the external pressure on the quantum correlations of molecular magnets. Europhysics Letters (Print), v. 117, p. 20004, 2017.

3 **Cruz, C.**. Quantum correlations and Bell's inequality violation in a Heisenberg spin dimer via neutron scattering. INTERNATIONAL JOURNAL OF QUANTUM INFORMATION, v. 5, p. 1750031, 2017.

Not associated with this thesis

4 Leite Ferreira, B. J. M. ; Brandão, Paula ; dos Santos, A.M. ; Gai, Z. ; **Cruz, C.** ; Reis, M. S. ; Santos, T. M. ; Félix, V. . Heptacopper(II) and dicopper(II)-adenine complexes: Synthesis, structural characterization and magnetic properties. Journal of Coordination Chemistry (Print), v. 2, p. 1, 2015.

5 Pedro, S. S. ; Caraballo Vivas, R. J. ; Andrade, V. M. ; **Cruz, C.** ; Paixão, L. S. ; Contreras, C. ; Costa-Soares, T. ; Caldeira, L. ; Coelho, A. A. ; Carvalho, A. Magnus G. ; Rocco, D. L. ; Reis, M. S. . Effects of Ga substitution on the structural and magnetic properties of half metallic Fe2MnSi Heusler compound. Journal of Applied Physics, v. 117, p. 013902, 2015.

6 Tedesco, J C G ; Pedro, S S ; Caraballo Vivas, R J ; **Cruz, C** ; Andrade, V M ; dos Santos, A M ; Carvalho, A M G ; Costa, M ; Venezuela, P ; Rocco, D L ; Reis, M S . Chemical disorder determines the deviation of the Slater-Pauling rule for Fe MnSi-based Heusler alloys: evidences from neutron diffraction and density functional theory. Journal of Physics. Condensed Matter (Print), v. 28, p. 476002, 2016.

7 Caraballo Vivas, R.J. ; Pedro, S.S. ; **Cruz, C. S.** ; Tedesco, J.C.G. ; Coelho, A.A. ; Carvalho, A. Magnus G. ; Rocco, D.L. ; Reis, M.S. . Experimental evidences of enhanced magnetocaloric properties at room temperature and half-metallicity on Fe2MnSi-based Heusler alloys. Materials Chemistry and Physics, v. 174, p. 23, 2016.

8 Paixao, L. ; **Cruz, C.** ; Costa-Soares, T. . Refrigeração Magnética. In: Thales Costa Soares ; Eloi Teixeira César ; Edson E. Reinerh. (Org.). Ciência em dia : Jornadas de divulgação cientifica. 1ed.: Editora livraria da fisica, 2016, v. , p. 103-112.

9 Shi, Fa-Nian ; Bai, Yi-Wen ; Lu, Miao ; **Cruz, C.** ; Reis, M. S. ; Gao, Jun . A one-dimensional Mn(II)-based metal organic oxide: structure and properties. Transition Metal Chemistry, v. 42, p. 1-10, 2017.

10 EscobarL. B. L., P. Brandão, D. Ananias, A.M. dos Santos, **C. Cruz**, M.S. Reis. Effect of hydrostatic pressure on magnetocaloric properties of two dinuclear Gd III-based complexes. Submitted to Dalton Transitions.

11 **Cruz, C.** Espalhamento de nêutrons em sistemas magnéticos de baixa dimensionalidade: Uma abordagem didática. Submitted to Revista Brasileira de Ensino de Física.

1 Introduction

The study of theoretical quantum information quantifiers has attracted considerable attention, since they are a key resource for several information-processing protocols [1–7]. For example, the constituents of interacting many-body systems are generally correlated and the presence of genuinely quantum correlations is usually related to the existence of quantum entanglement, a well-known and useful resource for quantum tasks. However, the notion of quantum correlations has been expanded [2, 8–19], and it has been shown that quantum entanglement does not encompass all possible quantum correlations in a system. Such nonclassical correlations beyond entanglement have been called *quantum discord* [9–11]. In recent years, it has been understood that these nonclassical correlations play an important role in many quantum information processing applications, especially when entanglement is absent [2, 9, 15, 16, 20].

The emergence of new quantum devices based on condensed matter systems requires one to understand its fundamental concepts, which can provide the opportunity for full control of quantum properties of such systems, thus reinforcing new applications and providing fascinating and innovative perspectives. However, the development of quantum systems that allow the application with great accuracy of any quantum information processing protocol is compromised by the inevitable coupling of this system with the external environment. This coupling promotes the destruction of the quantum properties of the system of interest. This has been a major hurdle in developing technological devices based on large-scale quantum information. In this scenario, the characterization and full knowledge of nonclassical correlations constitute a rather complicated task from the theoretical [21] and experimental [22] points of view. This scenario is even worse for condensed matter systems, because, for these, the number of constituents in the system is often close to the Avogadro constant of $\sim 6 \times 10^{23}$. However, molecular magnetic systems appear as strong candidates for platforms for processing of quantum information [2, 20, 23–32]. In this class of materials, intermolecular interactions are extremely weak, when com-

pared to intramolecular interactions [23]. Therefore, these systems can be seen as an excellent realization of clusters and chains of spins with interesting topological conformations [2, 30–33], whose magnetic behavior is described through its fundamental magnetic unit, such as dimers [2, 33], trimers [30], large clusters [31], and chains [32].

The recent demonstration that quantum correlations can be measured by the thermodynamic properties of solids, such as magnetic susceptibility, internal energy [2, 20], specific heat, or even difractive properties of neutron scattering [12, 24], shows that quantum correlations can be related to significant macroscopic and structural effects allowing the measurement and control of quantum correlations in solid state systems in customized molecular magnetic materials. Consequently, the design of novel materials, with operational properties for quantum information coding, processing, and distribution, becomes an actual challenge to overcome.

In the past few years, it has been demonstrated that molecular magnetic materials can contain quantum correlations [2, 20, 25, 27–29, 34–36], with high stability and resistance to external disturbances, such as high temperatures, pressures, and magnetic fields [2, 20, 27, 28]. The large gap between the ground state and the first-excited state found in some materials, allowing the existence of quantum correlations at higher temperatures [25, 28, 29]. In this context, molecular magnetic systems may be somewhat immune to decoherence mechanisms, which leads to the destruction of the quantum properties of the system of interest, owing to the inevitable coupling of the quantum system with the external environment, and promotes the aim of greater efficiency and lower costs for the production of new devices based on quantum information technologies. Recently, it has been demonstrated that these materials can combine classical properties (i.e., those found in conventional magnets [37]) with quantum properties, such as quantum interference [38], quantum tunneling of magnetization [39, 40], entangled quantum states [2, 25, 28, 29], and quantum correlations [2, 20], so that these systems hold promise for use as the basis of new devices, including quantum logic keys, a key ingredient for the large-scale production of computers and quantum devices.

Consequently, the study of these systems offers an opportunity to enable full control of their quantum properties, providing fascinating and innovative research perspectives and enabling promising applications in emerging quantum technologies, paving the way toward the limits of quantum mechanics. Several aspects are worthy of thorough research: (i) how robust are their quantum features against temperature and (ii) how

large a system can support these properties. In this context, the aim of this thesis is to explore fundamental aspects of quantum information theory, through the development of models for the theoretical characterization of the quantum properties of molecular magnetic systems, seeking to propose new materials with different topologies, aiming at the optimization of their quantum properties, and highlighting the design and characterization of isotropically coupled spin-1/2 pairs, i.e., a molecular magnetic system in a d^9 electronic configuration such as Cu ions in the 2+ oxidation state. The overall concept of this thesis is to explore the potential of these materials to be prototype materials for quantum information technology by addressing three principal issues: (i) design and synthesis of novel materials, (ii) characterization of their magnetic and quantum behavior, and (iii) detection of quantum information quantifiers, such as entanglement of formation and entropic and geometric quantum discord in molecular magnets by the measurement of thermodynamic properties of solids, such as magnetic susceptibility, internal energy, specific heat, and even neutron scattering properties.

The thesis is divided as follows: Chapters 2 and 3 present an introduction to the concepts and techniques that we use in the works related to this thesis. Chapter 2 contains an introduction to low-dimensional molecular magnetism, where we show its theoretical foundations and we describe the step-by-step process of developing models for low-dimensional molecular magnets, an essential step for the connection of thermodynamic properties with quantum ones. In Chapter 3, we discuss the forms of characterization and quantification of quantum correlations, as well as their influence on molecular magnetic systems. We show the analytical expressions for quantum information quantifiers, such as entanglement witness, entanglement of formation, and entropic and geometric quantum discord, based on the Schatten 1-norm, in bipartite systems. In Chapter 4, we present a literature review and the state of the art in quantum information in molecular magnetic systems. Chapters 5 to 7 present the main results of this thesis. In Chapter 5, we show that carboxylate-based molecular magnets can support quantum correlations at thousands of kelvins above room temperature. We provide the literature on engineered materials with high stability of quantum correlations against external perturbations. In Chapter 6, we show that and external pressure can induce structural contraction in a metal–silicate framework, leading to a change of its magnetic alignment and decreasing the degree of quantum correlations in the system. In addition, in Chapter 7 we establish a relationship between the detection of quantum correlations and diffractive properties

of neutron scattering, allowing the measurement of nonclassical correlations in molecular magnetic materials via neutron scattering experiments. Finally, in Chapter 8, we present the general conclusions of the thesis and provide some outlooks for future works.

2 Low-Dimensional Molecular Magnetism

In this chapter, we show the theoretical foundations used in the characterization of molecular magnets, highlighting the analysis of clusters, also called zero-dimensional systems (as spin-1/2 interacting pairs in a quantum spin lattice). We give a theoretical description of magnetic coupling based on the Heisenberg model and present the process of construction of analytical models for the description of the magnetic behavior of some molecular magnets and first principles calculatiosn. In addition, we also quote the analysis of single-crystal and powder average inelastic neutron scattering structure factors. For more detailed discussions about the topics covered in this chapter, see Refs. [1, 23, 41–44].

2.1   Introduction

In the past few decades, the development of new technologies has provided great advances in materials preparation techniques. New compounds have been synthesized and, as a consequence, several new physical phenomena can be studied: among them is molecular magnetism, a multidisciplinary research area that has emerged from the intersection of magnetism, quantum mechanics, and organic and molecular chemistry. According to Kahn [41], it is a subarea of condensed matter physics, based on rational planning and the synthesis of new compounds, aiming at the achievement of properties coupled to magnetism [44].

Molecular magnetic materials are synthesized by methods of organic and molecular chemistry, particularly conducted in solution at room temperatures and generally composed by nonmetals with or without ions or metal atoms in their structure. Therefore, they have some unique magnetic properties, because their magnetic behavior can originate exclusively from the unpaired electrons of some types of organic radicals (p electrons) [44]. In addition, they may be in the form of metal compounds or coordination polymers, where organic molecules are attached to metallic ions with d and f orbitals. In

this scenario, the organic component may act passively, only as a mediator of the magnetic interaction, or actively, contributing to the magnetic moment through p orbitals [44]. For these and other reasons, which will be discussed in this chapter, the study of molecular magnets allows an approach along several strands that transcend the conventional description of magnetism [23, 41, 44], leading to interesting research perspectives.

2.1.1   Brief History of Molecular Magnetism

The phenomenological nature of magnetism has been known since antiquity, and, after all these years, the study of magnetic materials has, and still does, play a fundamental role in the development of society by providing the production of various materials and devices indispensable to modern life [45]. However, the main interest in magnetic phenomena grew exponentially in the mid-19th century, primarily for applications to the production of electrical energy, and later (in the 20th century) with the advent of information technology for storing and reading data. The theory of magnetism formulated by Heisenberg [46] introduces the concept of exchange as one of the fundamental forms for the construction of a phenomenological model for a description of the magnetic properties of physical systems. For decades, it was believed that magnetic phenomena only manifested themselves in compounds that contained transition metals in their structure, such as iron, cobalt, nickel, or the rare-earth elements samarium, praseodymium, and neodymium [45]. Magnetic properties emerge from long-range interactions, directly between orbitals (in the case of pure elements and metallic alloys) or indirectly, mediated by a nonmagnetic anion (in the case of manganitites and ferrites) [23]. In most cases, the magnetic materials studied at this moment in history have exhibited conventional magnetic properties, such as spontaneous ordering and phase transitions, as well as having three-dimensional crystalline structure. They are opaque, dense, and generally conductive, in addition to being synthesized through ubiquitous techniques derived from metallurgy and ceramics, whose processes involve high temperatures of hundreds of kelvins above room temperature.

On the other hand, the history of molecular magnetism is recent compared to the millennial history of the phenomenological observation of magnetic phenomena, owing to the huge experimental limitations up to the second half of the 20th century [23], because its physical effects are detected at low temperatures. Historically, the advent

of molecular magnetism, in its most comprehensive definition, actually occurred in 1952 with the observation of magnetic interactions originating from an isolated copper dimer ($Cu^{II}(CH_3COO)_2$), made by the physicists Bleaney and Bowers, in a paper published that year [47], where they explained the observed magnetism at low temperatures as a result of the antiferromagnetic interaction between the two copper ions. Since then, there has been a huge evolution in research on molecular magnets. Because of their ease of synthesis, great versatility, low toxicity, biocompatibility, and the stability of their quantum properties against decoherence processes, molecular magnets are extremely promising materials in the development of new technological devices, high-density data storage [37], magneto-optics [48], magnetic refrigeration [49–51], and quantum computing and information [2, 20, 25, 27–29, 34, 35], etc. [30–33].

However, despite the potential technological interest of this class of materials, the scientific community is still looking up systems with technologically useful performances at room temperature. In this way, the search for high-coercivity molecular magnets, that is, high magnetic information capacity, high resiliency, and basic capacities for the development of technology, has driven research in low-dimensional magnetic systems in recent years. The synthesis of mixed compounds containing organic radicals and transition metals has been a good alternative [52], providing fascinating and innovative research perspectives and paving the way for promising applications in emerging technologies.

2.1.2   Fundamental Aspects and Main Properties

From a structural point of view, molecular magnetic systems can be seen as an excellent realization of isolated molecules or chains, forming spin clusters owing to their low dimensionality. This fact leads to some interesting perspectives on the design of novel compounds with different topological conformations. These materials usually have a few metal centers connected to each other, where their magnetic properties are often reflections of their quantum behavior [23]. They can present as an isolated molecule or spin cluster, which may be dimers, trimers, tetramers, or they may form larger structures such as unidimensional chains, surfaces, and interacting sheets of magnetic ions, forming three-dimensional networks.

In addition, in most cases, this class of materials presents intermolecular interactions that are extremely weak when compared to intramolecular interactions. Therefore,

the magnetic behavior of a molecular magnet can be described by considering its lower unit, such as a monomer, dimer, trimer and so forth [23]. Owing to its low-dimensional characteristics, the theoretical models that describe the magnetic behavior of these materials are generally analytically soluble [44], which allows us to discern their physical properties in details.

In this context, establishing a relationship between magnetic interactions and the crystal lattice is one of the fundamental aspects behind the study of molecular magnetic systems. The general rules governing the interactions of these systems have been exhaustively studied since the advent of molecular magnetism in 1952, and although these rules have been chemically consolidated [53], there are several degrees of freedom that are extremely important from the physical point of view but still unexplored (especially from a quantum point of view). For example, various molecular magnetic systems, such as metal–organic crystal systems, have an immense variety of topologies and compositions, leading to dramatic effects on magnetic behavior and, consequently, their physical properties [44]. For this reason, chemists and physicists have combined their knowledge to systematically understand the relationship between structure and magnetism and its implications on the magnetic properties of these systems and its advantages on the development of emerging technologies [44].

Magnetic molecular compounds are usually organized according to the chemical nature of the spin carriers, these can be: (i) inorganic, where its magnetic phenomena emerges from transition metals and rare earth ions, without the presence of carbon-hydrogen bound; (ii) organic, where organic radicals with p electrons are the ones responsible for its magnetic behavior; or (iii) metal-organic, where its the magnetic nature is emerging from transition metal ions bounded to organic molecules or radicals.

Inorganic Molecular Magnetic Systems

There are numerous observations of low-dimensional magnetism in inorganic systems, such as the wide range of composites formed by transition metals and rare-earth ions, from where many of the traditional magnetic systems originate [1, 23]. The low-dimensional properties in inorganic magnetic systems emerge mostly from their chemical aspects, related to systems with low value of their spin angular momentum $s = 1/2$, typically observed in systems composed of Cu^{2+} ions or V^{4+} ions [1,23], and $s = 1$ typically

observed in systems composed of nickel Ni^{2+} [1,23], allowing the emergence of interactions of quantum order that characterize the magnetic properties of these systems and may lead these compounds to interesting applications in the study of the quantum information processing in these materials [1,23]. In addition, topological aspects are also relevant, because they allow us to incorporate these ions into particular private units, such as clusters and chains, guaranteeing the low dimensionality of these systems. Consequently, low-dimensional inorganic molecular magnetic compounds exhibit fascinating properties that can be extremely useful from the point of view of technology, such as higher ordination and transition temperatures, as well as easy crystallization, allowing large-scale production of reasonably sized magnetic crystals of specific structural and magnetic characteristics [1,23].

Organic Molecular Magnetic Systems

Purely organic molecular magnetic systems are characterized by having only p electrons as the ones responsible for the magnetic properties. These compounds consist basically of carbon, hydrogen, oxygen, nitrogen, and, in some cases, phosphorus, sulfur, and fluorine [1,23,44,54]. The main organic radicals used in molecular magnetic systems are nitronyl-nitroxide, nitroxide, verdazil, and thiazyl [1,54]. Among the most studied organic magnets in the literature, it is worth mentioning the nitronyl-nitroxide radicals [1,54]. These radicals have an electronic delocalization, which makes materials based on organic radicals good transmitters of magnetic information [1]. Therefore, these materials are widely used as paramagnetic building blocks to obtain magnetic molecular compounds.

Another important attribute of organic molecular magnetic compounds is their versatility of synthesis, because modifications of the radical group[1] influence the crystal structure in the organization of the molecules by modifying the distances and angles between sites with magnetic moment, leading to the emergence of intermolecular interactions, having dramatic consequences on their magnetic properties.

However, although organic metal magnetic systems are extremely interesting from a physical and chemical point of view, the low magnetic ordering temperatures observed in these systems constitute a major phenomenological obstacle to their technological application.

---

[1]The R group comprises nitronyl-nitroxide, nitroxide, verdazil, and thiazyl.

Metal-Organic Molecular Magnetic Systems

One approach used to obtain systems with properties technologically useful performances at room temperature such as, for instance, the stability of their quantum properties against thermal decoherence processes, is the synthesis of organic compounds containing transition metals, the so-called metal-organic molecular magnets. In metal-organic systems, the magnetic nature emerges from transition metal ions and/or organic radicals. Consequently, the magnetic properties of these compounds are determined primarily by the d electrons of the transition metal and/or the p electrons of the organic radicals [1].

In general, these systems are divided into two classes: the so-called *open-shell magnetic systems* [55, 56], where the organic component acts actively in magnetism through one or more free radicals [1], and the so-called *closed-shell magnetic systems* [57, 58], where the organic component does not contain free radicals, acting passively in the magnetism only as a mediator of the magnetic interaction, in which case the magnetic properties are only emerging from transition metals.

In this thesis, we focus on closed-shell molecular magnetic systems, because the relationships between their magnetic and structural properties are well understood chemically but are still unexplored from the quantum point of view, especially in the characterization of quantum correlations between the components of these systems, opening a wide avenue to the rational development of new compounds with interesting quantum characteristics with high stability and resistance to external disturbances, such as high temperatures, pressures, and magnetic fields [2, 20, 27, 28].

Because of their ease of synthesis and great versatility, metal-organic molecular magnets have been the subject of intense study. Their properties make them promising materials to be used in several technological devices and they have a wide range of fascinating applications; e.g., their low toxicity and biocompatibility are very useful in the development of new drugs for the treatment of cancer diseases [31]; they can be used in high-density data storage devices [37] and quantum computing devices using the stability of their quantum properties against decoherence processes [2,25,28,29]; they have applications in magnetic refrigeration [49–51] and spintronics [37]; and they have other interesting potential characteristics for applications as prototype materials. A deep understanding of the fundamental aspects of the physical nature of these materials still needs careful atten-

tion. In this context, novel materials are synthesized and characterized from a magnetic and structural point of view to be used in those applications previously mentioned.

2.2   Theoretical Foundations

Since their advent, the unique properties of molecular magnetic systems have allowed a deep study of fundamental aspects of several new physical phenomena that challenge a series of well-established concepts. One of the advantages of the study of low-dimensional molecular magnets lies in the relative simplicity of the description of their magnetic properties. Depending on the size of the Hilbert space associated with these systems, it is possible to characterize their thermodynamic properties analytically, because the Hamiltonian models that describe their quantum behavior are already known and their physical aspects are well known in the literature.

2.2.1   Hamiltonians and Interactions

Heisenberg Hamiltonian

One of the simplest Hamiltonian models, which emerges from the problem of two electrons close to the vicinity of two closed-shell atoms, used to describe the magnetic nature of interactions in molecular magnets is the Heisenberg–Dirac–Van Vleck Hamiltonian [23]

$$\mathcal{H} \;=\; -\sum_{i,j} J\vec{S}_i \cdot \vec{S}_j \;, \tag{2.1}$$

in which the sum is taken over the exchange Hamiltonians for all the $\{i,j\}$ pairs of atoms, where $\vec{S}_i$ and $\vec{S}_j$ are the spin operators related to the ions on sites i and j, respectively, and J is the exchange parameter (magnetic coupling constant).

This Hamiltonian is defined by considering localized wavefunctions [1,23]. Because the hopping integral rules the kinetics of the electrons, localized wavefunctions are a consequence of small values of the hopping integral [1,23]. Due to this fact, this Hamiltonian, Eq. (2.1), is not a reliable description of the physical properties of metallic systems.

However, molecular magnets are, in most cases, insulators and are very well described by the Heisenberg models [1, 23].

In order to contextualize the mathematical description of this text with the main results of this thesis, let us consider a low-dimensional molecular magnetic system as an interacting pair of spin (e.g., a dimer) ruled by the Heisenberg-Dirac-Van Vleck Hamiltonian, Eq. (2.1),

$$\mathcal{H} \;=\; -J\vec{S}_i \cdot \vec{S}_j \;, \tag{2.2}$$

We can rewrite this Hamiltonian, to facilitate the calculation of its eigenvalues, using the following relation:

$$\vec{S}^2 = (\vec{S}_1 + \vec{S}_2)^2 = \vec{S}_1^2 + \vec{S}_2^2 + 2\vec{S}_1 \cdot \vec{S}_2 \;. \tag{2.3}$$

One can rewrite the Hamiltonian, Eq. (2.2), as

$$\mathcal{H} = -\frac{J}{2}(\vec{S}^2 - \vec{S}_1^2 - \vec{S}_2^2) \tag{2.4}$$

where $\vec{S} = \vec{S}_1 + \vec{S}_2$, from which we can obtain the energy eigenvalues

$$\mathcal{E}_s = -\frac{1}{2}J\left[s\left(s+1\right) - s_1\left(s_1+1\right) - s_2\left(s_2+1\right)\right] \;. \tag{2.5}$$

In this way, the most energetic state (parallel alignment) is

$$\mathcal{E}_{s_{MAX}} = -Js_1s_2 \;; \tag{2.6}$$

while the less energetic state (antiparallel alignment)is

$$\mathcal{E}_{s_{MIN}} = J(s_1 + 1)s_2 \;. \tag{2.7}$$

The difference between these energies is

$$\mathcal{E}_{s_{MIN}} - \mathcal{E}_{s_{MAX}} = J(2s_1 + 1)s_2 \;. \tag{2.8}$$

Therefore, the magnetic coupling constant J gives us information about the energy difference between the least and most energetic states:

$$J = \frac{\mathcal{E}_{s_{MIN}} - \mathcal{E}_{s_{MAX}}}{(2s_1 + 1)s_2} \;. \tag{2.9}$$

Thus, there are three different physical situations:

- $J = 0 \Rightarrow \mathcal{E}_{s_{MIN}} = \mathcal{E}_{s_{MAX}}$, in which case there is no magnetic interaction.

- $J > 0 \Rightarrow \mathcal{E}_{s_{MIN}} > \mathcal{E}_{s_{MAX}}$, in which case there is a parallel alignment.

- $J < 0 \Rightarrow \mathcal{E}_{s_{MIN}} < \mathcal{E}_{s_{MAX}}$, in which case there is an antiparallel alignment.

Zeeman Hamiltonian

Again, in order to contextualize this text to the main results of this thesis, we will address another Hamiltonian fundamental for the description of the molecular magnetic systems studied in this thesis. Another important magnetic interaction, which describes the magnetic properties of low-dimensional molecular magnetic systems, is the Zeeman interaction. This Hamiltonian is of extreme importance in physics, since it explains the phenomenon of splitting of the spectral lines of energies into several equidistant lines from an atom in the presence of an external magnetic field ($\vec{B}$). The phenomenological nature of the Zeeman effect depends essentially on the magnitude of the magnetic field relative to the spin-orbit coupling, as is completely described by the Dirac equation [23, 41].

The Zeeman Hamiltonian concerns the interaction of the orbital and spin magnetic moments with the external magnetic field:

$$\mathcal{H}_z = \frac{\mu_B}{\hbar}\vec{B}\cdot(\vec{L}+2\vec{S}) \ . \tag{2.10}$$

Therefore, we can separately write the purely spin and orbital parts as

$$\mathcal{H}^{(\mathcal{S})}{}_z = -\mu_{\mathbf{S}}\cdot\vec{B} \ , \tag{2.11}$$

$$\mathcal{H}^{(\mathcal{L})}{}_z = -\mu_{\mathbf{L}}\cdot\vec{B} \ , \tag{2.12}$$

where

$$\mu_{\mathbf{S}} = -g_S\mu_B\vec{S} \ , \tag{2.13}$$

$$\mu_{\mathbf{L}} = -g_L\mu_B\vec{L} \ . \tag{2.14}$$

Therefore, one can rewrite the Zeeman Hamiltonian, Eq.(2.10), as follows:

$$\mathcal{H}_z = \mathcal{H}^{\mathcal{L}}{}_z + \mathcal{H}^{\mathcal{S}}{}_z = -\vec{\mu_J}\cdot\vec{B} \ , \tag{2.15}$$

where

$$\vec{\mu_J} = -g_J\mu_B\vec{J}; \quad \vec{J} = \vec{L}+\vec{S} \ . \tag{2.16}$$

Finally, the Zeeman Hamiltonian can be rewritten as:

$$\mathcal{H}_z = g_j\mu_B\vec{B}\cdot\vec{J} \ . \tag{2.17}$$

The energy spectrum for this Hamiltonian is given by:

$$\mathcal{E}_z = g_j\mu_B(B_xj_x + B_yj_y + B_zj_z) \ . \tag{2.18}$$

Through some vector calculations [23] we can find the Landé factor:

$$g_j = 1 + \frac{j(j+1) - l(l+1) + s(s+1)}{2j(j+1)} \; . \tag{2.19}$$

This factor can be formally obtained from the calculation of the first-order perturbation in energies of an atom in a weak uniform magnetic field[2]. It is worth noting that, a spin Hamiltonian, Eq. (2.19), returns $g = 2$, thus any deviation from this result is due to the orbital contribution of the angular momentum.

2.2.2   Quench of the Orbital Angular Momentum

An important effect that occurs in many molecular magnets, being fundamental to the description of molecular magnetic systems studied in this thesis, is the quench of the orbital angular momentum. Let us consider the quenching of the orbital angular momentum that occurs in materials with a strong crystalline field, since the projection of the angular momentum of an atom in cubic symmetry is zero [1,59]. Crystalline field raises the degeneracy of the atomic states, canceling out the orbital angular momentum [1,23,59].

In order to analyze the physical nature of the lifting of degeneracy due to the crystalline field, that leads to the quench of the orbital angular momentum, let us consider a particular and ubiquitous phenomenon of a $3d$ shell atom, as a transition metal six-fold coordinated with sp ions in an octahedral symmetry [1,23,59]. Through the angular nature of the orbitals it is possible to estimate how the degeneracy of the d orbitals are raised when the atom is placed in a cubic lattice. The five $3d$ orbitals split in two groups, one with two most energetic orbitals, $d_{x^2-y^2}$ and d_{z^2}, oriented along Cartesian axes, also known as e_g orbitals, and another group with three orbitals, d_{xy}, d_{zx} and d_{yz}, oriented along the Cartesian planes, also known as t_{2g} orbitals [1,23,59]. Figure 2.1 shows a schematic representation of $d_{x^2-y^2}$, d_{z^2}, d_{xy}, d_{zx} and d_{yz} orbitals. A cubic crystal field causes partial lifting of the degeneracy, separating states belonging to the e_g and t_{2g} representations. This effect, which also happens for other symmetries, is usually called *crystal-field splitting*.

For the case of an isolated $3d$ atom its orbitals are occupied following the Hund rule, where each orbital is occupied with at most two electrons with its antiparallel spins, following the Pauli's exclusion principle. However, because of the orbital splitting, due

---

[2]In this case, we consider weak in comparison to the system's internal magnetic field.
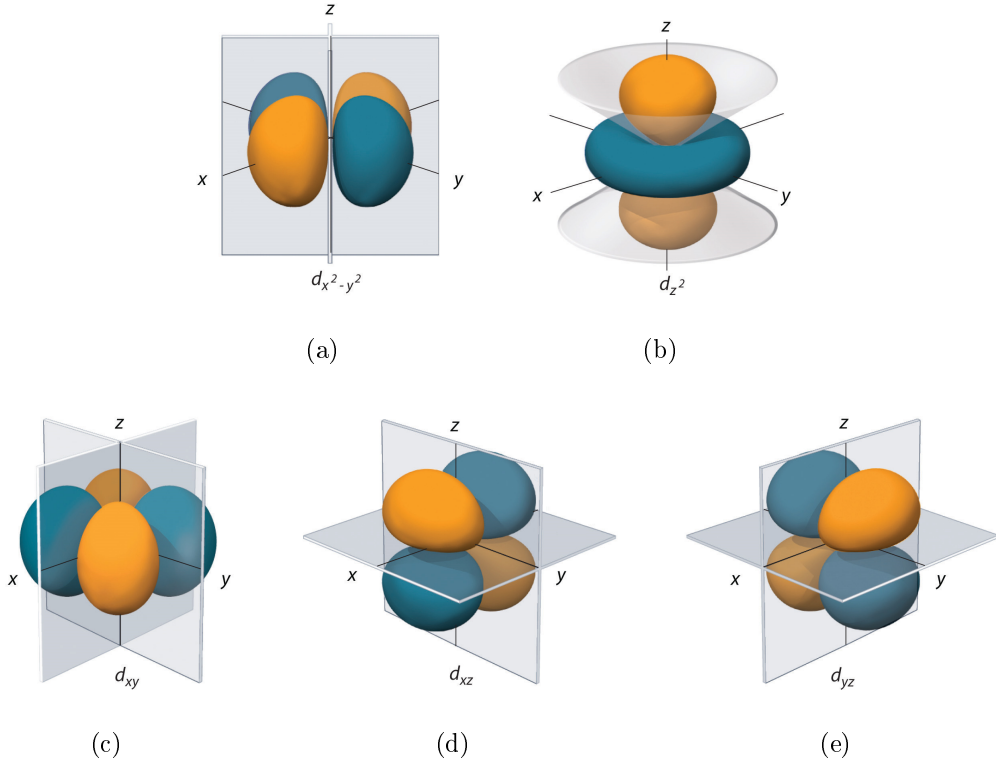
Figure 2.1: Schematic representation of (a) $d_{x^2-y^2}$, (b) d_{z^2}, (c) d_{xy}, (d) d_{zx} and (e) d_{yz} orbitals in a crystal with cubic symmetry [60].

to the crystalline field, the first electrons occupy the three degenerate orbitals of lower energy t_{2g}, while the other electrons will remain in these orbitals, if the pairing energy is greater than the also known splitting energy Δ (*low spin* case), or occupy e_g orbitals, otherwise (*high spin* case), following the Hund rule in both cases.

However, for each d electronic configuration the quench of orbital angular momentum may or may not happen. Because of the degeneracy of t_{2g} orbitals and the fact that they are oriented along the Cartesian planes, it is possible to carry an electron in any of these three orbitals by a simple rotation. This fact favors the appearance of an orbital angular momentum due to this electron mobility. Thus, electronic configurations such as d^1 and d^2, for example, do not have quench of orbital angular momentum, since the t_{2g} orbitals are not completely filled. Thus, the d^1 and d^2 configurations have no orbital angular momentum quench. In contrast, d^3 configuration, there will be the quench of the orbital momentum, since t_{2g} orbitals will be filled. On the other hand, in high spin d^4 and d^5, low spin d^6 and d^7 as well as d^8 and d^9 electronic configurations the quench is favorable since t_{2g} will be filled and there is no rotational symmetry between the e_g orbitals, while low spin d^4 and d^5 and high spin d^6 and d^7 do not have quench, since down spin electrons will have electronic mobility in the orbital. The expected/unexpected quench of orbital

Table 2.1: Expected/Unexpected quench of orbital angular momentum for octahedral coordination.

Number of d electrons	High/Low Spin	Expected Quench
1		No
2		No
3		Yes
4	HS	Yes
4	LS	No
5	HS	Yes
5	LS	No
6	HS	No
6	LS	Yes
7	HS	No
7	LS	Yes
8		Yes
9		Yes

angular momentum for octahedral coordination are given in the following Table 2.1:

On the other hand, an extra lifting of degeneracy is usually observed in octahedral complexes where its two axial bonds can be shorter or longer than those of the equatorial bonds changing the symmetry to a thetragonal distortion. This is the basis of the Jahn-Teller effect, that describes the geometrical distortion of molecules and ions that is associated with certain electron configurations. The above mentioned scenarios are also depicted on Figure 2.2. Due to a Coulombian repulsion, orbitals with z component increase in energy by compression , due to fact that d orbitals with z component have a greater overlap with the ligand orbitals (Figure 2.2 (c)), this thetragonal lifting of degeneracy leads to four orbital groups: a_{1g} (d_{z^2} orbital), b_{1g} ($d_{x^2-y^2}$ orbital), e_g (d_{zx} and d_{yz} orbitals) and b_{2g} (d_{xy} orbital). On the other hand, the thetragonal elongation (Figure 2.2 (d)) lower the electrostatic repulsion between the electron-pair in orbitals with a z component, thus lowering the energy of the complex. Hence, as opposed to compression, in the elongation Jahn-Teller distortions, the degeneracy is broken through the stabilization (lowering energy) of the d orbitals with a z component, while the orbitals without a z component are destabilized (higher energy) as shown in Figure 2.2 (d).
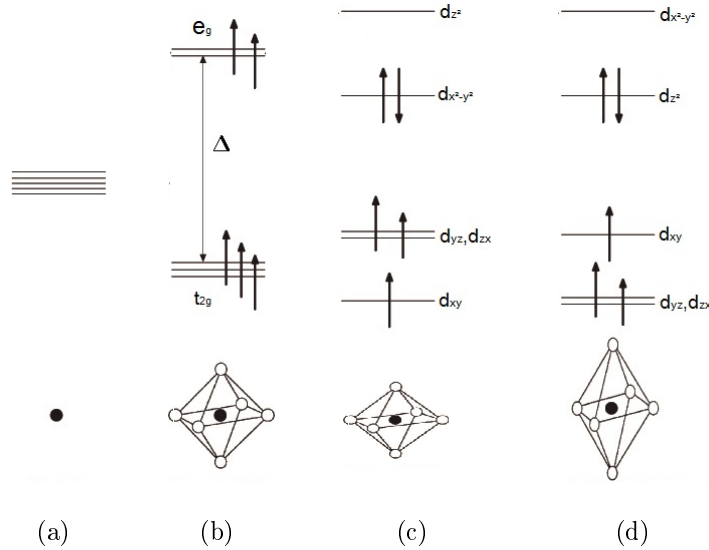
Figure 2.2: $3d$ Ion with its five degenerate orbitals. (a) Free ion, (b) cubic symmetry, (c) thetragonal compression and (d) expansion (from Ref. [1]).

The Jahn–Teller effect is most often encountered in low-dimensional molecular magnetic systems as octahedral complexes of the transition metals [61]. This is a ubiquitous phenomenon in six-coordinate copper(II) complexes [62], the main subject of study of this thesis. Because of its d^9 electronic configuration an elongated distortion is favorable (Figure 2.2 (d)), elongating the bonds to the ligands lying along the z axis, and leading to the quench of the angular momentum. Therefore, the orbital splitting, due to the crystaline field, allowing us to consider only the spin contribution to the total angular momentum and calculate the Landé factor, Eq. (2.19), using $j = s$ and $l = 0$. It is worth mentioning that this seems to be a good approximation for the transition metal ions, especially those with less than a half-filled $3d$ shell [1,23,59], because, in most cases, partial quenching occurs experimentally. This phenomenon is very common in many molecular magnets and thus allows us to consider from this point only the contribution of spin to the total angular momentum in several low-dimensional molecular magnetic systems.

2.2.3   Thermodynamic Quantities

From knowledge of the Hamiltonian, we can describe the microscopic nature of low-dimensional magnetic systems. However, we are interested in the description of its macroscopic properties. In this context, the connection between the microscopic and macroscopic characteristics of physical systems is made through the entropy functional

[23]. From the point of view of statistical mechanics, the entropy can be seen as an extensive property[3] of a thermodynamic system, related to the number of microscopic configurations, also known as microstates Ω that are consistent with the macroscopic quantities that characterize the system (such as its volume, pressure, and temperature). However, the concept of entropy arises naturally from the fundamental postulate that each microstate Ω is equally probable, where the entropy S is

$$S = k_B \ln (\Omega) \tag{2.20}$$

where k_B is the Boltzmann constant [4].

Let us consider p_i as the equilibrium probability of a certain state i, which can be obtained when the entropy is maximized under the correct constraints (Jaynes principle) [23,63,64]. From the constraint of an isolated system with energy and particle numbers constant, we have (the microcanonical ensemble) $p_i = \Omega^{-1}$ with $\Omega = \sum_i$. Thus the entropy can be written as

$$s = -\sum_i p_i \ln (p_i) \ , \tag{2.22}$$

the so-called Shannon entropy [23,65], with $S = k_B s$. From the Shannon entropy, Eq. (2.22), the probability p_i is normalized

$$\sum_i p_i = 1 \ , \tag{2.23}$$

because the fundamental postulate is that each microstate Ω is equally probable (microcanonical ensemble).

On the other hand, for the constraint of a system in thermal contact with a thermal reservoir, it exchanges energy, but its temperature remains constant (canonical

---

[3]An extensive property depends on the amount of matter in the system of interest. The phenomenological nature of entropy, as a measurement of the irreversibility of a thermodynamic process, is commonly interpreted as a measurement of unavailability of energy to do some useful work. As a result, the concept of entropy is in some way attached with energy. Phenomenologically, if the system's energy changes, the entropy also tends to change. Because energy is an extensive property, entropy is also an extensive property.

[4]The addition of the Boltzmann constant k_B was a mere convention, since Ω is dimensionless and historically the entropy was defined by Clausius as

$$dS = \frac{\delta Q_{rev}}{T} \tag{2.21}$$

with units of J/K, the same units as the Boltzmann constant.

ensemble) [23]. The internal energy of the thermodynamic system can be defined as the weighted average of all states i:

$$U = \sum_i p_i E_i \; . \tag{2.24}$$

These last two equations are the canonical constraints that maximize the entropy. From the Lagrange multiplier method,

$$s = -\sum_i p_i \ln (p_i) + \alpha \left(1 - \sum_i p_i \right) + \beta \left(U - \sum_i p_i E_i \right) \; , \tag{2.25}$$

where λ and β are the Lagrange multipliers related to the normalization and energy constraints, respectively.

Maximizing the entropy

$$\frac{\mathrm{d}s}{\mathrm{d}p_i} = 0 \; , \tag{2.26}$$

and from the Eq. (2.23) we obtain

$$p_i = \frac{e^{-\beta E_i}}{Z} \; , \tag{2.27}$$

where

$$Z(T,B) = \sum_i e^{-\beta \mathcal{E}_i} \tag{2.28}$$

is the so-called canonical partition function.

From Eqs. (2.25) and (2.27), we have

$$s = \beta U + \ln Z \; . \tag{2.29}$$

and from the thermodynamic relationship

$$\frac{\partial S}{\partial U} = \frac{1}{T} \tag{2.30}$$

we obtain

$$\beta = \frac{1}{k_B T} \; . \tag{2.31}$$

From the Hamiltonian of the system, we write the energy spectrum $\mathcal{E}_i$, in order to obtain the canonical partition function. Once we have the partition function, the connection with thermodynamics can be done through the Helmholtz free energy [42]:

$$F(T,B) = -N k_B T \ln[Z(B,T)] \; , \tag{2.32}$$

From this, we obtain the thermodynamic properties of interest for the description of the magnetic nature of several low-dimensional molecular magnetic systems.

From the free energy, Eq. (2.32), we can obtain the magnetization [23]

$$
\begin{aligned}
M_i(T,B) &= -\frac{\partial}{\partial B_i} F(T,B) \\
&= N k_B T \frac{1}{Z(B,T)} \frac{\partial}{\partial B_i} Z(B,T) \,, \qquad (2.33)
\end{aligned}
$$

and the magnetic susceptibility, which is the derivative with respect to the external magnetic field, at the limit of low fields [23],

$$
\chi_{ij} = \lim_{B \to 0} \mu_0 \frac{dM_j}{dB_i} \qquad (2.34)
$$

where $(i,j) = x,y,z$. χ_{ij} is a rank-2 tensor. Phenomenologically, it measures the magnetic properties of a material. A physical system is said to be paramagnetic when the magnetic field in the material is strengthened by the induced magnetization, which leads to a positive magnetic susceptibility, but the system does not possess permanent magnetization without an external magnetic field. In contrast, ferromagnetic, ferrimagnetic, or antiferromagnetic materials [1, 23] have positive susceptibility and possess permanent magnetization even without external magnetic field. However, if the material exhibits a negative magnetic susceptibility, it is said to be diamagnetic, because the magnetic field in the material is weakened by the induced magnetization. In addition, quantitative measurements of the magnetic susceptibility of a molecular material also can provide insight into its chemical nature, revealing precious information about its microscopic properties, such as bonding and energy levels [30–33, 37, 49–51].

Therefore, the magnetic susceptibility of magnetic materials is fundamental for the characterization of its macroscopic and microscopic properties. In the following chapter, we present how the measure of magnetic susceptibility can also provide us with valuable information about the quantum nature of low-dimensional molecular magnetic systems.

2.2.4   Modeling Low-Dimensional Molecular Magnets

From the fundamentals described in the last sections, we can construct magnetic models for characterization of low-dimensional molecular magnetic systems. In this section, we will describe the step-by-step process of how to develop models for low-dimensional molecular magnets, an essential step for the connection of thermodynamic properties with the quantum features of molecular magnets.

Geometric configuration

The first step is to obtain the crystallographic structure of the system under consideration, highlighting the magnetic centers (metallic and/or organic), the bond angles, and distances between magnetic ions. This makes it possible to associate one or more exchange interactions, because different angles and distances lead to different exchange interactions.

Let us exemplify what was said in the previous paragraph. Let us consider the designed compound $Cu_2(HCOO)_4(HCOOH)_2$(piperazine) [2]. In this structure, copper dimers are arranged in linear chains and these chains are separated from each other, thus forming sheets of copper dimers (see Fig. 2.3(b)). From a magnetic viewpoint, analyzing the intra- and interchain distances, we can identify one exchange parameter, J, related to an intra-dimer interaction, as can be seen in Fig. 2.3(a).

Hamiltonians

From the geometric configuration of spins, it is possible to write the Hamiltonian model. A discussion on the physical meaning of some Hamiltonian models is given by Reis (2013) [23].

Let us consider the magnetic system of Fig. 2.3. The Hamiltonian model of this system is simply written as

$$\mathcal{H} = -J\vec{S}_1 \cdot \vec{S}_2 - g\mu_B \vec{B} \cdot (\vec{S}_1 + \vec{S}_2). \tag{2.35}$$

Once Eq. (2.35) is invariant under spin rotation, the total spin $s = s_1 + s_2$ is a good quantum number [23, 43]. From the Clebsch–Gordon series, the spectrum consists of $s = 1$ triplet and a $s = 0$ singlet [23]. Diagonalizing it, we obtain the energy eigenvalues E_s and eigenvectors $|s, m_s\rangle$ [23, 43]:

$$\mathcal{E}_{s,m_s} = -\frac{1}{2}J\left[s\left(s+1\right) - s_1\left(s_1+1\right) - s_2\left(s_2+1\right)\right] - g\mu_B B m_s \tag{2.36}$$

where $|s_1 - s_2| \leq s \leq s_1 + s_2$ and $m_s = -s, -s+1, ..., +s-1, +s$. The eigenvectors are

(a)

(b)
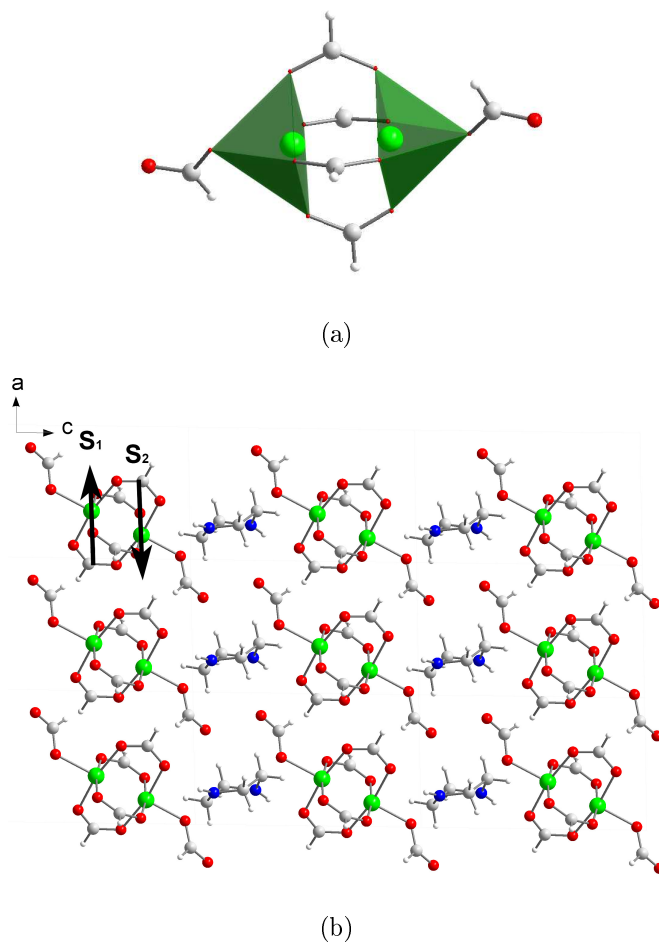
Figure 2.3: Crystal structure of $Cu_2(HCOO)_4(HCOOH)_2$(piperazine) compound [2] with (a) local dimer polyhedron representation and (b) dimeric sheet view, where the arrows represent the reduced magnetic structure of the compound. Color scheme: Cu - green; O - red; N - blue.

given by:

$$|s = 1, m_s = +1\rangle = |00\rangle \tag{2.37}$$

$$|s = 1, m_s = 0\rangle = \frac{1}{\sqrt{2}} \left(|01\rangle + |10\rangle\right) \tag{2.38}$$

$$|s = 1, m_s = -1\rangle = |11\rangle \tag{2.39}$$

$$|s = 0, m_s = 0\rangle = \frac{1}{\sqrt{2}} \left(|01\rangle - |10\rangle\right) \ . \tag{2.40}$$

Thermodynamic Quantities

From the energy spectra obtained in the previous step, we are able to obtain the desired thermodynamic quantities. These quantities are in most cases soluble analytically, enabling us to compare the analytical model with experimental data.

From the Hamiltonian of the system, we write the energy spectrum, Eq. (2.36), and, to obtain the desired thermodynamic quantities we write the partition function, using Eq. (2.28), as

$$Z = 1 + e^{\beta(J + g\mu_B B)} + e^{\beta(J)} + e^{\beta(J - g\mu_B B)} \ . \tag{2.41}$$

The connection with thermodynamics can be done through the Helmholtz free energy, Eq. (2.32), from which we finally obtain the magnetization, using Eq. (2.42),

$$M_i(T,B) \quad = \quad \frac{2Ng\mu_B e^{\frac{J}{k_B T}}}{Z(B,T)} \sinh\left\{\frac{g\mu_B B}{k_b T}\right\} \ . \tag{2.42}$$

From the theoretical point of view, the magnetic susceptibility is obtained from Eq.(2.34), as the Bleaney-Bowers equation for a two spin-1/2 system [2, 23, 34, 47, 66] as

$$\chi(T) = \frac{2N(g\mu_B)^2}{k_B T} \frac{1}{3 + e^{-J/k_B T}} \ . \tag{2.43}$$

Experimental Data

Finally, the analytical thermodynamic quantities obtained previously can be compared with the experimental data of interest to obtain the free parameters to the fitting, for instance, the exchange integrals J's of the isotropic Heisenberg Hamiltonian, Eq. (2.35), the Landé factor g, and other quantities [23]. With the optimized free parameter values, it is possible to understand the microscopic phenomena behind the magnetic behavior of a such molecular magnet [23]. These results are shown on Fig. 2.4.
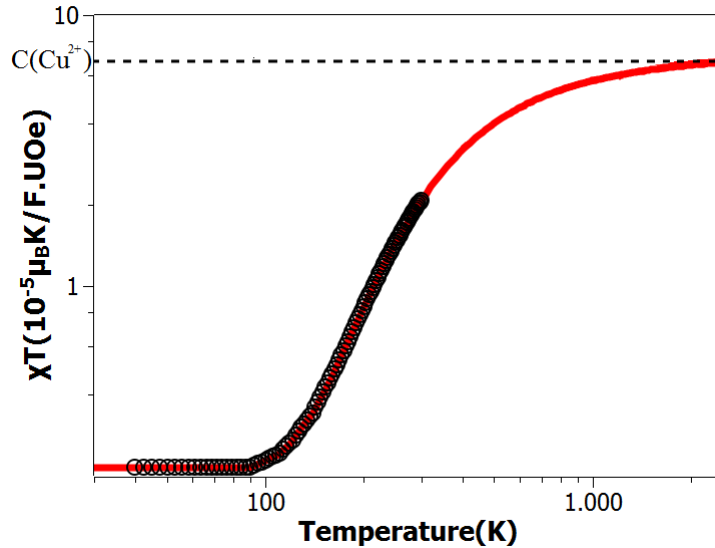
Figure 2.4: Experimental (open circles) and theoretical (solid line) magnetic susceptibility times temperature. The red line represents the fitting of Eq. (2.43) to the experimental data, where an extrapolation, up to higher temperatures, was done using the optimized parameters. The dashed line indicates the Curie constant for a Cu–Cu dimer.

This fitting was performed using DAVE-MagProp[5] [2, 44, 67], a software that analyzes and processes magnetic data.

2.2.5   First Principle Calculations in Low-Dimensional Molecular Magnets

In this section we briefly present the quantum formalism of first principle calculations on which part of the methodology used in the investigation of the magnetic properties of the molecular magnetic compounds studied in this thesis is based. From the computational materials science point of view, *ab initio*[6], or first principles DFT calculations are a powerful method for the prediction and calculation of material properties using fundamental concepts of quantum mechanics, without requiring higher order parameters such as phenomenological material properties. Usually, in electronic structure calculations, we use the approximation of clamped nuclei, where the nuclei of the treated molecules are seen as fixed. In such a case, the atomic dynamics of the nuclei and electron

---

[5]In the Appendices of this thesis a tutorial is provided on the use of DAVE-MagProp for the construction of theoretical models in molecular magnetism.

[6]Latin term "from the beginning".

cloud can be split as

$$\Psi_{Tot} = \psi_{eletronic} \otimes \psi_{nuclei} .\tag{2.44}$$

This is the Born–Oppenheimer approximation [68,69]. In this approach, the nuclei–nuclei interaction energy is constant and the nuclear kinetic energy term is neglected, so the atomic dynamics is given by the Hamiltonian

$$\begin{aligned}
\mathcal{H} &=& \mathcal{K}_e + \mathcal{V}_{ee} + \mathcal{V}_{en} + \mathcal{V}_{nn} \tag{2.45}\\
&=& \mathcal{H}_e + \mathcal{V}_{nn} , \tag{2.46}
\end{aligned}$$

where $\mathcal{K}_e$ is the electron kinetic energy, $\mathcal{V}_{ee}$ is the electron-electron potential, $\mathcal{V}_{en}$ is the electron-nuclei potential, $\mathcal{V}_{nn}$ is the nuclei-nuclei potential, and finally $mathcalH = \mathcal{K}_e + \mathcal{V}_{ee} + \mathcal{V}_{en}$ is the electronic Hamiltonian. Therefore, a stationary electronic state of an N-electron system $\psi(\vec{r}_1,...,\vec{r}_N)$ satisfies the many-electron time-independent Schrödinger equation [70]

$$\begin{aligned}
\mathcal{H}_e &=& \mathcal{K}_e + \mathcal{V}_{ee} + \mathcal{V}_{en}\psi(\vec{r}_1,...,\vec{r}_N) \tag{2.47}\\
&=& \left[\sum_i^N \left(-\frac{\hbar^2}{2m_i}\nabla_i^2 \right) + \sum_{i<j}^N V_{ee}(\vec{r}_i,\vec{r}_j) + \sum_i^N V_{en}(\vec{r}_i) \right] \psi(\vec{r}_1,...,\vec{r}_N) \tag{2.48}\\
&=& E\psi(\vec{r}_1,...,\vec{r}_N) . \tag{2.49}
\end{aligned}$$

There are many methods for solving this equation, one of the simplest methods is the Hartree–Fock method, based on the expansion of the wavefunction in Slater determinants [54]. However, these methods require a huge computational effort, which makes it virtually impossible to apply them effectively to larger systems. Density Functional Theory provides us a more versatile alternative, since it provides a way to systematically map the many-body problem using the electron density $n(\vec{r})$, for a normalized $\psi(\vec{r}_1,...,\vec{r}_N)$, given by

$$n(\vec{r}) = N \int d^3r_2 \cdots \int d^3r_N \, \psi^*(\vec{r}_1,...,\vec{r}_N)\psi(\vec{r}_1,...,\vec{r}_N) .\tag{2.50}$$

Then, given the ground-state density $n_0(\vec{r})$, it is possible to calculate the corresponding ground-state wave function

$$\psi_0(\vec{r}_1,...,\vec{r}_N) = \psi\left[n_0(\vec{r})\right]\tag{2.51}$$

that is a unique functional of $n_0(\vec{r})$.

Therefore, all physical observables are unique functionals of the electronic density of the ground state, that is,

$$\mathcal{O}\left[n_0\left(\vec{r}\right)\right] = \langle\psi\left[n_0\left(\vec{r}\right)\right]|\mathcal{O}|\psi\left[n_0\left(\vec{r}\right)\right]\rangle \tag{2.52}$$

In this way , the ground-state energy is written as

$$E\left[n_0\left(\vec{r}\right)\right] = \langle\psi\left[n_0\left(\vec{r}\right)\right]|\mathcal{H}_e|\psi\left[n_0\left(\vec{r}\right)\right]\rangle \tag{2.53}$$

$$= \langle\psi\left[n_0\left(\vec{r}\right)\right]|\mathcal{K}_e + \mathcal{V}_{ee} + \mathcal{V}_{en}\psi(\vec{r}_1,...,\vec{r}_N)|\psi\left[n_0\left(\vec{r}\right)\right]\rangle \tag{2.54}$$

Thus, the potential energy from the external field resulting from positively charged nuclei, $\mathcal{V}_{en}$, can be written in terms of the ground-state density as

$$\mathcal{V}_{en}\left[n_0\left(\vec{r}\right)\right] = \int V\left(\vec{r}\right)n_0\left(\vec{r}\right)\mathrm{d}^3r. \tag{2.55}$$

which leads to the first Hohenberg-Kohn Theorem [69,71,72], in which the external potential felt by the electrons is univocally determined by the electronic density of the ground state, $n_0\left(\vec{r}\right)$ [54,69].

More generally, the energy functional can be written as

$$E\left[n_0\left(\vec{r}\right)\right] = \mathcal{K}_e\left[n_0\left(\vec{r}\right)\right] + \mathcal{V}_{ee}\left[n_0\left(\vec{r}\right)\right] + \int V\left(\vec{r}\right)n_0\left(\vec{r}\right)\mathrm{d}^3r. \tag{2.56}$$

This gives us the second Hohenberg–Kohn theorem [69, 71, 72], where the ground-state energy is the global minimum of the energy $E\left[n\left(\vec{r}\right)\right]$ and the density that minimizes this functional is the exact density of the ground state, $n_0\left(\vec{r}\right)$ [54].

Although the Hohenberg–Kohn theorem ensures that knowledge of $n_0\left(\vec{r}\right)$ is sufficient to determine the ground-state properties of a quantum system, this theorem does not provide us with a practical procedure for obtaining $n_0\left(\vec{r}\right)$. This problem was solved with the emergence of the so-called Kohn–Sham equation [69,73], the one-electron Schrödinger-like equation of a fictitious system, also known as the Kohn–Sham system, of noninteracting electrons that generate the same electronic density as any given system of interacting particles [54,69]:

$$\left[-\frac{\hbar^2}{2m}\nabla^2 + V_s(\vec{r})\right]\phi_i(\vec{r}) = E_i\phi_i(\vec{r}) , \tag{2.57}$$

where $V_s(\vec{r})$ is the effective single-particle external potential in which the particles are moving, also known as the Kohn–Sham effective potential, and ϕ_i are the orbitals that yield the density

$$n(\vec{r}) = \sum_i^N |\phi_i(\vec{r})|^2 \ . \tag{2.58}$$

In a general way, the effective single-particle external potential $V_s(\vec{r})$ can be written as

$$V_s(\vec{r}) = V(\vec{r}) + \int \frac{e^2 n_{\rm s}(\vec{r'})}{|\vec{r} - \vec{r'}|} {\rm d}^3 r' + V_{\mathcal{XC}}[n_s(\vec{r})] \ , \qquad (2.59)$$

where

$$\int \frac{e^2 n_{\rm s}(\vec{r'})}{|\vec{r} - \vec{r'}|} {\rm d}^3 r'] \qquad (2.60)$$

is known as the Hartree term, which describes the electron–electron Coulomb repulsion and $V_{\mathcal{XC}}[n_s(\vec{r})]$ is the exchange-correlation potential that includes all the many-particle interactions. Therefore, the solution of the Kohn–Sham equation is obtained in the following self-consistent way:

- Start from an initial guess for $n(\vec{r})$.

- Calculate the corresponding Kohn–Sham effective potential $V_s(\vec{r})$,

- Solve the Kohn–Sham equation, Eq. (2.57), for the $\phi_i(\vec{r})$.

- Using Eq. (2.58), calculate a new density $n(\vec{r})$ and start again.

Then, we repeat this procedure until the convergence is reached.

In order to determine the eigenfunctions and eigenvalues of the Kohn–Sham equation, Eq. (2.57), it is fundamental to introduce a set of basic functions that allow it to be transformed into an algebraic equation whose solution can be obtained through matrix diagonalization methods. The Kohn–Sham equations, Eq. (2.57), can be solved by using the plane-wave pseudopotential method, to expand the Kohn-Sham orbitals, and pseudopotentials to describe the electron-ion interaction, as implemented in the Quantum ESPRESSO software [74]. Using this approach one can calculate the total ground state energy and the Kohn-Sham orbitals for isolated, periodic and extended systems, calculate the total ground state energy of magnetic systems, and optimize the crystal structure of the magnetic systems of interest. In addition to calculating the parameters of Electronic Paramagnetic Resonance (EPR) to study the creation of quantum logic gates based on low-dimensional molecular magnetic systems using gauge including projected augmented wave (GIPAW) approach [75–82].

2.2.6   Neutron Scattering

In the past few decades, neutrons have become a key resource for studying

the structural, magnetic, and even quantum properties of condensed matter systems [12,22,83,84,84–88]. Neutrons provide invaluable information about structure [83], atomic motion [84], magnetic order [12], phase transitions [84,85], magnetic excitations [84,89], and quantum entanglement [22,24,86–88]. Inelastic neutron scattering is a useful technique to address pairwise spin correlations in magnetic systems [84]. Recently, it was demonstrated that structure factors obtained from inelastic neutron scattering are good tools to detect quantum entanglement in condensed matter systems [22,86–88]. Structure factors are macroscopic quantities that can be measured in neutron scattering experiments in various physical systems, such as quantum spin lattices. They can be defined as two-point correlation functions [88] and are widely used to describe the crystal structure of molecular systems [84,90].

From a magnetic point of view, the study of molecular magnetic materials is typically done through the approach of using the magnetic parameters of a Hamiltonian model, by the fit of some thermodynamic properties, e.g., magnetic susceptibility, internal energy, and specific heat [2,23,30,31,31,43], as presented in the previous section. In this context, correlation functions have great importance in describing these properties; in addition, they can be directly measurable, e.g., in neutron scattering experiments via structure factors.

Magnetic Neutron Scattering

From an experimental point of view, neutrons are generally produced by specially designed pulsed sources or nuclear reactors, [84]. In both cases, a monochromatic neutron beam is generated and directed to the target sample. When the neutron beam hits the target sample, it can be scattered or absorbed by the nuclei of the sample and scattered through the magnetic interaction between the intrinsic neutron magnetic moment (μ) of the unpaired electrons in the sample or by orbital motion.

Nuclear scattering is responsible for phonon and elastic scattering, i.e., Bragg diffraction. The neutrons absorbed by the nuclei of the sample lead to a decrease of intensity that can greatly influence the time of measurement needed to obtain good statistics [84,90]. To determine magnetic and quantum properties of a condensed matter system, nuclear scattering and the absorption are undesirable in most cases. Therefore, they must influence the final result as little as possible [84,90]. However, because

the neutron magnetic moment couples to those of the unpaired electrons of the sample material, neutron scattering provides detailed information about its magnetic and quantum properties. In this scenario, elastic neutron scattering is widely used to study magnetic order transitions [84], whereas magnetic inelastic scattering is a useful tool to study magnetic excitations and pairwise classical and quantum correlations in magnetic systems [12,22,86–88,90]. Therefore, it is possible to study nonclassical correlations from inelastic neutron scattering, one of the main subjects of study of this thesis.

In a neutron scattering experiment, a beam is generated and scattered by the sample toward a network of detector tubes [84]. This network of detectors varies from one instrument to another, but usually it covers a wide range of scattering angles (θ). In inelastic scattering, neutrons with initial energy E_i and momentum k_i are scattered by the target sample. After being scattered, the neutrons will be detected with energy E_f and momentum k_f. The conservation laws during this process require that the energy transferred between the neutron and the sample is $\hbar\omega$, while the momentum transfer will be $\hbar\vec{q}$ [84,91]. Figure 2.5 shows a schematic representation of the neutron scattering process.
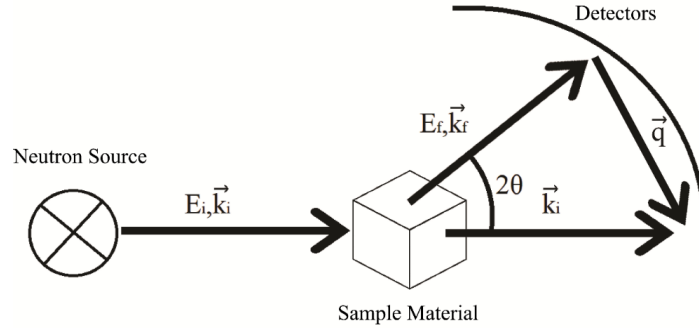
Figure 2.5: Schematic representation of the neutron scattering process. A monochromatic beam of neutrons is produced with a determined energy E_i and momentum k_i. After being scattered through the sample, the neutrons are measured in a network of detectors, the arrival time of these neutrons is measured, and their energy E_f is determined; its moment k_f is determined from the scattering angle 2θ [84,91].

In this way, the neutron beam is scattered and analyzed according to the transferred energy [12],

$$\hbar\omega = E_i - E_f = \frac{\hbar^2}{2m_n}\left(k_i^2 - k_f^2\right) \ , \tag{2.61}$$

where m_n is the neutron mass, and momentum transfer,

$$\hbar\vec{q} = \hbar\left(\vec{k}_i - \vec{k}_f\right) \tag{2.62}$$

where $\vec{q}$ is the scattering vector, i.e., the difference between the initial and scattered neutron momentum. It can be directly obtained from knowledge of the moments k_{in} and k_{out} and the scattering angle θ:

$$q = \sqrt{k_i^2 + k_f^2 + 2k_i^2 k_f cos(2\theta)} \ , \tag{2.63}$$

where $k_{i,f} = 2\pi/\lambda_{i,f}$, with $\lambda_{i,f}$ the wavelength of the neutron beams incident and scattered.

As the main objective of this section is to present the process of constructing models for the analysis of low-dimensional magnetic systems, by calculating structural factors, an effective spin must be attributed to the magnetic centers or to the whole unit cell [87]. The magnetic scattering cross section can be derived from first-order perturbation theory through Fermi's golden rule [91,92] that describes the probability of transition per unit time from one energy eigenstate of a quantum system into other energy eigenstates in a continuum, which is equivalent to Born's approximation in interacting systems [91], where we assume that the interaction potential between the neutrons and the unpaired electrons in the sample is small enough to be treated as a perturbation. Therefore, the magnetic cross section can be interpreted as the number of neutrons scattered per second into a solid angle element $d\Omega$ in the direction θ, with energy in the interval between ω and $\omega + d\omega$ [91], and calculated as [84,87,91,93]

$$\frac{d^2\sigma}{d\omega d\Omega} = \frac{1}{Z}\left(\frac{g_{l,\alpha}\gamma r_0}{2}\right)^2 \frac{k_{out}}{k_{in}} e^{-2W} \sum_{\alpha,\beta,l,m}\left(\delta_{\alpha,\beta} - \frac{\vec{q}_\alpha\vec{q}_\beta}{|\vec{q}|^2}\right)[F_l(\vec{q})g_{l,\alpha}]^* [F_m(\vec{q})g_{m,\beta}] \tag{2.64}$$

$$\times \ \int e^{i\left[\omega t + \vec{q}\cdot\vec{r}_{l,m}\right]}\langle S_l^\alpha S_m^\beta(t)\rangle dt \tag{2.65}$$

where Z is the partition function of the system; $\gamma = -1.913$ is the gyromagnetic ratio; $r_0 = e^2/m_e c^2$ is the classical electron radius [12, 84, 87, 90]; $g_{l,\alpha}$ is the Landé factor; e^{-2W} is the Debye–Weller factor, responsible for the exponential decay of the magnetic cross section as a function of the scattering vector $\vec{q}$ [12,84]; $F_l(\vec{q})$ is the magnetic form factor, which results from the finite extension of the orbitals seen by the neutrons with wavelengths of the order of the interatomic distances [87,91], for which detailed knowledge on the electronic wavefunctions of magnetic ions is required to determine it and whose values can be found in the literature [84,87,91]; the factor $(\delta_{\alpha,\beta} - \vec{q}_\alpha\vec{q}_\beta/|\vec{q}|^2)$ means that the neutron can only couple to components of the magnetic moment perpendicular to the

scattering vector $\vec{q}$ [84]; l and m denote the lth and mth spins in the cluster; ω represents the energy transferred to the target sample; Ω is the solid angle under which the scattered neutrons are observed; $\vec{r}_{l,m} = \vec{r}_l - \vec{r_m}$ is the spatial vector; $(\alpha,\beta) = x,y,z$; and, finally, S_l^α are the spin operators. It is worth mentioning that the following term

$$\delta_{\alpha,\beta} - \frac{\vec{q}_\alpha \vec{q}_\beta}{|\vec{q}|^2} \; , \tag{2.66}$$

means that the neutrons can only couple with the components of the magnetic moment perpendicular to the scattering vector $\vec{q}$ [84]. For this reason, the neutrons that are scattered are correlated to the magnetic centers of the sample. Therefore, we can define the dynamic structure factor $\mathcal{S}(\vec{q},\omega)$ [94] as a fundamental quantity that contains all the information about the magnetic structure, spin dynamics, and the nonclassical correlations of quantum magnets [22, 43, 84, 86–88, 90, 94, 95]. It can be obtained from Eq. (2.65) as

$$\mathcal{S}(\vec{q},\omega) = \frac{1}{2\pi N} \sum_{l,m} \sum_{\alpha,\beta} \int e^{i\left[\omega t + \vec{q}\cdot\vec{r}_{l,m}\right]} \langle S_l^\alpha S_m^\beta(t)\rangle dt \; . \tag{2.67}$$

Through a simple visual inspection of Eq. (2.67), we see that the dynamic structure factor can be described as a Fourier transform in space and time of the time-dependent correlation function between the spin pairs, $\langle S_l^\alpha S_m^\beta(t)\rangle$. Determining the dynamic structure factor is the primary objective of any magnetic scattering experiment [43, 84, 90, 94, 95]. It contains information about the nonclassical correlations of the spin pairs [22, 86–88, 94, 95].

From transitions between discrete energy levels, the time integral shown in Eq. (2.67) gives a delta function $\delta\left(E_{out} - E_{in} - \hbar\omega\right)$, where $\hbar\omega$ is the transferred energy, Eq. (6.3) [12, 43]. Taking the time integral over energy gives us the so-called integrated (or static) structure factor,

$$\mathcal{S}(\vec{q}) = \sum_{\alpha\beta} \mathcal{S}^{\alpha\beta}(\vec{q}) = \frac{1}{N} \sum_{\alpha\beta} \sum_{l,m} e^{i\vec{q}\cdot\vec{r}_{l,m}} \langle S_l^\alpha S_m^\beta\rangle \tag{2.68}$$

Considering the excitation of a given initial state $|\psi_i\rangle$ for a final state in the magnetic multiplet $|\psi_f\rangle$, we can write the unique structure factor $\mathcal{S}_{fi}^{(\alpha,\beta)}(\vec{q})$ [43] as

$$\mathcal{S}_{fi}^{(\alpha,\beta)}(\vec{q}) = \sum_f \langle\psi_i|\mathcal{U}_\alpha^\dagger(\vec{q})|\psi_f\rangle\langle\psi_f|\mathcal{U}_\beta(\vec{q})|\psi_i\rangle \; , \tag{2.69}$$

where

$$\mathcal{U}_{\alpha,\beta}(\vec{q}) = \sum_{\vec{r}_1} S_{(1,2)}^{(\alpha)} e^{i\vec{q}\cdot\vec{r}_1}, \tag{2.70}$$

whose summation is taken over all the ions of the unit cell [12,43,87]. In this way, we can define the known monocrystal structure factor, $\mathcal{S}(q)$, for a molecular magnetic system, such as

$$\mathcal{S}_{fi}^{(\alpha,\beta)}(\vec{q}) = \delta_{\alpha,\beta}\mathcal{S}(q) \ . \tag{2.71}$$

This result is applied to neutron scattering from single crystals. In neutron scattering experiments, one measures the powder average structure factors from powder samples, but how often these measurements are made in powder samples and our intention is the construction of models for the interpretation of neutron scattering experiments by calculating the structure factor. We need to define an average of the structure factor $\bar{\mathcal{S}}(q)$. Thus, we integrate Eq.(2.71) over the solid angle element Ω on which the neutrons are detected. The powder average can be defined as

$$\bar{\mathcal{S}}(\vec{q}) = \int \frac{d\Omega_q}{4\pi}\mathcal{S}(\vec{q}) \ . \tag{2.72}$$

Given the Hamiltonian model, it is possible to predict its scalar structure factor. One can then compare experiments of neutron scattering on real materials with these theoretical model calculations. [43].

From the experimental point of view, the intensity peaks from inelastic scattering are controlled by the magnetic form factor $F_l(\vec{q})$ and are directly proportional to the average structure factor of the material:

$$I \quad \propto \quad [F_l(\vec{q})^* F_m(\vec{q})] \ .\bar{\mathcal{S}}(q) \tag{2.73}$$

In this context, from the positions of inelastic peaks, the q dependence, and intensity of the peaks, one can obtain information about energy levels and, therefore, the quantum properties of magnetic systems. The position of the energy levels and the peak intensities are determined by the microscopic magnetic Hamiltonian and the magnetic form factor $F_{l,m}(\vec{q})$, respectively. From the experimental access to the inelastic peak positions, q dependence allows the characterization of the quantum properties of magnetic systems [22, 84, 86–88, 94, 95]. Therefore, from the intensity peaks of inelastic neutron scattering, we can experimentally extract information about the structure factor and thereby obtain useful information about the magnetic, structural, and quantum magnetic properties of molecular magnetic systems [12, 22, 24, 83–88, 96].

Generally, the study of the magnetic properties of molecular magnetic systems is done through the optimization of free parameters of the magnetic model (Hamiltonian)

by adjusting its thermodynamic properties, such as magnetic susceptibility and specific heat [2, 23, 30, 31, 31, 32, 43]. In contrast, the inelastic neutron scattering structure factor provides us with a more sensitive and microscopic test of our magnetic Hamiltonian, because this is determined by the relative positions $\vec{r}_{l,m}$ of the magnetic ions.

Therefore, through the neutron scattering intensity peaks, we obtain very valuable information about the microscopic properties of the sample material without the need to access the macroscopic properties of the target system, such as its magnetic susceptibility or specific heat, or make any assumption about any other external conditions under which the neutrons are scattered, such as temperature, pressure, or magnetic field.

We can thus compare neutron scattering experiments in real materials [12, 96–100] with the theoretical models previously constructed by adjusting the intensity peaks, Eq. (2.73). In this context, the positions of the peaks are related to the scattering vector; therefore, through them we obtain information about the energy levels and, as a consequence, we can evaluate microscopically the magnetic and quantum properties of the sample. Therefore, given the Hamiltonian of the system, we can construct a model that allows us to predict the structure factor for neutron inelastic scattering.

Structure Factors of a Molecular Magnetic System

For a given molecular magnetic system, one can evaluate the inelastic structure factor, which allows a sensitive test of an assumed Hamiltonian, because it is affected by the relative positions $\vec{r}_1$ and $\vec{r}_2$ of the interacting magnetic ions. Usually, to obtain certain parameters of a model Hamiltonian, a fitting to a thermodynamic quantity (magnetic susceptibility, specific heat, magnetization, and so forth) is performed [2, 23, 30, 31, 43].

Let us consider a low-dimensional magnetic system, such as a small two spin-1/2 cluster, as an interacting pair of spin-1/2 particles ruled by the Heisenberg–Dirac–Van Vleck Hamiltonian, Eq. (2.1), so that we can analytically calculate the static structure factor of inelastic neutron scattering[7]. This is an ideal realization of a two-qubit system and, therefore, makes molecular magnetic systems of this type promising platforms for quantum information processing [2, 12, 20, 24], the main subject of study of this thesis.

---

[7]This example relates to actual materials such as $VO(HPO_4)0.5H_2O$, where the structure factor is obtained by the analysis of magnetic excitations in the inelastic neutron scatter data in isolated dimers of V^{4+} [12, 43, 99].

Once Eq. (2.1) is invariant under spin rotation, the total spin $s = s_1 + s_2$ is a good quantum number [23, 43]. From the Clebsch–Gordon series, the spectrum consists of $s = 1$ triplet and a $s = 0$ singlet [23]. We obtain the following energy eigenvalues E_s, Eq. (2.5), and eigenvectors $|s, m_s\rangle$ [23, 43]:

$$E_{s=1} = \frac{1}{4}J \tag{2.74}$$

$$E_{s=0} = -\frac{3}{4}J \tag{2.75}$$

$$|\psi_0\rangle = |s = 0, m_s = 0\rangle = \frac{1}{\sqrt{2}}\left(|01\rangle - |10\rangle\right) \tag{2.76}$$

$$|\psi_1\rangle = |s = 1, m_s = +1\rangle = |00\rangle \tag{2.77}$$

$$|\psi_2\rangle = |s = 1, m_s = 0\rangle = \frac{1}{\sqrt{2}}\left(|01\rangle + |10\rangle\right) \tag{2.78}$$

$$|\psi_3\rangle = |s = 1, m_s = -1\rangle = |11\rangle \ . \tag{2.79}$$

Therefore, for this specific case of a Heisenberg spin dimer, Eq. (2.1), one can define the so-called exclusive structure factor as a function of the scattering vector $\vec{q}$ [43], for the excitation of the final states in the magnetic multiplet $|\psi_f\rangle$, Eqs. (2.77)–(2.76), from the given initial state $|\psi_i\rangle$. For the $|\psi_0\rangle = |s = 0, m_s = 0\rangle$ initial state (antiparallel magnetic alignment), Eq. (2.76), only $s = 1$ final states are excited, Eqs. (2.77)–(2.79). In this way, using Eqs. (2.69) and (2.70), we obtain

$$\mathcal{S}_{s=1,s=0}^{(\alpha,\beta)}(\vec{q}) = \sum_{f=1}^{3}\langle\psi_0|\left[\sum_{\vec{r}_1} S_{(1,2)}^{(\alpha)}e^{i\vec{q}\cdot\vec{r}_{(1,2)}}\right]^{\dagger}|\psi_f\rangle\langle\psi_f|\left[\sum_{\vec{r}_{(1,2)}} S_{(1,2)}^{(\beta)}e^{i\vec{q}\cdot\vec{r}_1}\right]|\psi_0\rangle \ , \tag{2.80}$$

where Eq.(2.80) is related to the exclusive differential inelastic neutron scattering cross section by

$$\frac{d\sigma}{d\Omega} = (\gamma r_0)^2\frac{k_{out}}{k_{in}}(\delta_{\alpha\beta} - \bar{q}_\alpha\bar{q}_\beta)\{\sum_{f=1}^{3}\langle\psi_0|\left[\sum_{\vec{r}_{(1,2)}} S_{(1,2)}^{(\alpha)}e^{i\vec{q}\cdot\vec{r}_1}\right]^{\dagger}|\psi_f\rangle\langle\psi_f|\left[\sum_{\vec{r}_1} S_{(1,2)}^{(\beta)}e^{i\vec{q}\cdot\vec{r}_{(1,2)}}\right]|\psi_0\rangle\}|F(\vec{q})|^2 \tag{2.81}$$

where $\gamma \approx -1.913$ is the neutron gyromagnetic ratio, $r_0 = e^2/m_ec^2$ is the classical electron radius and $\bar{q} = \vec{q}/|q|$.

Considering point-like ions $(F(\vec{q}) = 1)$, one can define the scalar neutron scattering structure factor $\mathcal{S}(\vec{q})$ for the Heisenberg spin-1/2 dimer [43]. Simplifying the presentation by quoting, the result $\langle\mathcal{S}_{s=1,s=0}^{(\alpha,\beta)}(\vec{q})\rangle$, can be obtained by summing over final and averaging over initial polarizations [43]. Replacing the eigenvectors given by Eqs. (2.77)–(2.76) in Eq. (2.80), and using Eq. (2.71), we can evaluate the inelastic neutron

scattering intensities that are given by structure factors [43] for the Heisenberg spin-1/2 dimer, Eq. (2.1). In this manner, we obtain the scalar neutron scattering structure factor as calculated in Ref. [43]:

$$\mathcal{S}(\vec{q}) = \frac{1}{2}\left[1 - cos(\vec{q} \cdot (\vec{r_1} - \vec{r_2}))\right]. \tag{2.82}$$

Therefore, for systems ruled by the Heisenberg models, the neutron scattering structure factors can be analytically calculated. In Chapter 7, we show that nonclassical correlations can be accessed through diffractive properties obtained via neutron scattering experiments, since they can be defined as two-point correlation functions [88], without making any assumption about the macroscopic properties of the target system, such as its magnetic susceptibility or specific heat, or imposing any other external conditions under which the neutrons are scattered, such as temperature or magnetic field.

3 Quantum Correlations

The quantum properties of composite systems can be explored to allow for a revolution in quantum information technology. Characterizing the quantum nature of correlations is of paramount importance since these correlations refer to statistical properties of quantum systems. In this chapter, we will discuss quantum correlations in a general way, the forms of its characterization and quantification, and their influence on finite-temperature systems such as molecular magnetic systems. We show the analytical expressions for quantum information quantifiers, such as entanglement witness, entanglement of formation, and entropic and geometric quantum discord, based on the Schatten 1-norm, in bipartite systems as a function of the thermodynamic properties of solids. Throughout this thesis, discussions will be concentrated on finite-dimensional bipartite systems, for which a more complete understanding can be found in the literature [4, 65, 101]. Consequently, we present one path toward identifying the presence of quantum correlations in a molecular magnet, as a Heisenberg spin-1/2 dimer.

3.1 Quantum Entanglement

Quantum entanglement is one of the most interesting phenomena in quantum mechanics. Nowadays, quantum entanglement has received considerable attention as a remarkable resource for quantum information processing [4,65,102] and for understanding of correlations in composite systems. Althought in 1932 von Neumann had completed the fundamental elements of a nonrelativistic quantized description of nature [4,103], it was in 1935 that Einstein, Podolsky, and Rosen (EPR), through the perception of the violation of uncertainty relations, and then Schrödinger, the firsts to recognize the existence of the phenomenon called quantum entanglement[1]. EPR introduced the idea that quantum

---

[1]The original name "Verschränkung" was given by Schrödinger in his work *Die gegenwärtige Situation in der Quantenmechanik* (*The Current Situation in Quantum Mechanics*) [104].

states of a composite system can present nonlocal correlations among their components [105]. Schrödinger analyzed some physical consequences of quantum mechanics, noticing that some bipartite quantum states (EPR states [4]) do not admit ascribing individual states of subsystems, implying some *entangled predictions* for the quantum nature of subsystems [4, 104]. In the words of Schrödinger, "The best knowledge of a whole does not include the knowledge of its parts" [4, 104, 106]. Therefore, entanglement implies the existence of global quantum states of composite systems that cannot be written as a product of the quantum states of individual subsystems [4].

Let us consider the Hilbert space of a composite system

$$\mathbb{H} = \mathbb{H}_1 \otimes \mathbb{H}_2 \otimes \cdots \otimes \mathbb{H}_n \ , \tag{3.1}$$

if the quantum state of the composite system is perfectly described by the wavefunction

$$|\Psi\rangle \neq |\phi_1\rangle \otimes |\phi_2\rangle \otimes \cdots \otimes |\phi_n\rangle \ , \tag{3.2}$$

we cannot specify any pure quantum state $|\phi_i\rangle$ $(i = 1, \ldots, n)$ of the subsystems separately; that is, knowledge of a whole does not imply knowledge of the parts.

In a general way, for mixed states, the state of the composite system is specified by the density operator ρ [65] that acts on Hilbert space $\mathbb{H}$. This state is defined to be separable if there is a probability distribution p_i and a set of states $\{\rho_1^{(i)}, \rho_2^{(i)}, \ldots, \rho_n^{(i)}\}$ acting in $\mathbb{H}_1$, $\mathbb{H}_2$, $\ldots$, $\mathbb{H}_n$, such that it can be written as

$$\rho = \sum_i p_i \rho_1^{(i)} \otimes \rho_2^{(i)} \otimes \cdots \otimes \rho_n^{(i)} \ . \tag{3.3}$$

A quantum state is said to be entangled if it cannot be written as Eq. (3.3).

3.1.1   Entanglement and Correlations in Quantum Mechanics

We can define correlation as the information gained about one system by measuring another. Let us consider the classical situation, an imagined experiment with macroscopic objects (balls and boxes). There are two balls with printed numbers 0 and 1 on each ball, respectively, and we hide each ball in one box. Each box can be considered as a subsystem of a composite system. The content of each box is one bit of information[2]. Since the content of the boxes is unknown to an external observer in advance, only the probability distribution is known, as can be seen from Table 3.1.

---

[2]A bit (binary digit) is the smallest unit of information that can be stored or transmitted and is used in computational and information theory. A bit can only assume two values: 0 or 1, true or false, etc.

Table 3.1: Probability distribution of a classical correlation experiment.

Event	Box A	Box B	Probability
1	0	1	50%
2	1	0	50%

An observer can acquire information or determine the contents of one box by opening the other. This is because the subsystems (the boxes) are classically correlated. If we consider each box as a single quantum system with respective Hilbert spaces $\mathbb{H}_A$ (box 1) and $\mathbb{H}_B$ (box 2), the state of each box is

$$|\phi_A\rangle \;=\; |\phi_B\rangle = \frac{1}{\sqrt{2}}\left(|0\rangle + |1\rangle\right) \; . \tag{3.4}$$

However, we could imagine a composite quantum system $\mathbb{H} = \mathbb{H}_A \otimes \mathbb{H}_B$ in this scenario. The quantum state of this prepared composite can be described as the superposition of the probability of each event as[3]

$$\begin{aligned}|\Psi\rangle \;&=\; \frac{1}{\sqrt{2}}\left(|0\rangle_A \otimes |1\rangle_B + |1\rangle_A \otimes |0\rangle_B\right)\\ &\neq\; |\phi_A\rangle \otimes |\phi_B\rangle \; .\end{aligned} \tag{3.5}$$

Therefore, the entanglement arises from the quantum superposition; a local measurement in any of the subsystems returns us states $|0\rangle$ or $|1\rangle$ with equal probabilities, while measurements of both subsystems are perfectly correlated. We know nothing about the subsystems, although we have knowledge of the system as a whole and although $|\Psi\rangle$ is a pure state. This contrasts with the classical situation, in which we can always consider individual states of the subsystems. This is a clue that entangled states are special correlated states whose physical nature cannot be simulated or represented from classical correlations. We say that entangled states contain quantum correlations.

Thus, we know that pure entangled states contain purely quantum correlations, whereas entangled statistical mixtures may also contain classical correlations, but they must necessarily have quantum ones [15,34,66]. The fact that entangled states cannot be simulated or represented from local classical correlations can be expanded to the property that, unlike separable states, entangled states cannot be created by local operations and classical communications (LOCC) [65].

---

[3]This is one of the Bell states, states that maximally violate Bell's inequality [4,107,108].

Local Operations and Classical Communications

The fundamental concept of mixed separable states, Eq.(3.3), can be redefined in a more operational way because such quantum states can be produced by LOCC [4,65], which is an operation that generates classical correlation accomplished by classical communication among the parts that are creating its states [4,35,65,109].

Let us consider an initial state ρ_{in}, that interacts with a ancillary system ρ_{aux}. Since the evolution of a quantum system is described by unitary transformations, $\mathcal{U}\rho\mathcal{U}^\dagger$, we have that for this joint system

$$\rho = \rho_{aux} \otimes \rho_{in} \ . \tag{3.6}$$

In other words, the auxiliary system is correlated with the initial system. Consequently, to obtain only the evolution of the system of interest we must calculate the partial trace over the auxiliary system

$$\rho_{in}{}' = \mathrm{Tr}\left[\mathcal{U}\rho\mathcal{U}^\dagger\right] \ . \tag{3.7}$$

Thus, the state corresponding to the measurement of element i of the basis, whose probability

$$p_i = \mathrm{Tr}\left[\mathcal{E}_i\rho_{in}\mathcal{E}_i^\dagger\right] \ , \tag{3.8}$$

is a mapping of the form

$$\rho_i = \frac{\mathcal{E}_i\rho_{in}\mathcal{E}_i^\dagger}{\mathrm{Tr}\left[\mathcal{E}_i\rho_{in}\mathcal{E}_i^\dagger\right]} \ . \tag{3.9}$$

where $\mathcal{E}_i$ are the set of generalized quantum operations (Kraus operators) [65], with $\sum_i \mathcal{E}_i^\dagger\mathcal{E}_i = \mathbb{I}$. That is an extremely useful representation for correcting information loss through the decoherence process, induced, for instance, by the transmission of quantum states. In this way, we can coordinate these operations locally with a classical communication channel in order to obtain the transmission of quantum states with the least possible loss.

Let us consider two subsystems A and B, spatially separable by an arbitrary distance, with no quantum interaction between these subsystems. Meanwhile, we can perform local operations in each subsystem separately. In addition, the operators of each subsystem can communicate classically and coordinate local operations. Together these two processes are called Local Operations and Classical Communication (LOCC). In this way, we can classically correlate A and B, but we cannot create entanglement from this,

because it cannot be simulated or represented purely by classical correlations [4,65]. It is reasonable to say that there is no entanglement in separable states, Eq. (3.3), since they can be created by LOCC and, as a consequence, it can be described by local classical correlations[4].

Another consequence that arises from LOCC applied to entangled states is in the fact that state entanglement does not increase under LOCC transformations. Let us consider that an entangled state ρ' is transformed into another state ρ'' by LOCC. Therefore, one can attest that at best ρ'' is as entangled as ρ' [4, 35, 109]. This fact can be expressed in the existence of maximally entangled states, in which from LOCC we can generate any other entangled state with equal or less degree of entanglement.

Entanglement Basic Properties

In this way, we can condense the definition of entanglement in an operational way through the basic properties common to any entangled state:

- **Separable states, (Eq. 3.3), do not contain entanglement.**

A quantum state is said to be separable if it can be written in the form

$$\sigma = \sum_i p_i \sigma_1^{(i)} \otimes \sigma_2^{(i)} \otimes \cdots \otimes \sigma_n^{(i)} . \tag{3.10}$$

A separable quantum state do not contain entanglement because we can define them operationally through LOCC, and, consequently, these can be defined by classical correlations.

- **Entanglement does not increase under LOCC.**

Since, as mentioned before, the physical nature of entanglement can not be described or represented by any effect of a classical nature. Let us consider a set of separable quantum state $\mathbf{S}$, performing a LOCC transformation $\Lambda_{LOCC}(\sigma)$ in a general separable state σ

$$\Lambda_{LOCC}(\sigma) \in \mathbf{S}, \ \forall \ \sigma \in \mathbf{S} . \tag{3.11}$$

---

[4]It is worth noting that, in the light of discord theory [9,10], this does not necessarily mean that quantum correlations cannot exist in separable states [9,10,34,66].

Suppose a quantum entangled state $\rho_A B$ is transformed into another entanglement quantum state $\xi_A B$ by LOCC operations. So everything that can be done with ρ_A and LOCC operations can also be done with ρ_B and LOCC operations. Therefore, starting from an entangled state, ρ, applying LOCC, $\Lambda_{LOCC}(\rho)$, we can obtain at most another state, but with a degree of entanglement, $E(\rho)$, equal to or less than the state that created it.

$$E(\Lambda_{LOCC}(\rho)) \leq E(\rho) , \quad \forall E(\rho) . \tag{3.12}$$

In other words, one can define a general measurement of the degree of entanglement $E(\rho)$. Due to the fact that entanglement do not increase under LOCC, $E(\rho)$ is monotonically non-increasing under LOCC operations.

In order to clarify this point we will consider the following example [35]: Let us consider the entangled state

$$|\Phi_+\rangle = \frac{1}{\sqrt{2}} \left(|0\rangle_A \otimes |1\rangle_B + |1\rangle_A \otimes |0\rangle_B \right) , \tag{3.13}$$

where the qubits are shared by two distant laboratories A and B. Thus, one qubit is in laboratory A and the other qubit is in laboratory B. The main idea is after a measurement, they obtain other entangled state

$$|\phi\rangle = \alpha|0\rangle_A \otimes |1\rangle_B + \beta|1\rangle_A \otimes |0\rangle_B . \tag{3.14}$$

Then, A promotes the interaction of its qubit with an ancillary system $|0\rangle$ and obtain

$$\frac{1}{\sqrt{2}} \left(|00\rangle_A \otimes |1\rangle_B + |01\rangle_A \otimes |0\rangle_B \right) . \tag{3.15}$$

It then promotes the following local operations (LO)

$$|00\rangle \quad \rightarrow \quad \alpha|01\rangle + \beta|10\rangle , \tag{3.16}$$

$$|01\rangle \quad \rightarrow \quad \alpha|00\rangle + \beta|11\rangle , \tag{3.17}$$

and obtain

$$\frac{1}{\sqrt{2}} \left[|0\rangle_A \left(\alpha|0\rangle_A \otimes |1\rangle_B + \beta|1\rangle_A \otimes |0\rangle_B \right) + |1\rangle_A \left(\alpha|0\rangle_A \otimes |0\rangle_B + \beta|1\rangle_A \otimes |1\rangle_B \right) \right] . \tag{3.18}$$

In this way, A performs a measurement on its ancillary qubit. If the result $|0\rangle_A$ is found, A communicates laboratory B through a classical communication channel (CC), such as a telephone, that the desired state $|\phi\rangle$, Eq.(3.14), was obtained. Otherwise,

if the result $|1\rangle_A$ is found A communicates B (CC) to apply the local operation σ_x (qubit flip) on your qubit. Thus, the desired state $|\phi\rangle$, Eq.(3.14), is obtained.

Therefore, from this simple example we can see that from an entangled state $|\Phi_+\rangle$, Eq. (3.13), we can create another entangled state $|\phi\rangle$, Eq.(3.14), but at most with the same degree of entanglement of the state that created it. Then, entanglement does not increase under LOCC.

Similarly, the same result can be obtained using Eq.(3.9) and the following Kraus operators

$$\mathcal{E}_1 = p_1 \left(\alpha |0\rangle\langle 0| + \beta |1\rangle\langle 1| \right) \otimes \mathbb{I} \ , \tag{3.19}$$

$$\mathcal{E}_2 = p_2 \left(\alpha |1\rangle\langle 0| + \beta |0\rangle\langle 1| \right) \otimes \left(|1\rangle\langle 0| + |0\rangle\langle 1| \right) \ , \tag{3.20}$$

where $\mathcal{E}_i |\Phi_+\rangle = p_i |\phi\rangle$,and

$$\mathcal{E}_1^\dagger \mathcal{E}_1 + \mathcal{E}_2^\dagger \mathcal{E}_2 = \mathbb{I} \ , \tag{3.21}$$

in such a way that

$$|\phi\rangle\langle\phi| = \mathcal{E}_1 |\Phi_+\rangle\langle\Phi_+| \mathcal{E}_1^\dagger + \mathcal{E}_2 |\Phi_+\rangle\langle\Phi_+| \mathcal{E}_2^\dagger \ . \tag{3.22}$$

Thus, if the initial shared state between A and B is separable, Eq. (3.3), it can be shown that from Eqs. (3.9), (3.19) and (3.20), it is not possible, using only LOCC, obtain an entangled state [35].

- **Maximally entangled states**

The degree of information we can extract from a state in a quantum system is measured by the von Neumann entropy [65]

$$S(\rho) = -\text{Tr}\left[\rho\log\rho\right] \ . \tag{3.23}$$

For a pure state of a bipartite system, ρ_{AB}, the von Neumann entropy $S(\rho_{AB}) = 0$. However, if a state is entangled, the von Neuman entropy of any of the two reduced density operators is nonzero. We can then infer that the entropy of the constituent subsystems of a compound system for certain quantum states may be greater than the entropy of the global system

$$S(\rho_A) > S(\rho_{AB}) \ , \tag{3.24}$$

$$S(\rho_B) > S(\rho_{AB}) \ . \tag{3.25}$$

In addition, this never occurs in a classical domain, strengthening the fact that the physical nature of the entanglement cannot be represented in any classical way. This fact is a consequence of the entagled nature of this states, sumarized in the Schrödinger's observation [4,104,106], in which the knowledge global entangled system does not include the knowledge of its parts.

For pure states, the inequalities above, Eqs. (3.24) and (3.25), are valid if, and only if, ρ_{AB} is entangled. Therefore, one can define the maximally entangled quantum states of two qubits, such as those whose von Neumann entropy, of the reduced density matrices, is maximal, using $S(\rho_A) = S(\rho_B) = 1^5$. This only occurs if ρ_A and ρ_B are maximally mixed states. This class of states comprise the *Bell states* [4,35,65]

$$|\Psi_\pm\rangle = \frac{1}{\sqrt{2}} \left(|00\rangle \pm |11\rangle\right) \ , \tag{3.26}$$

$$|\Phi_\pm\rangle = \frac{1}{\sqrt{2}} \left(|01\rangle \pm |10\rangle\right) \ . \tag{3.27}$$

The Bell states are of great importance, because of their nonlocal characteristics, expressed in violation of Bell's inequality [4, 107, 108], being extremely useful as a fundamental tool for the implementation of several protocols for coding, processing, and distribution of quantum information [110–112].

Finally, the considerations presented in this section show basic characteristics about the nature of entangled states. They also suggest that some entangled states may present a greater degree of entanglement than others. Therefore, a measurement of this degree of entanglement becomes of extremely important for the characterization of this effect in physical systems. In the next section, we will discuss some ways to measure the degree of entanglement of a low dimensional molecular magnetic system.

3.1.2   Detection and Quantification of Entanglement

Entanglement is a physical resource, being used as a tool for processing, coding, and distribution of information in several quantum protocols. Therefore, there is a need to detect and quantify it as well as any physical resource. For pure states, Eqs. (3.24) and (3.25) are a good way to identify entanglement. However, because of the inevitable interaction between the quantum system of interest and the environment (decoherence),

---

[5]This is the normalized value for a maximally entangled state.

we have to work in the most of cases with statistical mixtures of quantum states.

To identify and/or quantify the entanglement of a given quantum state, functions are defined that satisfy the definitions of the separable and entangled states described above. However, it is not easy to know whether states cannot be written as Eq. (3.3) and thereby identify entanglement in the system, due to the fact that a state can be written in several forms in different basis. Despite the rigorous mathematical definition, the characterization and quantification of entanglement is a very complex task in most cases [4,35,65,102,109]. In this context, we present a way to define a separability criteria, which is a tool capable of detecting the presence of entangled states in a physical system.

Separability Criteria

We can establish a separability criteria for mixed states, since we define what are entangled states. A standard approach for determining whether a bipartite mixed state ρ_{AB} is separable is to use completely positive trace preserving (CPTP) map.

A positive map can be defined as a transformation $\Gamma(\rho)$ such that

$$\Gamma(\rho) \geq 0, \ \forall \ \rho \ , \tag{3.28}$$

since ρ is positive by definition[6] [65]. Meanwhile, the transformation $\mathbb{I} \otimes \Gamma$ is not necessarily positive and may have lead to negative eigenvalues.

Let us consider a separable bipartite quantum state ρ_{AB} by applying this transformation:

$$[\mathbb{I} \otimes \Gamma] \left(\rho_{AB} \right) = \sum_i p_i \rho_A^{(i)} \otimes \Gamma(\rho_B^{(i)}) \ . \tag{3.29}$$

By definition

$$\Gamma(\rho_B^{(i)}) \geq 0 \ \Rightarrow \ [\mathbb{I} \otimes \Gamma] \left(\rho_{AB} \right) \geq 0 \ . \tag{3.30}$$

In this way, any separable states must have $[\mathbb{I} \otimes \Gamma] \left(\rho_{AB} \right) \geq 0$[7] whereas entangled states necessarily have

$$[\mathbb{I} \otimes \Gamma] \left(\rho_{AB} \right) < 0 \ . \tag{3.31}$$

---

[6]That is, it does not have negative eigenvalues [65].

[7]This is not a sufficient condition for separability, since entangled states may also satisfy it.

To identify whether any bipartite state ρ_{AB} is separable, it must be shown that all transformations $[\mathbb{I} \otimes \Gamma] (\rho_{AB})$ are positive for all possible maps $\Gamma(\rho_B^{(i)})$. This fact makes it difficult to construct a general way to attest the separability of a quantum state, even for bipartite systems.

Peres-Horodecki Criteria

A fairly widespread completely positive trace preserving (CPTP) map in the literature is the well-known positive partial transposition [113–115]

$$
\begin{aligned}
PPT(\rho_{AB}) &= PPT(\sum_{i,j,k,l} p_{i,j,k,l}|i,j\rangle\langle k,l|) \\
&= \sum_{i,j,k,l} p_{i,j,k,l}|i,l\rangle\langle k,j| \; .
\end{aligned}
\tag{3.32}
$$

For this, we can infer that a bipartite state ρ_{AB} is entangled if

$$
PPT(\rho_{AB}) < 0 \; ,
\tag{3.33}
$$

If an eigenvalue of the matrix that underwent PPD is negative, we can attest the presence of entangled states. Otherwise, the condition

$$
PPT(\rho_{AB}) \geq 0
\tag{3.34}
$$

is insufficient to ensure separability in a general way. Only for Hilbert spaces of $2 \otimes 2$ and $2 \otimes 3$ dimensions is Eq. (3.34) a necessary and sufficient condition of separability [4,113,115]. In the literature, this criterion is also known as the *Peres–Horodecki criterion* [4, 113–116].

For qubits, the most widely used separability criterion is the Peres–Horodecki criterion. Despite this, there are several proposals for separability criteria and many new criteria have been proposed, especially for multipartite systems [117–125].

Entanglement Witness

Although there is no general and definitive understanding of classification and quantification of entanglement in multipartite systems with an arbitrary number of qubits, a useful tool to detect entanglement in a system of arbitrary dimension is the use of observables named *entanglement witnesses* [25, 26, 35, 109, 126, 127].

An entanglement witness W can be understood as a Hermitian operator that acts on the Hilbert space $\mathbb{H}$; it is not positive definite but yields positive expectation values for separable states [25, 26, 35, 109, 126, 127]. As an example, for a mixed separable state,

$$\langle W \rangle_S = \text{Tr}\left(\rho_S W\right) = \sum_i p_i \langle \psi_S | W | \psi_S \rangle \geq 0 \ , \tag{3.35}$$

since any separable mixed state ρ_S can be expressed as a convex sum of projectors onto pure separable states $|\psi_S\rangle$ [25, 26, 28, 35, 109, 126, 127]. It is worth noting that the positive expectation value does not imply the presence of separable quantum states [25, 26, 28, 35, 109, 126, 127]. However, if the given density matrix ρ leads to a negative expectation value, $\text{Tr}\left(\rho W\right) < 0$, then ρ is an entangled state.

We can interpret the entanglement witness under the view of the geometry of quantum states. Let $\boldsymbol{P}$ be the set of all density matrices and let $\boldsymbol{S}$ be a subset of $\boldsymbol{P}$ of all separable density matrices. The entanglement witness can be interpreted geometrically as the operator defining the surface $\boldsymbol{W}$, which separates the state space $\boldsymbol{P}$, as can be seen from Fig. 3.1
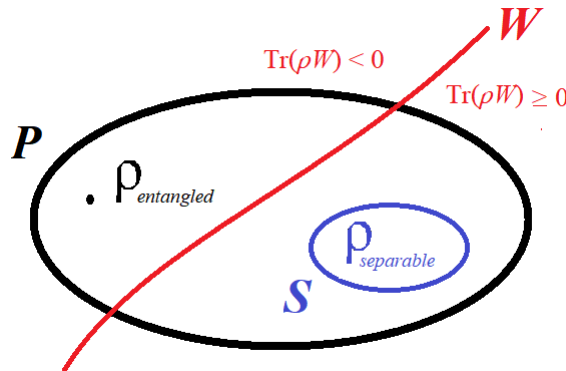
Figure 3.1: Geometric interpretation of an entanglement witness. $\boldsymbol{P}$ is the set of all density matrices (black), $\boldsymbol{S}$ is a subset of all separable density matrices (blue), and $\boldsymbol{W}$ is a surface (red) defined by Eq. (3.35), which separates the state space $\boldsymbol{P}$.

As can be seen, any state ρ at the left side of the surface, whose $\text{Tr}\left(\rho W\right) < 0$, is said entangled, while a state at the right side of the surface, whose $\text{Tr}\left(\rho W\right) \geq 0$, is indistinguishable from this witness. Here it is clear that, for a nonoptimized witness[8], this is a necessary but not sufficient condition of entanglement.

The entanglement witness method is very interesting from the operational

---

[8]Optimized witnesses can be defined as surfaces tangent to $\boldsymbol{S}$.

point of view, since it allows us to relate the presence of entanglement with the measurement of physical properties of the quantum system of interest [9].

Entanglement of Formation

The main idea behind the quantification of entanglement is its usefulness in terms of the processing, distribution, and coding of quantum information. Using entanglement as a resource, we can implement various computational and quantum information protocols. Only detecting the presence of entangled states is not enough—it is necessary to quantify it.

A useful measurement of entanglement is the *entanglement of formation*, $E_F(\rho)$, which can be understood as the amount of quantum pure states needed to create a mixed entangled state [4,34,66,128,129]. In this context, the main idea behind the entanglement of formation consists in thinking of the entanglement in statistical mixtures as being the average of the mixture of pure states [128].

Therefore, the entanglement of formation in a quantum system that is in any quantum state as a convex sum of pure states,

$$\rho_{AB} = \sum_i p_i |\Psi_i\rangle\langle\Psi_i| \ , \tag{3.36}$$

where p_i is the probability distribution, is equal to

$$E_F(\rho_{AB}) = \min_{\mathcal{E}} \sum_i p_i E(|\Psi_i\rangle) \ , \tag{3.37}$$

where the minimum is taken over all ensembles $\mathcal{E} = \{p_i, |\Psi_i\rangle\}$ and achieved for a *particular ensemble* [128].

In this particular ensemble, Eq. (3.37) will be an average. Therefore, the function $E(|\Psi_i\rangle)$ is the von Neumann entropy [65], Eq. (3.23), and, for the reduced density matrix $\rho_A^{(i)}$,

$$S(\rho_A^{(i)}) = -\mathrm{Tr}\left[\rho_A^{(i)} \log_2 \rho_A^{(i)}\right] \ , \tag{3.38}$$

denotes the entanglement of pure states, as mentioned above, with

$$\rho_A^{(i)} = \mathrm{Tr}_B\left[|\Psi_i\rangle\langle\Psi_i|\right] \ , \tag{3.39}$$

---

[9]In the next section, we associate the entanglement witness with a macroscopic property of a molecular magnetic system.

in this way

$$E_F(\rho_{AB}) = \min_{\mathcal{E}} \sum_i p_i \{-\text{Tr}\left[\text{Tr}_B\left[|\Psi_i\rangle\langle\Psi_i|\right]\log_2\left[\text{Tr}_B\left(|\Psi_i\rangle\langle\Psi_i|\right)\right]\right]\} , \qquad (3.40)$$

The minimization makes the definition of entanglement of a mixed state not constructive, so Eq. (3.40) is not easy to calculate in systems with large Hilbert space dimension [4,34,66,128,129]. However, for widespread case of two-qubit systems [4,34,66, 128,129], it was possible to handle successfully all the necessary calculations and derive a more general formula in a closed analytic form [2,4,34,66,128,129].

Let us consider an ensemble of two-qubit systems. The entanglement of formation, Eq. (3.40), is determined from the minimum number of maximally entangled pairs that are necessary to create a given state ρ_{AB} by using LOCC [34,66]. The entanglement of formation has the analytical solution

$$E_F(\rho_{AB}) = \lambda_+\log_2(\lambda_+) + \lambda_-\log_2(\lambda_-) , \qquad (3.41)$$

where $\lambda_\pm$ are the eigenvalues of the reduced density matrix $\rho_A^{(i)}$, Eq.(3.39), from the $\{p_i,|\Psi_i\rangle\}$ that minimizes Eq. (3.37).

Wootters [128] defined the *concurrence* to help calculate Eq. (3.40). The concurrence is related to similarity between a state and its qubit flip[10], defined as

$$\bar{\rho} = (\sigma_y \otimes \sigma_y)\rho^*(\sigma_y \otimes \sigma_y) \qquad (3.42)$$

where σ_y is the y-Pauli matrix [65] and where ρ^* is the complex conjugate of ρ. The qubit flip transformation is introduced primarily to handle mixed states. This foundation is also convenient for expressing the entanglement of a pure state of our special case of two qubits [128].

Therefore, performing some calculations[11], we found the concurrence as

$$\mathbb{C} = \max\left\{0, \sqrt{\lambda_1} - \sqrt{\lambda_2} - \sqrt{\lambda_3} - \sqrt{\lambda_4}\right\} , \qquad (3.43)$$

with λ_i being ($\lambda_1 \geq \lambda_2 \geq \lambda_3 \geq \lambda_4 \geq 0$) the eigenvalues of the matrix

$$R = \rho(\sigma_y \otimes \sigma_y)\rho^*(\sigma_y \otimes \sigma_y) . \qquad (3.44)$$

---

[10]Mathematically, this inversion operation can be done by any operator that only contains elements in the secondary diagonal; by convention we adopt σ_y.

[11]This calculation is not simple and its formal proof goes beyond the objectives of this text. More details can be found in Ref. [128].

Due to the fact that the product of Hermitian matrices is, in general, a non-Hermitian matrix, the matrix R is non-Hermitian, in general.

With the aid of concurrence, Eq. (3.43), we can express the entanglement of formation as

$$\mathbb{E} = -\mathbb{E}_+ - \mathbb{E}_- \tag{3.45}$$

where

$$\mathbb{E}_\pm = \frac{1 \pm \sqrt{1 - \mathbb{C}^2}}{2} \log_2 \left(\frac{1 \pm \sqrt{1 - \mathbb{C}^2}}{2} \right) \tag{3.46}$$

Therefore, through the concurrence we also obtain the entanglement of formation, where Eqs. (3.45) and (3.46) are the famous result for the entanglement of formation obtained by Wootters [128]. At this point of the text, we have obtained how to detect and quantify the entanglement in a quantum system. Now, we will apply what we have hitherto seen to the quantum systems of interest of this thesis, the low-dimensional molecular magnetic systems.

3.1.3   Thermal Entanglement

Until a few years ago, it was thought that quantum entanglement is fragile and can easily vanish through the inevitable interaction of the system with its environment [130] because of decoherence, i.e., the loss of quantum properties in macroscopic systems, and, because of this condition, it was thought that entanglement could only exist in microscopic systems. In 2003, Ghosh *et al.* [131] proved that larger systems can also remain entangled. Through the measurement of magnetic susceptibility they found that bulk lithium fluoride salt, in an external magnetic field, formed a hugely entangled system [131].

Nowadays, recent demonstrations have shown that quantum entanglement can be measured by the thermodynamic properties of solids, such as magnetic susceptibility [2, 25, 27–29, 34, 66, 132], internal energy [34, 66, 132], specific heat [34, 66], and even neutron scattering data [12, 24]. Therefore, quantum entanglement can be related to significant material properties, allowing the measurement and control of quantum properties of solid state systems by means of material engineering. Consequently, the design of novel materials becomes an actual challenge to overcome.

In this direction, molecular magnets can provide an excellent opportunity to

achieve this goal as prototype materials for quantum information technology. They combine classical properties, found in any macroscopic magnet, with quantum ones, such as quantum interference and entanglement. The large gap between the ground state and the first-excited state found in some materials allows the existence of entangled quantum states at higher temperatures [25, 28, 29, 133]. Recently, several works have shown that *thermal entanglement* [2, 25, 27–29, 34, 66, 132] can exist in solid state systems and remain at relatively high temperatures [2, 28, 29].

Let us address thermal entanglement in a molecular magnetic system through canonical formalism. In this case, the system is in contact with a thermal reservoir. We fix the external parameters of the problem and the variable energy

$$E = \mathrm{Tr}\left(\rho\mathcal{H}\right) \ , \tag{3.47}$$

is a statistical average of the Hamiltonian $\mathcal{H}$. From the definition

$$\mathrm{Tr}\left(\rho\right) = 1 \ , \tag{3.48}$$

the von Neumann entropy [65], Eq. (3.23), can be rewritten with these two bounds, Eqs. (3.47) and (3.48), using, for this, the Lagrange multipliers α and β, as

$$S(\rho) = -\mathrm{Tr}\left[\rho\mathrm{log}_2\rho\right] + \alpha\left[1 - \mathrm{Tr}\left(\rho\right)\right] + \alpha\left[E - \mathrm{Tr}\left(\rho\mathcal{H}\right)\right] \ , \tag{3.49}$$

in whichc we are only adding zero to the entropy.

Maximizing in relation to ρ gives

$$\frac{\mathrm{d}S(\rho)}{\mathrm{d}\rho} = 0 \ , \tag{3.50}$$

and applying Eq. (3.48) we find that the density matrix of a system in thermal equilibrium has the Gibbs form [2, 23, 34, 66]

$$\rho \ = \ \frac{e^{-\mathcal{H}/k_B T}}{Z} \tag{3.51}$$

$$= \ \frac{1}{Z}\left(e^{-E_0/k_B T}|E_0\rangle\langle E_0| + \sum_{i=1}^{N-1} e^{-E_i/k_B T}|E_i\rangle\langle E_i|\right) \ , \tag{3.52}$$

E_i are the energy eigenvalues and

$$Z = \mathrm{Tr}\{e^{-\mathcal{H}/k_B T}\} \tag{3.53}$$

is the canonical partition function. Therefore, if it is not possible to write this density matrix like that in Eq. (3.3), we can say that this system exhibits entanglement; otherwise, the system is separable [4, 35, 65, 102, 109].

As an example, let us consider a system consisting of two isotropically coupled spin-1/2 particles as a Heisenberg dimer in a d^9 electronic configuration in thermodynamic equilibrium. This system is ruled by a Heisenberg Hamiltonian $\mathcal{H} = -J\vec{S}_1 \cdot \vec{S}_2$ [16, 23], where J is the magnetic coupling constant [23]. The density matrix of the system under consideration also has the Gibbs form, Eq. (3.52). It can be written on the Bell's diagonal mixed state in the computational basis $\{|00\rangle, |01\rangle, |10\rangle, |11\rangle\}$ [34, 66] as

$$
\begin{aligned}
\rho(T) &= \frac{1}{4}
\begin{bmatrix}
1 + c(T) & 0 & 0 & 0 \\
0 & 1 - c(T) & 2c(T) & 0 \\
0 & 2c(T) & 1 - c(T) & 0 \\
0 & 0 & 0 & 1 + c(T)
\end{bmatrix} \\
&= \frac{1}{4}(1 + c(T)\vec{S}_1 \otimes \vec{S}_2) ,
\end{aligned}
\tag{3.54}
$$

where

$$
c(T) = \langle \vec{S}_A^{(\alpha)} \otimes \vec{S}_B^{(\alpha)} \rangle = -1 + \frac{4}{3 + e^{-J/k_B T}} ,
\tag{3.55}
$$

is the pairwise correlation function and $\alpha = \{x, y, z\}$. The pairwise correlation function assumes values from -1 to 0 for antiparallel coupling ($J < 0$) between the spins and values of 0 to $1/3$ for parallel coupling ($J > 0$).

As calculated in Refs. [2, 23, 34, 47, 66], this system satisfies the Bleaney–Bowers equation [23, 47] [23, 47]

$$
\chi(T) = \frac{2N(g\mu_B)^2}{k_B T} \frac{1}{3 + e^{-J/k_B T}} .
\tag{3.56}
$$

Thus, it is possible to write the pairwise correlation function of the Heisenberg dimer as a function of its magnetic susceptibility at finite temperature [2, 34, 66]:

$$
c(T) = \frac{2k_B T}{N(g\mu_B)^2}\chi(T) - 1 ,
\tag{3.57}
$$

thus associating the pairwise correlation function to the macroscopic physical properties of a solid state system.

Therefore, since we can calculate the density matrix, Eq. (3.54) in terms of magnetic susceptibility, using Eq. (3.57), we can associate the entanglement quantifiers presented in the previous section with a thermodynamic quantity of a macroscopic material, such as magnetic susceptibility. In the following we present an entanglement witness based on the measurement of magnetic susceptibility and the entanglement of formation as a function of magnetic susceptibility.

Thermal Entanglement Witness

As mentioned before in Section 3.1.2, the entanglement witness can tell whether, for the condition given by Eq. (3.35), a given quantum system is entangled. If Eq. (3.35) is violated, the system's state is entangled; otherwise, if Eq. (3.35) is satisfied, we cannot state with certainty that the system's state is separable.

Several thermodynamic quantities, such as internal energy [127,134–136], magnetization, and heat capacity [137], have been proposed as an entanglement witness, but they depend on the complete knowledge of the specific macroscopic model that describes the quantum system and they are not usually directly measurable quantities. Fortunately, as has been shown by Wieśniak, Vedral and Brukner, from a theoretical point of view, the magnetic susceptibility of a condensed matter system can reveal thermal spin entanglement between the constituents of a solid as an entanglement witness [36].

This witness is directly measured and can be applicable, *a priori*, without the full knowledge of the Hamiltonian model that describes the macroscopic properties of the condensed matter system of interest or the dimensionality of the Hilbert space associated with the quantum system.

First, let us consider a magnetic system, whose total Hamiltonian can be given by

$$\mathcal{H} = \mathcal{H}_0 + \mathcal{H}_1 \ , \tag{3.58}$$

where $\mathcal{H}_0$ is the spin Hamiltonian and $\mathcal{H}_1$ is the Zeeman interaction [23] of each spin,

$$\mathcal{H}_1 = g\mu_B B \sum_i S_z^i \ . \tag{3.59}$$

Given the bound $[\mathcal{H}_0, \mathcal{H}_1] = 0$, the Hamiltonian model H_0 that describes the magnetic behavior of our magnetic system has to commute with the S_z component of spin [25,28,36]. Then the magnetic susceptibility can be written in terms of the correlation functions $\langle S_\alpha^i S_\alpha^j \rangle$ as

$$\chi_\alpha \ = \ \frac{(g\mu_B)^2}{k_B T} \Delta^2(M_\alpha) \tag{3.60}$$

$$= \ \frac{(g\mu_B)^2}{k_B T} \left(\sum_{i,j}^{N} \langle S_\alpha^i S_\alpha^j \rangle + \langle \sum_i^N S_\alpha^i \rangle^2 \right) \tag{3.61}$$

where g is the Landé factor, μ_B is the Bohr magneton and $\Delta^2 M_\alpha$ is the variance of the magnetization and $\alpha = \{x, y, z\}$ specify the spin direction.

For any separable state given by Eq. (3.3), one finds that

$$
\begin{aligned}
\chi(T) &= \chi_x + \chi_y + \chi_z \\
&= \frac{(g\mu_B)^2}{k_B T} \left(\Delta^2 M_x + \Delta^2 M_y + \Delta^2 M_z \right)
\end{aligned}
\tag{3.62}
$$

For an arbitrary state of a spin-S particle, the relations

$$
\langle S_x^2 \rangle + \langle S_y^2 \rangle + \langle S_z^2 \rangle = S(S+1)
\tag{3.63}
$$

$$
\langle S_x \rangle^2 + \langle S_y \rangle^2 + \langle S_z \rangle^2 \leq S^2
\tag{3.64}
$$

are valid [28, 36, 138], since the projection of the spin in any direction cannot be higher than S. Taking the difference between Eqs. (3.63) and (3.64) gives

$$
\Delta^2 S = \Delta^2 S_x + \Delta^2 S_y + \Delta^2 S_z \geq S \ .
\tag{3.65}
$$

If the thermal state was actually a product one of N spins, the variance of magnetization would be the sum of variances of individual spins [36]

$$
\begin{aligned}
\chi(T) &= \frac{(g\mu_B)^2}{k_B T} \sum_n p_n \sum_i^N \left((\Delta^2 S_x)_i^n + (\Delta^2 S_y)_i^n + (\Delta^2 S_z)_i^n \right) \ , \\
&= \frac{(g\mu_B)^2}{k_B T} \sum_n p_n \Delta^2 S_i^n \ , \\
&\geq \frac{(g\mu_B)^2 N S}{k_B T} \ .
\end{aligned}
\tag{3.66}
$$

where this bound is also valid in the general case of separable states [36].

Finally, the magnetic susceptibility is an entanglement witness due to the fact that separable states can not violate the relation in Eq. (3.35). For isotropic systems, where $\chi_x = \chi_y = \chi_z$, one can define the entanglement witness based in a thermodynamical observable:

$$
\langle W \rangle = \frac{3 k_B T \overline{\chi}(T)}{(g\mu_B)^2 N S} - 1 \ ,
\tag{3.67}
$$

where there must be entangled states if $\langle W \rangle < 0$ [25, 26, 28, 35, 109, 126, 127]. With $\langle W \rangle$ obtained from the measurement of the magnetic susceptibility we can identify the presence of entanglement in molecular magnetic systems, establishing a solid relationship between a quantum entanglement observer and the macroscopic properties of a condensed matter system.

Thermal Entanglement of Formation

Let us consider our molecular magnetic system (isotropically coupled spin-1/2 pairs) at thermal equilibrium, described by the canonical ensemble, Eq. (3.52), ruled by the Hamiltonian $\mathcal{H}$ that exhibits invariance under π rotation around a given spin axis ($\mathbb{Z}_2$ symmetry) [16, 23][12], with the partition function $\mathcal{Z} = \text{Tr}(e^{-\mathcal{H}/k_B T})$. The two-spins' reduced density matrix at sites labeled by A and B in the computational basis $\{|00\rangle, |01\rangle, |10\rangle, |11\rangle\}$ will be given by an X-shaped mixed state:

$$\rho_{AB} = \begin{pmatrix} \rho_{11} & & & \rho_{14} \\ & \rho_{22} & \rho_{23} & \\ & \rho_{23}^* & \rho_{33} & \\ \rho_{14}^* & & & \rho_{44} \end{pmatrix}. \tag{3.68}$$

The concurrence has the analytical solution

$$\mathbb{C} = \max\left\{0, |\rho_{23}| - \sqrt{\rho_{11}\rho_{44}}, |\rho_{14}| - \sqrt{\rho_{22}\rho_{33}}\right\}. \tag{3.69}$$

Therefore, by using Eq. (3.69) the entanglement of formation is calculated with the aid of concurrence using Eq. (3.45).

As an example, let us consider the main system of this thesis, an isotropically coupled pair of spin-1/2 particles ruled by a Heisenberg Hamiltonian $\mathcal{H} = -J\vec{S}_1 \cdot \vec{S}_2$. The density matrix of the system under consideration can be written on the Bell's diagonal mixed state in the computational basis, Eq. (3.54), as a function of the magnetic susceptibility of this system satisfying the Bleaney–Bowers equation [23, 47]:

$$\chi(T) = \frac{2N(g\mu_B)^2}{k_B T} \frac{1}{3 + e^{-J/k_B T}} \tag{3.70}$$

where g is the Landé factor, μ_B is the Bohr magneton, k_B is the Boltzmann constant, and N is the number of dimers. Therefore, it is possible to write the pairwise correlation function of the Heisenberg dimer as a function of its magnetic susceptibility at finite temperature .

To quantify the amount of entanglement in this spin system, the concurrence [65, 128, 129] of this molecular magnetic system is written as a function of the magnetic

---

[12]A number of spin models are enclosed within these requirements, e.g., the Heisenberg models [23].

susceptibility as [2, 34, 66]

$$\mathbb{C} = \begin{cases} -\frac{1}{2}\left[2 + 3\frac{2k_B T}{N(g\mu_B)^2}\chi(T)\right] & T < T_t \\[2em] 0 & T \geq T_e \end{cases} \tag{3.71}$$

where

$$T_t \approx 0.91|J|/k_B \tag{3.72}$$

is the threshold temperature of entanglement, the maximum temperature below which there is entanglement in the system [25, 28].

Replacing Eq. (3.71) in Eq. (3.45) we obtain the entanglement of formation for a set of isotropically coupled pairs of spin-1/2. A molecular magnetic system in a d^9 electronic configuration, ruled by a Heisenberg Hamiltonian and therefore an ideal realization of a two-qubit system

$$\mathbb{E} = -\mathbb{E}_+ - \mathbb{E}_- \tag{3.73}$$

$$\mathbb{E}_\pm = \frac{1 \pm \sqrt{1 - \frac{1}{4}\left[2 + 3\frac{2k_B T}{N(g\mu_B)^2}\chi(T)\right]^2}}{2} \times$$

$$\times \log_2\left(\frac{1 \pm \sqrt{1 - \frac{1}{4}\left[2 + 3\frac{2k_B T}{N(g\mu_B)^2}\chi(T)\right]^2}}{2}\right) \qquad T < T_t \tag{3.74}$$

and zero otherwise. Therefore, using Eq. (3.74), we quantify the amount of entanglement in a condensed matter system by the measurement of its macroscopic properties.

3.2   Quantum Discord

The boundaries between the quantum and classical nature of pure quantum states are solidly established through Bell's inequality [4, 107, 108]. However, when it comes to statistical mixtures, this applicability is not straightforward. In the 1990s, it was widely believed that the states are classically correlated only when they are separable [66]. Therefore, the existence of genuinely quantum correlations was usually inferred by the presence of entanglement among the parts of the systems [16]. Nowadays, it is understood that, although quantum entanglement provides a way to determine pure quantum correlations, it does not encompass all quantum correlations of the system [2, 5–

$8, 10, 11, 14$–$16, 19, 34, 66, 102, 139$–$148]$ and the measure of quantum excess of correlations has been termed *quantum discord* $[9, 10, 149]$.

In 2000, Zurek greatly expanded the notion of quantum correlations by introducing the concept of quantum discord a good indicator of the quantum nature of the correlations [9]. In 2001, Henderson and Vedral, independently, analyzed the correlations in a bipartite system, suggesting, from the theory of measurement, a way to separate purely classical and quantum correlations [10]. Hence, the study of quantum discord has been attracting considerable attention owing to its important role in many quantum information processes even when entanglement is absent $[2, 16, 34, 66, 150$–$152]$, showing that quantum entanglement does not encompass all possible quantum correlations in a system. Using the model of deterministic quantum computation with one qubit [153], Datta demonstrated, in 2008 [17], that a quantum processor can be built over mixed states by using quantum correlations, measured by the entropic quantum discord, in the absence of entanglement.

3.2.1 Mutual Information

The concept of correlations, like information of one system about another, is a key feature in condensed matter systems $[9, 10, 16, 149]$. In a physical viewpoint, system's properties can be strongly affected by the correlations among the constituents of the system, leading to remarkable phenomena, i.e., quantum phase transitions $[9, 10, 16, 149]$.

In statistics, correlation can be interpreted by the dependence or association in any mathematical viewpoint between two random variables. The amount of correlation between two sets of random variables X and Y with probability distribution function $p(x,y)$, with $x \in X$ and $y \in Y$, is measured by the covariance (correlation moment):

$$\mathcal{C}(X,Y) = \langle (X - \langle X \rangle)(Y - \langle Y \rangle) \rangle \, . \tag{3.75}$$

Another reliable measurement of the correlation between two sets of random variables X and Y is the the Pearson correlation coefficient [154]

$$R_{XY} = \frac{\mathcal{C}(X,X)}{\Delta_X \Delta_Y} \, , \tag{3.76}$$

where Δ_X and Δ_Y are the standard deviation of X and Y, respectively. The standard

deviation defined as

$$\Delta_X = \sqrt{\frac{\sum_{i=i}^{N}(x_i - \bar{X})^2}{N-1}} \qquad (3.77)$$

is a measurement of the amount of variation or dispersion of a set of random variables X and Y, which indicates that the distribution tends to be close to the average of the set (low standard deviation) and how the distribution is spread out over a wide range of values [155].

However, in a informational point of view, it is well known that the disappearance of the covariance, Eq.(3.75), or correlation coefficient, Eq.(3.76), does not necessarily mean that random variables are independent, $p(x,y) = p(x)p(y)$; in other words, the vanishing of the quantities is not a sufficient condition for the informational independence of X and Y [65]. In order to quantify the information content of a set of random variable X, related to the information content of other set of random variable Y, let us introduce the concept of *mutual information.*

From classical information theory, the information obtained after knowing the value of a random variable X, which takes values within a set of probabilities $\{p_x\}$, with $x \in X$, is quantified by its Shannon entropy

$$H(X,Y) = -\sum_x p_x \log p_x \ . \qquad (3.78)$$

Therefore, the Shannon entropy quantifies, on average, the information produced by a stochastic source of data X [65].

In this context, taking two random variables X and Y, we can measure the correlation between them by their mutual information [9, 10, 16, 149]

$$\mathcal{I}(X:Y) = H(X) + H(Y) - H(X,Y) \ , \qquad (3.79)$$

where

$$H(X,Y) = -\sum_{x,y} p_{xy} \log p_{xy} \ . \qquad (3.80)$$

is the joint Shannon entropy for X and Y.

It is worth noting that, $\mathcal{I}(X:Y) \geq 0$, due to this fact, in contrast to the covariance, Eq.(3.75), or correlation coefficient, Eq.(3.76), the vanishing of the mutual information, $\mathcal{I}(X:Y) = 0$, is a necessary and suficient condition for the informational independence of X and Y [65,66]. Due to this fact, we can use the mutual information,

Eq.(3.79), as a reliable measurement of correlation between two physical systems X and Y

Using Beyes rule [66, 156], well known in probability theory, we introduce the conditional entropy

$$H(X|Y) = H(X,Y) - H(Y) \; , \tag{3.81}$$

which quantifies, on average, the ignorance about the value of a random variable X given that Y is known. The mutual information, Eq. (3.79), can be written as

$$\mathcal{I}(X : Y) = H(X) - H(X|Y) \; . \tag{3.82}$$

Therefore, the mutual information can be understood as the ignorance about the system that remains after the information about it has been extracted from another system [66].

In statistical physics and quantum mechanics, the mean values of certain dynamic variables (system correlation functions) are of great interest. The correlation functions are directly measurable quantities (i.e., in scattering experiments). Knowledge of the correlation functions allows us to find different macroscopic characteristics of physical systems such as magnetic susceptibility, specific heat, internal energy, and magnetization. In this section, we aim to discuss in more detail that quantum correlations can be directly associated with macroscopic characteristics of solid state systems through the usual statistical correlations. Through the formalism of the density matrix, the elements of the density matrix bring us information about the correlations between the systems that make up the statistical ensemble that describes the state of the physical system of interest.

3.2.2   Entropic Quantum Discord

The main aspect behind the description of genuinely quantum correlations consists in splitting its nature into classical aspects and quantum ones. Mutual information of the two subsystems can be used as a measure of full correlations. To generalize the Eqs. (3.79)-(3.82) to quantum theory, we replace the classical probability distributions by density matrices. Thus, quantum mutual information can be defined as

$$\mathcal{I}(\rho_A : \rho_B) = S(\rho_A) - S(\rho_A|\rho_B) \tag{3.83}$$

where

$$S(\rho) = -\mathrm{Tr}\left[\rho \log_2 \rho\right] \; , \tag{3.84}$$

is the von Neumann entropy, ρ_{AB} is the density matrix of the composite system $AB = A \cup B$, with ρ_A and ρ_B being the reduced density matrices for the subsystems A and B, respectively, and

$$S(\rho_A|\rho_B) = S(\rho_{AB}) - S(\rho_B) \; , \tag{3.85}$$

is the quantum generalization of the conditional entropy, Eq. (3.81).

Consider a measurement performed locally only on part B, described by a set of positive-operator-valued measurements (POVMs)[13] $\{B_k\}$. The state of the quantum system conditioned on the measurement of outcome k can be written as

$$\rho_k = (\mathbb{I}_A \otimes B_k)\rho(\mathbb{I}_A \otimes B_k)/p_k \tag{3.86}$$

where

$$p_k = \text{Tr}\left[(\mathbb{I}_A \otimes B_k)\rho(\mathbb{I}_A \otimes B_k)\right] \tag{3.87}$$

is the probability of obtaining outcome k.

The conditional density operator, Eq. (3.86), allows an alternative definition of the quantum conditional entropy:

$$S(\rho_A|\{B_k\}) = \sum_k p_k S\left(\rho_k\right) \; . \tag{3.88}$$

Quantum mutual information, Eq. (3.83), can thus be alternatively defined as

$$J(\rho_A : \{B_k\}) = S(\rho_A) - S(\rho_A|\{B_k\}) \; . \tag{3.89}$$

Eq. (3.83) and (3.89) are equivalents for a set of states

$$\xi_{AB} = \sum_{i,j} p_{i,j} \Pi_A^{\{i\}} \otimes \Pi_B^{\{j\}} \; , \tag{3.90}$$

where $p_{i,j}$ is the joint probability and the reduced density matrices of systems A and B are described in terms of the set of orthogonal projectors $Pi_A^{\{i\}}$ and $\Pi_b^{\{j\}}$ of each subsystem, respectively. In other words, a local observable associated with these projectors could be measured without being disturbed. In this way, we can then define a set ω_{cc} of states, where a local measurement in any state $\xi_{AB} \in \omega_{cc}$ is done without disturbing the system, so we call this state classical–classical (cc). However, this is completely different in the

[13]A POVM is a measure whose values are positive self-join operators over the associated Hilbert space. Therefore, it is a very general measurement formulation in quantum mechanics and quite useful in quantum information theory. A more complete explanation can be found in Ref. [65].

quantum scenario, due to the quantum effects on the correlation between subsystems A and B. Therefore, this difference provides a measurement for the quantumness of the correlations, which has been called quantum discord [9, 10, 16, 149].

Quantum mutual information, which is the information theoretical measure of the total correlation in a quantum system, can be divided into the quantum part $\mathcal{Q}$ and the classical ones $\mathcal{C}(\rho_{AB})$ [2, 9–18, 148, 157], where the classical correlation of the composite system ρ_{AB} is defined as

$$\mathcal{C}(\rho_{AB}) = \max\left[J(\rho_A : \{B_k\})\right] \tag{3.91}$$

where the maximum is taken over all POVMs $\{B_k\}$ performed locally only on subsystem B, with the conditional state and the probability p_k of obtaining outcome k [2, 9–18].

Quantum discord can then be introduced as an entropic measurement of genuinely quantum correlations in a quantum state, defined as the difference between the total and the classical correlation,

$$\mathcal{Q}(\rho_{AB}) = \mathcal{I}(\rho_A : \rho_B) - \mathcal{C}(\rho_{AB}) , \tag{3.92}$$

where this difference is due to the quantum nature effects on the correlation between the subsystems A and B.

Therefore, a reliable discord-like quantifier, Eq. (3.92), is defined by the following properties:

- $\mathbb{Q}(\rho_{AB})$ is positive

$$\mathbb{Q}(\rho_{AB}) \geq 0 \; \forall \; \rho_{AB} . \tag{3.93}$$

- $\mathbb{Q}(\rho_{AB}) = 0$ if, and only if $\rho \in \omega_{cc}$.

- $\mathbb{Q}(\rho_{AB})$ is invariant on local unit transformations $\{U_A, U_B\}$:

$$\mathbb{Q}\left([U_A \otimes U_B]\, \rho_{AB}\, [U_A \otimes U_B]^\dagger\right) = \mathbb{Q}(\rho_{AB}) . \tag{3.94}$$

- $\mathbb{Q}(\rho_{AB})$ is decreasing and monotonic under any local transformations $\Gamma(\rho_{A(B)})$ that preserve local commutativity:

$$\left[\Gamma(\rho_{A(B)}), \Gamma(\xi_{A(B)})\right] = 0 \iff \left[\rho_{A(B)}, \xi_{A(B)}\right] = 0 . \tag{3.95}$$

- $\mathbb{Q}(\rho_{AB})$ is a convex function

$$\sum_i p_i \mathbb{Q}(\rho_{AB}^{(i)}) \geq \mathbb{Q}\left(\sum_i p_i \rho_{AB}^{(i)}\right) \tag{3.96}$$

• For any set of pure states, $\mathbb{Q}(\rho_{AB})$ is reduced to an entanglement measurement.

Therefore, a zero discord state ρ_{AB} is achieved if $\rho_{AB} \in \omega_{cc}$. Consequently, the states can be measured with maximal precision, without disturbing the quantum system. This fact was recently explored from an experimental point of view by Girolami [5, 7, 158, 159], which relies on discord-type quantum correlations with a metrological interpretation in a black-box quantum phase estimation paradigm. The discord of a quantum state guarantees that the minimum precision can be obtained by using this state in a metrological configuration of phase estimation, providing a strong indication that states with nonzero quantum discord play a central role in the context of quantum metrology.

3.2.3   Geometric Quantum Discord

The analytical maximization over POVM's, Eq. (3.91), involved in the entropic measurements of quantum discord, Eq. (3.92), is a hard task even for a two-qubit system [9–11, 157]. Computing entropic quantum discord (and a large class of entropic measurements including entanglement of formation) is an NP-complet problem even for bipartite mixed states [21][14]. Therefore, the problem of computing entropic measurements of quantum discord is computationally intractable [21]. The execution time of any algorithm for quantum discord computation grows exponentially with the Hilbert space dimension, making the computation of quantum discord in a quantum system of moderate size not possible in practice [21].

Consequently, there are only a few results for the analytical expression of entropic quantum discord, and only for certain classes of states are exact solutions known [11, 13–17, 160]. Numerous quantifiers of quantum correlations have been proposed [5, 7, 11, 13–19, 142, 157–166], especially quantifiers based on geometric arguments [15, 18, 19, 142, 157, 159, 161–166].

A reliable geometric-based discord-like quantifier can be built by employing a general distance measurement $D(\rho, \rho_{cq})$, which is a metric used to measure how far the

---

[14]In computational complexity theory, an NP-complete problem belongs to nondeterministic polynomial time (NP) complexity classes, whose solutions can be verified in polynomial time.

state under investigation ρ is from the closest *classical–quantum* state [19] ρ_{cq}, given by

$$\zeta = \sum_k p_k \Pi_A^{\{k\}} \otimes \zeta_B^{\{k\}}, \tag{3.97}$$

with $0 \leq p_k \leq 1$ and $\sum_k p_k = 1$; $\{\Pi_A^{\{k\}}\}$ being a set of orthogonal projectors for subsystem A, and $\zeta_B^{\{k\}}$ being a reduced density operator for subsystem B [18].

Geometric quantum discord can be defined as a measurement of the amount of quantum correlations in a quantum state in terms of its minimal distance from the set ω_{cq} of closest classical–quantum states ζ, Eq. (3.97) [2, 18]. Therefore, geometric quantum discord can be expressed as

$$\mathbb{Q}_G(\rho) = \min_{\omega_{cq}} D(\rho, \zeta) \tag{3.98}$$

We can interpret $D(\rho, \zeta)$ under the view of the geometry of quantum states, as can be seen from Fig. 3.2. Let $\boldsymbol{P}$ be the set of all density matrices and let ω_{cq} be a subset of $\boldsymbol{P}$ of all closest classical–quantum states ζ, Eq. (3.97). The geometric quantum discord is the minimal distance between ρ and ζ.
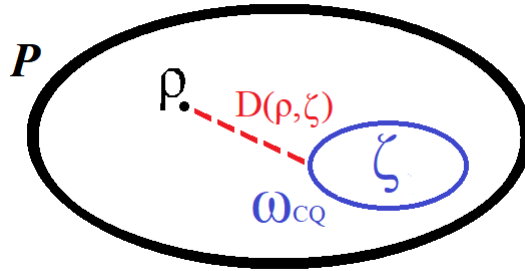

Figure 3.2: Schematic representation of a measure of quantum discord based on a measurement of distance $D(\rho, \zeta)$.

Since the geometric quantifier of quantum discord $\mathbb{Q}_G(\rho)$, Eq. (3.98), depends on the choice of the metric $D(\rho, \zeta)$, it must satisfy some conditions so that $\mathbb{Q}_G(\rho)$ can be considered a reliable discord-like quantifier.

- $D(\rho, \zeta)$ must be monotonic under any Completely Positive and Trace Preserving map $\Gamma(\rho)$:

$$D(\rho, \zeta) \geq D\left[\Gamma(\rho), \Gamma(\zeta)\right] . \tag{3.99}$$

A map $\Gamma(\rho)$ is defined as positive if, and only if

$$\rho \to \Gamma(\rho) = \sum_i E_i \rho E_i^\dagger . \tag{3.100}$$

where $\{E_i\}$ are the set of Krauss operators [65] with $\sum_i E_i E_i^\dagger = \mathbb{I}$, which leads to the trace-preserving and completely positive map if $[\mathbb{I} \otimes \Gamma] \, (\rho) \geq 0$. Thus, $[\Gamma(\rho)]^\dagger = \Gamma(\rho)$ and $\text{Tr} \, [\Gamma(\rho)] = 1$.

- $D(\rho,\zeta)$ must be invariant under transposition:

$$D(\rho,\zeta) = D(\rho^T,\zeta^T) \ . \tag{3.101}$$

Despite its remarkable features, geometric discord is known to be sensitive to the choice of distance measures; given a chosen metric $D(\rho,\zeta)$, the nearest classical state will be determined. Hereafter, we list some of the main metrics used in the literature for the geometric measurement of quantum correlations.

Relative Entropy

Relative entropy is a useful quantifier, especially in classical information theory, as a measure of the distance between two probability distributions. In the context of quantum information theory, relative entropy appears as a metric option for the measurement of geometric correlations:

$$\mathbb{Q}_G(\rho) = \min_{\omega_{cq}} D(\rho,\zeta) = \min_{\omega_{cq}} S(\rho\|\zeta) = \min_{\omega_{cq}} \text{Tr} \, [\rho\ln(\rho) - \rho\ln(\zeta)] \ . \tag{3.102}$$

Nonetheless, strictly speaking, relative entropy $S(\rho\|\zeta)$ is not a mathematical metric, since it is not a symmetric function.

Bures Metric

In quantum information geometry, the Bures metric[15] [168, 169] (or Helstrom metric [169]) defines a distance measurement between a density matrix ρ and the set of classical–quantum states:

$$\mathbb{Q}_G(\rho) = \min_{\omega_{cq}} D_B(\rho,\zeta) = \min_{\omega_{cq}} \left[2 - 2\sqrt{F(\rho,\zeta)} \right] \ , \tag{3.103}$$

where

$$F(\rho,\zeta) = \{\text{Tr} \, [\sqrt{\rho}\zeta\sqrt{\rho}]^{\frac{1}{2}}\}^2 \tag{3.104}$$

is the *Fidelity* [170–172]. However, the Bures metric does not reduce to a measure of entanglement for pure states, not being considered a reliable quantifier of quantum discord.

---

[15]It can be seen as a quantum generalization of the Fisher information metric [158, 167] and is reduced to the Fubini–Study [167] metric when restricted to pure states.

Hilbert-Schmidt Norm

The Hilbert–Schmidt norm (or Schatten 2-norm) is a metric based on the distance from a given quantum state ρ to the closest classical–quantum state ζ, Eq. (3.97), and can be expressed as

$$\mathcal{Q}_G(\rho) = \min_{\omega_{cq}} D_{HS}(\rho,\zeta) = \min_{\omega_{cq}} \|\rho - \zeta\|_2^2 \tag{3.105}$$

where $\|X\|_2 = \sqrt{\mathrm{Tr}\left[X^\dagger X\right]}$ is the Hilbert-Schmidt Norm.

As pointed out in Refs. [150, 163, 173], the geometric discord based on the Hilbert–Schmidt norm[16] [19] cannot be regarded as a good measure for the quantumness of correlations, because it may increase under local operations on the unmeasured sub-system B [162], whose reduced density matrix is written in terms of the set of orthogonal projectors $Pi_A^{\{i\}}$ and $\Pi_b^{\{j\}}$. This leads us to the creation of quantum discord in a reversible way, without cost to the total correlation of the system [163].

Schatten 1-norm

On the other hand, geometric quantum discord based on the Schatten 1-norm is a well-defined measurement of the amount of quantum correlations of a state in terms of its minimal distance from the set ω_{cq} of classical states [18, 162]. Geometric quantum discord can then be expressed as

$$\mathcal{Q}_G(\rho) = \min_{\omega_{cq}} \|\rho - \rho_c\| \tag{3.106}$$

where $\|X\|_1 = \mathrm{Tr}\left[\sqrt{X^\dagger X}\right]$ is the 1-norm, ρ is a given quantum state and ρ_c a closest classical-quantum state [18, 162].

This norm has been widely used in the literature as a reliable geometric measurement of quantum discord. In addition, this metric has a conceptual importance, because it is the only p-norm capable of producing a well-defined quantum correlation measure. In addition, it exhibits remarkable properties under decoherence for simple diagonal Bell states [18, 140, 162], under certain conditions in which abrupt transitions can

---

[16]The other Schatten p-norms $\|X\|_p = \{\mathrm{Tr}\left[X^\dagger X\right]^{\frac{p}{2}}\}^{\frac{1}{p}}$ for $p \geq 2$ cannot be regarded as a good measure for the quantumness of correlations either [157, 162].

be observed, the *sudden change* of quantum correlations [174,175], or an invariant behavior of the degree of quantum correlation in the system interacting with the extraneous environment, the *freezing* of quantum correlations [140,166,176].

3.2.4   Thermal Discord

Until 2010, the measurement of quantum correlations in macroscopic systems had only been related to the measurement of entanglement. Then, in 2011, Yurishchev [34,66] related the measurement of entropic quantum discord [9,10,153] with the magnetic susceptibility of a spin cluster material [34,66] from a theoretical point of view, associating the measurement of quantum discord with a thermodynamic property of a condensed matter system. Let us consider the main subject of study of this thesis, a system consisting of two isotropically coupled spin-1/2 particles such as a Heisenberg dimer in a d^9 electronic configuration in thermodynamic equilibrium.

Thermal Entropic Discord

The density matrix given by Eq. (3.54) is a Bell diagonal state, an therefore, it has the form from which the entropic quantum discord, Eq. (3.92), can be evaluated exactly. The mutual information $\mathcal{I}$, Eq. (3.83), can be calculated as a function of the pairwise correlation function $c(T)$, Eq. (3.55)

$$\mathcal{I}(T) = \frac{1}{4} \left[(1 - 3c(T)) \log_2(1 - 3c(T)) + 3(1 + c(T)) \log_2(1 + c(T)) \right] . \qquad (3.107)$$

Thus, the classical part of the total thermodynamic correlations, Eq. (3.107), can be calculated as a function of the pairwise correlations $c(T)$, Eq. (3.55), by using Eq.(3.91) and Eq.(3.54):

$$\mathcal{C}(T) = \frac{1}{2} \left[(1 + |c(T)|) \log_2(1 + |c(T)|) + (1 - |c(T)|) \log_2(1 - |c(T)|) \right] . \qquad (3.108)$$

Eq. (3.92), (3.107) and (3.108) define the so called *Thermal Discord*, [2,34,66]

$$
\begin{aligned}
\mathcal{Q}(\rho_{AB}) \;=\;& \mathcal{I}(T) - \mathcal{C}(T) & (3.109) \\
=\;& \frac{1}{4} \left[(1 - 3c(T)) \log_2(1 - 3c(T)) + 3(1 + c(T)) \log_2(1 + c(T)) \right] - & (3.110) \\
& -\frac{1}{2} \left[(1 + |c(T)|) \log_2(1 + |c(T)|) + (1 - |c(T)|) \log_2(1 - |c(T)|) \right] & (3.111)
\end{aligned}
$$

Thus, from Eq. (3.55), the entropic quantum discord can be calculated as a function of the magnetic susceptibility of a Heisenberg dimer in a d^9 electronic configuration in thermodynamic equilibrium:

$$
\begin{aligned}
\mathcal{Q}_E(T) = &\frac{1}{4}\{[4 - 3\alpha T\chi(T)]\log_2[4 - 3\alpha T\chi(T)] + 3\alpha T\chi(T)\log_2[\alpha T\chi(T)]\} - \\
&\frac{1}{2}\{[1 + |\alpha T\chi(T) - 1|]\log_2[1 + |\alpha T\chi(T) - 1|] + [1 - |\alpha T\chi(T) - 1|] \\
&\log_2[1 - |\alpha T\chi(T) - 1|]\}
\end{aligned} \tag{3.112}
$$

where $\alpha = 2k_B/N(g\mu_B)^2$ [2]. This result was first published in Ref. [34] in 2011, being one of the first quantifiers of quantum discord in terms of a thermodynamic property of a condensed matter system such as a molecular magnet.

Thermal Geometric Discord

Until 2016, connections between the quantum state geometry, associated with the measurement of geometric quantum correlations, and the thermodynamic properties of molecular magnetic systems had not yet been made. Inspired by the works of Ciccarello *et al.* [177] and Paula *et al.* [18, 162], the author of this thesis has calculated the geometric quantum discord based on the Schatten 1-norm, Eq. (3.106), as a function of the magnetic susceptibility of a molecular magnet as a coupled spin-1/2 Heisenberg dimer.

First, let us consider a set of isotropically coupled pairs of spin 1/2, i.e., a molecular magnetic system in a d^9 electronic configuration, ruled by a Hamiltonian $\mathcal{H}$ that exhibits invariance under π rotation around a given spin axis ($\mathbb{Z}_2$ symmetry) [16, 23]. The two-spin reduced density matrix at sites labeled 1 and 2 in the computational basis $\{|00\rangle, |01\rangle, |10\rangle, |11\rangle\}$ will be given by an X-shaped mixed state

$$
\rho_X = \begin{bmatrix} \rho_{11} & 0 & 0 & \rho_{41}^* \\ 0 & \rho_{22} & \rho_{32}^* & 0 \\ 0 & \rho_{32} & \rho_{33} & 0 \\ \rho_{41} & 0 & 0 & \rho_{44} \end{bmatrix}, \tag{3.113}
$$

where the positive semidefiniteness and the normalization of ρ_X require $\rho_{11}\rho_{44} \geq |\rho_{41}|^2$, $\rho_{22}\rho_{33} \geq |\rho_{23}|^2$, and $\text{Tr}[\rho_X] = 1$ [161, 177].

By decomposing the Eq.(3.113) in the Pauli basis, we obtain [16, 178–180]

$$
\rho_X = \frac{1}{4}(\mathbb{I} \otimes \mathbb{I} + \sum_{\alpha=x,y,z} c_\alpha \vec{\sigma}^\alpha \otimes \vec{\sigma}^\alpha + c_\beta \mathbb{I} \otimes \vec{\sigma}^z + + c_\gamma \vec{\sigma}^z \otimes \mathbb{I}) \tag{3.114}
$$

with

$$c_x = \langle \sigma_1^x \sigma_2^x \rangle = \mathrm{Tr}\,[\sigma_1^x \otimes \sigma_2^x \rho] = 2(\rho_{32} + \rho_{41}) \tag{3.115}$$

$$c_y = \langle \sigma_1^y \sigma_2^y \rangle = \mathrm{Tr}\,[\sigma_1^y \otimes \sigma_2^y \rho] = 2(\rho_{32} - \rho_{41}) \tag{3.116}$$

$$c_z = \langle \sigma_1^z \sigma_2^z \rangle = \mathrm{Tr}\,[\sigma_1^z \otimes \sigma_2^z \rho] = 1 - 2(\rho_{22} + \rho_{33}) \tag{3.117}$$

$$c_\beta = \mathrm{Tr}(\vec{\sigma}_1^z \otimes \mathbb{I}\rho_X) = 2(\rho_{11} + \rho_{22}) - 1 \tag{3.118}$$

$$c_\gamma = \mathrm{Tr}(\mathbb{I} \otimes \vec{\sigma}_2^z \rho_X) = 2(\rho_{11} + \rho_{33}) - 1 \tag{3.119}$$

where all these parameters assume values in the interval $-1 \leq c_{\alpha;\beta;\gamma} \leq 1$ ($\alpha = x,y,z$) [161].

Eq. (3.114) describes the so-called X-state which has nonzero elements only on the diagonal and antidiagonal as a consequence of the $\mathbb{Z}_2$-symmetry of the quantum spin model. Also, we stress the fact that ρ_{41} and ρ_{32} are reals due to the invariance of the quantum spin model under symmetrical operations.

In terms of the parameters $\{c_j\}$, for $c_x^2 - c_z^2 + c_\gamma^2 < 0$ the Schatten 1-norm quantum correlation can be written as

$$\mathcal{Q}_G(\rho_X) = \frac{|c_x|}{2} \tag{3.120}$$

and in case of $c_x^2 - c_z^2 + c_\gamma^2 \geq 0$:

if, $|c_x| \geq |c_z| \Rightarrow \mathcal{Q}_G(\rho_X) = \frac{|c_y|}{2},$ \hfill (3.121)

if, $|c_x| < |c_z| \Rightarrow \mathcal{Q}_G(\rho_X) = \Theta\left(c_y^2 - c_z^2 + c_\gamma^2\right) \frac{1}{2}\sqrt{\frac{c_x^2\left(c_y^2 + c_\gamma^2\right) - c_y^2 c_z^2}{c_x^2 - c_z^2 + c_\gamma^2}} \Theta\left(c_z^2 - c_y^2 - c_\gamma^2\right) \frac{|c_z|}{2}$

\hfill (3.122)

where $\Theta\left(x\right)$ is Heaviside step function (with $\Theta\left(0\right) = 1/2$).

Eq. (3.120)-(3.122) can be simplified in terms of the matrix elements of the X-shaped density matrix Eq. (3.113) as

$$\mathcal{Q}_G(\rho_X) = \frac{1}{2}\sqrt{\frac{\phi_1 \phi_{\max} - \phi_2 \phi_{\min}}{\phi_{\max} - \phi_{\min} + \phi_1^2 - \phi_2^2}} \tag{3.123}$$

where

$$
\begin{aligned}
\phi &= 2(\rho_{11} + \rho_{22}) - 1, \\
\phi_1 &= 2(\rho_{23} + \rho_{14}), \\
\phi_2 &= 2(\rho_{23} - \rho_{14}), \\
\phi_3 &= 1 - 4\rho_{22} , \\
\phi_{\max} &= \max\{\phi_3^2, \phi_2^2 + \hat{\phi}\}, \\
\phi_{\min} &= \min\phi_3^2, \phi_1^2
\end{aligned}
\tag{3.124}
$$

$$
\tag{3.125}
$$

As calculated in reference [161] the corresponding classical and total correlations are respectively:

$$
\mathbb{C}_G(\rho_X) = \hat{c}_+ \tag{3.126}
$$

$$
\mathbb{T}_G(\rho_X) = \frac{1}{2}\left[\hat{c}_+ + \max\left[\hat{c}_+, \hat{c}_0 + \hat{c}_-\right]\right] , \tag{3.127}
$$

where

$$
\hat{c}_- = \min\{|c_{11}|, |c_{22}|, |c_{33} - \mathrm{Tr}(\mathbb{I} \otimes \vec{S}_j^z \rho_X) \cdot \mathrm{Tr}(\vec{S}_i^z \otimes \mathbb{I}\rho_X)|\} \tag{3.128}
$$

$$
\hat{c}_+ = \max\{|c_{11}|, |c_{22}|, |c_{33} - \mathrm{Tr}(\mathbb{I} \otimes \vec{S}_j^z \rho_X) \cdot \mathrm{Tr}(\vec{S}_i^z \otimes \mathbb{I}\rho_X)|\} \tag{3.129}
$$

$$
\hat{c}_0 = \mathrm{int}\{|c_{11}|, |c_{22}|, |c_{33} - \mathrm{Tr}(\mathbb{I} \otimes \vec{S}_j^z \rho_X) \cdot \mathrm{Tr}(\vec{S}_i^z \otimes \mathbb{I}\rho_X)|\} \tag{3.130}
$$

are the minimum, maximum and intermediate values of the spin-spin correlation functions.

For Heisenberg models with $U(1)$ symmetry, namely, $[\mathcal{H}, \sigma^z]$ we obtain a stronger constraint over the elements of the density matrix [16]. The $U(1)$ invariance ensures that the element ρ_{41} vanishes in the reduced density matrix of Eq.3.113. In this case, ρ_X is a Bell diagonal state [161, 177], and this yields that they fulfil $c_\beta = c_\gamma = 0$. Therefore, the corresponding density matrix can be expanded as

$$
\rho_{Bell} = \frac{1}{4}\left(\mathbb{I} \otimes \mathbb{I} + c_\alpha \vec{\sigma}_1^\alpha \otimes \vec{\sigma}_2^\alpha\right) . \tag{3.131}
$$

Hence, $c_x^2 - c_z^2 \pm c_\gamma^2 \to c_x^2 - c_z^2$. Therefore, the geometric quantum discord in Eq.(3.121) reduces to Eq.(3.120), if $|c_x| \geq |c_z|$, and Eq.(3.122) for $|c_z| < |c_x|$ reduces to

$$
\mathcal{Q}_G(\rho_{Bell}) = \frac{1}{2}\max\{|c_z|, |c_y|\} . \tag{3.132}
$$

Therefore, from Eqs. (3.132) and (3.57), the geometric quantum discord can be written as a function of the magnetic susceptibility as

$$\mathcal{Q}_G(T) = \frac{1}{2} \left| \frac{2k_B T}{N(g\mu_B)^2} \chi(T) - 1 \right| \ . \tag{3.133}$$

This result [2] is a connection between the geometry of quantum states, through the measure of geometric discord, based on the Schatten 1-norm [162], with a thermodynamic property of a molecular magnetic system.

4 Literature Review and State of the Art

In recent years, it has been demonstrated by studying the quantum properties of molecular magnetic systems that these materials have highly stable quantum correlations against external perturbations such as temperature, pressure, and magnetic fields. In this context, molecular magnetic systems present themselves as strong candidates as prototype materials for processing, codification, and distribution of the quantum information, since they may be immune to decoherence mechanisms, which leads to the destruction of the quantum properties of the system of interest through the inevitable coupling of the quantum system with the external environment. Consequently, studying these systems gives us an opportunity to gain total control of their quantum properties, providing fascinating and innovative research perspectives and paving the way for promising applications in emerging quantum technologies, such as new devices based on quantum correlations and quantum computation. In this chapter, we present the state of the art of the study of quantum correlations in molecular magnetic systems.

4.1 Quantum Information in Molecular Magnetic Systems

Nowadays, we have reached the point where the miniaturization of electronic devices will inevitably lead to molecular size components. However, designing components with molecular properties requires a deep understanding of the laws of quantum mechanics applied to these components. This fact has led to a technological breakthrough that will be achieved through employing quantum information theory.

Quantum information theory is a field in increasing development, involving the intersection of two major areas of scientific knowledge: quantum mechanics and information theory [3,4,65,181]. It is based on the study of the properties of compound quantum

systems in order to explore them for codification, processing, and distribution of the information contained in a quantum state or encapsulated in a quantum system [3,4,65]. Due to the fact that the science of quantum information is an extremely multidisciplinary area, it involves lines of research ranging from the study of algorithms for quantum computation to forms of relation with other areas such as condensed matter physics, [3,4,65,181,182], optics [3,4,65,181,183], and thermodynamics [3,4,65,181,184], passing through questions related to the fundamentals of theoretical physics, and arriving at experimental implementations of a wide range of protocols in different physical platforms [4,111,185–187].

4.1.1 Quantum Information Theoretical Quantifiers

One of the most striking results in the field of computation and quantum information was the discovery that entanglement is a physical resource with which we can perform tasks like processing and transmission of information. Initially, entanglement was only considered as a quantum correlation [3, 4, 65]. It was the entanglement, in which, from the 1990s, hope was placed on ambitious projects of radical improvement in computer performance, designing secure data networks, implementing teleportation of states, etc. [4, 111, 185–187]. However, entanglement is fragile and can easily vanish through the inevitable interaction of the system with its environment [130]. Despite the rapid growth of quantum information science in recent years, especially with regard to the development of marketable technologies related to encryption [3, 4, 65, 111, 181, 188, 189] and quantum computation [3, 4, 65, 181, 190], large-scale development of technological devices based on quantum information is compromised by the decoherence process that leads to the destruction of the quantum properties of the system of interest through the inevitable coupling of the quantum system with the external environment.

Most of the research so far has focused on the use of highly entangled states, which are, however, difficult to produce and stabilize for a large number of constituents. Because of this, in the 21st century we saw a further development of ideas about the physical nature of quantum correlations and the development of new quantum enhanced measurements without entanglement [101] and new quantum information quantifiers. The study of theoretical quantum information quantifiers has attracted considerable attention as a key resource for several information processing protocols [3–7].

In 2000, Zurek introduced the concept of quantum discord as a reliable in-

dicator of the quantum nature of the correlations [9]. In 2001, Henderson and Vedral, independently, analyzed the correlations in a bipartite system, suggesting, from the theory of measurement, a way to separate purely classical and quantum correlations [10], as we show in Section 3.3.1. In 2008, using the model of deterministic quantum computation with one qubit [153], Datta demonstrated that a quantum processor can be built over mixed states by using quantum correlations, measured by the entropic quantum discord, in the absent of entanglement. This fact has led to an expansion of the notion of quantum correlations and it has been shown that the quantum entanglement does not encompass all possible quantum correlations in a system.

However, there are only a few results for the analytical expression of entropic quantum discord, and only for certain classes of states are exact solutions known [11, 13–17, 160]. Most recently, in 2014, Huang [21] proved that computing entropic quantum discord (and a large class of entropic measurements including entanglement of formation) is an NP-complet problem even for bipartite mixed states. As a result, the problem of computing entropic measurements of quantum discord is computationally intractable [21]. Therefore, devising efficient algorithms or even establishing closed analytical formulas for such quantifiers of quantum correlations is a very difficult task. This motivated the introduction of alternative measures of quantum discord from a theoretical point of view [12, 14, 34, 66, 191, 192].

In 2010, Dakić *et al.* demonstrated that a reliable geometric quantifier of discord-like correlations can be built by employing the so-called trace distance, which is used to measure how far the state under investigation is from the closest *classical–quantum* state [19]. Despite its remarkable features, as we showed in Section 3.3.2, geometric discord is known to be sensitive to the choice of distance measures, as pointed out by Tufarelli *et al.* [150] and Piani in 2012 [163] and Hu *et al.* in 2013 [173]. The geometric discord as proposed by Dakić *et al.* [19] cannot be regarded as a good measure for the quantumness of correlations, because it may increase under local operations on the unmeasured subsystem [162]. In this context, in 2013 Paula [162], following the above-mentioned works, studied the fundamental aspects of geometric discord by considering general Schatten p-norms, explicitly showing that only the 1-norm is able to define a consistent quantum correlation measure.

Nowadays, numerous quantifiers of quantum correlations have been proposed [5, 7, 11, 13–19, 142, 157, 158, 160, 162–166], especially quantifiers based on geometric argu-

ments [15, 18, 19, 142, 157, 162–166]. In addition, the scientific community has proposed numerous alternative measurements of general quantum correlations based on discord-like quantifiers through metrological measures of nonclassical correlations [165, 193, 194] and phenomenological aspects of quantum systems [195, 196]. Among all possible measurements of general quantum correlations, the scientific community has paid particular attention to the concepts of *quantum interferometric power* proposed by Girolami *et al.* in 2014 [158] and *quantum coherence quantifiers* proposed by Baumgratz *et al.* in 2014 [195].

Quantum interferometric power can be seen as a nonclassical correlation quantifier with a metrological interpretation in a black-box quantum phase determination paradigm [101], which relies on discord-type quantum correlations [158, 197]. Girolami *et al.* [158] showed that the discord of a quantum state guarantees that the minimum precision can be obtained by using this state in a metrological configuration of phase estimation, providing a strong indication that states with nonzero quantum discord play a central role in the context of quantum metrology.

In order to understand its conception, let's consider an interferometric protocol where a phase φ is implemented in one branch of a bipartite initial state ρ_{12} via the unitary transformation $U_\varphi = e^{-i\varphi\mathcal{H}_1}$, where $\mathcal{H}_1$ is the generator of the rotation. After such implementation, the resulting phase, $\tilde{\varphi}$, can be estimated and compared to the intended one. The optimum result, where $\tilde{\varphi}$ is as close as φ as possible, is obtained when the Cramer-Rao bound is saturated [198] since, it determines the maximum achievable precision for any initial state ρ_{12} with the generator of rotation $\mathcal{H}_1$, providing a lower bound on the variance of any unbiased estimator function φ which maps observed data obtained from arbitrary quantum measurements [101]. Therefore, for a given input state ρ_{AB}, a relevant figure of merit for such a setup is the minimum *Quantum Fisher Information*, $\mathcal{F}(\rho_{AB}; \mathcal{H}_A)$, over all $\mathcal{H}_A$ [158, 197], given by:

$$\mathcal{P}^A(\rho_{AB}) = \frac{1}{4} \min_{\mathcal{H}_A} \mathcal{F}(\rho_{AB}; \mathcal{H}_A) \tag{4.1}$$

In 2017, Bromley *et al.* [197] demonstrated that entanglement cannot entirely capture the worst-case sensitivity in quantum interferometry, proving that quantum interferometric power relies on more general quantum correlations beyond entanglement and captures the relevant resource [197].

On the other hand, Baumgratz, Cramer, and Plenio define a phenomenological characteristic of quantum systems as a quantum information theoretical quantifier, the

quantum coherence [195]. As the main resource of the quantum interference phenomena, quantum coherence plays an important role in quantum information theory, enabling applications that are impossible within the classical realm. For any distance between quantum states D Baumgratz [195] define a general distance based coherence quantifier as

$$\mathcal{C}_D = \min_{\sigma \in \mathcal{I}} D(\rho, \sigma) \ , \tag{4.2}$$

where the minimal distance of ρ from a set of incoherent states $\sigma \in \mathcal{I}$. For an arbitrary fixed reference basis $\{|i\rangle_{i=1,...,d}\}$ of a d-dimensional Hilbert space $\mathcal{H}$ in which we consider the quantum state of interest ρ, the set of all density matrices

$$\sigma = \sum_{i=1}^{d} s_i |i\rangle\langle i| \ , \tag{4.3}$$

that are diagonal in this reference basis, with s_i being the probabilities. Any state which cannot be written as above is defined as coherent. In a manner analogous to that proposed in Chapter 3 for entanglement and quantum discord any reliable measure of coherence, Eq. (4.2), is $\mathcal{C}_D = 0$ only for incoherent states $\sigma \in \mathcal{I}$.

Thus, unlike other information theoretic quantifiers coherence is basis-dependent. This reference basis $\{|i\rangle_{i=1,...,d}\}$ may be dictated by the physics of the problem under investigation or by a task for which coherence is required [195, 196]. In addition, the definition of coherence quantifiers [195] requires the definition of incoherent operations, analog to the entanglement monotones requires a definition of non-entangling operations, determined by phenomenological considerations, which leads to LOCC operations, as described on chapter 3. A completely positive trace preserving map Λ is said to be an incoherent operation if it can be written in the form

$$\Lambda[\rho] = \sum_i K_i \rho K_i^\dagger \in \mathcal{I} \subset \mathcal{H} \ , \tag{4.4}$$

where the defining operator K_i are the so-called incoherent Krauss operators[1], which maps every incoherent state σ.

With this definitions, Baumgratz *et al.* [195] set the framework for a resource theory for quantum coherence. They performed a wide variety of measurements of quantum coherence on solid bases by establishing a quantitative theory of quantum coherence

---

[1]Incoherent Krauss operators have a great importance for open quantum system dynamics, since it defines the depolarizing, phase-damping and amplitude-damping channels [195]

as a resource of quantum information quantifying process [196], presenting basic assumptions of their approach and using it to identify quantitative measurements of quantum coherence. In analogy to that already defined in Chapter 3 for the calculation of the quantum discord the relative entropy measure is defined for the quantum coherence as

$$\mathcal{C}_{ent}(\rho) = S(\rho_{diag}) - S(\rho) , \tag{4.5}$$

where $S(\rho)$ is the von Neumann entropy and ρ_{diag} is the diagonal density matrix obtained from the diagonal elements of ρ written on the reference basis. On the other hand, a reliable geometric coherence quantifier can be built by employing a general distance measurement $D(\rho,\rho_{diag})$, which is a metric used to measure how far the state under investigation ρ is from the closest set of incoherent states $\mathcal{I}$. Thus, all the metrics used in Chapter 3 to define reliable quantifiers of quantum discord can be used as geometric measures of quantum coherence.

In a general way, these discord-like quantifiers exhibit monotonic behavior as the environment acts on the system. Otherwise, under certain conditions, abrupt transitions can be observed, the *sudden change* of quantum correlations [174, 175], or an invariant behavior of the degree of quantum correlation in the system interacting with the extraneous environment, the *freezing* of quantum correlations [140, 166, 176]. Therefore, in addition to defining quantifiers capable of providing the degree of quantum correlations in a physical system, the state of the art of quantum correlation quantification lies in the study of the dynamics and the behavior of these correlations versus effects from interaction with the external environment (decoherence processes).

4.1.2 Decoherence in Magnetic Materials

The identification of qubits in magnetic materials has attracted the attention of the scientific community of quantum information theory and condensed matter physics. Moreover, there are also quantum correlations among the magnetic components of these materials [2]. However, the main obstacle to the development in large scale of instruments and devices that employ quantum correlations is decoherence process [199, 200]. To develop coherent quantum devices based on a given magnetic material, a few static qubits are insufficient; rather, large sets of coherent qubits whose dynamics can be monitored and controlled for a sufficiently long time [66], i.e., for a quantum computer, are needed,

and the lifetime of the coherent state must be long enough to perform a certain number of computational protocols required by an arbitrary quantum algorithm. As pointed by Krojanski and Suter [201], the decoherence time is expected to get shorter with the number of correlated qubits, thus it decreases rapidly with increasing number of qubits in the system [66, 201], but experimental data are only available for small numbers of qubits.

Remarkable results in the manipulation of qubits have recently been achieved using nuclear magnetic resonance (NMR) methods in nuclear spins of atoms in different molecules [202–204]. In this technique, the spin dynamics is characterized by the spin–lattice relaxion time, which is responsible for the longitudinal magnetization decay of the system [203], and the spin–spin relaxion time, which responsible for the transverse magnetization component dephasing [66, 203], and therefore the decohering process of the quantum states of nuclear spin magnetic materials.

It should be noted that the spin–lattice relaxion time in nuclear spins can be seconds or even minutes [204]. However, there is a great disadvantage of nuclear spins: due to the small nuclear magneton [203][2], operating qubits in nuclear magnetic materials must be done at extremely low temperatures, on the order of millikelvins.

The recent results strengthen the fact that electronic magnetic materials, such as molecular magnetic systems, may be somewhat immune to decohering mechanisms [2, 20, 25, 27–29, 34–36]. Owing to the large gap between the ground state and the first-excited state found in some materials, these materials can contain quantically correlated states with high stability and resistance to external disturbances, such as high temperatures, pressures, and magnetic fields [2, 20, 25, 27–29, 34–36]. It is an undoubted advantage over the qubits based on nuclear magnetic atoms and molecules. However, unfortunately, the prospect of using these materials, as qubit systems, in the processing and distribution of quantum information still is currently impractical because the large spin–lattice interaction leads to extremely short relaxation times (10^{-10}–10^{-6} s). Nevertheless, the state of the art for study the decohering process in electronic spin qubits relies on the creation and design of novel materials with large electron spin relaxation times [66].

---

[2]This is a factor of almost 10^3 smaller when compared to the electronic one.

4.1.3 Quantifying Quantum Correlations in Molecular Magnetic Systems

Nowadays, the demand for the development of new materials has guided several research groups to the study of structures that, besides exhibiting remarkable physical properties, are useful in technological and everyday applications. The search for the understanding, optimization, and development of new systems is the main motivation for conducting research projects in the area of condensed matter physics. In recent years, the scientific community has learned how to use the emerging quantum properties of condensed matter physics systems through the study of quantum information theoretical quantifiers by measuring thermodynamic properties of solids [2, 20, 23, 25, 27–29, 34–36], paving the way for a promising future in the development of new quantum technologies.

The technological challenges of quantum information science lead us to consider fundamental aspects of Molecular Magnetism, because of its ease of synthesis, great versatility, and low-dimensional features. In 2000, inspired by the paper published by Ahn *et al.* [205], in which they implemented a Grover algorithm [206, 207] in Rydberg atoms [205], Leuenberger and Loss [208] published a paper in which they proposed an implementation of Grover's algorithm using molecular magnets, theoretically showing that molecular magnets can be used to construct dense and efficient memory devices based on Grover's algorithm. However, the superposition of single-particle quantum states is sufficient for Grover's algorithm [205–208], and quantum entanglement was still unexplored.

Until 2000s, most of the demonstrations of quantum correlations in condensed matter physics were related to the detection of entanglement involving at most a handful of atoms. The components of these systems are likelier to become entangled with stray components, obscuring their original interconnections. Because of decohering processes, too much information leaks out to the environment, causing the system to behave through a classical probability distribution. In this scenario, the difficulty of preserving quantum correlations poses a major challenge for those of us seeking to exploit these novel effects behind the quantum nature of physical systems for practical use, such as quantum computers and emerging quantum technologies.

In 2003, Ghosh *et al.* [131] proved that larger systems can also remain entangled. They put a lithium fluoride salt in an external magnetic field and observed that the

atoms in the salt can be seen as spinning magnets that try to align themselves with the external field. Through the measurement of the magnetic susceptibility, they found that the atoms responded much faster than the strength of their mutual interactions would suggest. Therefore, some additional effect was boosting the atoms to align with the external magnetic field, and the researchers argued that this was due to the entanglement between the magnetic dipoles. Therefore, the 10^{23} atoms of the salt formed a hugely entangled system [131]. However, to avoid the confounding effects on the magnetic dipoles resulting from heat energy, which leads to thermal decoherence, Ghosh $et\ al.$ [131] had to perform their experiments at extremely low temperatures of a few millikelvins.

In the middle of the 2000s, several thermodynamic quantities, such as internal energy [127, 134–136], magnetization, and heat capacity [137], were proposed as an way to identify the presence of entanglement in a macroscopic condensed matter system, but they all depended on complete knowledge of the specific model that describes the macroscopic properties of the quantum system of interest and they were not usually directly measurable quantities. Therefore, in 2005, Wieśniak, Vedral, and Brukner showed from a theoretical point of view that magnetic susceptibility of a condensed matter system can reveal thermal spin entanglement between the constituents of a solid, as an entanglement witness [36]. This witness can be directly measured and can be applicable, in principle, without full knowledge of the Hamiltonian model that describes the physical nature of the system or the dimensionality of the Hilbert space associated with the quantum system, thereby establishing a solid relationship between the quantum properties of a condensed matter system and its macroscopic properties. In 2009, Pinto [25] investigated quantum thermal entanglement in molecular magnetic systems composed of S spin dimers using Wieśniak's entanglement witness, where the maximum temperature below which entanglement [3, 4, 25, 28] is directly associated with the intra-dimeric magnetic coupling and that the entanglement appears only for the antiferromagnetic coupling.

On the other hand, from an experimental point of view, Souza $et\ al.$ [27] measured thermal entanglement in spin clusters through the magnetic susceptibility measurements in a molecular magnetic system. They found the entanglement exists below 240 K. This was the first clue that a molecular magnetic system could be somewhat resistant to the thermal decohering process. Then, in 2009, Souza $et\ al.$ [29] measured quantum entanglement and quantum nonlocality at higher temperatures in a copper-carboxylate-based molecular magnet. In these materials, the magnetic coupling is strong enough

to resist thermal decoherence. Although the system remained entangled up to 630 K, hundreds of kelvins above room temperature, Bell's inequality is violated up to 290 K, which is a remarkable feature, because violation of Bell's inequality has great importance to quantum information science from an operational viewpoint for the implementation of several protocols. In 2012, Reis *et al.* [28] showed, through an engineered molecular system, that molecular magnets could remain up to 730 K, significantly above the highest temperature where a system could be quantum correlated as reported up that time.

Until 2011, the measurement of quantum correlations in molecular magnetic systems was only related to the measurement of entanglement. However, in 2011, Yurishchev related the measurement of entropic quantum discord [9,10,153] with the magnetic susceptibility of a spin cluster material [34,66] from a theoretical point of view.

At this point, the main results of this thesis, presented in the next chapters, are placed on the state of the art of the study of quantum information in molecular magnetic systems. Based on the demand for functional quantum systems, with high stability in their quantum properties, against the inevitable decoherence process, and aiming for greater efficiency and lower production costs of new devices based on quantum information technologies, the state of the art of the study of condensed matter systems applied to quantum information lies in the exploration of potential systems as prototypes for coding, processing, and distribution of quantum information.

One of the fundamental aspects behind the state of the art of molecular magnetic systems is the relationship between magnetic interactions and the crystalline lattice. Although some general rules governing the interactions of these systems are qualitatively understood from the chemical point of view [53], there are numerous degrees of freedom, such as metal center bounds and local distortions that are extremely physically important but still unexplored from the quantum point of view. For example, there are several molecular magnetic systems, such as metal–organic crystalline systems [2,31], that have an immense variety of topologies [2,30,31] and compositions, leading to dramatic effects on magnetic behavior and, consequently, on their quantum properties [2], allowing the study of the way that multiple topological conformations [31] affect the quantum characteristics of these materials.

Our main results have been aimed at proposing and providing engineered materials with a high stability of its quantum correlations against external perturbations.

In 2016, we found that carboxylate-based molecular magnetic systems can achieve stable quantum correlations up to 10^4 K above room temperature [2]. It is worth mentioning that we make the connection between the geometry of quantum states, through the measure of geometric discord based on the Schatten 1-norm [162], with a thermodynamic property of a molecular magnetic system. We add to the literature an engineered material with a high stability of its quantum correlations against external perturbations. The study of carboxylate-based molecular magnets will lead to new research toward the limits of quantum information processing, with promising applications in emerging quantum technologies, especially devices based on quantum correlations.

In 2017, we showed through the density functional theory (DFT) that an external pressure yields a minimization on the degree of quantum correlations in a spin cluster [20]. Also remarkable is the possibility of handling the ground state of the system by controlling its temperature and pressure, showing that quantum properties of spin clusters can be controlled and manipulated by the management of significant macroscopic effects [20].

Still in 2017, based on the works of Cramer [22] and Marty [87] that associated the structure factor of inelastic neutron scattering in a condensed matter system, as an entanglement witness, we showed that it is possible to quantify the presence of geometric quantum correlations, through structure factors obtained through inelastic neutron scattering. We have provided one path toward identifying the presence of quantum correlations in a two-qubit system, only using diffractive properties of inelastic neutron scattering without making any assumption about its macroscopic properties or the external conditions under which the neutrons are scattered, being an alternative way to describe the quantum properties of a two-qubit system via neutron scattering experiments.

These results open a new and exciting prospect for quantum information processing in spin cluster materials, leading to promising applications in quantum information science such as the development of novel candidate platforms for the processing and transmission of quantum information.

5 Stable Quantum Correlations at Room Temperature in a Carboxylate Based Molecular Magnet

In this chapter, we begin the presentation of the results obtained in this thesis, showing that carboxylate-based compounds can support quantum correlations thousands of kelvins above room temperature. We report the crystal structure and magnetic suscepti-bility of a carboxylate-based molecular magnet with the formula $Cu_2(HCOO)_4(HCOOH)_2$ $(C_4H_{10}N_2)$, a metal–organic framework, from which the quantum correlations quanti-fiers, derived as a function of the temperature using the magnetic susceptibility of the compound, shown in Chapter 3 are explored. The analytical formulas for the quantum correlations and the analysis of the data suggest the existence of entanglement up to tem-peratures of 681 K, while the measure of quantum discord reveals that this system remains at the singlet ground state up to ~ 80 K. In addition, quantum correlations would remain up to 9540 K, thousands of kelvins above room temperature, even without entanglement. Therefore, we obtain very stable quantum correlations up to 513 K, the limit at which this material can exist—hundreds of kelvins above room temperature [157]. These results could only be achieved as a result of the material topology, because of the carboxylate group promoting a huge metal-to-metal magnetic interaction. These results represent the highest temperatures, reported to date, wherein quantum correlations can be supported.

5.1 Design of the Carboxylate-Based Molecular Magnet: Synthesis and Crystal Structure

To obtain strongly entangled states at high temperature, we need to maximize the gap between the ground state and the first-exited state, and metal organic frameworks are one path toward achieving this goal. Metal–organic frameworks (MOFs) are essentially polymers formed from the bonding of metal ions with polytopic organic compounds, often

resulting in fascinating structural topologies such as chains, layers, and three-dimensional structures with high porosity. Because of this and other factors, they present a wide variety of applications in the processes of adsorption, gas storage and catalysis, drug storage, magnetic refrigeration, and magnetic data storage [209, 210]. It is well known that the preparation of such compounds is extremely sensitive to synthetic conditions, including observations indicating that the degree of hydration yields different structures [209–212]. The use of chemical and crystal engineering techniques allows us to systematically design structures with chemical and magnetic properties that are adjustable to the synthesis conditions. In this way, we can design materials with such features to enhance their quantum properties and then study the quantum correlations.

To obtain a low-dimensional system of two qubits, under which the quantum correlations were calculated, we use copper(II) ions as a Heisenberg dimer in a d^9 electronic configuration and therefore an ideal realization of a two-qubit system (spin-1/2 dimer) ruled by a Heisenberg–Dirac–Van Vleck Hamiltonian $\mathcal{H} = -J\vec{S}_1 \cdot \vec{S}_2$ [23]. In this context, we present the synthesis, structural characterization, and magnetic properties of Cu(II) MOFs, using as a binder piperazine ($C_4H_{10}N_2$), a vermifuge compound, the derivatives of which are widely used in the treatment of different parasites [213]. The use of piperazine as a binder allows the formation of porous environments, thus allowing the production of MOFs.

The compounds were synthesized in collaboration with the Center for Research in Ceramic and Composite Materials (CICECO) Chemistry of the University of Aveiro (Portugal), using the standard procedure of reflux synthesis[1] using piperazine ($C_4H_{10}N_2$), distilled water, ethanol, formic acid, and copper(II) carbonate ($CuCO_3Cu(OH)_2$). For the synthesis of our compound, we used a mixture of dehydrated copper(II) nitrate, piperazine ethanol, and/or distilled water, refluxed for 3 h at a temperature of $\sim$425 K.

The dinuclear copper(II) complex $Cu_2(HCOO)_4(HCOOH)_2(C_4H_{10}N_2)$ was successfully synthesized, and its crystalline structure was characterized by single-crystal X-ray diffraction. Its molecular structure is presented in Fig. 5.1 and the spatial groups and lattice parameters and angles, obtained from X-ray diffraction, are presented in Table 5.1.

---

[1]These materials are readily prepared under hydrothermal conditions using conventional heating (300–500 K) for a period of a few days or by crystallization at room temperature.
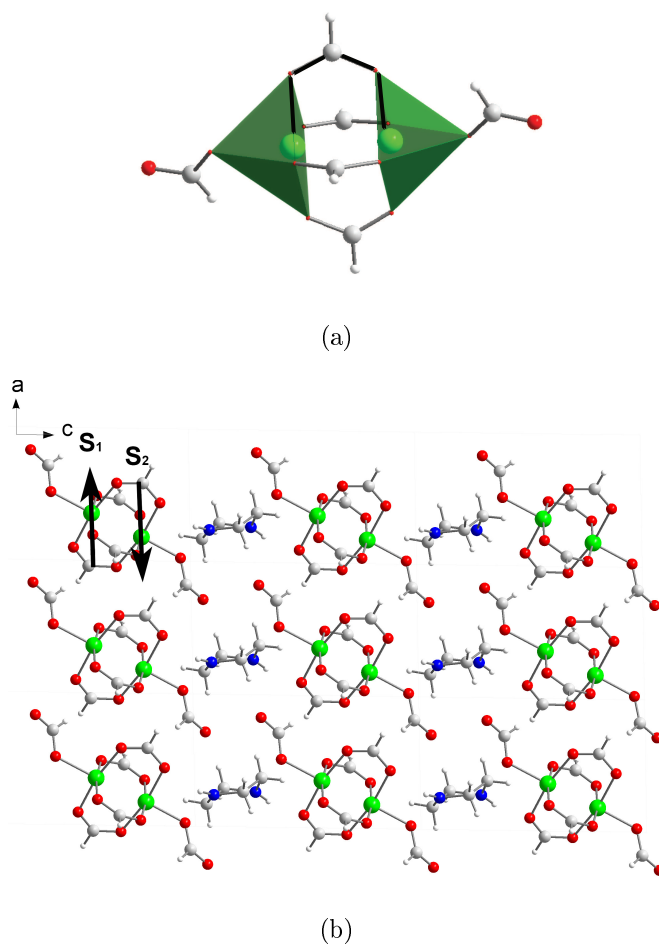
(a)

(b)

Figure 5.1: Crystal structure of $Cu_2(HCOO)_4(HCOOH)_2(C_4H_{10}N_2)$ compound with (a) local dimer polyhedron representation and (b) dimeric sheet view, where the arrows represent the reduced magnetic structure of the compound. Color scheme: Cu - green; O - red; N - blue.

Table 5.1: Crystalline data and refined parameters obtained in the X-ray diffraction

Space Group	Triclinic P-1
a(Å)	6.3927(4)
b(Å)	6.7758(4)
c(Å)	10.4418(5)
$\alpha(^o)$	93.825(3)
$\beta(^o)$	90.544(3)
$\gamma(^o)$	107.214(3)

Single-crystal structure analysis revealed that the compound is composed of a dimeric cupric tetraformate unit, with a short Cu–Cu internuclear separation of 2.628(2) Å and one piperazine molecule. The dimer is formed by opposing square pyramidal CuO$_5$ with a very small distortion (see Fig. 5.1(a)). The base oxygen atoms on the adjoining pyramids are part of the four connecting carboxylate groups in a syn–syn conformation, leading to a strong magnetic interaction between the dimer ions. The apical oxygen of the pyramid is connected via an HCOO group (Cu–O = 2.12(1) Å) to another carboxylate group. The crystal structure is stabilized by intermolecular N–HO hydrogen bonding with N(10)$\cdots$O(7) = 2.722(2) Å and N(10)$\cdots$O(8)^{ii} = 2.745(2) Å ($ii = 1 + x, y, z$), forming an infinite two-dimensional network.

5.2 Magnetic Properties

Our designed compound Cu$_2$(HCOO)$_4$(HCOOH)$_2$(C$_4$H$_{10}$N$_2$) is of highest interest, it shows a short interaction path between the metal centers, a crucial factor for the emergence of strongly entangled states at high temperature, since from its short interaction path maximizes the gap between the ground state and the first-exited state.

From the previously described crystal structure, it is possible to extract the magnetic structure, as shown in Fig. 5.1(b). In this structure, copper dimers, with an intramolecular separation of 2.628(2) Å, are separated from each other by a distance of 6.776(1) Å. These dimers are arranged in linear chains along the a axis, and these chains are separated from each other along c axis by a distance of 8.176(1) Å, thus forming sheets of copper dimers (see Fig. 5.1(b)).

From a magnetic viewpoint, owing to the much higher intra- and interchain distances, in comparison to the Cu–Cu intra-dimer distance, we considered a model of isolated dimers, a low-dimensional molecular magnetic system as described in Chapter 2. Given that the Cu(II) ions under consideration have a d^9 electronic configuration, this material is an ideal realization of a spin-1/2 dimer, in which the quantum correlations presented in Chapter 3 were calculated as

$$\mathcal{H} = -J\vec{S}_1 \cdot \vec{S}_2 - g\mu_B \vec{B} \cdot (\vec{S}_1 + \vec{S}_2) \ . \tag{5.1}$$

where g is the isotropic Landé factor. The present model has one exchange parameter, J, which related to an intra-dimer interaction corresponding to the syn–syn conformation
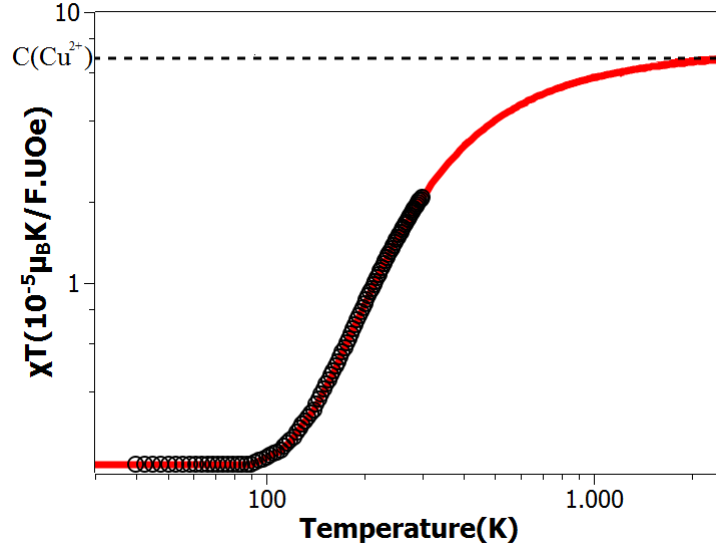
Figure 5.2: Experimental (open circles) and theoretical (solid line) magnetic susceptibility times temperature. The red line represents the fitting of Eq.(5.2) to the experimental data, where an extrapolation, up to higher temperatures, was done using the optimized parameters. The dashed line indicates the saturation of the χT curve (Curie constant) for copper ions in a 2+ oxidation state.

between the copper ions, as can be seen by the dark lines in Fig. 5.1(a). As pointed in Chapter 3, the quantum properties of several materials have been deeply analyzed by means of thermodynamic quantities [3, 19, 25–29, 126, 127, 131, 133, 214, 215], and the measurement of the magnetic susceptibility χ is a good benchmark [3, 19, 25–29, 126, 133] owing to easy experimental access.] From the theoretical point of view, through the model presented in Chapter 2, the magnetic susceptibility from the Hamiltonian of Eq. 7.11 can be described as [23, 47]

$$\chi(T) = \frac{2N(g\mu_B)^2}{k_B T} \frac{1}{3 + e^{-J/k_B T}} \; . \tag{5.2}$$

Figure 5.2 shows the experimental data from the magnetic susceptibility of $Cu_2(HCOO)_4(HCOOH)_2(C_4H_{10}N_2)$, as well as, a fitting of the above to the experimental data, where this data were corrected to account for both the temperature-independent paramagnetism and the diamagnetic contribution obtained from the fitting using the software DAVE-MagProp [67].

From the curve of $\chi T(T)$ for this compound, we can identify the profile of a strong antiferromagnetic arrangement at high temperatures between the metal centers. This can be interpreted as a negative intra-dimer short-range interaction related to the

distances between the metal centers. The optimized parameters were obtained from the fitting with $J = -748.5$ K (antiferromagnetically coupled ions) and $g = 2.07$. From these fitting parameters, it was possible to extrapolate this thermodynamic quantity to higher temperatures and it is clear that the system indeed dimerizes at rather elevated temperatures, and these dimers remain isolated down to the lowest measured temperature.

It is worth noting that, for the material under consideration, the experimental $\chi T(T)$ quantity, for the whole range of temperature considered (<300 K), is smaller than the Curie constant of the dimer $C = 1.34 \times 10^{-4}$ μ_BK/FU-Oe; and it is a clear signature that at least one exchange interactions into the system is larger than the thermal energy at room temperature. As a consequence, the paramagnetic region is not reached for the temperature range in which the susceptibility is measured and therefore these experimental data cannot be described within the Curie–Weiss law [23].

5.3   Thermal Quantum Correlations

In order to analyze the quantum correlations by means of magnetic susceptibility, first, let us analyze the thermal entanglement in $Cu_2(HCOO)_4(HCOOH)_2(C_4H_{10}N_2)$, since we calculated in Chapter 3 the thermal quantum correlation quantifiers in terms of the magnetic susceptibility of a two 1/2-spin molecular magnetic system.

As mentioned before in Section 3.1, an entanglement witness is an observable that can tell us whether, for the condition given by Eq. (3.35), a given quantum system is entangled. If Eq. (3.35) is violated, the system's state is entangled; otherwise, if Eq. (3.35) is satisfied, we cannot state with certainty that the system's state is separable. This witness is directly measured, as a function of the magnetic susceptibility, Eq. (3.67), from which we can identify the presence of entanglement in $Cu_2(HCOO)_4(HCOOH)_2(C_4H_{10}N_2)$, using the experimental data and the developed model shown in Fig. 5.2, establishing a relationship between a quantum entanglement observer and a thermodynamic property of this compound.

In Fig. 5.3, we obtain the entanglement witness from the magnetic suscepti-bility shown in Fig. 5.2; the witness is negative up to 420 K ($\text{Tr}(\rho W) < 0$), showing the presence of entangled states in our $Cu_2(HCOO)_4(HCOOH)_2(C_4H_{10}N_2)$ compound below this temperature, while the states above this temperatures, for which $\text{Tr}(\rho W) \geq 0$, are
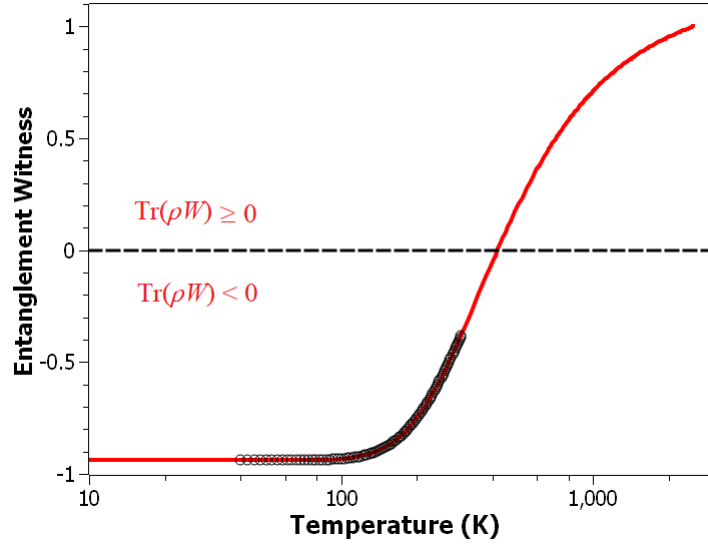
Figure 5.3: Experimental (open circles) and theoretical (solid line) Entanglement Witness for the carboxylate based molecular magnet $Cu_2(HCOO)_4(HCOOH)_2(C_4H_{10}N_2)$. The red line represents the fitting of Eq.(3.67) to the experimental data, where an extrapolation, up to higher temperatures, was done using the optimized parameters obtained from the fitting of the magnetic susceptibility. The dashed line indicates when Eq. (3.35) is violated.

indistinguishable from this witness.

Furthermore, to quantify the amount of quantum correlations discussed in Chapter 3 of this molecular magnetic system, as a function of the magnetic susceptibility, shown in 5.2, we adopt the measurements of (i) entanglement of formation, which is often used as a measurement of entanglement, defined by [128, 129] and discussed in Section 3.2, (ii) entropic quantum discord, which is a measurement of the amount of genuinely quantum correlations, and (iii) geometric quantum discord, based on the Schatten 1-norm, a well-defined measurement of the amount of quantum correlations of a state in terms of its minimal distance from the set of classical states [18, 162], as widely discussed in Section 3.3.

Figure 5.4 shows the entanglement of formation, Eq. (3.74), entropic quantum discord (Eq. (3.112)), as well as the geometric quantum discords, Eq. (3.133), as a function of temperature, obtained from the experimental magnetic susceptibility data (open circles) and the extrapolated ones (solid lines), shown in 5.2.

Note that, up to ~ 80 K, above the liquid nitrogen temperature, the entropic discord and the entanglement achieve the maximum value of unity; i.e., the system is
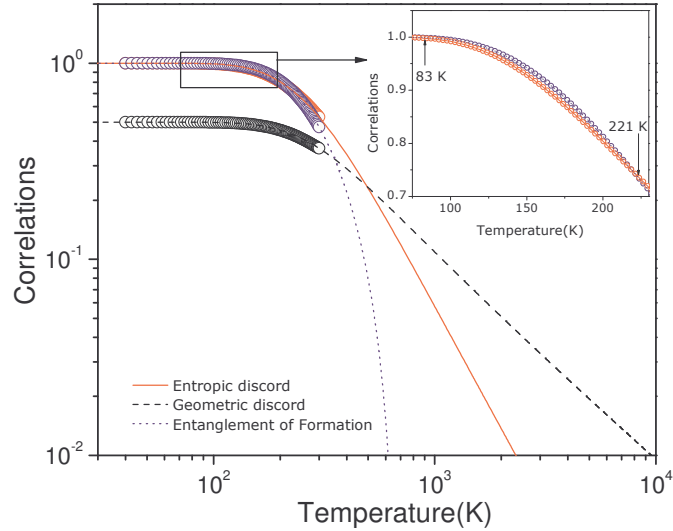
Figure 5.4: Temperature dependence of entropic (solid red) and geometric (dashed black) quantum discords, as well as entanglement of formation (dotted blue). Owing to technical limitations, experimental data (open circles) are measured only up to room temperature, but the theoretical extrapolation (solid lines) goes further. The inset shows the region where the entanglement is larger than entropic quantum discord, as well as the pure state up to ~ 80 K.

absolutely in the singlet ground state (pure state). Above this temperature, the entanglement is larger than entropic quantum discord and intercepts back to this curve at 221 K. This phenomenon in which the entanglement is larger than the quantum correlations can be explained because entanglement is a mixture of purely classical and purely quantum correlations. In addition, a direct comparison may lead to a misunderstanding, because entanglement is a different measure of quantum correlation, as already discussed in Section 3.3., where pure entangled states contain purely quantum correlations, because the measurement of quantum discord is reduced to an entanglement measurement, while entangled statistical mixtures may also contain classical correlations, but they must necessarily have quantum ones [15, 34, 66], because entangled states cannot be simulated or represented from classical correlations.

From the entanglement of formation, we can verify that these copper dimers are entangled up to temperatures of $T_e = 681$ K when the entanglement has a sudden death, in contrast with the entanglement witness when we identify the presence of entangled states up to 420 K. However, from the entropic quantum discord, we can verify that this material can support correlated quantum states up to temperatures as high as 2320 K.

However, above 500 K, the geometric quantum discord is larger than the entropic one and it can survive up to 9540 K, thousands of kelvins above room temperature and above the entropic quantum discord. These are the highest temperatures that have been reported in the literature wherein quantum correlation can be supported in solid state systems [2]. This means that the quantum correlations in this material are very stable and survive up to the temperatures at which the material exists: 523 K [157]. It is important to emphasize that these results are only possible because of the engineered metal–carboxylate compound and its syn–syn conformation, which leads to a strong magnetic interaction ($J = -748.5$ K). Therefore, carboxylate-based molecular magnets are one path toward achieving stable quantum correlations at room temperature.

5.4 Partial Conclusions

In summary, our aim was to provide an engineered material with high stability of its quantum correlations against external perturbations. The dinuclear copper(II) metal–organic framework complex $Cu_2(HCOO)_4(HCOOH)_2(C_4H_{10}N_2)$ was successfully synthesized, and its crystalline structure was characterized by single-crystal X-ray diffraction. From the crystal structure and the plot of $\chi T(T)$, it was possible to extract a magnetic interaction map, where each possible interaction was analyzed and compared with the results obtained by describing its crystal structure, and where we identified the profile of a strong antiferromagnetic arrangement at high temperatures between the metal centers, interpreted as a negative intra-dimer short-range interaction ascribed to the distances between the metal centers. In this way, we construct a model with the intention of describing its magnetic behavior from the measurement of its magnetic susceptibility, where the optimized parameters were obtained from the fitting of $\chi T(T)$. Finally, the quantum correlations were analyzed based on the magnetic model. We found that geometric quantum discord was significantly different from zero (10^{-3}) up to 9540 K, while the entropic one shows the existence of quantum correlations up to 2320 K, even when the entanglement is absent. It is worth noting that we identified pure states up to 80 K, close to the liquid nitrogen temperature.

This prototype material has been achieved only after successful material engineering to ensure the highest exchange interaction between spin-1/2 Cu ions into a dimeric

structure. The core element to this realization is the carboxylate group, which yielded a very short and direct metal-to-metal extraordinarily high magnetic interaction, leading the material to be almost immune to thermal decohering mechanisms. Therefore, the study of metal–organic frameworks, such as carboxylate-based molecular materials, can now open a new and exciting prospect for research in quantum information processing toward the limits of quantum mechanics in macroscopic materials, leading to promising applications in quantum information science such as the development of novel candidate platforms for the processing and transmission of quantum information.

6 Influence of the External Pressure on the Quantum Correlations of Molecular Magnets

In this chapter we proceed presenting the results of this thesis and show that the degree of correlation in a spin cluster system can be affected by the structural parameters by applying external hydrostatic pressure. We performed first-principles calculations to investigate the dependence, under external pressure, of the magnetic coupling constant of the metal–silicate framework $KNaCuSi_4O_{10}$ [33]—a Heisenberg dimer with a d^9 electronic configuration. From this we obtain the entropic quantum discord and the entanglement of formation as a function of its magnetic susceptibility. Our results show that it is possible to manipulate the degree of quantum correlation in a magnetic system inducing a structural contraction by applying an external pressure. This leads to a better management of the quantum properties of these systems and facilitates experimental and theoretical research of quantum correlations via first principles.

6.1 Material Description

Using the Density Funtional Theory (DFT), we performed first-principles calculations to investigate the dependence of the magnetic coupling constant of a well-known low-dimensional molecular magnetic system, a metal–silicate framework $KNaCuSi_4O_{10}$ [33, 216–218], under external pressure to evaluate the influence on the quantum correlations obtained as a function of the magnetic susceptibility of this compound.

This compound was chosen because it has synthetic analogs to the naturally occurring mineral litidionite[1] (Fig. 6.1)—a Cu^{2+} dimer, i.e., with a d^9 electronic configuration, this material is an ideal realization of a spin-1/2 dimer, and therefore it is an

---

[1] This name was given by Scacchin in the 1980s because of its very small crystals associated with glass of the same color found in the crater of the Vesuvius volcano [33].

ideal realization of a two-qubit system under which we calculate the thermal quantum correlations described in Chapter 3.

Figure 6.1: Lithionite (KNaCuSi$_4$O$_{10}$), a mineral found in the Vesuvius volcano, Campania region, in the Gulf of Naples, Italy (font:`http://www.catalogomultimediale.unina.it/wp-content/uploads`).

Its crystal structure was first determined in Ref. [216] and it was successfully synthesized in Refs. [33, 217, 218]. The crystal structure consists of complex silicate chains interconnected by edge-sharing CuO_5 square pyramids dimerized in Cu$_2$O$_8$ units [33]. These dimers are magnetically isolated from each other, separated by two SiO$_4$ corners. According to Ref. [33], there is only one crystallographically independent metal position, because the center of the triclinic cell inversion is at the midpoint of the metal–metal bond; with the square pyramid distorted, litidionite exhibits a typical Jahn–Teller distortion, as expected from Cu^{2+} ions in a d^9 electronic configuration [33].

6.2 First-Principles Calculations on KNaCuSi$_4$O$_{10}$

In order to obtain the properties of KNaCuSi$_4$O$_{10}$, this problem was approached by using the computational quantum mechanical modeling method of DFT [54, 69, 71], one of the most popular and versatile methods available in condensed matter physics. The calculations were performed at the National Center for High Performance Processing in São Paulo (CENAPAD-SP), in collaboration with the State University of

Feira de Santana (UEFS) and the Federal University of Bahia (UFBA).

By using the Density Functional Theory [71] in the generalized gradient approximation (GGA), the exchange and correlation function can be written generically as

$$E_{\mathcal{XC}}^{GGA}[n] = \int f\left[n(\vec{r}),\nabla n(\vec{r})\right]\lceil^3 r. \tag{6.1}$$

where $f\left[n(\vec{r}),\nabla n(\vec{r})\right]$ is a parametrized analytic function, whose expression is not unique [54,69]. Therefore, in the literature, there are several types of functional $f\left[n(\vec{r}),\nabla n(\vec{r})\right]$ [219] with the Perdew-Burke-Ernzerhof parametrization for the exchange-correlation functional $V_{\mathcal{XC}}[n_s(\vec{r})]$ [219–224]. The so called PBE functional has no empirical parameters and is considered one of the most accurate, so it is widely used in electronic structure calculations [54,69]. The Kohn–Sham equations as presented on Chapter 2, Eq. (2.57), were solved by using the plane-wave pseudopotential method as implemented in the Quantum ESPRESSO software [74], using the CENAPAD facilities in collaboration with UEFS and UFBA. The plane-wave energy cutoff was 47.5 Ha for the wavefunction and 237.5 Ha for the charge density. The k-point sampling of the Brillouin zone was done with a $5 \times 5 \times 5$ grid following the Monkhorst–Pack scheme [225] and with a Marzari–Vanderbilt smearing width of 5×10^{-4} Ha [226].

Therefore, from these parameters, the crystal structure was optimized at each volume of the unit cell. During the ionic relaxation, all positions were relaxed until Hellmann–Feynman forces were <0.05 Ha/bohr and the total energy converged to <5 $\times$ 10^{-6} Ha with respect to the Brillouin zone integration.

The equation of state (EOS) of the KNaCuSi$_4$O$_{10}$ compound was obtained by fitting the total energy as a function of volume to the third-order Birch–Murnaghan equation of state [227]:

$$P(V) = \frac{3B_0}{2}\left[\left(\frac{V_0}{V}\right)^{\frac{7}{3}} - \left(\frac{V_0}{V}\right)^{\frac{5}{3}}\right]\left\{1 + \frac{3}{4}\left(B_0' - 4\right)\left[\left(\frac{V_0}{V}\right)^{\frac{2}{3}} - 1\right]\right\}, \tag{6.2}$$

where P, V_0, B_0, and B_0' are the pressure, equilibrium volume, bulk modulus at ambient pressure, and the pressure derivative of the bulk modulus at ambient pressure, respectively. The values found for the parameters were as follows: $V_0 = 3271$ a.u., $B_0 = 54.1$ GPa, and $B_0' = 3.3$. At each volume, we obtained the energies

$$E(V) = E_0 + \frac{9V_0B_0}{16}\left\{\left[\left(\frac{V_0}{V}\right)^{\frac{2}{3}} - 1\right]^3 B_0' + \left[\left(\frac{V_0}{V}\right)^{\frac{2}{3}} - 1\right]^2\left[6 - 4\left(\frac{V_0}{V}\right)^{\frac{2}{3}}\right]\right\}. \tag{6.3}$$

The values found for these parameters were the following: $V_0 = 3271$ Bohr^3, $B_0 = 54.1$ GPa and $B_0' = 3.3$ GPa. Figure 6.2 shows the structural optimization curve, i.e., results for the total energy versus volume of the unit cell obtained for DFT calculations and fitted by the third-order Birch–Murnaghan equation of state (Eq. (6.3)).
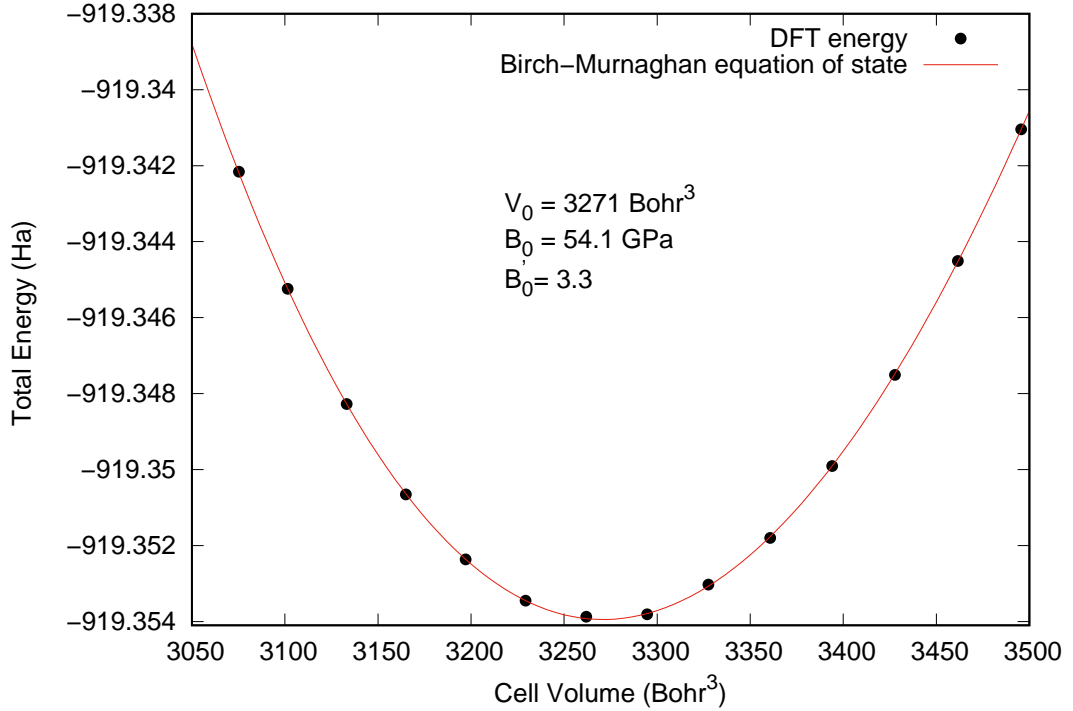

Figure 6.2: Total energy versus cell volume for KNaCuSi$_4$O$_{10}$ calculated by using DFT and fitted with the third-order Birch–Murnaghan equation of state.

For a Heisenberg spin-1/2 dimer there are two eigenvalues of energy, one being E_T for the triplet state and the other being E_S for the singlet state of the dimeric unit. Hence, its magnetic coupling constant (J) is the difference between these two states, $J = E_S - E_T$. On the other hand, the Hohenberg-Kohn theorem asserts that the total energy of a system is a functional of the charge density. Thus, we have used this theorem along with the Kohn-Sham scheme to calculate the total energy for each spin alignment for several volumes and fitted them by using the above equation of state. Based on such a procedure, it is possible to write the total energy as a function of pressure and we can therefore calculate the other physical quantities from first principles accordingly.

By calculating the energies in Eq. (6.3) for each configuration it is possible to obtain the magnetic coupling for different values of pressure using first principles calculations. Consequently, it was possible to obtain the magnetic coupling for different values of hydrostatic pressure using first principles calculations, as can be seen from Table 6.1;

in addition, the temperature of entanglement (T_e), Eq. (3.72), was obtained from these values of the exchange parameters.

Table 6.1: Summary of the parameters obtained by first principles calculations: exchange parameter (J), lattice parameter (a), volume of unit cell (V), and pressure applied (P); as well as the threshold temperature of entanglement (T_e) obtained from the values of the exchange parameters.

J(K)	a(Bohr)	V(Bohr^3)10^3	P(GPa)	T$_e$(K)
-2.86	—	—	$\sim10^{-4}$	2.60
-2.91	13.053	3.229	0.708	2.648
-2.03	12.966	3.164	1.881	1.847
-1.40	12.923	3.133	2.499	1.274
-1.03	12.879	3.101	3.141	0.937
-0.45	12.842	3.075	3.692	0.41
1.09	12.778	3.029	4.696	—
2.38	12.769	3.023	4.845	—

As can be seen from Table 6.1, as we increase the hydrostatic pressure in the system, we decrease the lattice parameter (a) and volume of the unit cell (V). However, by applying hydrostatic pressure, the exchange parameter of the system increases and becomes positive, i.e., the system ceases to be ordered antiferromagnetically (an entangled ground state) and becomes ferromagnetically ordered (a separable ground state) and due to this there is no entanglement between the metallic centers. Hence, the temperature of entanglement decreases with the increase of the hydrostatic pressure in the system (see Table 6.1). It is thus possible to increase the maximum temperature below which the system is entangled by reducing the external hydrostatic pressure.

6.2.1   Quantum Correlations as a Function of Temperature and Pressure

The external pressure applied on a molecular magnetic system induces a structural contraction that reduces its lattice parameters, leading to strengthening or weak-

ening of the magnetic coupling of the system, owing to its strong dependence on the structural properties of the sample material. For the prototype material KNaCuSi$_4$O$_{10}$, its magnetic coupling constant (J) increases and becomes positive, i.e., the system changes from an antiparallel alignment ($J < 0$, the entangled ground state) to a parallel alignment ($J > 0$, the separable ground state) from the application of external pressure, as can be seen in Fig. 5.4(a). Hence, we obtain the threshold temperature (T_e), Eq. (3.72), using the magnetic coupling constant. Figure 5.4(b) shows the dependence of T_e for the prototype compound under pressure. As can be seen, the change in magnetic alignment leads to a decrease of T_e down to the disappearance of the entanglement (see Fig. 6.3(b)), when the system achieves a parallel alignment. This means that the degree of entanglement in a magnetic system can be controlled by significant macroscopic effects when applying external pressure.

On the other hand, in order to evaluate the influence of external pressure on the quantum correlations, we calculate the magnetic susceptibilities, Eq. (2.43), for the spin-1/2 Heisenberg dimer from each magnetic coupling constant presented in Fig. 6.3(a). By using Eqs. (3.74) and (3.112), it is possible to evaluate the quantum correlations as a function of these susceptibilities. We obtain the quantum correlation curves measured by this thermodynamic property for each magnetic configuration of the system. In this way, we establish a relationship between the quantum properties and macroscopic effects.

Fig. 6.4 shows the entropic (Eq. (3.112)) and geometric (Eq. (3.133)) quantum discords, as well as the entanglement of formation (Eq. (3.74)) as a function of temperature. These curves are calculated for different values of the exchange parameter J, as presented in Table 6.1. Owing to this change of the sign of the exchange parameter, there is a gap in the correlations that maximize the quantum correlation in the system and it can be achieved by reducing the external hydrostatic pressure. From the entanglement of formation (see Fig. 6.4(c)), we can verify that the system remains entangled up to its temperature of entanglement (see Table 6.1) when the entanglement drops to zero. However, the calculations of entropic and geometric quantum discord reveal that this system remains quantum correlated even when the entanglement is absent, even in a separable ground state; i.e., despite the absence of entanglement, the quantum discord is not zero. In this way, Figs. 6.5(a), (b), and (c) show the entanglement of formation ((Eq. 3.74)) and the entropic discord (Eq. (3.112)) and geometric quantum discord (Eq. (3.133)) curves as a function of temperature and pressure, respectively. Note that the
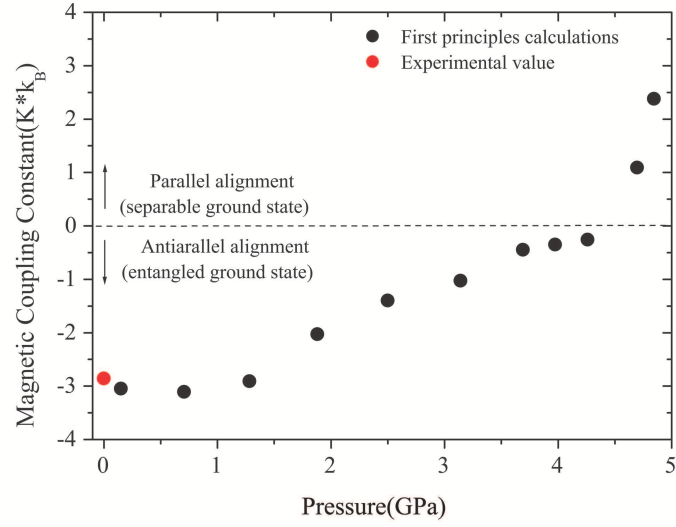
(a)
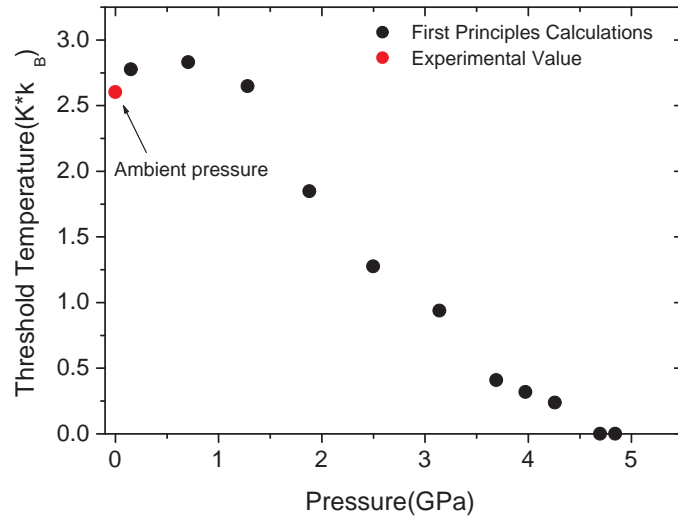
(b)

Figure 6.3: (a) Magnetic coupling constant and (b) threshold temperature of entanglement T_e, Eq. (3.72), obtained in terms of the external pressure. The red circle is the experimental value obtained at ambient pressure taken from Ref. [33]. The external pressure induces a structural contraction on the prototype material, leading to a change of the magnetic alignment of the system. This change yields a decrease in the degree of entanglement by reducing T_e.

degree of quantum correlations in the system decreases by increasing the external pressure as a consequence of the changes of the magnetic coupling constant, as shown in Fig. 6.3(a). Also remarkable is the management of the ground state in the system by reducing the temperature and controlling the external pressure; it achieves this state when the entropic discord (Fig. 6.5(a)) and entanglement (Fig. 6.5(b)) reach the maximum value of unity. As pointed out before, the system changes from the entangled ground state to a separable one owing to the changes of the magnetic configuration of the system induced by the external pressure. This is reflected in the quantum correlations when entanglement goes to zero (see Fig. 6.5(b)); i.e., system reaches the threshold temperature $T = T_e$, Eq. (3.72). Hence, a minimization of the quantum discord in the system is obtained (see Fig. 6.5(a)). However, it remains significantly different from zero even in separable states when the entanglement is absent, as can be seen in Fig. 6.5(a). In this way, we can control the quantum correlations of this molecular magnet by means of macroscopic properties such as temperature and pressure.

Therefore, the structural contractions of the system, achieved by increasing the external pressure, leads to a change in the magnetic configuration of the system, as can be seen in Fig. 6.3. As a consequence, the quantum correlations (Fig. 6.5) are drastically affected, because these quantum properties are directly related to the magnetic behavior of the system (Eqs. (3.74), (3.112), and (3.133)). Therefore, it is possible to manage the degree of quantum correlation in a magnetic system by the control of external pressure and temperature. Furthermore, this external pressure can be achieved experimentally by reducing the lattice parameter of the system by chemical substitution or hydrostatically, for example. This result can open up great opportunities for research in experimental detection and manipulation of quantum correlations. It allows a better understanding of the quantum properties of molecular magnets by the management of significant macroscopic properties, leading to promising applications in quantum information science such as the development of novel candidate platforms for quantum information processing by means of materials engineering.
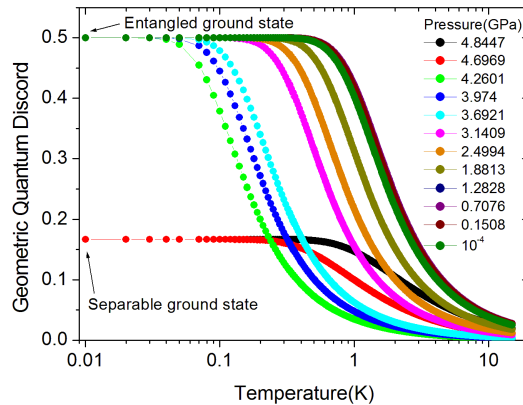
6.3   Partial Conclusions

In summary, we performed first-principles calculations to investigate the de-
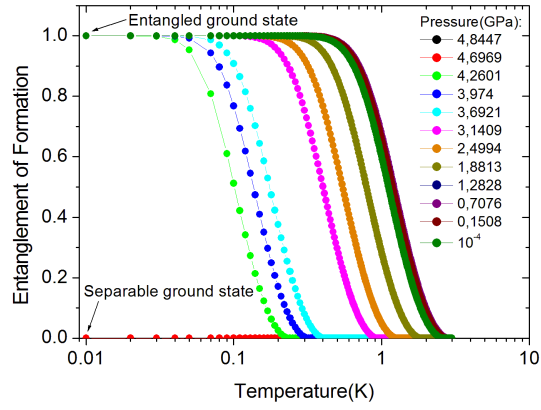
(a)
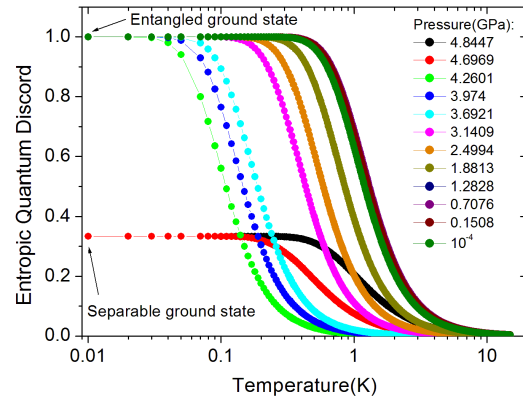
(b)

(c)

Figure 6.4: Temperature dependence of entropic (a) and geometric (b) quantum discords, as well as the entanglement of formation (c) calculated for each value of magnetic coupling constant J obtained by first-principles calculations (see Fig. 6.3). By applying hydrostatic pressure, the system changes from the entangled ground state to a separable ground state, yielding a gap in the correlations; in spite of that, the quantum discord reveals that this system remains quantum correlated even when the entanglement is absent.
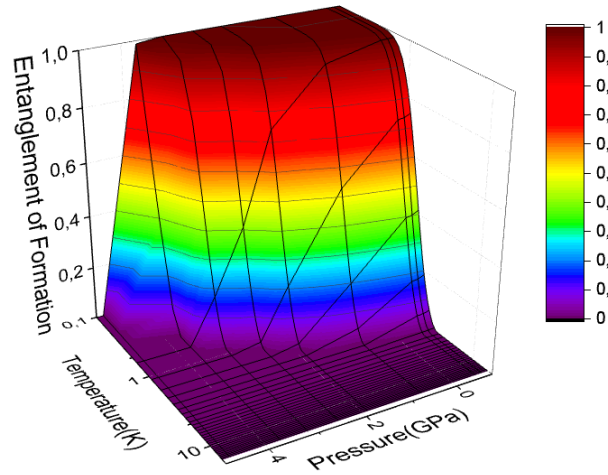
(a)
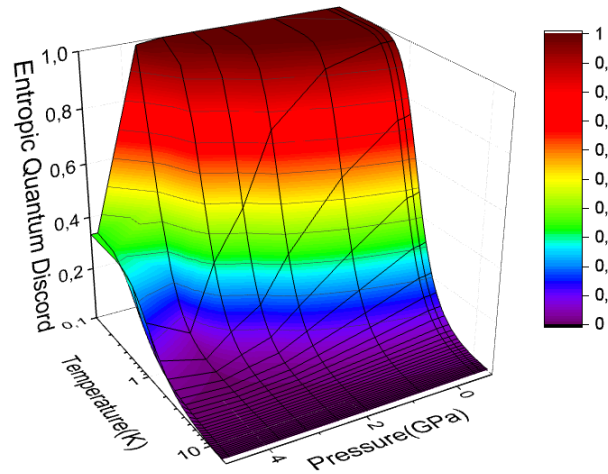
(b)
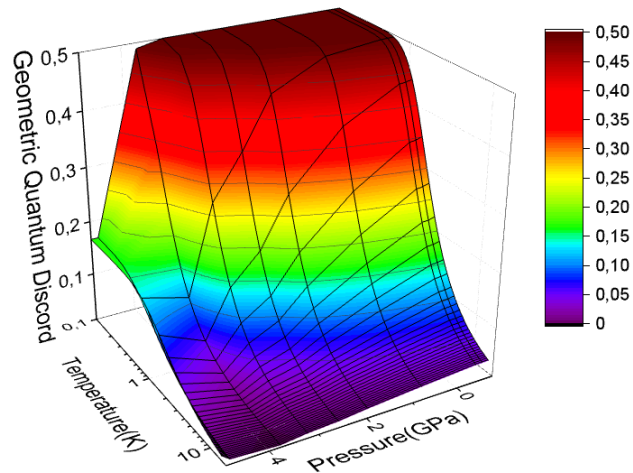
(c)

Figure 6.5: (a) Entanglement of formation and (b) entropic and (c) geometric quantum discord as a function of the temperature and pressure. It is worth noting that it is possible to manage the degree of quantum correlation in a magnetic system by controlling the external pressure and temperature.

pendence under hydrostatic pressure of the quantum correlations of the metal–silicate framework $KNaCuSi_4O_{10}$ compound, which is a Heisenberg dimer in a $3d^9$ electronic configuration, an ideal realization of a two-qubit system (spin-1/2 dimer). We observed that increasing the external hydrostatic pressure induces a structural contraction of the prototype material, leading to a change of its magnetic alignment. This change yields a minimization on the degree of quantum correlations in the system, because the system changes from an antiparallel alignment (entangled ground state) to a parallel alignment (separable ground state), induced by the sign of the magnetic coupling constant. In spite of that, the entropic and geometric quantum discords reveal that this system remains quantum correlated even when the entanglement is absent.

Our results have shown that the degree of correlation in a spin cluster system can be affected by applying external hydrostatic pressure, demonstrating that quantum correlations of a molecular magnetic system, such as the metal–silicate framework $KNaCuSi_4O_{10}$, are related to significant macroscopic effects, such as an external hydrostatic pressure, leading us to better control of quantum correlations in solid state systems by means of materials control and engineering. Our results enable better management of the quantum properties in magnetic systems and provides opportunities for experimental and theoretical research of quantum correlations in these systems via first principles, leading to a better understanding of their quantum properties with promising applications in emerging quantum technologies.

7 Quantum Correlations in a Heisenberg Spin Dimer via Neutron Scattering

In the present chapter, we show analytical expressions for the entanglement witness, entanglement of formation, and geometric quantum discord, based on the Schatten 1-norm as a function of quantities typically obtained in neutron scattering via a scalar structure factor. Our results provide one path toward identifying the presence of quantum correlations in a molecular magnet such as a Heisenberg spin-1/2 dimer by using diffractive properties of single crystal magnetic scattering. This is an alternative way to describe the quantum properties of a sample material via neutron scattering experiments, without making any assumption about their macroscopic quantities, leading to promising applications in quantum information science.

7.1 Neutron Scattering for a Heisenberg Spin Dimer

The study of the magnetic properties of molecular materials is typically done by approximating magnetic parameters of a Hamiltonian model by the fit of some thermodynamic properties, such as magnetic susceptibility, internal energy and specific heat [2, 23, 30, 31, 31, 43]. In this context, correlation functions have great importance in describing these properties; in addition, they can be directly measurable, e.g., in neutron scattering experiments via *structure factors*. Structure factors can be defined as two-point correlations [88] and are widely used to describe the crystal structure of molecular systems ruled by Hamiltonians [88, 228, 229], e.g., Heisenberg models [23].

Quantum information quantifiers are expressed in terms of statistical correlation functions [2, 34, 66], due to the fact that these functions are present in the elements of the density matrix of the quantum system, linking their macroscopic properties with the quantum ones. Therefore, it is possible to quantify the presence of quantum correlations

in a system via structure factors [12, 22, 87, 88], since these factors are directly associated to the correlation functions; thus allowing the measurement of quantum information quantifiers by neutron scattering experiments.

Inspired by the papers of Cramer [22] and Marty [87], in which the structure factor of inelastic neutron scattering in condensed matter systems was associated with an entanglement witness, we show that it is possible to quantify the presence of quantum correlations through structure factors obtained through inelastic neutron scattering. We provide one path toward identifying the presence of quantum correlations in a two-qubit system, only using diffractive properties of inelastic neutron scattering without making any assumption about its macroscopic properties or the external conditions under which the neutrons are scattered, being an alternative way to describe the quantum properties of a two-qubit system via neutron scattering experiments.

As discussed in Chapter 2 and Section 2.2.5, for a given Hamiltonian model, one can evaluate the inelastic structure factor. Let us consider a molecular magnet as an interacting pair of spin-1/2 particles ruled by the Heisenberg–Dirac–Van Vleck Hamiltonian, Eq. (2.1), an ideal realization of a two-qubit system, and, therefore, a promising platform in quantum information processing. The so-called scalar neutron scattering structure factor, Eq. (2.82), allows a sensitive test of the assumed Hamiltonian model, since its properties are affected by the relative positions of the metallic centers of a sample material [43].

For the system ruled by the Hamiltonian of, Eq.(2.1), from the relation

$$\bar{\mathcal{S}}(\vec{q}) = \sum_{\alpha,\beta} \mathcal{S}^{\alpha\beta}(\vec{q}) = \sum_{\alpha,\beta} \sum_{l,m} e^{i\vec{q}\cdot(\vec{r_l}-\vec{r_m})} \langle S_l^{\alpha} S_m^{\beta} \rangle. \tag{7.1}$$

by using Eq.(2.71) the pairwise spin correlation function can be extracted and written as

$$\mathcal{C}^{\alpha\alpha} = \sum_{q} e^{-i\vec{q}\cdot\vec{r}_{l,m}} \mathcal{S}^{\alpha\alpha}(\vec{q}) \tag{7.2}$$

In this way, the correlations can be accessed through diffractive properties obtained via neutron scattering experiments, without making any assumption about the macroscopic properties of the target system, such as its magnetic susceptibility or specific heat, or about the external conditions under which the neutrons are scattered, such as temperature or magnetic field. Given the Hamiltonian model, it is possible to predict the scalar structure factor, which can be compared to the neutron scattering experimental results [43], as widely discussed in Chapter 1.

7.2 Quantum Information Theoretical Quantifiers in a Heisenberg Spin Dimer

In this section, we will present the analytical expressions for quantum informa-
tion quantifiers, such as entanglement witness, entanglement of formation, and geometric
quantum discord, based on the Schatten 1-norm as a function of quantities typically ob-
tained in neutron scattering via the scalar structure factor, allowing their measurement
via neutron scattering experiments.

7.2.1 Spin-Spin Correlation Function

Correlation functions have a great importance in statistical physics and quan-
tum mechanics, allowing us to find different properties of a physical system. In addition,
they can be directly measurable, e.g., in scattering experiments [66]. Quantum infor-
mation quantifiers are expressed in terms of statistical correlation functions [2, 34, 66],
because these functions are present in the elements of the density matrix of the quantum
system, linking their macroscopic and structural properties with the quantum ones.

For the system ruled by the Hamiltonian of Eq. (2.1), from Eqs. (7.1) and
(2.71) the spin–spin correlation function can be extracted and written in terms of inte-
grated structure factor as

$$\mathcal{C} \;=\; \langle S_1^\alpha S_2^\alpha \rangle = e^{-i\vec{q}\cdot(\vec{r_1}-\vec{r_2})} \mathcal{S}^{\alpha\alpha}(\vec{q}), \tag{7.3}$$

where $\alpha = x,y,z$.

Therefore, spin–spin correlation function can be accessed through diffractive
properties obtained via neutron scattering experiments, without making any assumption
about the macroscopic properties of the measured system or the external conditions under
which the neutrons are scattered.

The density matrix of the Heisenberg spin-1/2 dimer has the Gibbs form
$\rho(T) = e^{-\mathcal{H}/k_B T}/Z$ [2, 23, 34, 66], where $Z = \text{Tr}\{e^{-\mathcal{H}/k_B T}\}$ is the partition function. By
disregarding spontaneous symmetry breaking, the reduced density matrix at sites labeled
as 1 and 2 in the computational basis $\{|00\rangle,|01\rangle,|10\rangle,|11\rangle\}$ can be written on the Bell's

diagonal mixed state [34,66]:

$$\rho_{12} = \frac{1}{4} \begin{bmatrix} 1+\mathcal{C} & & & \\ & 1-\mathcal{C} & 2\mathcal{C} & \\ & 2\mathcal{C} & 1-\mathcal{C} & \\ & & & 1+\mathcal{C} \end{bmatrix}, \tag{7.4}$$

$$= \frac{1}{4}(1 + \mathcal{C}\vec{S}_1 \otimes \vec{S}_2), \tag{7.5}$$

where $\mathcal{C} = \langle S_1^x S_2^x \rangle = \langle S_1^y S_2^y \rangle = \langle S_1^z S_2^z \rangle$ is the Heisenberg dimer spin–spin correlation function, that using Eq. (2.82) can be written as a function of the scattering vector, $\vec{q} = \vec{k}_{out} - \vec{k}_{in}$, i.e., the difference between the final and the initial wave vectors, and the difference between the position vectors $\vec{r_1}$ and $\vec{r_2}$ of the metallic centers,

$$\mathcal{C} = \frac{e^{-i\vec{q}(\vec{r_1}-\vec{r_2})}}{2}\left[1 - \cos(\vec{q}\cdot(\vec{r_1} - \vec{r_2}))\right]. \tag{7.6}$$

This last ranges from $-1 \leq \mathcal{C} \leq 0$ for antiparallel magnetic alignment ($J < 0$, the entangled ground state) and $0 < \mathcal{C} \leq 1/3$ for parallel magnetic alignment ($J > 0$, the separable ground state) [2,34,66].

The spin–spin correlation function, Eq. (7.6), is depicted in Fig. 7.1 as a function of the scattering vector $\vec{q}$ times the distance between the metallic centers of a sample material, $\vec{r_1} - \vec{r_2}$, which can be obtained by neutron scattering experiments. It is worth noting that the location of the zero-point correlation can provide a convenient estimate from which distances in the system can be found in an antiparallel magnetic alignment ($\pi q^{-1}/2 \leq r_1 - r_2 \leq 3\pi q^{-1}/2$) or a parallel magnetic alignment ($0 < r_1 - r_2 < \pi q^{-1}/2$ and $3\pi q^{-1}/2 < r_1 - r_2 < 2\pi q^{-1}$), without any assumption about macroscopic quantities, such as the temperature, magnetic field, magnetic susceptibility, internal energy, or specific heat. This result has great importance in guiding us through the study of quantum information quantifiers in a Heisenberg spin dimer, because these quantifiers depend directly on the spin–spin correlation function.

7.2.2   Entanglement Witness

The detection of entanglement is usually done using an observable which identifies the presence of entanglement in a quantum system [4, 29, 36, 115]. As mentioned in Section 3.1, an entanglement witness is an useful tool to identify the presence of entanglement, since it can tell us whether, for the condition given by Eq. (3.35), a given
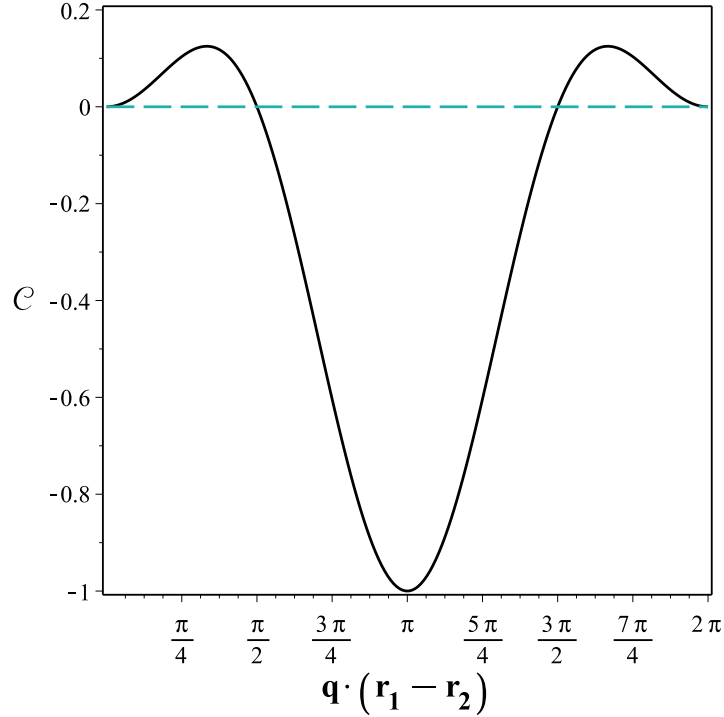
Figure 7.1: Spin–spin correlation as a function of $\vec{q} \cdot (\vec{r_1} - \vec{r_2})$, Eq. (7.6). The dashed (green) horizontal line separates the regions with antiparallel magnetic alignment ($\pi/2 \leq \vec{q} \cdot (r_1 - r_2) \leq 3\pi/2$) and parallel magnetic alignment ($0 < \vec{q} \cdot (r_1 - r_2) < \pi/2$ and $3\pi/2 < \vec{q} \cdot (r_1 - r_2) < 2\pi$).

quantum system is entangled. If Eq. (3.35) is violated, the system's state is entangled; otherwise, if Eq. (3.35) is satisfied, we cannot state with certainty that the system's state is separable.

As widely discussed on Chapter 3, magnetic susceptibility was proposed as a thermodynamical entanglement witness [4, 29, 36, 115]. For a system in which $[\mathcal{H}, S_z]$ the average magnetic susceptibility in a complete separable state satisfies [29, 36]

$$\bar{\chi} = \frac{\chi_x + \chi_y + \chi_z}{3} \leqslant \frac{(g\mu_B)^2 NS}{3k_B T}, \tag{7.7}$$

where N is the number of magnetic ions with spins-S, k_B is the Boltzmann constant, μ_B is the Bohr magneton, g is the Landé factor, and $\bar{\chi}$ is the average of the magnetic susceptibility.

As calculated by Wieśniak, Vedral and Brukner in the reference [36], the entanglement witness can be calculated in terms of the average magnetic susceptibility. In reference [230], the magnetic susceptibility of an antiferromagnetic spin-1/2 chain is compared to the correlation function measured by neutron diffraction [25]. Consequently,

we can analytically calculate the entanglement witness for a molecular magnet such as a Heisenberg spin-1/2 dimer in terms of its scalar structure factor using Eq.(7.6) as

$$\begin{aligned} \mathbb{W} & = 2 + 3e^{-i\vec{q}(\vec{r_1} - \vec{r_2})}\mathcal{S}(\vec{q}) \\ & = 2 + \frac{3e^{-i\vec{q}(\vec{r_1} - \vec{r_2})}}{2}\left[1 - \cos(\vec{q}\cdot(\vec{r_1} - \vec{r_2}))\right]. \end{aligned} \tag{7.8}$$
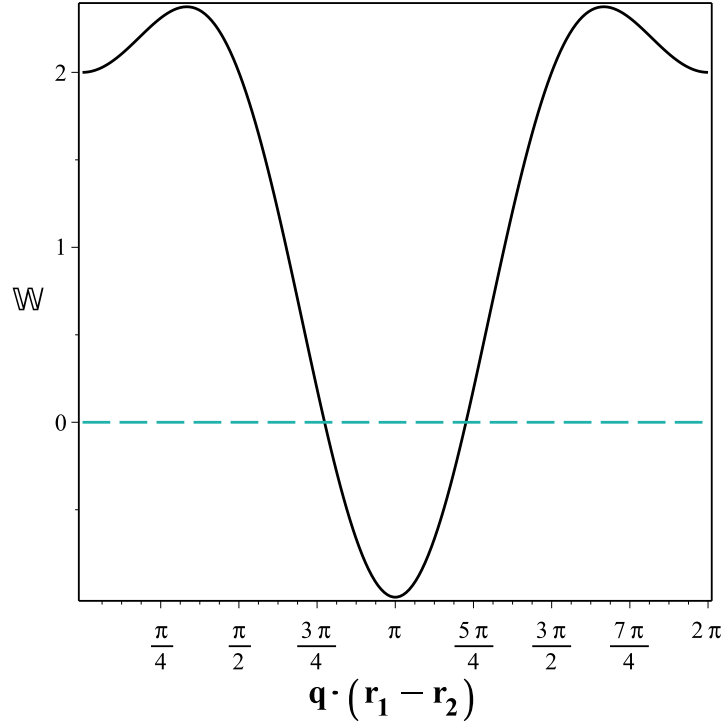

Figure 7.2: Entanglement witness of a Heisenberg spin dimer, Eq.(7.8). The dashed (green) horizontal line separates the region where the witness has a negative expectation value, i.e., the system is in an entangled quantum state $2.45 < \vec{q}\cdot(\vec{r_1} - \vec{r_2}) < 3.85$.

In Fig. 7.2, we show the entanglement witness for a Heisenberg spin dimer, Eq. (7.8), as a function of $\vec{q}\cdot(r_1 - r_2)$. The witness has a negative expectation in the range $2.45 < \vec{q}\cdot(\vec{r_1} - \vec{r_2}) < 3.85$, revealing the presence of entangled states. This result is compatible with the last ones, because in this band the system is found in an antiparallel magnetic alignment (entangled ground state), as can be seen in Fig. 7.1. We have thus provided one way to identify the presence of entanglement in a molecular magnet, such as a Heisenberg spin dimer, by using diffractive properties obtained via neutron scattering experiments, without making any assumption about macroscopic quantities.

7.2.3   Entanglement of Formation

In order to quantify the amount of entanglement in the Heisenberg spin-1/2 dimer and make a comparison with the entanglement witness, we will adopt the measurement of *entanglement of formation* defined by [128, 129]

$$\mathbb{E} = -\Gamma_+ \log_2\left(\Gamma_+\right) - \Gamma_- \log_2\left(\Gamma_-\right), \tag{7.9}$$

with

$$\Gamma_\pm = \frac{1 \pm \sqrt{1 - \mathbb{C}^2}}{2}, \tag{7.10}$$

where $\mathbb{C}$ is the concurrence [4,65,128,129]. The concurrence can be written as a function of the scalar structure factor, Eq.(**??**), in terms of spin-spin correlation function, Eq.(7.6), as follows:

$$\mathbb{C} = \max\left[0, -\frac{1}{2}\left(1 + 3e^{-i\vec{q}(\vec{r_1} - \vec{r_2})}\mathcal{S}(\vec{q})\right)\right]. \tag{7.11}$$

The equation above shows that the concurrence of a Heisenberg spin-1/2 dimer is also related to the diffractive properties, which can be obtained by neutron scattering experiments.

In sequence, we show in Fig. 7.3 (a) the entanglement of formation as a function of the scattering vector $\vec{q}$ times the distance between the metallic centers $\vec{r_1} - \vec{r_2}$ of a Heisenberg spin-1/2 dimer, Eq.(7.9). It is possible to identify a maximum of entanglement at $r_1 - r_2 = \pi q^{-1}$, where the system is found in an antiparallel magnetic alignment with an entangled pure state. It is worth noting that there are entangled states at $2.0 \lesssim \vec{q} \cdot (r_1 - r_2) \lesssim 4.2$, above the band where the entanglement is identified on the entanglement witness. In Fig. 7.3 (b), we make a comparison between the entanglement of formation and the entanglement witness. As can be seen, the positive expectation value of the witness, separated by the dashed (green) line, does not imply separability. However, the negative expectation value necessarily implies the presence of entangled quantum states in the system.

7.2.4   Geometric Quantum Discord

Despite quantum entanglement providing one path toward finding pure quantum correlations, it does not encompass all quantum correlations in a system. The
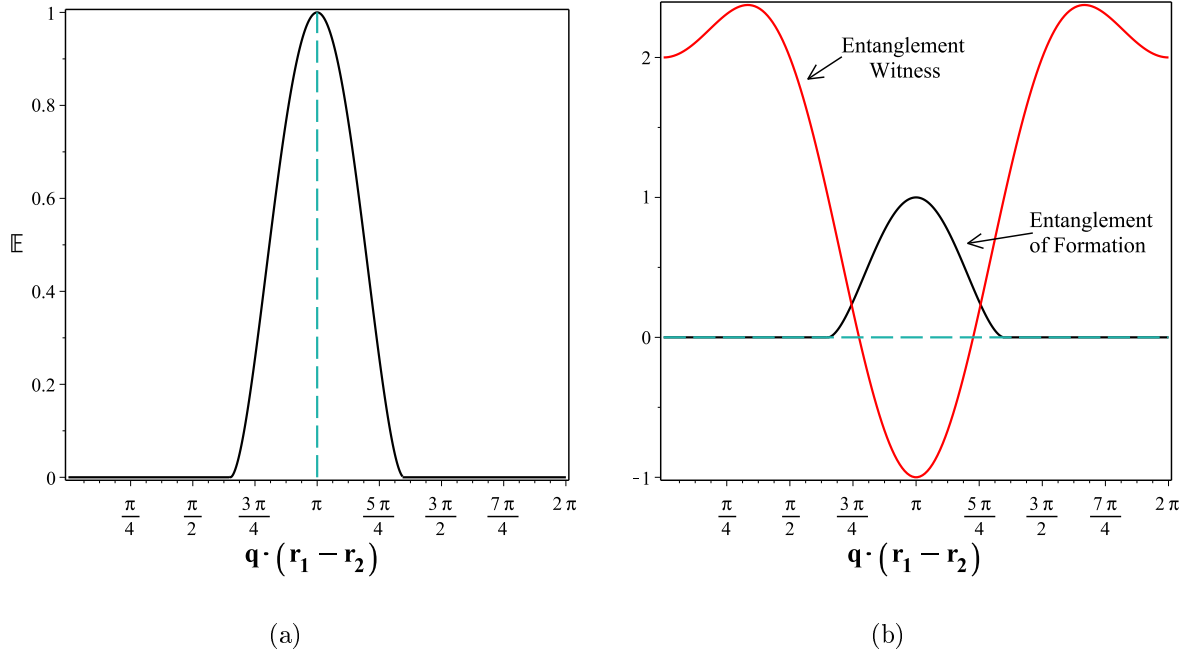
Figure 7.3: (a) Entanglement of formation as a function of $\vec{q} \cdot (\vec{r_1} - \vec{r_2})$, Eq.(7.9). The dashed (green) vertical line highlights the maximum of entanglement, where the system is in an antiparallel magnetic alignment with an entangled pure state. (b) We make a comparison between the entanglement of formation and the entanglement witness. The dashed (green) horizontal line separates the region where the witness has a negative expectation value, i.e., the system is in an entangled quantum state.

measurement of the total amount of quantum correlations has been called *quantum discord* [2, 9–18, 148, 157].

As discussed in Chapter 3 the calculation of quantum discord is a rather complicated task, even for a two-qubit system, such as a Heisenberg spin-1/2 dimer [2, 157]. This fact has stimulated alternative measurements of quantum information theoretical quantifiers as the *geometric quantum discord* [2]. In this context, the geometric quantum discord, based on the Schatten 1-norm, is one path toward achieving a well-defined measurement of quantum correlations in a quantum system [2] and it can be defined as

$$\mathbb{Q}_G(\rho) = \min_{\omega} \|\rho - \rho_c\|, \tag{7.12}$$

where $\|X\| = \text{Tr}\left[\sqrt{X^\dagger X}\right]$ is the 1-norm, ρ is a given quantum state and ω is the set of closest classical-quantum states ρ_c [2, 18, 157], whose general form is given by

$$\rho_c = \sum_k p_k \Pi_k^{\{1\}} \otimes \rho_k^{\{2\}}, \tag{7.13}$$

with $0 \leq p_k \leq 1$ and $\sum_k p_k = 1$; $\{\Pi_k^{\{1\}}\}$ denotes a set of orthogonal projectors for

subsystem 1, and $\rho_k^{\{2\}}$ is a general reduced density operator for the subsystem 2 [18, 157].

Then, for a Heisenberg spin dimer, the geometric quantum discord, based on the Schatten 1-norm, can be written as a function of the scalar structure factor as:

$$\begin{aligned} \mathbb{Q}_G(\mathcal{S}) &= \left| \frac{1}{4} \mathcal{S}(\vec{q}) \right| \\ &= \left| \frac{1 - cos(\vec{q} \cdot (\vec{r_1} - \vec{r_2}))}{4} \right| . \end{aligned} \tag{7.14}$$
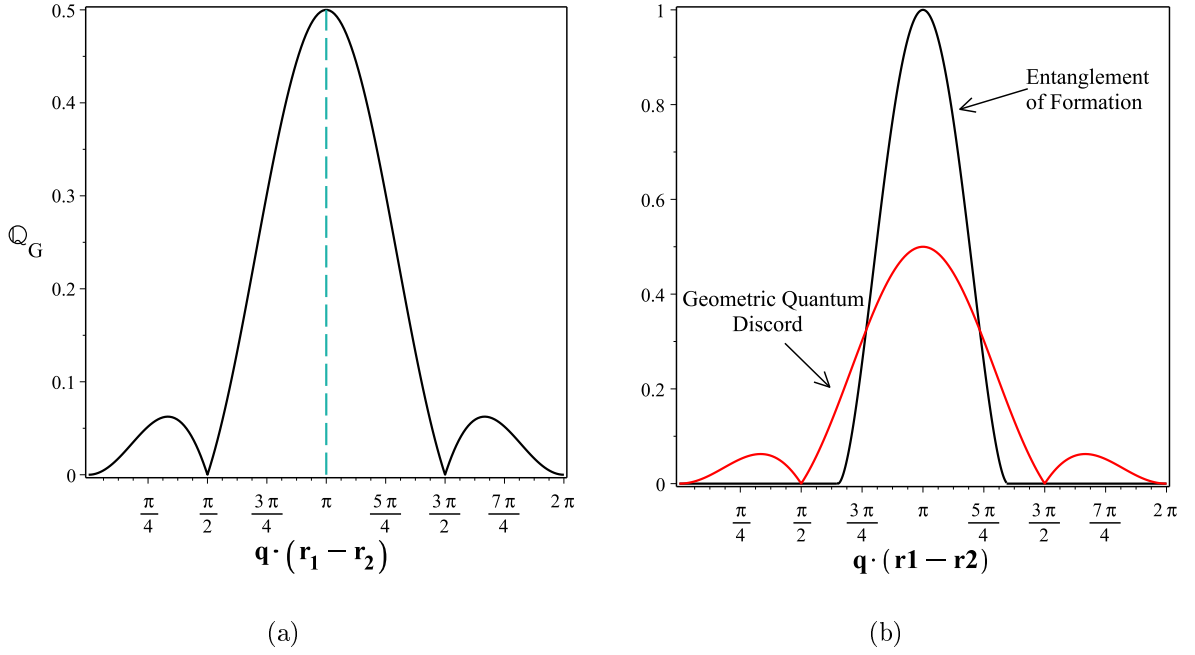

(a)   (b)

Figure 7.4: (a) Geometric quantum discord as a function of $\vec{q} \cdot (\vec{r_1} - \vec{r_2})$. The dashed (green) vertical line highlights the point where the system is in an antiparallel magnetic alignment with an entangled pure state. (b) Comparison between the geometric quantum discord and the entanglement of formation; it is possible to identify the presence of quantum correlations when the entanglement is absent and even when the system is found in a parallel magnetic alignment with a separable quantum state.

Fig. 7.4 (a) shows the geometric quantum discord as a function of the scattering vector $\vec{q}$ times the distance between the metallic centers, $\vec{r_1} - \vec{r_2}$, of the sample material, Eq. (7.14). We identify a maximum of quantum correlation at $r_1 - r_2 = \pi q^{-1}$. This is compatible with the previous results, where at this point the system is found in an entangled pure state (see Fig. 7.3(a)). Fig. 7.4(b) makes a comparison between the geometric quantum discord and the entanglement of formation. As can be seen, it is possible to identify the presence of quantum correlations when the entanglement is absent

and even when the system is found in a parallel magnetic alignment with a separable quantum state ($0 < \vec{q} \cdot (r_1 - r_2) < \pi/2$ and $3\pi/2 < \vec{q} \cdot (r_1 - r_2) < 2\pi$) (see Fig. 7.1); furthermore, the points of zero discord coincide with the points of zero correlation ($\pi/2$ and $3\pi/2$), indicating the absence of magnetic interaction ($J = 0$) between the magnetic ions.

Therefore, we have provided one way to find the geometric quantum correlations in a Heisenberg spin dimer by using diffractive properties obtained via neutron scattering experiments, without making any assumption about their macroscopic quantities.

7.3   Partial Conclusions

In summary, our main result was to provide to the literature analytical expressions for quantum information quantifiers, such as the entanglement witness, entanglement of formation, and geometric quantum discord as a function of quantities typically obtained in neutron scattering via a scalar structure factor. We provided one path toward identifying the presence of quantum correlations and quantum nonlocality in a two-qubit system such as a Heisenberg spin-1/2 dimer, using diffractive properties and without making any assumption about macroscopic properties or the external conditions under which the neutrons are scattered. We presented an alternative way to describe the quantum properties of a sample material via neutron scattering experiments. Our results open opportunities for the detection and manipulation of quantum correlations through neutron scattering experiments in magnetic systems, such as the molecular magnets ruled by Heisenberg Hamiltonians, leading to promising applications in quantum information science, since these materials can be promising platforms in quantum information processing.

8 General Conclusions and Outlooks

8.1 Conclusions

In this thesis we explore the potential of molecular magnetic systems to be prototype materials for quantum information technology, highlighting the design and characterization of isotropically coupled pairs of spin 1/2 particles, i.e., a molecular magnetic system in a d^9 electronic configuration such as Cu ions in the 2+ oxidation state. We addressed the detection and manipulation of quantum information quantifiers, such as entanglement of formation, entropic and geometric quantum discord by measuring the thermodynamic properties of solids, such as magnetic susceptibility, internal energy, specific heat, and, in addition we propose the measurement of magnetic neutron scattering data to the characterization of quantum correlations in low-dimensional molecular magnetic systems.

Our results strengthen the fact that molecular magnets may be somewhat immune to decohering mechanisms. In Chapter 5, we showed that carboxylate-based molecular magnets can support quantum correlations thousands of kelvins above room temperature. We provided an engineered material with a high stability of its quantum correlations against external perturbations, from which the entropic and geometric quantum discord, based on the Schatten 1-norm, was extensively explored. The analytical formulas for the quantum correlations were derived as a function of temperature by using the magnetic susceptibility of the compound and the analysis of the data suggests the existence of entanglement up to temperatures of 681 K, while the measure of quantum discord reveals that this system remains in the singlet ground state up to ~ 80 K. In addition, quantum correlations would remain up to 9540 K, thousands of Kelvin above room temperature, even without entanglement. As a result, we obtained very stable quantum correlations up to 513 K, the limit at which this material can exist—hundreds of Kelvin

above room temperature.

In Chapter 6, we showed that external pressure can induce structural contraction in a metal–silicate framework, leading to a change of its magnetic alignment and decreasing the degree of quantum correlations in the system. As a consequence, the ground state of this system can be handled by controlling the temperature and pressure. Therefore, the quantum properties of molecular magnetic systems can be controlled and manipulated by the management of significant macroscopic properties, opening a new and exciting prospect for processing and implementation of quantum information, as well as for discovering and understanding the limits of the quantum world, leading to promising applications in quantum information science such as the enhancement of quantum properties in low-dimensional molecular magnets by material engineering to the development of novel candidate platforms for the processing and transmission of quantum information.

In addition, in Chapter 7, we established a relationship between the detection of quantum correlations and diffractive properties of neutron scattering, enabling the measurement of nonclassical correlations in molecular magnetic materials via neutron scattering experiments, paving the way for research in experimental detection of quantum information quantifiers, and leading to a better understanding of its quantum properties. Our main result was to provide analytical expressions for quantum information quantifiers, such as the entanglement witness, entanglement of formation, Bell's inequality violation, and geometric quantum discord as a function of quantities typically obtained in neutron scattering in single crystal materials via the scalar structure factor. We provided one path toward identifying the presence of quantum correlations in a two-qubit system such as a Heisenberg spin-1/2 dimer, using diffractive properties and without making any assumption about macroscopic properties or the external conditions under which the neutrons are scattered.

In summary, the study of molecular magnets can now open a large range of opportunities for research toward the limits of quantum mechanics. These results allow better management of the quantum properties in molecular magnetic systems and provide new opportunities for experimental and theoretical research of quantum correlations in these systems, leading to a better understanding of their quantum properties with promising applications in emerging quantum technologies, such as the development of new devices based on molecular magnetic systems for quantum computation.

8.2   Future Works

Through the results presented in this thesis, we show that the electronic spin of low-dimensional molecular magnetic systems are promising candidates for the codification and processing of quantum information. Thus, as a perspective for future works, based on the works of Leuenberger and Loss [208], which propose an implementation of Grover's algorithm using molecular magnets,showing that molecular magnetic systems can be used to construct dense and efficient memory devices based on Grover's algorithm, we intend to study the implementation of quantum algorithms through quantum logic gates in low-dimensional molecular magnetic systems. From the computational materials science point of view, we intend to simulate electronic paramagnetic resonance (EPR) technique, through density functional theory (DFT) in the gauge including projected augmented wave (GIPAW) approach on the Quantum ESPRESSO software [75–82], using CENAPAD facilities.

Therefore, we can study the creation of quantum logic gates with the molecular magnet spins in a theoretical point of view. In addition, we could theoretically plan the implementation of a quantum logic gate, proposing new prototype materials with the structure and properties required for such a logic gate, by the development of first principles calculations, in order to study how different topological aspects affect the quantum properties of molecular magnetic systems, by using DFT. We will evaluate the effect of topology on the quantum correlations of a molecular magnetic systems, through the analysis of quantum information theoretical quantifiers and the development of theoretical models for the characterization of the thermodynamic properties of proposed prototype materials through DFT calculations.

As a consequence, from these theoretical results, we expect to obtain new topologies of molecular magnetic systems with optimized quantum properties. This can be seen as a molecular engineering for quantum computing. In this context, exploring these results is extremely interesting because we can test the creation and improvement of quantum correlations in several prototype material, and the protection of the quantum states of molecular magnetic systems against decoherence mechanisms through a deep analysis of the effects of external agents such as temperature, pressure and magnetic fields, on the quantum properties of low-dimensional molecular magnetic systems. Aiming to detect, quantify and manipulate the quantum properties of these materials, and propose

future experiments using EPR in the molecular magnet to test whether to implement some logic gates.

In addition, we intend to study thermal effects in discord-like quantum correlations as quantum interferometric power, and phenomenological characteristics of quantum systems as quantum coherence through the measurement of the thermodynamic properties of low dimensional molecular magnetic systems. In order to investigate how a metrological quantities and phenomenological properties of the quantum nature of a magnetic system can be used to infer the degree of its quantum correlations, and analyze the quantum properties of multipartite molecular magnetic systems such as larger spin clusters and chains as well as to study the nonequilibrium thermodynamics of quantum processes in molecular magnets by using the magnetocaloric effect.

Bibliography

[1] Mario Reis and António Moreira dos Santos. *Magnetismo molecular*. Editora Livraria da Física, 2011. Citado 11 vezes nas páginas xii, 1, 5, 8, 9, 10, 11, 12, 14, 17 e 20.

[2] C. Cruz, D. O. Soares-Pinto, P. Brandao, A. M. dos Santos, and M. S. Reis. Carboxylate-based molecular magnet: One path toward achieving stable quantum correlations at room temperature. *EPL (Europhysics Letters)*, 113(4):40004, 2016. Citado 31 vezes nas páginas 1, 2, 7, 10, 21, 22, 23, 24, 28, 33, 48, 49, 50, 51, 55, 56, 60, 62, 65, 66, 69, 75, 76, 77, 79, 80, 89, 102, 104, 105 e 109.

[3] V. Vedral. *Introduction to Quantum Information Science*. Oxford University Press, 2006. Citado 5 vezes nas páginas 1, 70, 71, 78 e 85.

[4] Ryszard Horodecki, Paweł Horodecki, Michał Horodecki, and Karol Horodecki. Quantum entanglement. *Reviews of modern physics*, 81(2):865, 2009. Citado 19 vezes nas páginas 1, 36, 37, 38, 39, 40, 43, 44, 45, 47, 48, 50, 55, 70, 71, 78, 105, 106 e 108.

[5] Davide Girolami, Tommaso Tufarelli, and Gerardo Adesso. Characterizing non-classical correlations via local quantum uncertainty. *Physical review letters*, 110(24):240402, 2013. Citado 5 vezes nas páginas 1, 55, 61, 71 e 72.

[6] Mile Gu, Helen M Chrzanowski, Syed M Assad, Thomas Symul, Kavan Modi, Timothy C Ralph, Vlatko Vedral, and Ping Koy Lam. Observing the operational significance of discord consumption. *Nature Physics*, 8(9):671–675, 2012. Citado 3 vezes nas páginas 1, 55 e 71.

[7] Davide Girolami, Alexandre M Souza, Vittorio Giovannetti, Tommaso Tufarelli, Jefferson G Filgueiras, Roberto S Sarthour, Diogo O Soares-Pinto, Ivan S Oliveira, and Gerardo Adesso. Quantum discord determines the interferometric power of quantum states. *Physical Review Letters*, 112(21):210401, 2014. Citado 5 vezes nas páginas 1, 55, 61, 71 e 72.

[8] Kavan Modi, Aharon Brodutch, Hugo Cable, Tomasz Paterek, and Vlatko Vedral. The classical-quantum boundary for correlations: discord and related measures. *Reviews of Modern Physics*, 84(4):1655, 2012. Citado 2 vezes nas páginas 1 e 55.

[9] Harold Ollivier and Wojciech H Zurek. Quantum discord: a measure of the quantumness of correlations. *Physical Review Letters*, 88(1):017901, 2001. Citado 10 vezes nas páginas 1, 40, 56, 57, 60, 61, 65, 72, 79 e 109.

[10] Leah Henderson and Vlatko Vedral. Classical, quantum and total correlations. *Journal of Physics A: Mathematical and General*, 34(35):6899, 2001. Citado 11 vezes nas páginas 1, 40, 55, 56, 57, 60, 61, 65, 72, 79 e 109.

[11] V Vedral. Classical correlations and entanglement in quantum measurements. *Physical Review Letters*, 90(5):050401, 2003. Citado 6 vezes nas páginas 1, 55, 60, 61, 72 e 109.

[12] Ben-Qiong Liu, Lian-Ao Wu, Guo-Mo Zeng, Jian-Ming Song, Wei Luo, Yang Lei, Guang-Ai Sun, Bo Chen, and Shu-Ming Peng. Estimation of quantum correlations in magnetic materials by neutron scattering data. *Physics Letters A*, 378(46):3441–3444, 2014. Citado 13 vezes nas páginas 1, 2, 28, 29, 30, 31, 32, 33, 49, 60, 72, 103 e 109.

[13] Zhihao Ma, Zhihua Chen, Felipe Fernandes Fanchini, and Shao-Ming Fei. Quantum discord for $d \otimes 2$ systems. *Scientific Reports*, 5, 2015. Citado 5 vezes nas páginas 1, 60, 61, 72 e 109.

[14] Takafumi Nakano, Marco Piani, and Gerardo Adesso. Negativity of quantumness and its interpretations. *Physical Review A*, 88(1):012117, 2013. Citado 6 vezes nas páginas 1, 55, 60, 61, 72 e 109.

[15] Shunlong Luo. Quantum discord for two-qubit systems. *Physical Review A*, 77(4):042303, 2008. Citado 9 vezes nas páginas 1, 38, 55, 60, 61, 72, 73, 88 e 109.

[16] MS Sarandy. Classical correlation and quantum discord in critical systems. *Physical Review A*, 80(2):022108, 2009. Citado 12 vezes nas páginas 1, 51, 54, 55, 56, 57, 60, 61, 66, 68, 72 e 109.

[17] Animesh Datta, Anil Shaji, and Carlton M Caves. Quantum discord and the power of one qubit. *Physical Review Letters*, 100(5):050502, 2008. Citado 6 vezes nas páginas 1, 56, 60, 61, 72 e 109.

[18] JD Montealegre, FM Paula, A Saguia, and MS Sarandy. One-norm geometric quantum discord under decoherence. *Physical Review A*, 87(4):042115, 2013. Citado 11 vezes nas páginas 1, 60, 61, 62, 64, 66, 72, 73, 87, 109 e 110.

[19] Borivoje Dakić, Vlatko Vedral, and Časlav Brukner. Necessary and sufficient condition for nonzero quantum discord. *Physical Review Letters*, 105(19):190502, 2010. Citado 8 vezes nas páginas 1, 55, 61, 62, 64, 72, 73 e 85.

[20] C Cruz, ÁS Alves, RN dos Santos, DO Soares-Pinto, JCO de Jesus, JS de Almeida, and MS Reis. Influence of the external pressure on the quantum correlations of molecular magnets. *EPL (Europhysics Letters)*, 117(2):20004, 2017. Citado 8 vezes nas páginas 1, 2, 7, 10, 33, 76, 77 e 80.

[21] Yichen Huang. Computing quantum discord is np-complete. *New journal of physics*, 16(3):033027, 2014. Citado 3 vezes nas páginas 1, 61 e 72.

[22] M Cramer, MB Plenio, and H Wunderlich. Measuring entanglement in condensed matter systems. *Physical review letters*, 106(2):020401, 2011. Citado 7 vezes nas páginas 1, 28, 29, 31, 32, 80 e 103.

[23] Mario Reis. *Fundamentals of magnetism.* Elsevier, 2013. Citado 31 vezes nas páginas 1, 2, 5, 6, 7, 8, 9, 11, 12, 13, 14, 17, 18, 19, 20, 21, 23, 28, 33, 34, 50, 51, 52, 54, 66, 77, 82, 85, 86, 102 e 104.

[24] Clebson Cruz. Quantum correlations and bell's inequality violation in a heisenberg spin dimer via neutron scattering. *International Journal of Quantum Information*, page 1750031, 2017. Citado 6 vezes nas páginas 1, 2, 28, 32, 33 e 49.

[25] DO Soares-Pinto, AM Souza, RS Sarthour, IS Oliveira, MS Reis, P Brandao, J Rocha, and AM dos Santos. Entanglement temperature in molecular magnets composed of s-spin dimers. *EPL (Europhysics Letters)*, 87(4):40008, 2009. Citado 16 vezes nas páginas 1, 2, 7, 10, 45, 46, 49, 50, 52, 53, 55, 76, 77, 78, 85 e 106.

[26] O. S. Duarte, C. S. Castro, D. O. Soares-Pinto, and M. S. Reis. Witnessing spin-orbit thermal entanglement in rare-earth ions. *EPL (Europhysics Letters)*, 103(4):40002, 2013. Citado 5 vezes nas páginas 1, 45, 46, 53 e 85.

[27] AM Souza, MS Reis, DO Soares-Pinto, IS Oliveira, and RS Sarthour. Experimental determination of thermal entanglement in spin clusters using magnetic susceptibility measurements. *Physical Review B*, 77(10):104402, 2008. Citado 10 vezes nas páginas 1, 2, 7, 10, 49, 50, 76, 77, 78 e 85.

[28] Mario S Reis, Stephane Soriano, Antonio M dos Santos, Brian C Sales, DO Soares-Pinto, and Paula Brandao. Evidence for entanglement at high temperatures in an engineered molecular magnet. *EPL (Europhysics Letters)*, 100(5):50001, 2012. Citado 15 vezes nas páginas 1, 2, 7, 10, 46, 49, 50, 52, 53, 55, 76, 77, 78, 79 e 85.

[29] AM Souza, DO Soares-Pinto, RS Sarthour, IS Oliveira, Mario S Reis, Paula Brandao, and AM Dos Santos. Entanglement and bell's inequality violation above room temperature in metal carboxylates. *Physical Review B*, 79(5):054408, 2009. Citado 12 vezes nas páginas 1, 2, 7, 10, 49, 50, 76, 77, 78, 85, 105 e 106.

[30] D Esteves, JCD Tedesco, SS Pedro, C Cruz, MS Reis, and P Brandao. New manganese (ii) structures derived from 2, 6-dichlorobenzoic acid: Syntheses, crystal structures and magnetism. *Materials Chemistry and Physics*, 147(3):611–616, 2014. Citado 8 vezes nas páginas 1, 2, 7, 20, 28, 33, 79 e 102.

[31] BJM Leite Ferreira, Paula Brandão, AM Dos Santos, Z Gai, C Cruz, MS Reis, TM Santos, and V Félix. Heptacopper (ii) and dicopper (ii)-adenine complexes: synthesis, structural characterization, and magnetic properties. *Journal of Coordination Chemistry*, 68(16):2770–2787, 2015. Citado 9 vezes nas páginas 1, 2, 7, 10, 20, 28, 33, 79 e 102.

[32] Fa-Nian Shi, Yi-Wen Bai, Miao Lu, C. Cruz, M. S. Reis, and Jun Gao. A one-dimensional mn(ii)-based metal organic oxide: structure and properties. *Transition Metal Chemistry*, Jul 2017. Citado 5 vezes nas páginas 1, 2, 7, 20 e 33.

[33] Paula Brandao, Joao Rocha, Mario S Reis, AM Dos Santos, and Rongying Jin. Magnetic properties of knamsi4o10 compounds (m= mn, fe, cu). *Journal of Solid State Chemistry*, 182(2):253–258, 2009. Citado 6 vezes nas páginas 2, 7, 20, 91, 92 e 97.

[34] Mikhail A Yurishchev. Quantum discord in spin-cluster materials. *Physical Review B*, 84(2):024418, 2011. Citado 22 vezes nas páginas 2, 7, 23, 38, 40, 47, 48, 49, 50, 51, 55, 56, 65, 66, 72, 76, 77, 79, 88, 102, 104 e 105.

[35] Diogo de Oliveira Soares Pinto. Emaranhamento térmico e simulações quânticas de sistemas magnéticos por ressonância magnética nuclear. *Centro Brasileiro de Pesquisas Físicas Rio de Janeiro*, 2009. Citado 14 vezes nas páginas 2, 7, 39, 40, 41, 42, 43, 44, 45, 46, 50, 53, 76 e 77.

[36] Marcin Wieśniak, Vlatko Vedral, and Časlav Brukner. Magnetic susceptibility as a macroscopic entanglement witness. *New Journal of Physics*, 7(1):258, 2005. Citado 8 vezes nas páginas 2, 52, 53, 76, 77, 78, 105 e 106.

[37] Lapo Bogani and Wolfgang Wernsdorfer. Molecular spintronics using single-molecule magnets. *Nature materials*, 7(3):179, 2008. Citado 4 vezes nas páginas 2, 7, 10 e 20.

[38] Christopher M Ramsey, Enrique Del Barco, Stephen Hill, Sonali J Shah, Christopher C Beedle, and David N Hendrickson. Quantum interference of tunnel trajectories between states of different spin length in a dimeric molecular nanomagnet. *Nature Physics*, 4(4):277–281, 2008. Citado na página 2.

[39] Leon Gunther and Bernard Barbara. *Quantum tunneling of magnetization—QTM'94*, volume 301. Springer Science & Business Media, 2012. Citado na página 2.

[40] Dante Gatteschi and Roberta Sessoli. Quantum tunneling of magnetization and related phenomena in molecular materials. *Angewandte Chemie International Edition*, 42(3):268–297, 2003. Citado na página 2.

[41] Olivier Kahn. Molecular magnetism. *VCH Publishers, Inc.(USA), 1993,*, page 393, 1993. Citado 3 vezes nas páginas 5, 6 e 13.

[42] Roman Boča. *Theoretical foundations of molecular magnetism*, volume 1. Elsevier, 1999. Citado 2 vezes nas páginas 5 e 19.

[43] JT Haraldsen, T Barnes, and JL Musfeldt. Neutron scattering and magnetic observables for s= 1/ 2 spin clusters and molecular magnets. *Physical Review B,*

71(6):064403, 2005. Citado 10 vezes nas páginas 5, 21, 28, 31, 32, 33, 34, 35, 102 e 103.

[44] Clebson dos Santos Cruz. Propriedades magnéticas de magnetos moleculares. Master's thesis, Universidade Federal Fluminense, 2017. Citado 5 vezes nas páginas 5, 6, 8, 9 e 24.

[45] Alberto P Guimarães. A pedra com alma–a fascinante história do magnetismo. *Civilização Brasileira. Rio de Janeiro*, 2011. Citado na página 6.

[46] Werner Heisenberg. Zur theorie des ferromagnetismus. *Zeitschrift für Physik*, 49(9-10):619–636, 1928. Citado na página 6.

[47] B Bleaney and KD Bowers. Anomalous paramagnetism of copper acetate. In *Proceedings of the Royal Society of London A: Mathematical, Physical and Engineering Sciences*, volume 214, pages 451–465. The Royal Society, 1952. Citado 5 vezes nas páginas 7, 23, 51, 54 e 85.

[48] Kazuhito Hashimoto and Hashimoto Ohkoshi. Design of novel magnets using prussian blue analogues. *Philosophical Transactions of the Royal Society of London A: Mathematical, Physical and Engineering Sciences*, 357(1762):2977–3003, 1999. Citado na página 7.

[49] Marco Evangelisti, Andrea Candini, Alberto Ghirri, Marco Affronte, Euan K Brechin, and Eric JL McInnes. Spin-enhanced magnetocaloric effect in molecular nanomagnets. *Applied Physics Letters*, 87(7):072504, 2005. Citado 3 vezes nas páginas 7, 10 e 20.

[50] Maria Manoli, Russell DL Johnstone, Simon Parsons, Mark Murrie, Marco Affronte, Marco Evangelisti, and Euan K Brechin. A ferromagnetic mixed-valent mn supertetrahedron: Towards low-temperature magnetic refrigeration with molecular clusters. *Angewandte Chemie*, 119(24):4540–4544, 2007. Citado 3 vezes nas páginas 7, 10 e 20.

[51] Yan-Zhen Zheng, Marco Evangelisti, and Richard EP Winpenny. Large magnetocaloric effect in a wells–dawson type {Ni6Gd6P6} cage. *Angewandte Chemie International Edition*, 50(16):3692–3695, 2011. Citado 3 vezes nas páginas 7, 10 e 20.

[52] Guilherme P Guedes, Rafael A Allão, Luiza A Mercante, Maria GF Vaz, and Miguel A Novak. Compostos magnéticos moleculares-o desenvolvimento de novos materiais magnéticos nanoestruturados. *Quim. Nova*, 33(8):1756–1764, 2010. Citado na página 7.

[53] John B Goodenough. Theory of the role of covalence in the perovskite-type manganites [la, m (ii)] mn o 3. *Physical Review*, 100(2):564, 1955. Citado 2 vezes nas páginas 8 e 79.

[54] Álvaro Santos Alves. *Estudo de magnetos moleculares através de cálculos de primeiros princípios*. PhD thesis, Universidade Federal Fluminense, 2011. Citado 5 vezes nas páginas 9, 25, 26, 92 e 93.

[55] Masayoshi Nakano, Ryohei Kishi, Suguru Ohta, Hideaki Takahashi, Takashi Kubo, Kenji Kamada, Koji Ohta, Edith Botek, and Benoit Champagne. Relationship between third-order nonlinear optical properties and magnetic interactions in open-shell systems: a new paradigm for nonlinear optics. *Physical review letters*, 99(3):033001, 2007. Citado na página 10.

[56] Georg Kresse and J Hafner. Ab initio molecular dynamics for open-shell transition metals. *Physical Review B*, 48(17):13115, 1993. Citado na página 10.

[57] ND Lang. Interaction between closed-shell systems and metal surfaces. *Physical Review Letters*, 46(13):842, 1981. Citado na página 10.

[58] Howard D Cohen and CCJ Roothaan. Electric dipole polarizability of atoms by the hartree—fock method. i. theory for closed-shell systems. *The Journal of Chemical Physics*, 43(10):S34–S39, 1965. Citado na página 10.

[59] MS Dresselhaus. *Solid State Physics: Part III, Magnetic Properties of Solids*. MIT Lecture Notes, 2001. Citado 2 vezes nas páginas 14 e 17.

[60] David Manthey. Orbital viewer. *A program for drawing orbitals [program]. Verze*, 1, 1998. Citado na página 15.

[61] Peter Atkins. *Shriver and Atkins' inorganic chemistry*. Oxford University Press, USA, 2010. Citado na página 17.

[62] Rob Janes and Elaine A Moore. *Metal-ligand bonding*. Royal Society of Chemistry, 2004. Citado na página 17.

[63] Edwin T Jaynes. Information theory and statistical mechanics. *Physical review*, 106(4):620, 1957. Citado na página 18.

[64] Edwin T Jaynes. Information theory and statistical mechanics. ii. *Physical review*, 108(2):171, 1957. Citado na página 18.

[65] Michael A Nielsen and Isaac L Chuang. *Quantum computation and quantum information*. Cambridge university press, 2010. Citado 19 vezes nas páginas 18, 36, 37, 38, 39, 40, 42, 43, 44, 47, 48, 50, 54, 57, 59, 63, 70, 71 e 108.

[66] SM Aldoshin, EB Fel'dman, and MA Yurishchev. Quantum entanglement and quantum discord in magnetoactive materials (review article). *Low Temperature Physics*, 40(1):3–16, 2014. Citado 21 vezes nas páginas 23, 38, 40, 47, 48, 49, 50, 51, 55, 56, 57, 58, 65, 72, 75, 76, 79, 88, 102, 104 e 105.

[67] Richard Tumanjong Azuah, Larry R Kneller, Yiming Qiu, Philip LW Tregenna-Piggott, Craig M Brown, John RD Copley, and Robert M Dimeo. Dave: a comprehensive software suite for the reduction, visualization, and analysis of low energy neutron spectroscopic data. *Journal of Research of the National Institute of Standards and Technology*, 114(6):341–358, 2009. Citado 2 vezes nas páginas 24 e 85.

[68] Max Born and Robert Oppenheimer. Zur quantentheorie der molekeln. *Annalen der physik*, 389(20):457–484, 1927. Citado na página 25.

[69] Weitao Yang and Paul W Ayers. Density-functional theory. In *Computational Medicinal Chemistry for Drug Discovery*, pages 103–132. CRC Press, 2003. Citado 4 vezes nas páginas 25, 26, 92 e 93.

[70] Erwin Schrödinger. An undulatory theory of the mechanics of atoms and molecules. *Physical review*, 28(6):1049, 1926. Citado na página 25.

[71] Pierre Hohenberg and Walter Kohn. Inhomogeneous electron gas. *Physical review*, 136(3B):B864, 1964. Citado 3 vezes nas páginas 26, 92 e 93.

[72] Eugene S Kryachko. Hohenberg-kohn theorem. *International Journal of Quantum Chemistry*, 18(4):1029–1035, 1980. Citado na página 26.

[73] Walter Kohn and Lu Jeu Sham. Self-consistent equations including exchange and correlation effects. *Physical review*, 140(4A):A1133, 1965. Citado na página 26.

[74] Paolo Giannozzi, Stefano Baroni, Nicola Bonini, Matteo Calandra, Roberto Car, Carlo Cavazzoni, Davide Ceresoli, Guido L Chiarotti, Matteo Cococcioni, Ismaila Dabo, et al. Quantum espresso: a modular and open-source software project for quantum simulations of materials. *Journal of physics: Condensed matter*, 21(39):395502, 2009. Citado 2 vezes nas páginas 27 e 93.

[75] Thibault Charpentier. Calculation of solid-state nmr and epr parameters using the gipaw method. Citado 2 vezes nas páginas 27 e 114.

[76] Chris J Pickard and Francesco Mauri. First-principles theory of the epr g tensor in solids: Defects in quartz. *Physical review letters*, 88(8):086403, 2002. Citado 2 vezes nas páginas 27 e 114.

[77] Davide Ceresoli. Ab-initio epr spectroscopy. Citado 2 vezes nas páginas 27 e 114.

[78] Amy L Webber, Benedicte Elena, John M Griffin, Jonathan R Yates, Tran N Pham, Francesco Mauri, Chris J Pickard, Ana M Gil, Robin Stein, Anne Lesage, et al. Complete 1 h resonance assignment of β-maltose from 1 h–1 h dq-sq cramps and 1 h (dq-dumbo)–13c sq refocused inept 2d solid-state nmr spectra and first principles gipaw calculations. *Physical Chemistry Chemical Physics*, 12(26):6970–6983, 2010. Citado 2 vezes nas páginas 27 e 114.

[79] Cory M Widdifield and David L Bryce. Solid-state 127i nmr and gipaw dft study of metal iodides and their hydrates: structure, symmetry, and higher-order quadrupole-induced effects. *The Journal of Physical Chemistry A*, 114(40):10810–10823, 2010. Citado 2 vezes nas páginas 27 e 114.

[80] Christel Gervais, Laure Bonhomme-Coury, Francesco Mauri, Florence Babonneau, and Christian Bonhomme. Gipaw (gauge including projected augmented wave) and local dynamics in 13 c and 29si solid state nmr: the study case of silsesquioxanes (rsio 1.5) 8. *Physical Chemistry Chemical Physics*, 11(32):6953–6961, 2009. Citado 2 vezes nas páginas 27 e 114.

[81] Cory M Widdifield and David L Bryce. A multinuclear solid-state magnetic reso-
nance and gipaw dft study of anhydrous calcium chloride and its hydrates. *Canadian
Journal of Chemistry*, 89(7):754–763, 2011. Citado 2 vezes nas páginas 27 e 114.

[82] Thibault Charpentier. The paw/gipaw approach for computing nmr parameters: A
new dimension added to nmr study of solids. *Solid state nuclear magnetic resonance*,
40(1):1–20, 2011. Citado 2 vezes nas páginas 27 e 114.

[83] JCG Tedesco, SS Pedro, RJ Caraballo Vivas, C Cruz, VM Andrade, AM Dos San-
tos, AMG Carvalho, M Costa, P Venezuela, DL Rocco, et al. Chemical disorder
determines the deviation of the slater–pauling rule for fe2mnsi-based heusler al-
loys: evidences from neutron diffraction and density functional theory. *Journal of
Physics: Condensed Matter*, 28(47):476002, 2016. Citado 2 vezes nas páginas 28
e 32.

[84] Reto Basler, Colette Boskovic, Grégory Chaboussant, Hans U Güdel, Mark Murrie,
Stefan T Ochsenbein, and Andreas Sieber. Molecular spin clusters: New synthetic
approaches and neutron scattering studies. *ChemPhysChem*, 4(9):910–926, 2003.
Citado 5 vezes nas páginas 28, 29, 30, 31 e 32.

[85] RJ Birgeneau, HJ Guggenheim, and G Shirane. Neutron scattering investigation of
phase transitions and magnetic correlations in the two-dimensional antiferromagnets
k 2 ni f 4, rb 2 mn f 4, rb 2 fe f 4. *Physical Review B*, 1(5):2211, 1970. Citado 2
vezes nas páginas 28 e 32.

[86] LC Kwek. Probing multipartite entanglement in spin chain via structure factors.
Laser Physics, 21(8):1511–1517, 2011. Citado 4 vezes nas páginas 28, 29, 31 e 32.

[87] O Marty, M Epping, H Kampermann, D Bruß, MB Plenio, and M Cramer. Quanti-
fying entanglement with scattering experiments. *Physical Review B*, 89(12):125117,
2014. Citado 7 vezes nas páginas 28, 29, 30, 31, 32, 80 e 103.

[88] Philipp Krammer, Hermann Kampermann, Dagmar Bruß, Reinhold A Bertlmann,
Leong Chuang Kwek, and Chiara Macchiavello. Multipartite entanglement detection
via structure factors. *Physical review letters*, 103(10):100502, 2009. Citado 7 vezes
nas páginas 28, 29, 31, 32, 35, 102 e 103.

[89] HA Mook, M Yethiraj, G Aeppli, TE Mason, and T Armstrong. Polarized neutron determination of the magnetic excitations in yba 2 cu 3 o 7. *Physical review letters*, 70(22):3490, 1993. Citado na página 28.

[90] Albert Furrer and Hans U Güdel. Neutron inelastic scattering from isolated clusters of magnetic ions. *Journal of Magnetism and Magnetic Materials*, 14(2-3):256–264, 1979. Citado 4 vezes nas páginas 28, 29, 30 e 31.

[91] Gordon Leslie Squires. *Introduction to the theory of thermal neutron scattering.* Cambridge university press, 2012. Citado 2 vezes nas páginas 29 e 30.

[92] Leon Van Hove. Correlations in space and time and born approximation scattering in systems of interacting particles. *Phys. Rev.*, 95:249, 1954. Citado na página 30.

[93] Igor A Zaliznyak and Seung-Hun Lee. Magnetic neutron scattering. *Modern Techniques for Characterizing Magnetic Materials, Springer, Heidelberg*, 2005. Citado na página 30.

[94] CJ Hamer, J Oitmaa, Zheng Weihong, and Ross H McKenzie. Critical behavior of one-particle spectral weights in the transverse ising model. *Physical Review B*, 74(6):060402, 2006. Citado 2 vezes nas páginas 31 e 32.

[95] P Schofield. Theory of thermal neutron scattering–the use of neutrons for the investigation of condensed matter, 1972. Citado 2 vezes nas páginas 31 e 32.

[96] MB Stone, F Fernandez-Alonso, DT Adroja, NS Dalal, D Villagrán, FA Cotton, and SE Nagler. Inelastic neutron scattering study of a quantum spin trimer. *Physical Review B*, 75(21):214427, 2007. Citado 2 vezes nas páginas 32 e 33.

[97] Y Qiu, C Broholm, S Ishiwata, M Azuma, M Takano, R Bewley, and WJL Buyers. Spin-trimer antiferromagnetism in la 4 cu 3 mo o 12. *Physical Review B*, 71(21):214439, 2005. Citado na página 33.

[98] Marshall Luban, Ferdinando Borsa, Sergey Bud'ko, Paul Canfield, Suckjoon Jun, Jae Kap Jung, Paul Kögerler, Detlef Mentrup, Achim Müller, Robert Modler, et al. Heisenberg spin triangles in {V6} type magnetic molecules: Experiment and theory. *Physical Review B*, 66(5):054407, 2002. Citado na página 33.

[99] DA Tennant, SE Nagler, AW Garrett, T Barnes, and CC Torardi. Excitation spectrum and superexchange pathways in the spin dimer vodpo$_4$12d$_2$o. *Physical review letters*, 78(26):4998, 1997. Citado na página 33.

[100] Brant Cage, F Albert Cotton, Naresh S Dalal, Elizabeth A Hillard, Boris Rakvin, and Chris M Ramsey. Observation of symmetry lowering and electron localization in the doublet-states of a spin-frustrated equilateral triangular lattice: Cu3(o2c16h23)1.2 c6h12. *Journal of the American Chemical Society*, 125(18):5270–5271, 2003. Citado na página 33.

[101] Daniel Braun, Gerardo Adesso, Fabio Benatti, Roberto Floreanini, Ugo Marzolino, Morgan W Mitchell, and Stefano Pirandola. Quantum enhanced measurements without entanglement. *arXiv preprint arXiv:1701.05152*, 2017. Citado 3 vezes nas páginas 36, 71 e 73.

[102] Kavan Modi, Tomasz Paterek, Wonmin Son, Vlatko Vedral, and Mark Williamson. Unified view of quantum and classical correlations. *Physical Review Letters*, 104(8):080501, 2010. Citado 4 vezes nas páginas 36, 44, 50 e 55.

[103] J Von Neumann. Mathematische grundlagen der quantenmechanik (berlin, 1932). *Springer*, 1955. Citado na página 36.

[104] Erwin Schrödinger. Die gegenwärtige situation in der quantenmechanik. *Naturwissenschaften*, 23(49):823–828, 1935. Citado 3 vezes nas páginas 36, 37 e 43.

[105] Albert Einstein, Boris Podolsky, and Nathan Rosen. Can quantum-mechanical description of physical reality be considered complete? *Physical review*, 47(10):777, 1935. Citado na página 37.

[106] JA Wheeler and W Zurek. Quantum mechanics and measurement, 1983. Citado 2 vezes nas páginas 37 e 43.

[107] Lawrence J Landau. On the violation of bell's inequality in quantum theory. *Physics Letters A*, 120(2):54–56, 1987. Citado 3 vezes nas páginas 38, 43 e 55.

[108] Časlav Brukner, Marek Żukowski, Jian-Wei Pan, and Anton Zeilinger. Bell's inequalities and quantum communication complexity. *Physical review letters*, 92(12):127901, 2004. Citado 3 vezes nas páginas 38, 43 e 55.

[109] Cleidson Castro. Quantum entanglement on magnetic materials and superconducting devices. *Universidade Federal Fluminense*, 2015. Citado 7 vezes nas páginas 39, 40, 44, 45, 46, 50 e 53.

[110] Charles H Bennett and Stephen J Wiesner. Communication via one-and two-particle operators on einstein-podolsky-rosen states. *Physical review letters*, 69(20):2881, 1992. Citado na página 43.

[111] Charles H Bennett, François Bessette, Gilles Brassard, Louis Salvail, and John Smolin. Experimental quantum cryptography. *Journal of cryptology*, 5(1):3–28, 1992. Citado 2 vezes nas páginas 43 e 71.

[112] Charles H Bennett, Gilles Brassard, Claude Crépeau, Richard Jozsa, Asher Peres, and William K Wootters. Teleporting an unknown quantum state via dual classical and einstein-podolsky-rosen channels. *Physical review letters*, 70(13):1895, 1993. Citado na página 43.

[113] Pawel Horodecki. Separability criterion and inseparable mixed states with positive partial transposition. *Physics Letters A*, 232(5):333–339, 1997. Citado na página 45.

[114] Rajiah Simon. Peres-horodecki separability criterion for continuous variable systems. *Physical Review Letters*, 84(12):2726, 2000. Citado na página 45.

[115] Michał Horodecki, Paweł Horodecki, and Ryszard Horodecki. Separability of mixed states: necessary and sufficient conditions. *Physics Letters A*, 223(1):1–8, 1996. Citado 3 vezes nas páginas 45, 105 e 106.

[116] Asher Peres. Separability criterion for density matrices. *Physical Review Letters*, 77(8):1413, 1996. Citado na página 45.

[117] Ming Li, Jing Wang, Shao-Ming Fei, and Xianqing Li-Jost. Quantum separability criteria for arbitrary-dimensional multipartite states. *Physical Review A*, 89(2):022325, 2014. Citado na página 45.

[118] Ting Gao, Yan Hong, Yao Lu, and Fengli Yan. Efficient k-separability criteria for mixed multipartite quantum states. *EPL (Europhysics Letters)*, 104(2):20007, 2013. Citado na página 45.

[119] Ting Gao and Yan Hong. Separability criteria for several classes of n-partite quantum states. *The European Physical Journal D*, 61(3):765–771, 2011. Citado na página 45.

[120] Géza Tóth and Otfried Gühne. Separability criteria and entanglement witnesses for symmetric quantum states. *Applied Physics B*, 98(4):617–622, 2010. Citado na página 45.

[121] AR Plastino, D Manzano, and JS Dehesa. Separability criteria and entanglement measures for pure states of n identical fermions. *EPL (Europhysics Letters)*, 86(2):20005, 2009. Citado na página 45.

[122] Heinz-Peter Breuer. Separability criteria and bounds for entanglement measures. *Journal of Physics A: Mathematical and General*, 39(38):11847, 2006. Citado na página 45.

[123] Michał Horodecki, Paweł Horodecki, and Ryszard Horodecki. Separability of mixed quantum states: linear contractions and permutation criteria. *Open Systems & Information Dynamics*, 13(1):103–111, 2006. Citado na página 45.

[124] Otfried Gühne and Michael Seevinck. Separability criteria for genuine multiparticle entanglement. *New Journal of Physics*, 12(5):053002, 2010. Citado na página 45.

[125] Andrew C Doherty, Pablo A Parrilo, and Federico M Spedalieri. Complete family of separability criteria. *Physical Review A*, 69(2):022308, 2004. Citado na página 45.

[126] OS Duarte, CS Castro, and MS Reis. Spin-orbit thermal entanglement in a rare-earth-metal ion: Susceptibility witness. *Physical Review A*, 88(1):012317, 2013. Citado 4 vezes nas páginas 45, 46, 53 e 85.

[127] Géza Tóth. Entanglement witnesses in spin models. *Physical Review A*, 71(1):010301, 2005. Citado 6 vezes nas páginas 45, 46, 52, 53, 78 e 85.

[128] William K Wootters. Entanglement of formation of an arbitrary state of two qubits. *Physical Review Letters*, 80(10):2245, 1998. Citado 6 vezes nas páginas 47, 48, 49, 54, 87 e 108.

[129] Scott Hill and William K Wootters. Entanglement of a pair of quantum bits. *Physical review letters*, 78(26):5022, 1997. Citado 5 vezes nas páginas 47, 48, 54, 87 e 108.

[130] Ting Yu and JH Eberly. Sudden death of entanglement. *Science*, 323(5914):598–601, 2009. Citado 2 vezes nas páginas 49 e 71.

[131] Sayantani Ghosh, TF Rosenbaum, G Aeppli, and SN Coppersmith. Entangled quantum state of magnetic dipoles. *Nature*, 425(6953):48–51, 2003. Citado 4 vezes nas páginas 49, 77, 78 e 85.

[132] Tanmoy Chakraborty, Harkirat Singh, Sourabh Singh, Radha Krishna Gopal, and Chiranjib Mitra. Probing quantum discord in a heisenberg dimer compound. *Journal of Physics: Condensed Matter*, 25(42):425601, 2013. Citado 2 vezes nas páginas 49 e 50.

[133] Vlatko Vedral. Living in a quantum world. *Scientific American*, 304(6):38–43, 2011. Citado 2 vezes nas páginas 50 e 85.

[134] Otfried Gühne and Geza Toth. Energy and multipartite entanglement in multi-dimensional and frustrated spin models. *Physical Review A*, 73(5):052319, 2006. Citado 2 vezes nas páginas 52 e 78.

[135] Mark R Dowling, Andrew C Doherty, and Stephen D Bartlett. Energy as an entanglement witness for quantum many-body systems. *Physical Review A*, 70(6):062113, 2004. Citado 2 vezes nas páginas 52 e 78.

[136] L-A Wu, Somshubhro Bandyopadhyay, MS Sarandy, and DA Lidar. Entanglement observables and witnesses for interacting quantum spin systems. *Physical Review A*, 72(3):032309, 2005. Citado 2 vezes nas páginas 52 e 78.

[137] Marcin Wieśniak, Vlatko Vedral, and Časlav Brukner. Heat capacity as an indicator of entanglement. *Physical Review B*, 78(6):064108, 2008. Citado 2 vezes nas páginas 52 e 78.

[138] Holger F Hofmann and Shigeki Takeuchi. Violation of local uncertainty relations as a signature of entanglement. *Physical Review A*, 68(3):032103, 2003. Citado na página 53.

[139] Zhong-Xiao Man, Yun-Jie Xia, and Rosario Lo Franco. Cavity-based architecture to preserve quantum coherence and entanglement. *Scientific reports*, 5, 2015. Citado na página 55.

[140] Benjamin Aaronson, Rosario Lo Franco, and Gerardo Adesso. Comparative investigation of the freezing phenomena for quantum correlations under nondissipative decoherence. *Physical Review A*, 88(1):012120, 2013. Citado 4 vezes nas páginas 55, 64, 65 e 75.

[141] Rosario Lo Franco, Bruno Bellomo, Sabrina Maniscalco, and Giuseppe Compagno. Dynamics of quantum correlations in two-qubit systems within non-markovian environments. *International Journal of Modern Physics B*, 27(01n03):1345053, 2013. Citado na página 55.

[142] Bruno Bellomo, R Lo Franco, and Giuseppe Compagno. Dynamics of geometric and entropic quantifiers of correlations in open quantum systems. *Physical Review A*, 86(1):012312, 2012. Citado 4 vezes nas páginas 55, 61, 72 e 73.

[143] R Lo Franco, Bruno Bellomo, Erika Andersson, and Giuseppe Compagno. Revival of quantum correlations without system-environment back-action. *Physical Review A*, 85(3):032318, 2012. Citado na página 55.

[144] Benjamin Aaronson, Rosario Lo Franco, Giuseppe Compagno, and Gerardo Adesso. Hierarchy and dynamics of trace distance correlations. *New Journal of Physics*, 15(9):093022, 2013. Citado na página 55.

[145] Isabela A Silva, Alexandre M Souza, Thomas R Bromley, Marco Cianciaruso, Raimund Marx, Roberto S Sarthour, Ivan S Oliveira, Rosario Lo Franco, Steffen J Glaser, Diogo O Soares-Pinto, et al. Observation of time-invariant coherence in a nuclear magnetic resonance quantum simulator. *Physical Review Letters*, 117(16):160402, 2016. Citado na página 55.

[146] Jin-Shi Xu, Kai Sun, Chuan-Feng Li, Xiao-Ye Xu, Guang-Can Guo, Erika Andersson, Rosario Lo Franco, and Giuseppe Compagno. Experimental recovery of quantum correlations in absence of system-environment back-action. *Nature communications*, 4, 2013. Citado na página 55.

[147] Thomas R Bromley, Marco Cianciaruso, Rosario Lo Franco, and Gerardo Adesso. Unifying approach to the quantification of bipartite correlations by bures distance. *Journal of Physics A: Mathematical and Theoretical*, 47(40):405302, 2014. Citado na página 55.

[148] Davide Girolami and Gerardo Adesso. Quantum discord for general two-qubit states: Analytical progress. *Physical Review A*, 83(5):052108, 2011. Citado 3 vezes nas páginas 55, 60 e 109.

[149] V Vedral. Classical correlations and entanglement in quantum measurements. *Physical review letters*, 90(5):050401, 2003. Citado 3 vezes nas páginas 56, 57 e 60.

[150] Tommaso Tufarelli, Davide Girolami, Ruggero Vasile, Sougato Bose, and Gerardo Adesso. Quantum resources for hybrid communication via qubit-oscillator states. *Physical Review A*, 86(5):052326, 2012. Citado 3 vezes nas páginas 56, 64 e 72.

[151] Stefano Pirandola. Quantum discord as a resource for quantum cryptography. *Scientific reports*, 4, 2014. Citado na página 56.

[152] T Werlang, C Trippe, GAP Ribeiro, and Gustavo Rigolin. Quantum correlations in spin chains at finite temperatures and quantum phase transitions. *Physical review letters*, 105(9):095702, 2010. Citado na página 56.

[153] Emanuel Knill and Raymond Laflamme. Power of one bit of quantum information. *Physical Review Letters*, 81(25):5672, 1998. Citado 4 vezes nas páginas 56, 65, 72 e 79.

[154] Jacob Benesty, Jingdong Chen, Yiteng Huang, and Israel Cohen. Pearson correlation coefficient. In *Noise reduction in speech processing*, pages 1–4. Springer, 2009. Citado na página 56.

[155] J Martin Bland and Douglas G Altman. Statistics notes: measurement error. *Bmj*, 313(7059):744, 1996. Citado na página 57.

[156] Wilton de O Bussab and Pedro A Morettin. Estatística básica. *Saraiva*, 9:14–15, 2010. Citado na página 58.

[157] FM Paula, Thiago R de Oliveira, and MS Sarandy. Geometric quantum discord through the schatten 1 norm. *Physical Review A*, 87(6):064101, 2013. Citado 9 vezes nas páginas 60, 61, 64, 72, 73, 81, 89, 109 e 110.

[158] Davide Girolami, Alexandre M Souza, Vittorio Giovannetti, Tommaso Tufarelli, Jefferson G Filgueiras, Roberto S Sarthour, Diogo O Soares-Pinto, Ivan S Oliveira, and Gerardo Adesso. Quantum discord determines the interferometric power of quantum states. *Physical Review Letters*, 112(21):210401, 2014. Citado 4 vezes nas páginas 61, 63, 72 e 73.

[159] Isabela Almeida Silva. *Correlações quânticas de caráter geral em sistemas de ressonância magnética nuclear*. PhD thesis, Universidade de São Paulo. Citado na página 61.

[160] Aharon Brodutch and Daniel R Terno. Quantum discord, local operations, and maxwells demons. *Physical Review A*, 81(6):062103, 2010. Citado 2 vezes nas páginas 61 e 72.

[161] Paola C Obando, Fagner M Paula, and Marcelo S Sarandy. Trace distance correlations for x states and the emergence of the pointer basis in markovian and non markovian regimes. *Physical Review A*, 92(3):032307, 2015. Citado 4 vezes nas páginas 61, 66, 67 e 68.

[162] FM Paula, Thiago R de Oliveira, and MS Sarandy. Geometric quantum discord through the schatten 1-norm. *Physical Review A*, 87(6):064101, 2013. Citado 8 vezes nas páginas 61, 64, 66, 69, 72, 73, 80 e 87.

[163] Marco Piani. Problem with geometric discord. *Physical Review A*, 86(3):034101, 2012. Citado 4 vezes nas páginas 61, 64, 72 e 73.

[164] FM Paula, A Saguia, Thiago R de Oliveira, and MS Sarandy. Overcoming ambiguities in classical and quantum correlation measures. *EPL (Europhysics Letters)*, 108(1):10003, 2014. Citado 3 vezes nas páginas 61, 72 e 73.

[165] D Spehner, F Illuminati, M Orszag, and W Roga. Geometric measures of quantum correlations with bures and hellinger distances. In *Lectures on General Quantum Correlations and their Applications*, pages 105–157. Springer, 2017. Citado 3 vezes nas páginas 61, 72 e 73.

[166] Marco Cianciaruso, Thomas R Bromley, Wojciech Roga, Rosario Lo Franco, and Gerardo Adesso. Universal freezing of quantum correlations within the geometric

approach. *Scientific reports*, 5:10177, 2015. Citado 5 vezes nas páginas 61, 65, 72, 73 e 75.

[167] Paolo Facchi, Ravi Kulkarni, VI Man'ko, Giuseppe Marmo, ECG Sudarshan, and Franco Ventriglia. Classical and quantum fisher information in the geometrical formulation of quantum mechanics. *Physics Letters A*, 374(48):4801–4803, 2010. Citado na página 63.

[168] Donald Bures. An extension of kakutani's theorem on infinite product measures to the tensor product of semifinite ω*-algebras. *Transactions of the American Mathematical Society*, 135:199–212, 1969. Citado na página 63.

[169] CW Helstrom. Minimum mean-squared error of estimates in quantum statistics. *Physics letters A*, 25(2):101–102, 1967. Citado na página 63.

[170] Armin Uhlmann. Fidelity and concurrence of conjugated states. *Physical Review A*, 62(3):032307, 2000. Citado na página 63.

[171] Richard Jozsa. Fidelity for mixed quantum states. *Journal of modern optics*, 41(12):2315–2323, 1994. Citado na página 63.

[172] Paulina Marian and Tudor A Marian. Uhlmann fidelity between two-mode gaussian states. *Physical Review A*, 86(2):022340, 2012. Citado na página 63.

[173] Xueyuan Hu, Heng Fan, DL Zhou, and Wu-Ming Liu. Quantum correlating power of local quantum channels. *Physical Review A*, 87(3):032340, 2013. Citado 2 vezes nas páginas 64 e 72.

[174] J Maziero, L C_ Celeri, RM Serra, and V Vedral. Classical and quantum correlations under decoherence. *Physical Review A*, 80(4):044102, 2009. Citado 2 vezes nas páginas 65 e 75.

[175] Laura Mazzola, Jyrki Piilo, and Sabrina Maniscalco. Sudden transition between classical and quantum decoherence. *Physical review letters*, 104(20):200401, 2010. Citado 2 vezes nas páginas 65 e 75.

[176] Titas Chanda, Amit Kumar Pal, Anindya Biswas, Aditi Sen, Ujjwal Sen, et al. Freezing of quantum correlations under local decoherence. *Physical Review A*, 91(6):062119, 2015. Citado 2 vezes nas páginas 65 e 75.

[177] F Ciccarello, T Tufarelli, and V Giovannetti. Toward computability of trace distance discord. *New Journal of Physics*, 16(1):013038, 2014. Citado 2 vezes nas páginas 66 e 68.

[178] Tobias J Osborne and Michael A Nielsen. Entanglement in a simple quantum phase transition. *Physical Review A*, 66(3):032110, 2002. Citado na página 66.

[179] Raoul Dillenschneider. Quantum discord and quantum phase transition in spin chains. *Physical Review B*, 78(22):224413, 2008. Citado na página 66.

[180] Ingemar Bengtsson and Karol Zyczkowski. *Geometry of quantum states: an introduction to quantum entanglement*. Cambridge University Press, 2007. Citado na página 66.

[181] Hoi-Kwong Lo, Tim Spiller, and Sandu Popescu. *Introduction to quantum computation and information*. World Scientific, 1998. Citado 2 vezes nas páginas 70 e 71.

[182] Nicolas Laflorencie. Quantum entanglement in condensed matter systems. *Physics Reports*, 646:1–59, 2016. Citado na página 71.

[183] Peter Lambropoulos and David Petrosyan. *Fundamentals of quantum optics and quantum information*, volume 23. Springer, 2007. Citado na página 71.

[184] Robert Alicki, Michał Horodecki, Paweł Horodecki, and Ryszard Horodecki. Thermodynamics of quantum information systems—hamiltonian description. *Open Systems & Information Dynamics*, 11(03):205–217, 2004. Citado na página 71.

[185] Dik Bouwmeester, Jian-Wei Pan, Klaus Mattle, Manfred Eibl, Harald Weinfurter, and Anton Zeilinger. Experimental quantum teleportation. *Nature*, 390(6660):575, 1997. Citado na página 71.

[186] Klaus Mattle, Harald Weinfurter, Paul G Kwiat, and Anton Zeilinger. Dense coding in experimental quantum communication. *Physical Review Letters*, 76(25):4656, 1996. Citado na página 71.

[187] David G Cory, MD Price, W Maas, E Knill, Raymond Laflamme, Wojciech H Zurek, Timothy F Havel, and SS Somaroo. Experimental quantum error correction. *Physical Review Letters*, 81(10):2152, 1998. Citado na página 71.

[188] Nicolas Gisin, Grégoire Ribordy, Wolfgang Tittel, and Hugo Zbinden. Quantum cryptography. *Reviews of modern physics*, 74(1):145, 2002. Citado na página 71.

[189] Artur K Ekert. Quantum cryptography based on bell's theorem. *Physical review letters*, 67(6):661, 1991. Citado na página 71.

[190] David DeMille. Quantum computation with trapped polar molecules. *Physical Review Letters*, 88(6):067901, 2002. Citado na página 71.

[191] Borivoje Dakić, Vlatko Vedral, and Časlav Brukner. Necessary and sufficient condition for nonzero quantum discord. *Physical review letters*, 105(19):190502, 2010. Citado na página 72.

[192] Shunlong Luo and Shuangshuang Fu. Geometric measure of quantum discord. *Physical Review A*, 82(3):034302, 2010. Citado na página 72.

[193] Pieter Bogaert and Davide Girolami. Metrological measures of non-classical correlations. In *Lectures on General Quantum Correlations and their Applications*, pages 159–179. Springer, 2017. Citado na página 73.

[194] Aharon Brodutch and Daniel R Terno. Why should we care about quantum discord? In *Lectures on General Quantum Correlations and their Applications*, pages 183–199. Springer, 2017. Citado na página 73.

[195] T Baumgratz, M Cramer, and MB Plenio. Quantifying coherence. *Physical review letters*, 113(14):140401, 2014. Citado 2 vezes nas páginas 73 e 74.

[196] Alexander Streltsov, Gerardo Adesso, and Martin B Plenio. Quantum coherence as a resource. *arXiv preprint arXiv:1609.02439*, 2016. Citado 3 vezes nas páginas 73, 74 e 75.

[197] Thomas R Bromley, Isabela A Silva, Charlie O Oncebay-Segura, Diogo O Soares-Pinto, Tommaso Tufarelli, Gerardo Adesso, et al. There is more to quantum interferometry than entanglement. *Physical Review A*, 95(5):052313, 2017. Citado na página 73.

[198] Matteo GA Paris. Quantum estimation for quantum technology. *International Journal of Quantum Information*, 7(supp01):125–137, 2009. Citado na página 73.

[199] Dirk Bouwmeester, Artur Ekert, Anton Zeilinger, et al. *The physics of quantum information*, volume 3. Springer, Berlin, 2000. Citado na página 75.

[200] Thaddeus D Ladd, Fedor Jelezko, Raymond Laflamme, Yasunobu Nakamura, Christopher Monroe, and Jeremy Lloyd O'Brien. Quantum computers. *Nature*, 464(7285):45, 2010. Citado na página 75.

[201] Hans Georg Krojanski and Dieter Suter. Scaling of decoherence in wide nmr quantum registers. *Physical review letters*, 93(9):090501, 2004. Citado na página 76.

[202] Lieven MK Vandersypen and Isaac L Chuang. Nmr techniques for quantum control and computation. *Reviews of modern physics*, 76(4):1037, 2005. Citado na página 76.

[203] Ivan Oliveira, Roberto Sarthour Jr, Tito Bonagamba, Eduardo Azevedo, and Jair CC Freitas. *NMR quantum information processing*. Elsevier, 2011. Citado na página 76.

[204] Paola Cappellaro, Chandrasekhar Ramanathan, and David G Cory. Dynamics and control of a quasi-one-dimensional spin system. *Physical Review A*, 76(3):032317, 2007. Citado na página 76.

[205] J Ahn, TC Weinacht, and PH Bucksbaum. Information storage and retrieval through quantum phase. *Science*, 287(5452):463–465, 2000. Citado na página 77.

[206] Lov K Grover. A fast quantum mechanical algorithm for database search. In *Proceedings of the twenty-eighth annual ACM symposium on Theory of computing*, pages 212–219. ACM, 1996. Citado na página 77.

[207] Artur Ekert and Richard Jozsa. Quantum computation and shor's factoring algorithm. *Reviews of Modern Physics*, 68(3):733, 1996. Citado na página 77.

[208] Michael N Leuenberger and Daniel Loss. Quantum computing in molecular magnets. *Nature*, 410(6830):789, 2001. Citado 2 vezes nas páginas 77 e 114.

[209] Ryan J Kuppler, Daren J Timmons, Qian-Rong Fang, Jian-Rong Li, Trevor A Makal, Mark D Young, Daqiang Yuan, Dan Zhao, Wenjuan Zhuang, and Hong-Cai Zhou. Potential applications of metal-organic frameworks. *Coordination Chemistry Reviews*, 253(23-24):3042–3066, 2009. Citado na página 82.

[210] Pieremanuele Canepa, Yves J Chabal, and Timo Thonhauser. When metal organic frameworks turn into linear magnets. *Physical Review B*, 87(9):094407, 2013. Citado na página 82.

[211] Joseph W Sharples and David Collison. Coordination compounds and the magnetocaloric effect. *Polyhedron*, 66:15–27, 2013. Citado na página 82.

[212] Alexandre R Rocha, Victor M Garcia-Suarez, Steve W Bailey, Colin J Lambert, Jaime Ferrer, and Stefano Sanvito. Towards molecular spintronics. *Nature materials*, 4(4):335, 2005. Citado na página 82.

[213] Mauro Longue Filho et al. Síntese e avaliação da atividade nematicida de derivados da piperazina. 1998. Citado na página 82.

[214] DO Soares-Pinto, J Teles, AM Souza, ER Deazevedo, RS Sarthour, TJ Bonagamba, MS Reis, and IS Oliveira. Writing electronic ferromagnetic states in a high-temperature paramagnetic nuclear spin system. *International Journal of Quantum Information*, 9(04):1047–1056, 2011. Citado na página 85.

[215] Jenny Hide, Wonmin Son, and Vlatko Vedral. Enhancing the detection of natural thermal entanglement with disorder. *Physical review letters*, 102(10):100503, 2009. Citado na página 85.

[216] Josr M Menrrn Pozest and Enn Vrrronto Tp Zzott. Reexamination and crystal structure analysis of litidionite. 1975. Citado 2 vezes nas páginas 91 e 92.

[217] JL GUTH, A Kalt, B Perati, and R Wey. Synthesis and formula of litidionite. *COMPTES RENDUS HEBDOMADAIRES DES SEANCES DE L ACADEMIE DES SCIENCES SERIE D*, 285(14):1221–1224, 1977. Citado 2 vezes nas páginas 91 e 92.

[218] Jesse Hefter and Malcolm E Kenney. Synthesis of the tube silicate litidionite and structural relationships between it and some other silicates. *Inorganic Chemistry*, 21(7):2810–2816, 1982. Citado 2 vezes nas páginas 91 e 92.

[219] John P Perdew, Kieron Burke, and Matthias Ernzerhof. Generalized gradient approximation made simple. *Physical review letters*, 77(18):3865, 1996. Citado na página 93.

[220] John P Perdew. Density-functional approximation for the correlation energy of the inhomogeneous electron gas. *Physical Review B*, 33(12):8822, 1986. Citado na página 93.

[221] Lee A Cole and JP Perdew. Calculated electron affinities of the elements. *Physical Review A*, 25(3):1265, 1982. Citado na página 93.

[222] JP Perdew and Y Wang. Pair-distribution function and its coupling-constant average for the spin-polarized electron gas. *Phys. Rev. B*, 45:13244, 1992. Citado na página 93.

[223] John P Perdew and Wang Yue. Accurate and simple density functional for the electronic exchange energy: Generalized gradient approximation. *Physical review B*, 33(12):8800, 1986. Citado na página 93.

[224] JP Perdew, K Burke, and M Ernzerhof. Perdew, burke, and ernzerhof reply. *Physical Review Letters*, 80(4):891, 1998. Citado na página 93.

[225] Hendrik J Monkhorst and James D Pack. Special points for brillouin-zone integrations. *Physical review B*, 13(12):5188, 1976. Citado na página 93.

[226] Nicola Marzari, David Vanderbilt, Alessandro De Vita, and MC Payne. Thermal contraction and disordering of the al (110) surface. *Physical review letters*, 82(16):3296, 1999. Citado na página 93.

[227] Francis Birch. Finite elastic strain of cubic crystals. *Physical Review*, 71(11):809, 1947. Citado na página 93.

[228] DA Tennant, C Broholm, DH Reich, SE Nagler, GE Granroth, T Barnes, K Damle, G Xu, Y Chen, and BC Sales. Neutron scattering study of two-magnon states in the quantum magnet copper nitrate. *Physical Review B*, 67(5):054414, 2003. Citado na página 102.

[229] T Huberman, R Coldea, RA Cowley, DA Tennant, RL Leheny, Rebecca J Christianson, and CD Frost. Two-magnon excitations observed by neutron scattering in the two-dimensional spin-5 2 heisenberg antiferromagnet rb 2 mn f 4. *Physical Review B*, 72(1):014413, 2005. Citado na página 102.

[230] Časlav Brukner, Vlatko Vedral, and Anton Zeilinger. Crucial role of quantum entanglement in bulk properties of solids. *Physical Review A*, 73(1):012110, 2006. Citado na página 106.

Appendices

A DAVE MagProp Tutorial

For the adjustment of the susceptibility data, and the calculation of the required parameters for the characterization of the molecular magnets studied in this thesis, we used DAVE - MagProp (Data Analysis and Visualization Environment) software (freeware) [67]. In this Appendix, we will present a brief tutorial for DAVE-MagProp, highlighting the construction of theoretical models in molecular magnetism.

Step 1: Opening the program and Importing the data.

Let us start by opening the DAVE program, go to *"Analysis"→"MagProp: Workup and Analysis of Magnetic Data"*. Let us import the $chiT$ data as a function of temperature as can be seen in Fig.A.1. In the *"File"→"Read Ascii File"* options click in *"Browse"*, select the file, set the position of the columns, and click *"Acept"*.
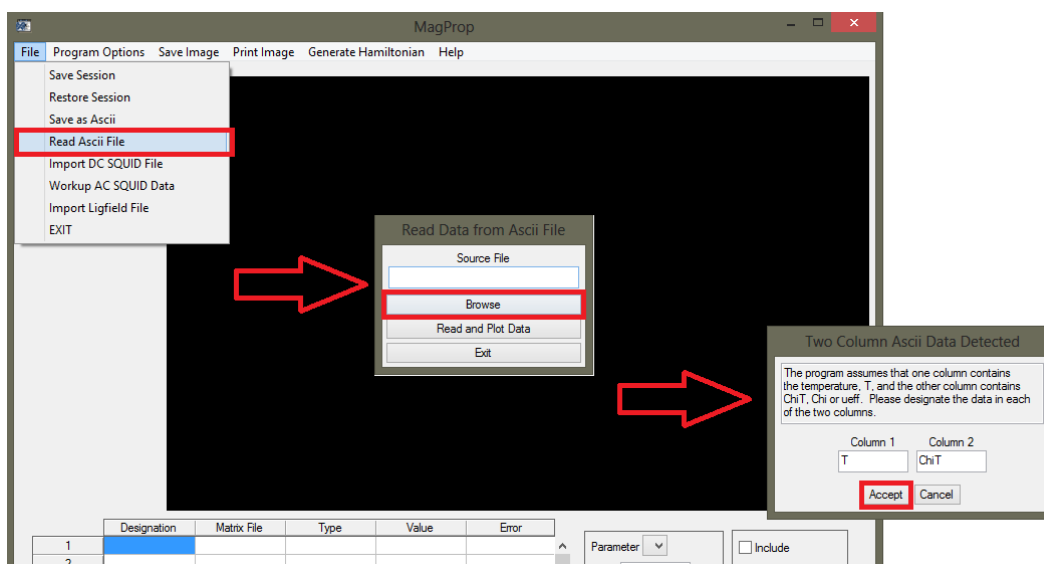
Figure A.1: Print from the DAVE-MagProp program screen. Import scheme of $chiT$ data as a function of temperature.

An important observation is that the data units of $chiT$ must be in emuK/mol,

and the temperature in Kelvin.

Step 2: Writing the Hamiltonian Model.

After importing the experimental data we will write the spin Hamiltonian. DAVE-MagProp has a Hamiltonian generator, to open it click *"Generate Hamiltonian"*→*"Hamiltonian Matrix Generator"*(see Fig.A.2).
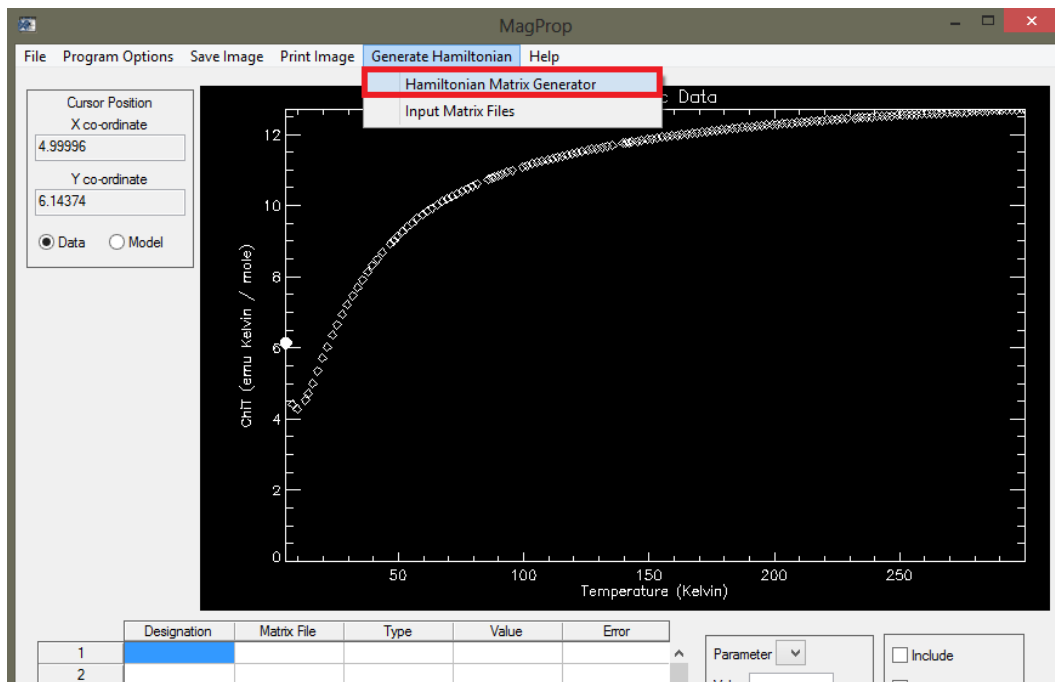
Figure A.2: Print from the DAVE-MagProp program screen. Opening *"Hamiltonian Matrix Generator"*

Open the Hamiltonian generator, click on *"New Hamiltonian"*, then define the name of the Hamiltonian file, and the number of metallic centers of the proposed model for the geometric spin configuration in question, then click *"Accept"*. In the following window, define the value of the angular momentum of each metallic center based on the state of oxidation and the symmetry of each magnetic ion (see Fig.A.3).

Then, use the menu on the right to define the scalar, and vector products between the spin operators and build the desired Hamiltonians (Fig.A.4). Then, click on *"Create Matrices"* to create the Hamiltonian matrix. Once this is done, return to the MagProp screen.
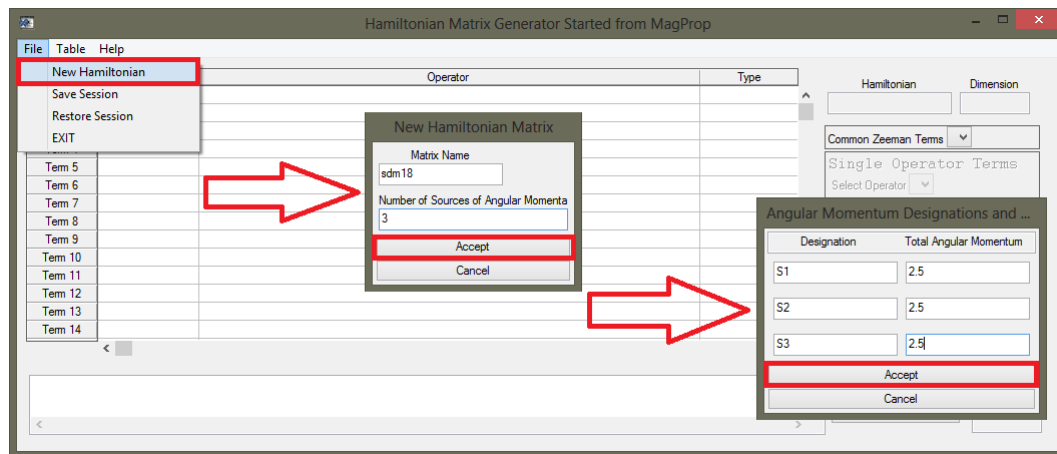
Figure A.3: Print screen from the Hamiltonian generator program of DAVE-MagProp software.
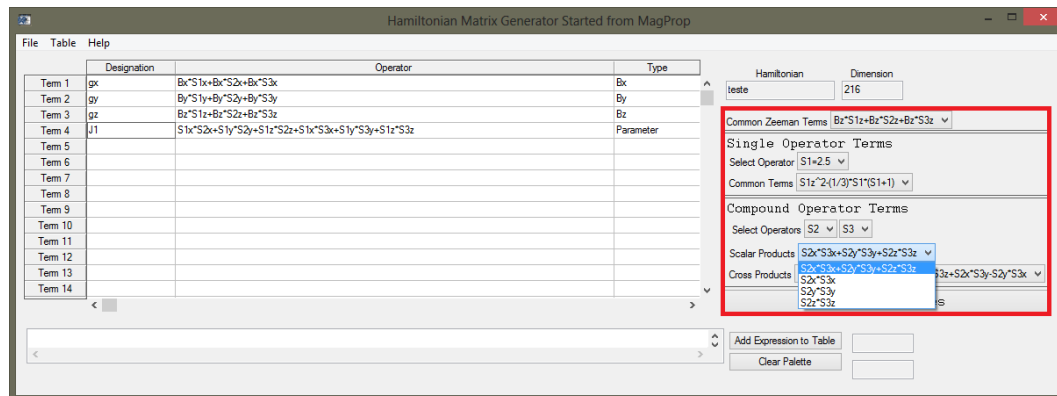
Figure A.4: Print screen from the Hamiltonian generator program of DAVE-MagProp software. Defining the products among the spin operators.
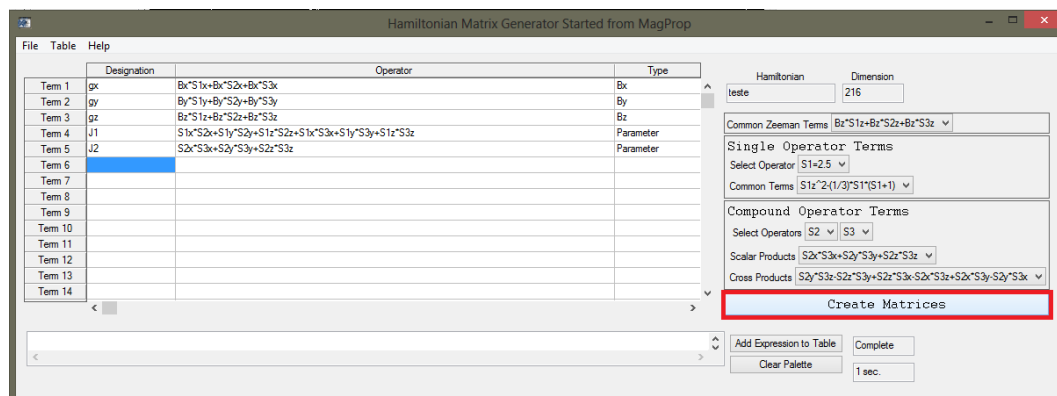
Figure A.5: Print screen from the Hamiltonian generator program of DAVE-MagProp software. Creating the Hamiltonian matrix.

Step 3: Adjusting the experimental data and extracting the optimized parameters.

It is also possible to include the diamagnetic contribution in the susceptibility model, for this click *"Diamagnetism/TIP"→"Include Diamagnetism Correction/TIP term in Model"*, as shown in Fig.A.6

Note that, in the lower left corner of the screen there will be a table with the respective optimized parameters introduced in the Hamiltonian (Fig.A.7). Click in *"Refine on data"*, the program will calculate the energy spectrum, and the magnetic susceptibility numerically and will give us the optimized parameters of the model.
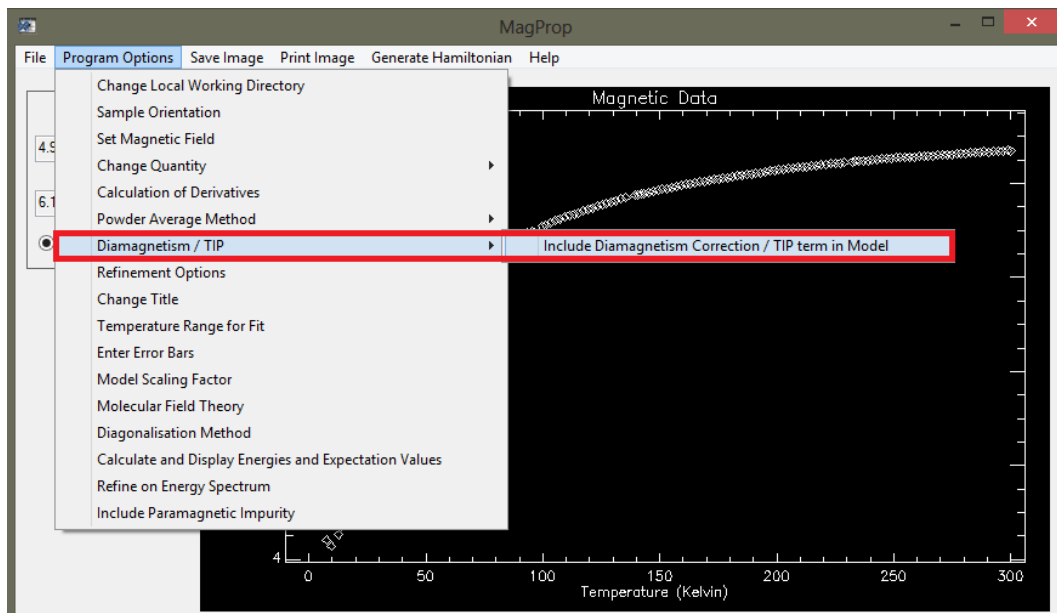
Figure A.6: Including the diamagnetic contribution in the susceptibility model.

The program displays the exchange parameters $J's$ in the unit of cm^{-1} (1.4K), and the diamagnetic contribution in $emu/Oe(9.274 \cdot 10^2 1\mu_B/Oe)$. Finally, to export the adjusted data with the parameters simply click on *"File"→"Save as Ascii"*.
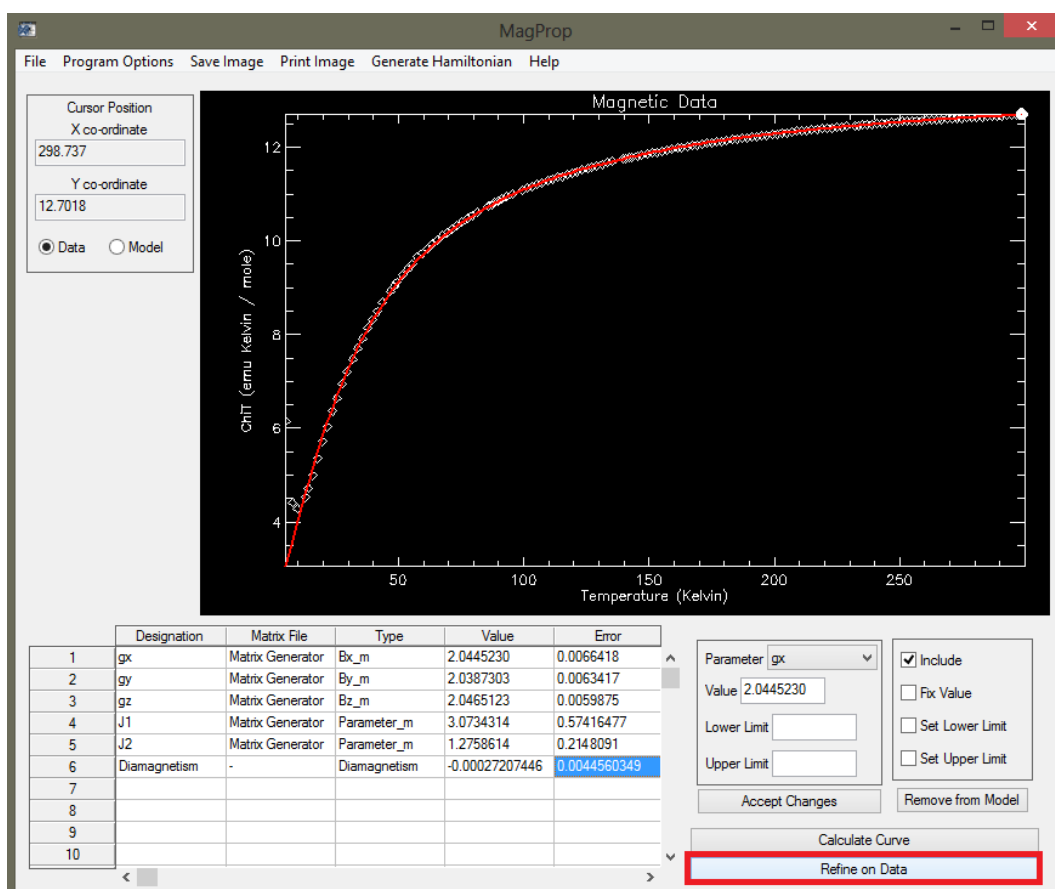
Figure A.7: Refining the experimental data.

B List of Papers

ASSOCIATED WITH THIS THESIS

1 **CRUZ, C. S.**; Soares-Pinto, D. O. ; Brandão, P. ; dos Santos, A. M. ; REIS, M.S. . Carboxylate-based molecular magnet: One path toward achieving stable quantum correlations at room temperature. Europhysics Letters (Print), v. 113, p. 40004, 2016.

2 **CRUZ, C**; ALVES, Á. S. ; DOS SANTOS, R. N. ; Soares-Pinto, D. O. ; DE JESUS, J. C. O. ; DE ALMEIDA, J. S. ; REIS, M.S. . Influence of the external pressure on the quantum correlations of molecular magnets. Europhysics Letters (Print), v. 117, p. 20004, 2017.

3 **CRUZ, C.**. Quantum correlations and Bell's inequality violation in a Heisenberg spin dimer via neutron scattering. INTERNATIONAL JOURNAL OF QUANTUM INFORMATION, v. 5, p. 1750031, 2017.

Carboxylate-based molecular magnet: One path toward achieving stable quantum correlations at room temperature

C. Cruz[1(a)], D. O. Soares-Pinto[2], P. Brandão[3], A. M. dos Santos[4] and M. S. Reis[1]

[1] *Instituto de Física, Universidade Federal Fluminense - Av. Gal. Milton Tavares de Souza s/n, 24210-346 Niterói, Rio de Janeiro, Brazil*
[2] *Instituto de Física de São Carlos, Universidade de São Paulo - CP 369, 13560-970, São Carlos, SP, Brazil*
[3] *CICECO, Universidade de Aveiro - 3810-205, Aveiro, Portugal, EU*
[4] *Quantum Condensed Matter Division, Oak Ridge National Laboratory - Oak Ridge, TN 37831-6475, USA*

Abstract – The control of quantum correlations in solid-state systems by means of material engineering is a broad avenue to be explored, since it makes possible steps toward the limits of quantum mechanics and the design of novel materials with applications on emerging quantum technologies. In this context, this letter explores the potential of molecular magnets to be prototypes of materials for quantum information technology. More precisely, we engineered a material and from its geometric quantum discord we found significant quantum correlations up to 9540 K (even without entanglement); and, in addition, a pure singlet state occupied up to around 80 K (above liquid nitrogen temperature). These results could only be achieved due to the carboxylate group promoting a metal-to-metal huge magnetic interaction.

Quantum entanglement has received a considerable attention as a remarkable resource for quantum information processing [1–3]. In spite of that, it is fragile and can easily vanish due to the inevitable interaction of the system with its environment [4]; and due to this condition, it was thought that entanglement could only exist at low temperatures. However, recently, it has been shown that entanglement can also exist at higher temperatures, and can be detected through the measurement of some thermodynamic observables [5–17].

Nevertheless, quantum entanglement does not encompass all quantum correlations in a system and recent studies have greatly expanded the notion of quantum correlations [18–29]; and the measure of quantum excess of correlations has been named as *quantum discord* [19–21]. In the last years, it was understood that quantum discord has an important role in many quantum information processing even without entanglement. Notably, this quantity can also detect quantum phase transitions [25,30,31].

Despite much effort by the scientific community, there are only a few results on the analytical expression of

quantum discord; and only for a certain class of states an exact solution is known [23–27,32,33]. This fact stimulated alternative measurements of quantum discord, theoretically and experimentally [22,24,29,34–36]. The recent demonstration that quantum discord can be measured by the thermodynamic properties of solids, such as magnetic susceptibility, internal energy [35–37], specific heat [35,36] and even neutron scattering data [22], shows that quantum correlations can be related to significant macroscopic effects allowing the measurement and the control of quantum correlations in solid-state systems by means of material engineering. Thus, the design of novel materials becomes an actual challenge to overcome.

In this direction, molecular magnets can be an excellent opportunity to achieve this goal as prototypes of materials for quantum information technology. They combine classical properties, found in any macroscopic magnet, with quantum ones, such as quantum interference and entanglement. The large gap between the ground state and the first-excited state found in some materials allows the existence of entangled quantum states at higher temperatures [6,11,13,17]. The study of molecular magnets opens thus the doors for new research toward the limits of

---

quantum mechanics; and several aspects are worthy of a thorough research, such as (i) how robust are their quantum features against temperature and (ii) how large systems can support these properties. These results would lead to promising applications in quantum technologies, specially devices based on quantum correlations.

In this context, we show in this letter that carboxylate-based compounds can support quantum correlations thousands of kelvins above room temperature. We report the crystal structure and magnetic susceptibility of a carboxylate-based molecular magnet with formula $[Cu_2(HCOO)_4(HCOOH)_2(piperazine)]$; from which the entropic and geometric quantum discord, based on the Schatten 1-norm [38,39], are extensively explored. The analytical formulas for the quantum correlations are derived as a function of the temperature using the magnetic susceptibility of the compound and the analysis of the data suggests the existence of entanglement up to temperatures of 681 K, while the measure of quantum discord reveals that this system keeps at the singlet ground state up to around 80 K. In addition, quantum correlations would remain up to 9540 K, thousands of kelvins above room temperature, even without entanglement. Thus, we obtain very stable quantum correlations up to 513 K, the limit where this material can exist —hundreds of kelvins above room temperature[1]. Due to the material topology, these results represent the highest temperatures, reported to date, wherein quantum correlations can be supported.

As pointed out before, to obtain such strongly entangled states at high temperature, we need to maximize the gap between the ground state and the first-exited state. Thus, we have designed materials with such features to enhance their quantum properties, and then study the entropic and geometric quantum discord. The dinuclear copper (II) complex $[Cu_2(\mu\text{-}HCOO)_4(HCOO)_2]$piperazine was the successful prototype synthesized, and its molecular structure is presented in fig. 1.

Single-crystal structure analysis revealed that the compound is composed of a dimeric cupric tetraformate unit, with a short Cu-Cu internuclear separation of 2.628(2) Å and one piperazine molecule. The dimer is formed by opposing square pyramidal CuO_5 with a very small distortion —see fig. 1(a). The base oxygen atoms on the adjoining pyramids are part of the four-connecting carboxylate groups in a syn-syn conformation leading to a strong magnetic interaction between the dimers ions. The apical oxygen of the pyramid is connected, via the HCOO group (Cu-O = 2.12(1) Å), to the other carboxylate group. The crystal structure is stabilized by the intermolecular N-HO hydrogen bonding with $N(10)\cdots O(7) = 2.722(2)$ Å and $N(10)\cdots O(8)^{ii} = 2.745(2)$ Å $(ii = 1+x, y, z)$ forming an infinite two-dimensional network.

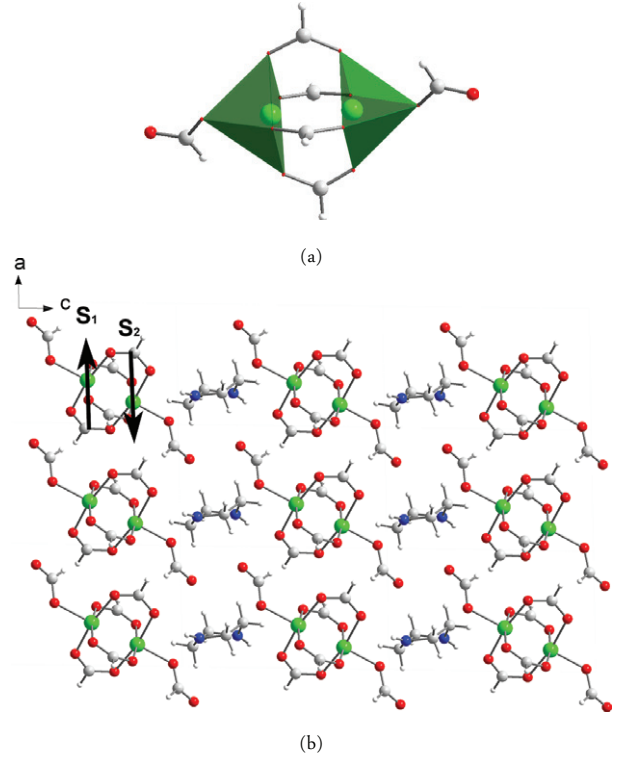From the magnetic point of view, the designed compound $[Cu_2(\mu\text{-}HCOO)_4(HCOO)_2]$piperazine is of highest

Fig. 1: (Color online) Crystal structure of $[Cu_2(\mu\text{-}HCOO)_4$ $(HCOO)_2]$piperazine compound with (a) local dimer polyhedron representation and (b) dimeric sheet view, where the arrows represent the reduced magnetic structure of the compound. Color scheme: Cu —green; O —red; N —blue.

interest, since it shows a short interaction path between the metal centers. From their crystal structure, previously described, it is possible to extract the magnetic structure, as shown in fig. 1(b). In this structure, copper dimers, with an intramolecular separation of 2.628(2) Å, are separated each other by a distance of 6.776(1) Å. These dimers are arranged in linear chains along the *a*-axis, and these chains are separated from each other, along the *c*-axis, by a distance of 8.176(1) Å, forming thus sheets of copper dimers —see fig. 1(b). Magnetically speaking, due to the much higher intra- and inter-chain distances, in comparison to the Cu-Cu intra-dimer distance, we considered a model of isolated dimers. Considering the Cu(II) ions under consideration have a d^9 electronic configuration, this material is an ideal realization of a spin-(1/2) dimer. The present model has one exchange parameter: J, related to an intra-dimer interaction corresponding to the syn-syn conformation, as can be seen in fig. 1(a). Thus, the Hamiltonian expression of this system is simply written as

$$\mathcal{H} = -J\vec{S}_1 \cdot \vec{S}_2 - g\mu_B \vec{B} \cdot (\vec{S}_1 + \vec{S}_2), \qquad (1)$$

where g is the isotropic Lande factor.

The quantum properties of several materials have been deeply analyzed by means of thermodynamic quantities [5–17], and the magnetic susceptibility χ has been

---

[1]This result was obtained by Thermogravimetric Analysis (TGA), not shown.
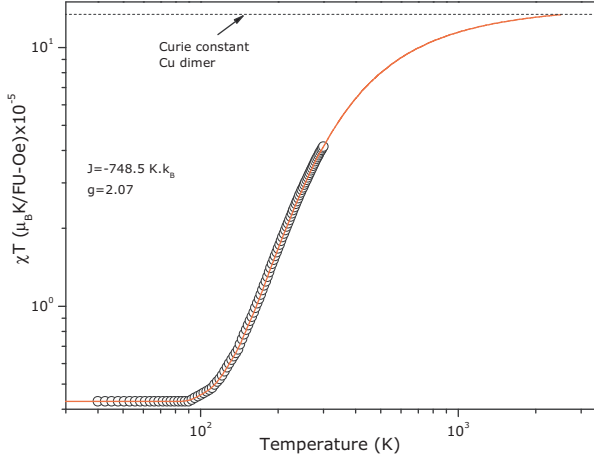
Fig. 2: (Color online) Experimental (open circles) and theoretical (solid line) magnetic susceptibility *vs.* temperature. The red line represents the fitting of eq. (2) to the experimental data, where an extrapolation, up to higher temperatures, was done using the optimized parameters. The dashed line indicates the Curie constant for a Cu-Cu dimer.

a good benchmark [5–8,10–13,17] due to the easy experimental access. For the material under consideration, the experimental χT quantity, for the whole range of temperature considered ($< 300\,\mathrm{K}$), is smaller than the Curie constant of the dimer $C = 1.34 \times 10^{-4}\ \mu_B\mathrm{K/FU\text{-}Oe}$; and it is a clear signature that at least one exchange interaction into the system is larger than the thermal energy at room temperature. As a consequence, the paramagnetic region is not reached for the temperature range in which the susceptibility is measured and therefore this experimental data cannot be described within the Curie-Weiss law. These results are shown in fig. 2. From the theoretical point of view, the magnetic susceptibility due to the Hamiltonian of eq. (4) can be described as [40,41]:

$$\chi(T) = \frac{2N(g\mu_B)^2}{k_B T} \frac{1}{3 + e^{-J/k_B T}} \tag{2}$$

and a fitting of the above to the experimental data (shown in fig. 2) were obtained with $J = -748.5\,\mathrm{K}$ (antiferromagnetically coupled ions) and $g = 2.07$. This fitting was performed using DAVE-MagProp [42], a software that analyzes and processes magnetic data. From these fitting parameters, it was possible to extrapolate this thermodynamic quantity to higher temperatures and it is clear that the system indeed dimerizes at rather elevated temperatures, and these dimers remain isolated down to the lowest measured temperature.

To go further and analyse the quantum correlations by means of magnetic susceptibility, firstly, the spin-spin correlation function $c(T) = \langle S_1^{(i)} S_2^{(i)} \rangle$, where $i = x, y, z$, must be written as a function of the magnetic susceptibility χ. For this prototype material, *i.e.*, an ideal spin-$(1/2)$ dimer, it reads as

$$c(T) = \frac{2k_B T}{N(g\mu_B)^2} \chi(T) - 1. \tag{3}$$

From the above, the quantum discord can now be written as a function of the magnetic susceptibility. Quantum discord can be defined in terms of the von Neumann entropy $S(\rho_{AB}) = -\mathrm{Tr}\,[\rho_{AB} \log_2 \rho_{AB}]$, where ρ_{AB} is the density matrix of a composite system. The total correlation $\mathcal{I}(\rho_A : \rho_B) = S(\rho_A) + S(\rho_B) - S(\rho_{AB})$ is split into the quantum part $\mathcal{Q}$ and the classical ones $\mathcal{C}(\rho_{AB})$ [19,20,23–28,43], where the classical correlation of the composite system ρ_{AB} is defined as

$$\mathcal{C}(\rho_{AB}) = \max \left[S(\rho_A) - \sum_k p_k S(\rho_k) \right], \tag{4}$$

where the maximum is taken over all positive operator-valued measurements (POVMs) $\{B_k\}$ performed locally only on subsystem B, with the conditional state $\rho_k = (\mathbb{I}_A \otimes B_k)\rho(\mathbb{I}_A \otimes B_k)/p_k$ and the probability to obtain the outcome k $p_k = \mathrm{Tr}\,[(\mathbb{I}_A \otimes B_k)\rho(\mathbb{I}_A \otimes B_k)]$.

Thus, the amount of genuinely quantum correlations, called *quantum discord* can be introduced as an entropic measure of quantum correlation in a quantum state, defined as the difference between the total and the classical correlation, $\mathcal{Q}(\rho_{AB}) = \mathcal{I}(\rho_A : \rho_B) - \mathcal{C}(\rho_{AB})$. Thus, the entropic quantum discord depending on the magnetic susceptibility reads as

$$\begin{aligned}
\mathcal{Q}_E(T) =\ & \frac{1}{4}\{[4 - 3\alpha T\chi(T)] \log_2 [4 - 3\alpha T\chi(T)] \\
& + 3\alpha T\chi(T) \log_2 [\alpha T\chi(T)]\} \\
& - \frac{1}{2}\{[1 + |\alpha T\chi(T) - 1|] \log_2 [1 + |\alpha T\chi(T) - 1|] \\
& + [1 - |\alpha T\chi(T) - 1|] \log_2 [1 - |\alpha T\chi(T) - 1|]\},
\end{aligned} \tag{5}$$

where $\alpha = 2k_B/N(g\mu_B)^2$.

On the other hand, the geometric quantum discord, based on Schatten 1-norm, is a well-defined measurement of the amount of quantum correlations of a state in terms of its minimal distance from the set ω of classical states [28,43]. Geometric quantum discord reads then as

$$\mathcal{Q}_G(\rho) = \min_\omega \|\rho - \rho_c\|, \tag{6}$$

where $\|X\| = \mathrm{Tr}\left[\sqrt{X^\dagger X}\right]$ is the 1-norm, ρ is a given quantum state and ρ_c a closest classical-quantum state [28,43].

It is described in refs. [28,38,39] and [43] for a Bell diagonal state and can now be written as a function of the magnetic susceptibility as

$$\mathcal{Q}_G(T) = \frac{1}{2} \left| \frac{2k_B T}{N(g\mu_B)^2} \chi(T) - 1 \right| \tag{7}$$

Furthermore, in order to make a comparison between the quantum discord and the amount of entanglement in the system under consideration, we adopt the measure of entanglement of formation, which is oftenly used as a measurement of entanglement, defined by [44,45]

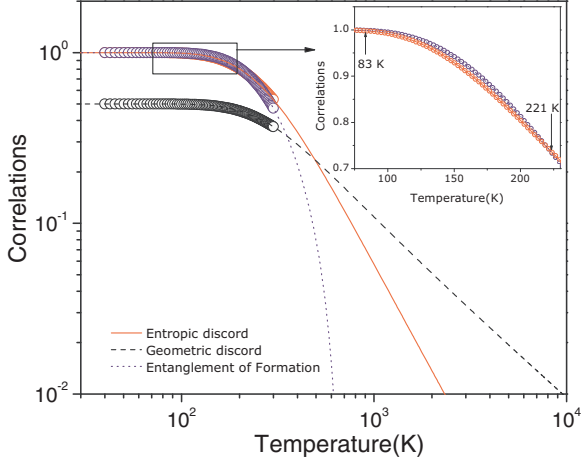$$\mathbb{E} = -\mathbb{E}_+ - \mathbb{E}_-, \tag{8}$$

Fig. 3: (Color online) Temperature dependence of entropic (solid red line) and geometric (dashed black line) quantum discords, as well as entanglement of formation (dotted blue line). Due to tecnhical limitations, experimental data (open circles) are measured only up to room temperature, but the theoretical extrapolation (solid lines) goes further. The inset shows the region where the entanglement is larger than entropic quantum discord, as well as the pure state up to around 80 K.

where

$$\mathbb{E}_{\pm} = \frac{1 \pm \sqrt{1 - \mathbb{C}^2}}{2} \log_2 \left(\frac{1 \pm \sqrt{1 - \mathbb{C}^2}}{2} \right) \qquad (9)$$

and $\mathbb{C}$ is the concurrence [1,44,45], that can now be written as a function of the magnetic susceptibility as

$$\mathbb{C} = -\frac{1}{2} \left[2 + 3 \frac{2k_B T}{N(g\mu_B)^2} \chi(T) \right], \qquad T < T_e \qquad (10)$$

and zero otherwise; where $T_e \approx |J|/k_B \ln(3) \approx 0.91|J|/k_B$ is the temperature of entanglement, the maximum temperature below which there is entanglement [3,6,11,12].

Figure 3 shows the entropic (eq. (5)) and geometric quantum discords (eq. (7)), as well as the entanglement of formation (eq. (8)), as a function of temperature, obtained from the experimental magnetic susceptibility data —open circles— and the extrapolated ones —solid lines. Note that, up to around 80 K (above the liquid nitrogen temperature) the entropic discord and the entanglement achieve the maximum value of unity, *i.e.*, the system is absolutely in the singlet ground state (pure state). Above this temperature, the entanglement is larger than entropic quantum discord and intercepts back this curve at 221 K. This phenomenon in which the entanglement is larger than the quantum correlations can be explained due to the fact that entanglement is a mixture of purely classical and purely quantum correlations. In addition, a direct comparison may lead to a misunderstanding, since entanglement is a different measurement of quantum correlation, as already discussed in refs. [26,35] and [36].

From the entanglement of formation we can verify that these copper dimers are entangled up to temperatures of $T_e = 681$ K when the entanglement has a sudden death. However, from the entropic quantum discord we can verify that this material can support correlated quantum states up to temperatures as high as 2320 K. However, above 500 K the geometric quantum discord is larger than the entropic one and it can survive up to 9540 K, thousands of kelvins above room temperature and above the entropic quantum discord. These are the highest temperatures reported in the literature wherein quantum correlation can be supported in solid-state systems. This means that the quantum correlations in this material are very stable and survives up to the temperatures in which the material exists: 523 K (see footnote [1]). It is important to emphasize that these results are only possible due to the engineered metal-carboxylate compound and its syn-syn conformation, that leads to a strong magnetic interaction ($J = -748.5$ K). Therefore, carboxylate-based molecular magnets are one path toward achieving stable quantum correlations at room temperature.

In summary, our main result was to provide to the literature an engineered material with a high stability of its quantum correlations against external perturbations. We found that geometric quantum discord is significantly different from zero up to 9540 K, while the entropic one shows the existence of quantum correlations up to 2320 K; even when the entanglement is absent. Also remarkable is the realization of a pure state up to 83 K. This prototype material has been achieved only after a successful material engineering to ensure the highest exchange interaction between spin-(1/2) Cu ions into a dimeric structure. The core element to this realization is the carboxylate group, that yielded a very short (and direct) metal-to-metal extraordinarily high magnetic interaction and leads the material to be immune to decohering mechanisms. The study of this class of materials can now open a large avenue for research towards the limits of quantum mechanics, leading to promising applications in quantum technologies.

$$* * *$$

Additional remark: Electronic Supplementary Information (ESI) available: CCDC 1428140 for compound

[Cu$_2(\mu$-HCOO)$_4$(HCOO)$_2$]piperazine, contains the supplementary crystallographic data for this paper. Copy of the data can be obtained free of charge on application to CCDC, see contact details at `http://www.ccdc.cam.ac.uk`.

REFERENCES

[1] NIELSEN M. A. and CHUANG I. L., *Quantum Computation and Quantum Information* (Cambridge University Press) 2010.
[2] VEDRAL V., *Introduction to Quantum Information Science* (Oxford University Press) 2006.
[3] HORODECKI R., HORODECKI P., HORODECKI M. and HORODECKI K., *Rev. Mod. Phys.*, **81** (2009) 865.
[4] YU T. and EBERLY J., *Science*, **323** (2009) 598.
[5] VEDRAL V., *Nature*, **453** (2008) 1004.
[6] SOARES-PINTO D., SOUZA A., SARTHOUR R., OLIVEIRA I., REIS M., BRANDAO P., ROCHA J. and DOS SANTOS A., *EPL*, **87** (2009) 40008.
[7] DUARTE O. S., CASTRO C. S., SOARES-PINTO D. O. and REIS M. S., *EPL*, **103** (2013) 40002.
[8] DUARTE O., CASTRO C. and REIS M., *Phys. Rev. A*, **88** (2013) 012317.
[9] SOARES-PINTO D., TELES J., SOUZA A., DEAZEVEDO E., SARTHOUR R., BONAGAMBA T., REIS M. and OLIVEIRA I., *Int. J. Quantum Inf.*, **9** (2011) 1047.
[10] SOUZA A., REIS M., SOARES-PINTO D., OLIVEIRA I. and SARTHOUR R., *Phys. Rev. B*, **77** (2008) 104402.
[11] REIS M. S., SORIANO S., DOS SANTOS A. M., SALES B. C., SOARES-PINTO D. and BRANDAO P., *EPL*, **100** (2012) 50001.
[12] WIEŚNIAK M., VEDRAL V. and BRUKNER Č., *New J. Phys.*, **7** (2005) 258.
[13] SOUZA A., SOARES-PINTO D., SARTHOUR R., OLIVEIRA I., REIS M. S., BRANDAO P. and DOS SANTOS A., *Phys. Rev. B*, **79** (2009) 054408.
[14] HIDE J., SON W. and VEDRAL V., *Phys. Rev. Lett.*, **102** (2009) 100503.
[15] TÓTH G., *Phys. Rev. A*, **71** (2005) 010301.
[16] GHOSH S., ROSENBAUM T., AEPPLI G. and COPPERSMITH S., *Nature*, **425** (2003) 48.
[17] VEDRAL V., *Sci. Am.*, **304** (2011) 38.
[18] MODI K., BRODUTCH A., CABLE H., PATEREK T. and VEDRAL V., *Rev. Mod. Phys.*, **84** (2012) 1655.
[19] OLLIVIER H. and ZUREK W. H., *Phys. Rev. Lett.*, **88** (2001) 017901.
[20] HENDERSON L. and VEDRAL V., *J. Phys. A: Math. Gen.*, **34** (2001) 6899.
[21] VEDRAL V., *Phys. Rev. Lett.*, **90** (2003) 050401.
[22] LIU B.-Q., WU L.-A., ZENG G.-M., SONG J.-M., LUO W., LEI Y., SUN G.-A., CHEN B. and PENG S.-M., *Phys. Lett. A*, **378** (2014) 3441.
[23] MA Z., CHEN Z., FANCHINI F. F. and FEI S.-M., *Sci. Rep.*, **5** (2015).
[24] GIROLAMI D. and ADESSO G., *Phys. Rev. A*, **83** (2011) 052108.
[25] SARANDY M., *Phys. Rev. A*, **80** (2009) 022108.
[26] LUO S., *Phys. Rev. A*, **77** (2008) 042303.
[27] DATTA A., SHAJI A. and CAVES C. M., *Phys. Rev. Lett.*, **100** (2008) 050502.
[28] PAULA F., DE OLIVEIRA T. R. and SARANDY M., *Phys. Rev. A*, **87** (2013) 064101.
[29] DAKIĆ B., VEDRAL V. and BRUKNER Č., *Phys. Rev. Lett.*, **105** (2010) 190502.
[30] PIRANDOLA S., *Sci. Rep.*, **4** (2014).
[31] WERLANG T., TRIPPE C., RIBEIRO G. and RIGOLIN G., *Phys. Rev. Lett.*, **105** (2010) 095702.
[32] MODI K., PATEREK T., SON W., VEDRAL V. and WILLIAMSON M., *Phys. Rev. Lett.*, **104** (2010) 080501.
[33] BRODUTCH A. and TERNO D. R., *Phys. Rev. A*, **81** (2010) 062103.
[34] LUO S. and FU S., *Phys. Rev. A*, **82** (2010) 034302.
[35] YURISHCHEV M. A., *Phys. Rev. B*, **84** (2011) 024418.
[36] ALDOSHIN S., FEL'DMAN E. and YURISHCHEV M., *Low Temp. Phys.*, **40** (2014) 3.
[37] CHAKRABORTY T., SINGH H., SINGH S., GOPAL R. K. and MITRA C., *J. Phys.: Condens. Matter*, **25** (2013) 425601.
[38] CICCARELLO F., TUFARELLI T. and GIOVANNETTI V., *New J. Phys.*, **16** (2014) 013038.
[39] OBANDO P. C., PAULA F. M. and SARANDY M. S., *Phys. Rev. A*, **92** (2015) 032307.
[40] REIS M., *Fundamentals of Magnetism* (Elsevier) 2013.
[41] BLEANEY B. and BOWERS K., *Proc. R. Soc. London, Ser. A*, **214** (1952) 451.
[42] AZUAH R. T., KNELLER L. R., QIU Y., TREGENNA-PIGGOTT P. L., BROWN C. M., COPLEY J. R. and DIMEO R. M., *J. Res. Natl. Inst. Stand. Technol.*, **114** (2009) 341.
[43] MONTEALEGRE J., PAULA F., SAGUIA A. and SARANDY M., *Phys. Rev. A*, **87** (2013) 042115.
[44] WOOTTERS W. K., *Phys. Rev. Lett.*, **80** (1998) 2245.
[45] HILL S. and WOOTTERS W. K., *Phys. Rev. Lett.*, **78** (1997) 5022.

Influence of the external pressure on the quantum correlations of molecular magnets

C. Cruz[1(a)], Á. S. Alves[2], R. N. dos Santos[2], D. O. Soares-Pinto[3], J. C. O. de Jesus[2], J. S. de Almeida[4] and M. S. Reis[1]

[1] *Instituto de Física, Universidade Federal Fluminense - Av. Gal. Milton Tavares de Souza s/n,*
24210-346, Niterói, Rio de Janeiro, Brazil
[2] *Projeto Física no Campus, Laboratório de Física de Materiais, Departamento de Física,*
Universidade Estadual de Feira de Santana - Avenida Transnordestina, s/n, Novo Horizonte,
44036-900, Feira de Santana, Bahia, Brazil
[3] *Instituto de Física de São Carlos, Universidade de São Paulo - CP 369, 13560-970, São Carlos, SP, Brazil*
[4] *Instituto de Física, Universidade Federal da Bahia - Campus Universitário de Ondina,*
40210-340, Salvador, Bahia, Brazil

Abstract – The study of quantum correlations in solid-state systems is a large avenue for research and their detection and manipulation are an actual challenge to overcome. In this context, we show by using first-principles calculations on the prototype material $KNaCuSi_4O_{10}$ that the degree of quantum correlations in this spin cluster system can be managed by external hydrostatic pressure. Our results pave the way for research in detection and manipulation of quantum correlations in magnetic systems with promising applications in quantum information science.

Introduction. – Quantum correlations play an important role in quantum information science as a remarkable resource in quantum information processing [1–4]. The existence of pure quantum correlations has been usually inferred by the presence of entanglement. Nevertheless, although quantum entanglement provides a way to find out pure quantum correlations, it does not encompass all quantum correlations of the system [5–28]. Nowadays, the notion of quantum correlations has been greatly expanded; and the measure of quantumness of the correlation has been named *quantum discord*. The study of quantum discord has been attracting considerable attention due to its important role in many quantum information processing even when the entanglement is absent [4,5,15,16,23].

Despite much effort by the scientific community, the characterization of quantum correlations consists in a rather complicated task, theoretically and experimentally speaking [5,24–30], specially in condensed-matter systems; since this difficulty increases with the number of constituents of the system. This fact has stimulated alternative measurements of quantum correlations, allowing a better control of these quantum properties in these systems [5,15,16,24–29].

In the past few years, it was understood that quantum discord can be evaluated through the measurement of some thermodynamic properties of solids, such as magnetic susceptibility [5,15,16], internal energy [15,16], specific heat [5,15,16] and diffractive properties of neutron scattering [29]. Recently, it has been shown that quantum discord can also exist at higher temperature, for instance, at thousands of kelvins above room temperature [5], showing that quantum correlations are related to significant macroscopic effects, allowing a better control of quantum correlations in solid-state systems by means of materials engineering [5].

In this context, we show in the present work that the degree of correlation in a spin cluster system can be affected by the structural parameters, by applying external hydrostatic pressure. We performed first-principles calculations to investigate the dependence, under external pressure,

(a)E-mail: clebsonscruz@if.uff.br

of the magnetic coupling constant of the metal-silicate framework KNaCuSi$_4$O$_{10}$ [31] —a Heisenberg dimer on a d^9 electronic configuration; from which we obtain the entropic quantum discord and the entanglement of formation as a function of its magnetic susceptibility. Our results show that it is possible to manipulate the degree of quantum correlation in a magnetic system inducing a structural contraction by applying an external pressure. This leads to a better management of the quantum properties of these systems and paves the way for experimental and theoretical research of quantum correlations via first principles, leading to a better understanding of these quantum properties with promising applications in emerging quantum technologies.

Pairwise quantum correlations in a prototype material. – Our prototype material in which we investigate the influence of an external pressure on the quantum correlations via first-principles calculations is the metal-silicate framework KNaCuSi$_4$O$_{10}$ [31]. This compound is synthetic analog to a natural occurring mineral litidionite, a Heisenberg dimer in a d^9 electronic configuration and, therefore, an ideal realization of a two-qubit system (spin-(1/2) dimer) ruled by a Heisenberg-Dirac-Van Vleck Hamiltonian $\mathcal{H} = -J\vec{S}_1 \cdot \vec{S}_2$ [23,32], where J is the magnetic coupling constant [32]. The magnetic susceptibility of this system satisfies the Bleaney-Bowers equation [32,33]:

$$\chi(T) = \frac{2N(g\mu_B)^2}{k_B T}\frac{1}{3 + e^{-J/k_B T}}, \tag{1}$$

where, g is the Landé factor, μ_B is the Bohr magneton, k_B is the Boltzmann constant and N is the number of dimers.

The density matrix of the system under consideration has the Gibbs form, $\rho(T) = e^{-\mathcal{H}/k_B T}/Z$ [5,15,16,32], where $Z = \text{Tr}\{e^{-\mathcal{H}/k_B T}\}$ is the partition function. It can be written on Bell's diagonal mixed state in the computational basis $\{|00\rangle, |01\rangle, |10\rangle, |11\rangle\}$ [15,16]:

$$\rho(T) = \frac{1}{4}\begin{bmatrix} 1+c(T) & 0 & 0 & 0 \\ 0 & 1-c(T) & 2c(T) & 0 \\ 0 & 2c(T) & 1-c(T) & 0 \\ 0 & 0 & 0 & 1+c(T) \end{bmatrix}$$

$$= \frac{1}{4}(1 + c(T)\vec{S}_1 \cdot \vec{S}_2), \tag{2}$$

where

$$c(T) = \langle \vec{S}_1^{(1)} \cdot \vec{S}_2^2 \rangle = -1 + \frac{4}{3 + e^{-2J/k_B T}} \tag{3}$$

is the pairwise correlation function.

As calculated in ref. [5], it is possible to write the pairwise correlation function of the Heisenberg dimer as a function of its magnetic susceptibility, eq. (1), at finite temperature,

$$c(T) = \frac{2k_B T}{N(g\mu_B)^2}\chi(T) - 1. \tag{4}$$

Hence, with $c(T)$, one can easily obtain the quantum correlations of KNaCuSi$_4$O$_{10}$, as a function of their magnetic susceptibility [15,16,28].

The total amount of correlation in the system which is identified by the mutual information $\mathcal{I}(\rho_A : \rho_B) = S(\rho_A) + S(\rho_B) - S(\rho_{AB})$ can be splitted into the quantum part $\mathcal{Q}$ and the classical ones $\mathcal{C}(\rho_{AB})$, where $S(\rho_{AB}) = -\text{Tr}[\rho_{AB}\log_2 \rho_{AB}]$ is the von Neumann entropy [5,17,18, 23–25,28,29,34–38]. The amount of genuinely quantum correlations, called *quantum discord* can be defined as the difference between the total and the classical correlation, $\mathcal{Q}(\rho_{AB}) = \mathcal{I}(\rho_A : \rho_B) - \mathcal{C}(\rho_{AB})$. This difference is due to the quantum effects on the correlation between the subsystems A and B. Thus, the entropic quantum discord depends on the magnetic susceptibility of the compound as

$$\mathcal{Q}(T) = \frac{1}{4}\left\{[2 - 3\alpha T\chi(T)]\log_2 [2 - 3\alpha T\chi(T)]\right.$$
$$+ 3\alpha T\chi(T)\log_2 [\alpha T\chi(T)]\}$$
$$- \frac{1}{2}\{[1 + |\alpha T\chi(T) - 1|]\log_2 [1 + |\alpha T\chi(T) - 1|]$$
$$\left. + [1 - |\alpha T\chi(T) - 1|]\log_2 [1 - |\alpha T\chi(T) - 1|]\right\}, \tag{5}$$

where $\alpha = 2k_B/N(g\mu_B)^2$ [5].

Furthermore, in order to quantify the amount of entanglement in this spin system and make a comparison with the measurements of quantum discord, we adopt the measurement of entanglement of formation defined by [39,40]

$$\mathbb{E} = -\Lambda_+ \log_2 (\Lambda_+) - \Lambda_- \log_2 (\Lambda_-), \tag{6}$$

where

$$\Lambda_\pm = \frac{1 \pm \sqrt{1 - \mathbb{C}^2}}{2} \tag{7}$$

and $\mathbb{C}$ is the concurrence [1,39,40] that is written as a function of the magnetic susceptibility as [5,15,16]

$$\mathbb{C} = \begin{cases} -\frac{1}{2}\left[2 + 3\frac{2k_B T}{N(g\mu_B)^2}\chi(T)\right], & T < T_t, \\ 0, & T \geq T_t, \end{cases} \tag{8}$$

where

$$T_t \approx 0.91|J|/k_B \tag{9}$$

is the threshold temperature, the maximum temperature below which there is entanglement in the system [41,42].

First-principles calculations. – We performed first-principles calculations to investigate the dependence of the magnetic coupling constant of the metal-silicate framework KNaCuSi$_4$O$_{10}$ [31] under external pressure in order to evaluate this influence on the quantum correlations obtained as a function of the magnetic susceptibility of this compound.

Technical details. We approached this problem by using the density functional [43] theory (DFT) in the generalized gradient approximation (GGA) with
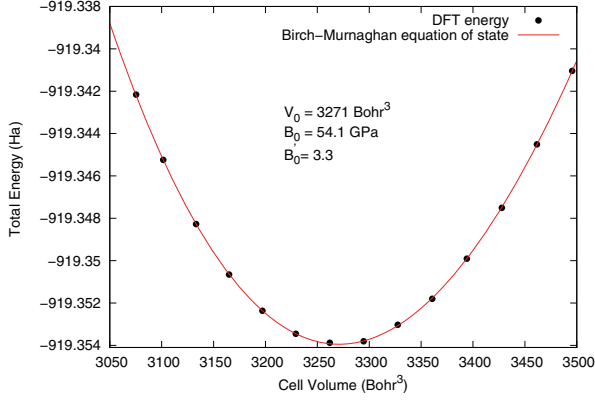
Fig. 1: (Colour online) Total energy *vs.* cell volume for $KNaCuSi_4O_{10}$ calculated by DFT and fitted using the third-order Birch-Murnaghan equation of state.

the Perdew-Burke-Ernzerhof parametrization for the exchange-correlation functional [44]. The Kohn-Sham equations were solved by using the plane-wave pseudopotential method as implemented in the Quantum ESPRESSO software [45]. The plane-wave energy cut-off was 47.5 Ha for the wave function and 237.5 Ha for the charge density. The k-point sampling of the Brillouin zone was done with an $5 \times 5 \times 5$ grid following the Monkhorst-Pack scheme [46] and with a Marzari-Vanderbilt smearing width of $5 \cdot 10^{-4}$ Ha [47]. The crystal structure was optimized at each volume of the unit cell. During the ionic relaxation, all positions were relaxed until Hellmann-Feynman forces were less than 0.05 Ha/bohr and the total energy converged below to $5 \cdot 10^{-6}$ Ha with respect to the Brillouin zone integration. The equation of state (EoS) of the $KNaCuSi_4O_{10}$ compound was obtained by fitting the total energy as a function of volume to the third-order Birch-Murnaghan equation [48]:

$$E(V) = E_0 + \frac{9V_0 B_0}{16} \left\{ \left[\left(\frac{V_0}{V} \right)^{\frac{2}{3}} - 1 \right]^3 B_0' \right.$$
$$\left. + \left[\left(\frac{V_0}{V} \right)^{\frac{2}{3}} - 1 \right]^2 \left[6 - 4 \left(\frac{V_0}{V} \right)^{\frac{2}{3}} \right] \right\}, \quad (10)$$

where V_0, B_0 and B_0' are the equilibrium volume, the bulk modulus at ambient pressure and its pressure derivative, respectively. The values found for these parameters were the following: $V_0 = 3271$ bohr^3, $B_0 = 54.1$ GPa and $B_0' = 3.3$. Figure 1 shows the structural optimization curve, *i.e.*, the results for the total energy *vs.* the volume of the unit cell obtained for DFT calculations and fitted by the third-order Birch-Murnaghan equation of state (eq. (10)).

For a Heisenberg spin-(1/2) dimer there are two eigenvalues of the energy, one being E_T the triplet state and the other E_S being the singlet state of the dimeric unit. Hence, its magnetic coupling constant (J) is the difference between these two states $J = E_S - E_T$. On the other hand,
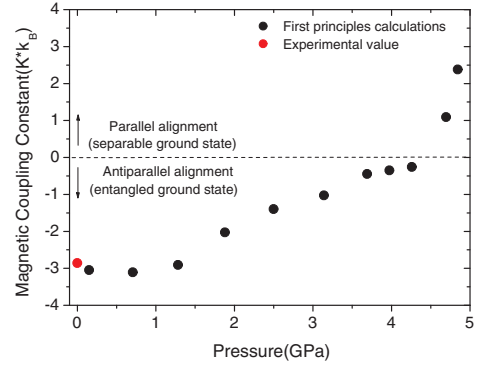
(a)
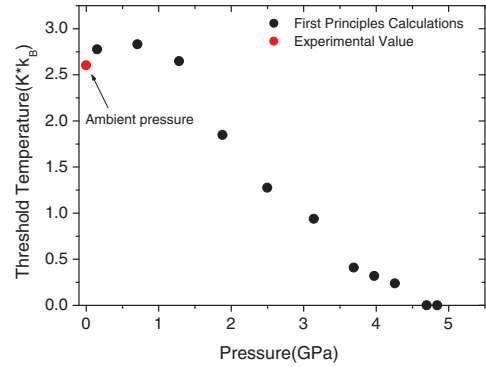
(b)

Fig. 2: (Colour online) (a) Magnetic coupling constant and (b) threshold temperature (T_t) obtained as a function of the external pressure. The red dot is the experimental value obtained at ambient pressure taken from ref. [31]. The external pressure induces a structural contraction on the prototype material leading to a change of the magnetic alignment of the system. This change yields a decrease on the degree of entanglement by reducing T_t.

the Hohenberg-Kohn theorem asserts that the total energy of a system is a functional of the charge density. Thus, we have used this theorem along with the Kohn-Sham scheme to calculate the total energy for each spin alignment for several volumes and fitted them by using the above equation of state. Based on such procedure it is possible to write the total energy as a function of pressure and we can therefore calculate the other physical quantities from first principles accordingly.

Results. The external pressure applied on a molecular magnetic system induces a structural contraction that reduces its lattice parameters leading to trengthening or weakening of the magnetic coupling of the system, due to its strong dependence with the structural properties of the sample material. For the prototype material $KNaCuSi_4O_{10}$ its magnetic coupling constant (J) increases and becomes positive, *i.e.*, the system changes from an antiparallel alignment ($J < 0$ —entangled ground state) to a parallel alignment ($J > 0$ —separable ground state) due to the application of an external pressure, as can be seen in fig. 2(a). Hence, we obtain the threshold
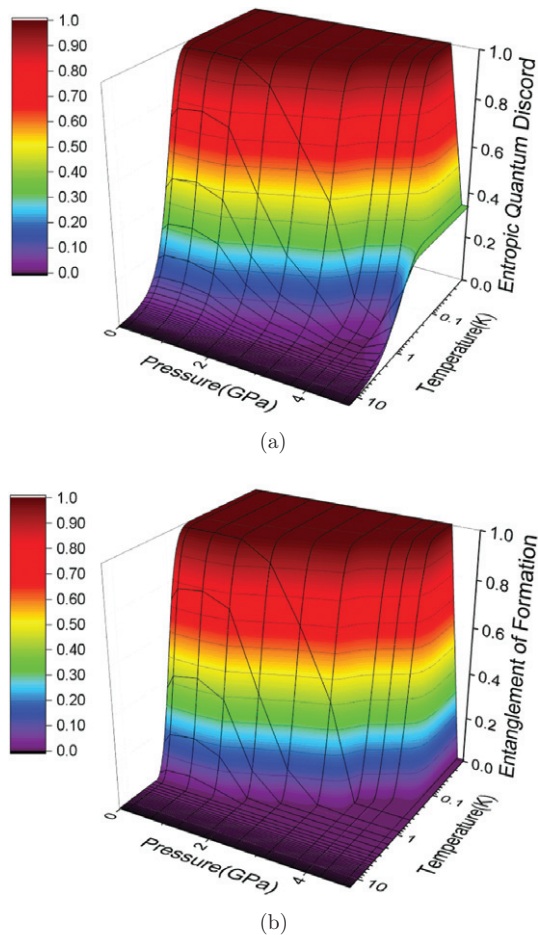
(a)

(b)

Fig. 3: (Colour online) (a) Entropic quantum discord and (b) entanglement of formation as a function of the temperature and pressure. It is worth noting that it is possible to manage the degree of quantum correlation in a magnetic system by the control of external pressure and temperature.

temperature (T_t), eq. (9), using the magnetic coupling constant. Figure 2(b) shows the dependence of T_t in the prototype compound under pressure. As can be seen, the change in the magnetic alignment leads to the decrease of T_t down to the disappearance of the entanglement (see fig. 2(b)), when the system achieves a parallel alignment. This means that the degree of entanglement in a magnetic system can be controlled by significant macroscopic effects when applying external pressure.

On the other hand, in order to evaluate the influence of external pressure on the quantum correlations, we calculate the magnetic susceptibilities (eq. (1)) from each magnetic coupling constant presented in fig. 2(a). Using eqs. (5), (6), it is possible to evaluate the quantum correlations as a function of these susceptibilities. We obtain the quantum correlation curves measured by this thermodynamic property for each magnetic configuration of the system. Thus, we establish a relationship between the quantum properties with significant macroscopic effects.

In sequence, fig. 3(a) and (b) shows the entropic quantum discord (eq. (5)) and entanglement of formation

(eq. (6)) curves as a function of the temperature and pressure, respectively. Note that the degree of quantum correlations in the system decreases by increasing the external pressure as a consequence of the changes of the magnetic coupling constant as shown in fig. 2(a). Also remarkable is the management of the ground state in the system by reducing the temperature and controlling the external pressure; it achieves this state when the entropic discord (fig. 3(a)) and entanglement (fig. 3(b)) reach the maximum value of unity. As pointed out before, the system changes from the entangled ground state to a separable one due to the changes of the magnetic configuration of the system induced by the external pressure. It is reflected in the quantum correlations when entanglement goes to zero (see fig. 3(b)), *i.e.*, the system reaches the threshold temperature $T = T_t$, eq. (9). Hence, this fact yields a minimization on the quantum discord in the system (see fig. 3(a)). However, it remains significantly different from zero even in separable states when the entanglement is absent as can be seen in fig. 3(a). In this way, we can control the quantum correlations of this molecular magnet by means of macroscopic properties such as temperature and pressure.

Therefore, the structural contraction on the system, achieved by increasing the external pressure, lead to a change in the magnetic configuration of the system, as can be seen in fig. 2. As a consequence, the quantum correlations (fig. 3) are drastically affected, since these quantum properties are directly related to the magnetic behaviour of the system (eqs. (5), (6)). Thus, it is possible to manage the degree of quantum correlation in a magnetic system by the control of external pressure and temperature. Furthermore, this external pressure can be achieved experimentally reducing the lattice parameter of the system by chemical substitution or hydrostatically, for example. This fact opens a large avenue for research in experimental detection and manipulation of quantum correlations. It allows a better understanding of the quantum properties of molecular magnets by the management of significant macroscopic properties, leading to promising applications in quantum information science such as the development of novel candidate platforms for quantum information processing by means of materials engineering.

Conclusions. – In summary, we performed first-principles calculations to investigate the dependence under hydrostatic pressure, of the quantum correlations of the prototype material $KNaCuSi_4O_{10}$, which is a Heisenberg dimer in a d^9 electronic configuration and, consequently, an ideal realization of a two-qubit system (spin-(1/2) dimer). We show that an external pressure induces a structural contraction on the prototype material, leading to a change of its magnetic alignment. This changes yields a minimization on the degree of the quantum correlations in the system; showing that quantum correlations are related to significant macroscopic effects. Also remarkable is the possibility to handle the ground state by controlling

the temperature and pressure. Our results allow a better management of the quantum properties in magnetic systems and pave the way for experimental and theoretical research of quantum correlations in these systems via first principles, leading to a better understanding of their quantum properties with promising applications in the emerging quantum technologies.

$* * *$

REFERENCES

[1] Nielsen M. A. and Chuang I. L., *Quantum Computation and Quantum Information* (Cambridge University Press) 2010.

[2] Vedral V., *Introduction to Quantum Information Science* (Oxford University Press) 2006.

[3] Horodecki R., Horodecki P., Horodecki M. and Horodecki K., *Rev. Mod. Phys.*, **81** (2009) 865.

[4] Tufarelli T., Girolami D., Vasile R., Bose S. and Adesso G., *Phys. Rev. A*, **86** (2012) 052326.

[5] Cruz C., Soares-Pinto D. O., Brandao P., dos Santos A. M. and Reis M. S., *EPL*, **113** (2016) 40004.

[6] Man Z.-X., Xia Y.-J. and Franco R. L., *Sci. Rep.*, **5** (2015) 13843.

[7] Aaronson B., Franco R. L. and Adesso G., *Phys. Rev. A*, **88** (2013) 012120.

[8] Franco R. L., Bellomo B., Maniscalco S. and Compagno G., *Int. J. Mod. Phys. B*, **27** (2013) 1345053.

[9] Bellomo B., Franco R. L. and Compagno G., *Phys. Rev. A*, **86** (2012) 012312.

[10] Franco R. L., Bellomo B., Andersson E. and Compagno G., *Phys. Rev. A*, **85** (2012) 032318.

[11] Aaronson B., Franco R. L., Compagno G. and Adesso G., *New J. Phys.*, **15** (2013) 093022.

[12] Silva I. A., Souza A. M., Bromley T. R., Cianciaruso M., Marx R., Sarthour R. S., Oliveira I. S., Franco R. L., Glaser S. J., Soares-Pinto D. O. *et al.*, *Phys. Rev. Lett.*, **117** (2016) 160402.

[13] Xu J.-S., Sun K., Li C.-F., Xu X.-Y., Guo G.-C., Andersson E., Franco R. L. and Compagno G., *Nat. Commun.*, **4** (2013) 2851.

[14] Bromley T. R., Cianciaruso M., Franco R. L. and Adesso G., *J. Phys. A: Math. Theor.*, **47** (2014) 405302.

[15] Yurishchev M. A., *Phys. Rev. B*, **84** (2011) 024418.

[16] Aldoshin S., Fel'dman E. and Yurishchev M., *Low Temp. Phys.*, **40** (2014) 3.

[17] Henderson L. and Vedral V., *J. Phys. A: Math. Gen.*, **34** (2001) 6899.

[18] Vedral V., *Phys. Rev. Lett.*, **90** (2003) 050401.

[19] Dakić B., Vedral V. and Brukner Č., *Phys. Rev. Lett.*, **105** (2010) 190502.

[20] Modi K., Paterek T., Son W., Vedral V. and Williamson M., *Phys. Rev. Lett.*, **104** (2010) 080501.

[21] Modi K., Brodutch A., Cable H., Paterek T. and Vedral V., *Rev. Mod. Phys.*, **84** (2012) 1655.

[22] Gu M., Chrzanowski H. M., Assad S. M., Symul T., Modi K., Ralph T. C., Vedral V. and Lam P. K., *Nat. Phys.*, **8** (2012) 671.

[23] Sarandy M., *Phys. Rev. A*, **80** (2009) 022108.

[24] Nakano T., Piani M. and Adesso G., *Phys. Rev. A*, **88** (2013) 012117.

[25] Girolami D. and Adesso G., *Phys. Rev. A*, **83** (2011) 052108.

[26] Girolami D., Tufarelli T. and Adesso G., *Phys. Rev. Lett.*, **110** (2013) 240402.

[27] Girolami D., Souza A. M., Giovannetti V., Tufarelli T., Filgueiras J. G., Sarthour R. S., Soares-Pinto D. O., Oliveira I. S. and Adesso G., *Phys. Rev. Lett.*, **112** (2014) 210401.

[28] Luo S., *Phys. Rev. A*, **77** (2008) 042303.

[29] Liu B.-Q., Wu L.-A., Zeng G.-M., Song J.-M., Luo W., Lei Y., Sun G.-A., Chen B. and Peng S.-M., *Phys. Lett. A*, **378** (2014) 3441.

[30] Huang Y., *New J. Phys.*, **16** (2014) 033027.

[31] Brandao P., Rocha J., Reis M. S., Dos Santos A. and Jin R., *J. Solid State Chem.*, **182** (2009) 253.

[32] Reis M., *Fundamentals of Magnetism* (Elsevier) 2013.

[33] Bleaney B. and Bowers K., *Anomalous Paramagnetism of Copper Acetate* (The Royal Society) 1952, pp. 451–465.

[34] Ollivier H. and Zurek W. H., *Phys. Rev. Lett.*, **88** (2001) 017901.

[35] Ma Z., Chen Z., Fanchini F. F. and Fei S.-M., *Sci. Rep.*, **5** (2015) 10262.

[36] Paula F., de Oliveira T. R. and Sarandy M., *Phys. Rev. A*, **87** (2013) 064101.

[37] Montealegre J., Paula F., Saguia A. and Sarandy M., *Phys. Rev. A*, **87** (2013) 042115.

[38] Datta A., Shaji A. and Caves C. M., *Phys. Rev. Lett.*, **100** (2008) 050502.

[39] Wootters W. K., *Phys. Rev. Lett.*, **80** (1998) 2245.

[40] Hill S. and Wootters W. K., *Phys. Rev. Lett.*, **78** (1997) 5022.

[41] Soares-Pinto D., Souza A., Sarthour R., Oliveira I., Reis M., Brandao P., Rocha J. and dos Santos A., *EPL*, **87** (2009) 40008.

[42] Reis M. S., Soriano S., dos Santos A. M., Sales B. C., Soares-Pinto D. and Brandao P., *EPL*, **100** (2012) 50001.

[43] Hohenberg P. and Kohn W., *Phys. Rev.*, **136** (1964) B864.

[44] Perdew J. P., Burke K. and Ernzerhof M., *Phys. Rev. Lett.*, **77** (1996) 3865.

[45] Giannozzi P., Baroni S., Bonini N., Calandra M., Car R., Cavazzoni C., Ceresoli D., Chiarotti G. L., Cococcioni M., Dabo I. *et al.*, *J. Phys.: Condens. Matter*, **21** (2009) 395502.

[46] Monkhorst H. J. and Pack J. D., *Phys. Rev. B*, **13** (1976) 5188.

[47] Marzari N., Vanderbilt D., De Vita A. and Payne M., *Phys. Rev. Lett.*, **82** (1999) 3296.

[48] Birch F., *Phys. Rev.*, **71** (1947) 809.

World Scientific
www.worldscientific.com

Quantum correlations and Bell's inequality violation in a Heisenberg spin dimer via neutron scattering

C. Cruz

Instituto de Física,
Universidade Federal Fluminense,
Av. Gal. Milton Tavares de Souza s/n, 24210-346 Niterói,
Rio de Janeiro, Brazil
clebsonscruz@if.uff.br

The characterization of quantum information quantifiers has attracted a considerable attention of the scientific community, since they are a useful tool to verify the presence of quantum correlations in a quantum system. In this context, in the present work we show a theoretical study of some quantifiers, such as entanglement witness, entanglement of formation, Bell's inequality violation and geometric quantum discord as a function of the diffractive properties of neutron scattering. We provide one path toward identifying the presence of quantum correlations and quantum nonlocality in a molecular magnet as a Heisenberg spin-1/2 dimer, by diffractive properties typically obtained via neutron scattering experiments.

Keywords: Neutron scattering; quantum correlations; entanglement production and manipulation; Bell's inequality violation.

1. Introduction

The study of quantum correlations has been subject of numerous investigations in the last few years, since it is a remarkable resource in quantum information science. In this regard, quantum information quantifiers[1–25] are useful tools to verify the presence of quantum correlations in a quantum system. In spite of that, the detection of quantum correlations is a difficult task, theoretically and experimentally speaking.[13,15–17,21,26–28] Nowadays, it is understood that quantum correlations can be quantified through the measurements of some macroscopic properties of magnetic systems.[13,17,29,30]

The study of the magnetic properties of molecular materials is typically done approximating magnetic parameters of a Hamiltonian model by the fit of some thermodynamic properties, such as magnetic susceptibility, internal energy and specific heat.[17,31–34] In this context, correlation functions have great importance in

describing these properties; in addition, they can be directly measurable, e.g. in neutron scattering experiments via *structure factors*. Structure factors can be defined as two-point correlations[35] and are widely used to describe the crystal structure of molecular systems ruled by Hamiltonians,[35–37] e.g. Heisenberg models.[31]

Quantum information quantifiers are expressed in terms of statistical correlation functions,[17,29,30] due to the fact that these functions are present in the elements of the density matrix of the quantum system, linking their macroscopic properties with the quantum ones. Therefore, it is possible to quantify the presence of quantum correlations in a system via structure factors,[13,35,38,39] since these factors are directly associated to the correlation functions; thus allowing the measurement of quantum information quantifiers by neutron scattering experiments.

In this scenario, the present work shows analytical expressions for the entanglement witness, entanglement of formation, Bell's inequality violation, and geometric quantum discord, based on the Schatten 1-norm as a function of quantities typically obtained in neutron scattering via a scalar structure factor. Our results provide one path towards identifying the presence of quantum correlations and quantum non-locality in a molecular magnet such as a Heisenberg spin-1/2 dimer, by diffractive properties. This is an alternative way to describe the quantum properties of a sample material via neutron scattering experiments, without making any assumption about their macroscopic quantities, leading to promising applications in quantum information science.

2. Neutron Scattering for a Heisenberg Spin Dimer

The study of molecular magnetic materials is typically done through the approach of the magnetic parameters of a Hamiltonian model, by the fit of some thermodynamic properties, e.g. magnetic susceptibility, internal energy, and specific heat.[17,31–34] For a given Hamiltonian model, one can evaluate the inelastic structure factor, which allows a sensitive test of the assumed model, since their properties are affected by the relative positions of the metallic centers of a sample material.[32]

Let us consider a molecular magnet as an interacting pair of spin-1/2 ruled by the Heisenberg-Dirac-Van Vleck Hamiltonian,

$$\mathcal{H} = -J\mathbf{S}_1 \cdot \mathbf{S}_2. \tag{1}$$

This is an ideal realization of a two qubit system; and therefore, a promising platform in the quantum information processing.

Once Eq. (1) is invariant under spin rotation, the total spin $s = s_1 + s_2$ is a good quantum number.[31,32] From the Clebsch–Gordon series the spectrum consists in an $s = 1$ triplet and $s = 0$ singlet.[31] Diagonalizing it, we obtain the energy eigenvalues E_s and eigenvectors $|s, m_s\rangle$[31,32]:

$$E_{s=1} = \frac{1}{4}J, \tag{2}$$

$$E_{s=0} = -\frac{3}{4}J, \tag{3}$$

$$|s=1, m_s = +1\rangle = |00\rangle, \tag{4}$$

$$|s=1, m_s = 0\rangle = \frac{1}{\sqrt{2}}(|01\rangle + |10\rangle), \tag{5}$$

$$|s=1, m_s = -1\rangle = |11\rangle, \tag{6}$$

$$|s=0, m_s = 0\rangle = \frac{1}{\sqrt{2}}(|01\rangle - |10\rangle). \tag{7}$$

In magnetic neutron scattering, neutrons interact magnetically with the atoms of the target sample. From the Van Hove formalism,[40] the partial differential cross section of an incident neutron in a magnetic system with initial state $|\psi_i\rangle$ is expressed in terms of time-dependent correlation functions

$$\frac{d^2\sigma}{d\omega d\Omega} = \frac{1}{Z}\left(\frac{g_{i,\alpha}\gamma r_0}{2}\right)^2 \sum_{\alpha,\beta,l,m}\left(\delta_{\alpha,\beta} - \frac{\mathbf{q}_\alpha \mathbf{q}_\beta}{|\mathbf{q}|^2}\right)[F_l(\mathbf{q})g_{l,\alpha}]^*[F_m(\mathbf{q})g_{m,\beta}]$$
$$\times \int \frac{dt}{2\pi}e^{i[\omega t + \mathbf{q}\cdot(\mathbf{r}_l - \mathbf{r}_m)]}\langle\psi_i|S_l^\alpha S_m^\beta(t)|\psi_i\rangle, \tag{8}$$

where the sum run over all magnetic sites l and m, which are the lth and mth spins with position vectors $\mathbf{r}_l$ and $\mathbf{r}_m$, respectively. Furthermore, γ is the neutron magnetic moment; $r_0 = e^2/m_e c^2$ is the classical electron radius; $F_i(\mathbf{q})$ is the magnetic form factor; α, $\beta = x, y, z$; ω is the energy transferred to the target magnetic system; $\mathbf{q} = \mathbf{k}_{\text{out}} - \mathbf{k}_{\text{in}}$ is the difference between the final and the initial wave vectors (scattering vector); and finally, S_l^α are the spin operators. Thus, the differential cross-section is proportional to the neutron scattering structure factor tensor that is written in terms of the pairwise correlation function[13,38,39,41]:

$$\mathcal{S}^{(\alpha,\beta)}(\mathbf{q},\omega) = \int \frac{dt}{2\pi}\sum_{l,m}e^{i[\omega t + \mathbf{q}\cdot(\mathbf{r}_l - \mathbf{r}_m)]}\langle\psi_i|S_l^\alpha S_m^\beta(t)|\psi_i\rangle. \tag{9}$$

Due to the transitions between the discrete energy levels, Eqs. (2) and (3), the time integral shown in Eq. (9) gives a delta function $\delta(E_f - E_i - \hbar\omega)$, where $\hbar\omega$ is the transfer energy.[32] Integrating Eq. (9) over energies, we obtain the integrated structure factor [35,38,39]

$$\mathcal{S}(\mathbf{q}) = \sum_{\alpha,\beta}\mathcal{S}^{\alpha\beta}(\mathbf{q}) = \sum_{\alpha,\beta}\sum_{l,m}e^{i\mathbf{q}\cdot(\mathbf{r}_l - \mathbf{r}_m)}\langle S_l^\alpha S_m^\beta\rangle. \tag{10}$$

Therefore, for the specific case of a Heisenberg spin dimer, Eq. (1), one can define the so-called exclusive structure factor as a function of the scattering vector $\mathbf{q}$,[32] for the excitation of the final states in the magnetic multiplet $|\psi_f\rangle$, Eqs. (4)–(7), from the given initial state $|\psi_i\rangle$

$$\mathcal{S}_{fi}^{(\alpha,\beta)}(\mathbf{q}) = \sum_f \langle\psi_i|\mathcal{U}_\alpha^\dagger(\mathbf{q})|\psi_f\rangle\langle\psi_f|\mathcal{U}_\beta(\mathbf{q})|\psi_i\rangle, \tag{11}$$

where

$$\mathcal{U}_{\alpha,\beta}(\mathbf{q}) = \sum_{\mathbf{r}_l} S_l^{(\alpha,\beta)} e^{i\mathbf{q}\cdot r_l}, \tag{12}$$

and the sum taken over all magnetic ions in a unit cell.[13,32,39]

For the $|s = 0, m_s = 0\rangle$ initial state (antiparallel magnetic alignment), Eq. (7), only $s = 1$ final states are excited, Eqs. (4)–(6). Thus, one can define the scalar neutron scattering structure factor, $\mathcal{S}(\mathbf{q})$, for the Heisenberg 1/2-spin dimer[32] by

$$\mathcal{S}_{fi}^{(\alpha,\beta)}(\mathbf{q}) = \delta_{\alpha,\beta}\mathcal{S}(\mathbf{q}). \tag{13}$$

Using the eigenvectors given by Eqs. (4)–(7) in Eq. (11), we evaluate the inelastic neutron scattering intensities, that are given by structure factors[32] for the Heisenberg spin-1/2 dimer, Eq. (1). Thus, we obtain the scalar neutron scattering structure factor as calculated in Ref. 32:

$$\mathcal{S}(\mathbf{q}) = \frac{1}{2}[1 - \cos(\mathbf{q}\cdot(\mathbf{r}_1 - \mathbf{r}_2))]. \tag{14}$$

Thus, given the Hamiltonian model, it is possible to predict their scalar structure factor, which can be compared to the neutron scattering experiments results.[32]

3. Quantum Information-Theoretic Quantifiers in a Heisenberg Spin Dimer

In this section, we will present the analytical expressions for quantum information quantifiers, such as entanglement witness, entanglement of formation, Bell's inequality violation and geometric quantum discord, based on the Schatten 1-norm as a function of quantities typically obtained in neutron scattering via scalar structure factor, allowing their measurement via neutron scattering experiments.

3.1. *Spin-spin correlation function*

Correlation functions have a great importance in statistical physics and quantum mechanics, allowing us to find different properties of a physical system. In addition, it can be directly measurable, e.g. in scattering experiments.[30] Quantum information quantifiers are expressed in terms of statistical correlation functions,[17,29,30] due to the fact that these functions are present in the elements of the density matrix of the quantum system, linking their macroscopic and structural properties with the quantum ones.

For the system ruled by the Hamiltonian, Eq. (1), from Eqs. (10) and (13) the spin-spin correlation function can be extracted and written in terms of integrated structure factor

$$\mathcal{C} = \langle S_1^{\alpha} S_2^{\alpha} \rangle = e^{-i\mathbf{q}\cdot(\mathbf{r}_1 - \mathbf{r}_2)}\mathcal{S}^{\alpha\alpha}(\mathbf{q}), \tag{15}$$

where $\alpha = x, y, z$.

Thus, spin-spin correlation function can be accessed through diffractive properties obtained via neutron scattering experiments, without making any assumption about the macroscopic properties of the measured system or the external conditions under which the neutrons are scattered.

Using Eq. (14), spin-spin correlation function can be written as a function of the scattering vector, $\mathbf{q} = \mathbf{k}_{\text{out}} - \mathbf{k}_{\text{in}}$, i.e. the difference between the final and the initial wave vectors, and the difference between the position vectors $\mathbf{r}_1$ and $\mathbf{r}_2$ of the metallic centers.

$$\mathcal{C} = \frac{e^{-i\mathbf{q}(\mathbf{r}_1 - \mathbf{r}_2)}}{2} \left[1 - \cos(\mathbf{q} \cdot (\mathbf{r}_1 - \mathbf{r}_2)) \right]. \tag{16}$$

This ranges from $-1 \leq \mathcal{C} \leq 0$ for antiparallel magnetic alignment ($J < 0$ — entangled ground state) and $0 < \mathcal{C} \leq 1/3$ for parallel magnetic alignment ($J > 0$ — separable ground state).[17,29,30]

The spin-spin correlation function, Eq. (16), is depicted in Fig. 1 as a function of the scattering vector $\mathbf{q}$ times the distance between the metallic centers of a sample material $\mathbf{r}_1 - \mathbf{r}_2$, which can be obtained by neutron scattering experiments. It is worth noting that, the location of the zero point correlation can provide a convenient estimate for which distances in the system can be found in an antiparallel magnetic alignment ($\pi q^{-1}/2 \leq r_1 - r_2 \leq 3\pi q^{-1}/2$) or a parallel magnetic alignment ($0 < r_1 - r_2 < \pi q^{-1}/2$ and $3\pi q^{-1}/2 < r_1 - r_2 < 2\pi q^{-1}$), without any assumption about macroscopic quantities, such as the temperature, magnetic field, magnetic susceptibility,
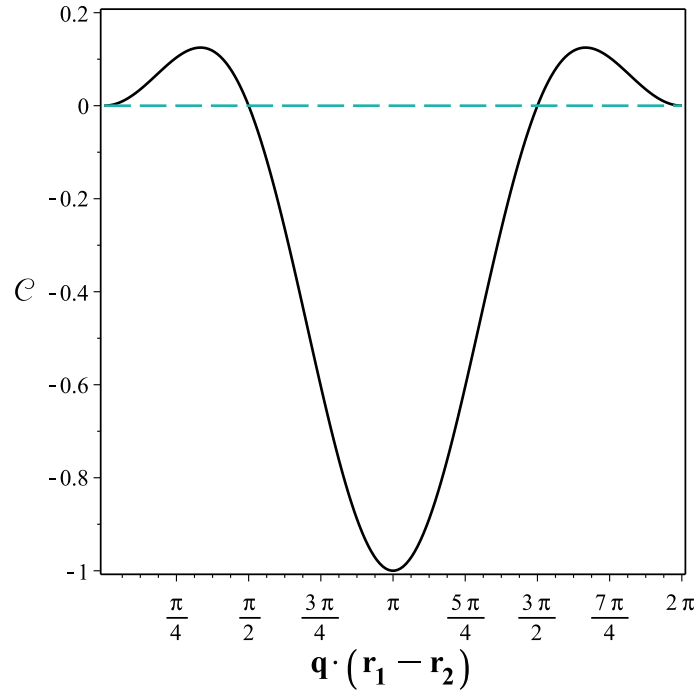

Fig. 1. (Color online) Spin-spin correlation as a function of $\mathbf{q} \cdot (\mathbf{r}_1 - \mathbf{r}_2)$, Eq. (16). The dashed (green) horizontal line separates the regions with antiparallel magnetic alignment ($\pi/2 \leq \mathbf{q} \cdot (\mathbf{r}_1 - \mathbf{r}_2) \leq 3\pi/2$) and parallel magnetic alignment ($0 < \mathbf{q} \cdot (r_1 - r_2) < \pi/2$ and $3\pi/2 < \mathbf{q} \cdot (r_1 - r_2) < 2\pi$).

internal energy or specific heat. This result has a great importance to guide us through the study of the quantum information quantifiers in a Heisenberg spin dimer, since these quantifiers depend directly on the spin-spin correlation function.

3.2. *Entanglement witness*

The detection of entanglement is usually done using an observable which identifies the presence of entanglement in a quantum system.[2–5] This observable, the so-called *entanglement witness* ($\mathcal{W}$), has a negative expectation value whether the system is in an entangled quantum state ($\mathcal{W} < 0$) and otherwise positive. However, the positive expectation value does not imply the presence of separable quantum states. Recently, magnetic susceptibility was proposed as a thermodynamical entanglement witness.[2–5] As calculated by Wieśniak, Vedral and Brukner in Ref. 4, the entanglement witness can be calculated in terms of the average magnetic susceptibility. In Ref. 8 the magnetic susceptibility of an antiferromagnetic spin-1/2 chain is compared to the correlation function measured by neutron diffraction.[42] Thus, we can analytically calculate the entanglement witness for a molecular magnet such as a Heisenberg spin-1/2 dimer, in terms of its scalar structure factor using Eq. (16) as follows:

$$\mathbb{W} = 2 + 3e^{-i\mathbf{q}(\mathbf{r_1}-\mathbf{r_2})}\mathcal{S}(\mathbf{q})$$
$$= 2 + \frac{3e^{-i\mathbf{q}(\mathbf{r_1}-\mathbf{r_2})}}{2}[1 - \cos(\mathbf{q}\cdot(\mathbf{r_1}-\mathbf{r_2}))]. \tag{17}$$

In Fig. 2, we show the entanglement witness for a Heisenberg spin dimer, Eq. (17), as a function of $\mathbf{q}\cdot(r_1 - r_2)$. The witness has a negative expectation at the range $2.45 < \mathbf{q}\cdot(\mathbf{r_1} - \mathbf{r_2}) < 3.85$, revealing the presence of entangled states. This result is compatible to the last ones, since in this band the system is found in an antiparallel magnetic alignment (entangled ground state), as can be seen in Fig. 1. Thus, we provide one way to identify the presence of entanglement in a molecular magnet, such as a Heisenberg spin dimer, by diffractive properties obtained via neutron scattering experiments, without making any assumption about their macroscopic quantities.

3.3. *Entanglement of formation*

In order to quantify the amount of entanglement in the Heisenberg spin-1/2 dimer and make a comparison with the entanglement witness, we will adopt the measurement of *entanglement of formation* defined by[6,7]:

$$\mathbb{E} = -\Gamma_+\log_2(\Gamma_+) - \Gamma_-\log_2(\Gamma_-), \tag{18}$$

with

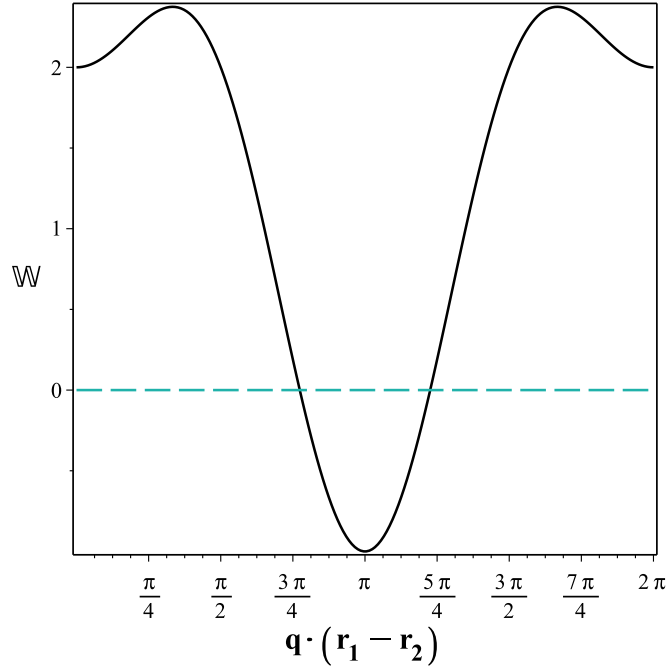$$\Gamma_\pm = \frac{1 \pm \sqrt{1 - \mathbb{C}^2}}{2}, \tag{19}$$

Fig. 2. (Color online) Entanglement witness of a Heisenberg spin dimer, Eq. (17). The dashed (green) horizontal line separates the region where the witness has a negative expectation value, i.e. the system is in an entangled quantum state $2.45 < \mathbf{q} \cdot (\mathbf{r}_1 - \mathbf{r}_2) < 3.85$.

where $\mathbb{C}$ is the concurrence.[1,2,6,7] The concurrence can be written as a function of the scalar structure factor, Eq. (14), in terms of spin–spin correlation function, Eq. (16), as follows:

$$\mathbb{C} = \max\left[0, -\frac{1}{2}\left(1 + 3e^{-i\mathbf{q}(\mathbf{r}_1 - \mathbf{r}_2)}\mathcal{S}(\mathbf{q})\right)\right]. \qquad (20)$$

The equation above shows that the concurrence of a Heisenberg spin-1/2 dimer is also related to the diffractive properties, which can be obtained by neutron scattering experiments.

In sequence, we see in Fig. 3 (a) the entanglement of formation as a function of the scattering vector $\mathbf{q}$ times the distance between the metallic centers $\mathbf{r}_1 - \mathbf{r}_2$ of a Heisenberg spin dimer, Eq. (18). It is possible to identify a maximum of entanglement at $r_1 - r_2 = \pi q^{-1}$, where the system is found in an antiparallel magnetic alignment with an entangled pure state. It is worth noting that there are entangled states at $2.0 \lesssim \mathbf{q} \cdot (r_1 - r_2) \lesssim 4.2$, above the band where the entanglement is identified on the entanglement witness. In Fig. 3(b), we make a comparison between the entanglement of formation and the entanglement witness. As can be seen, the positive expectation value of the witness, separated by the dashed (green) line, does not imply separability. However, the negative expectation value necessarily implies in the presence of entangled quantum states in the system.
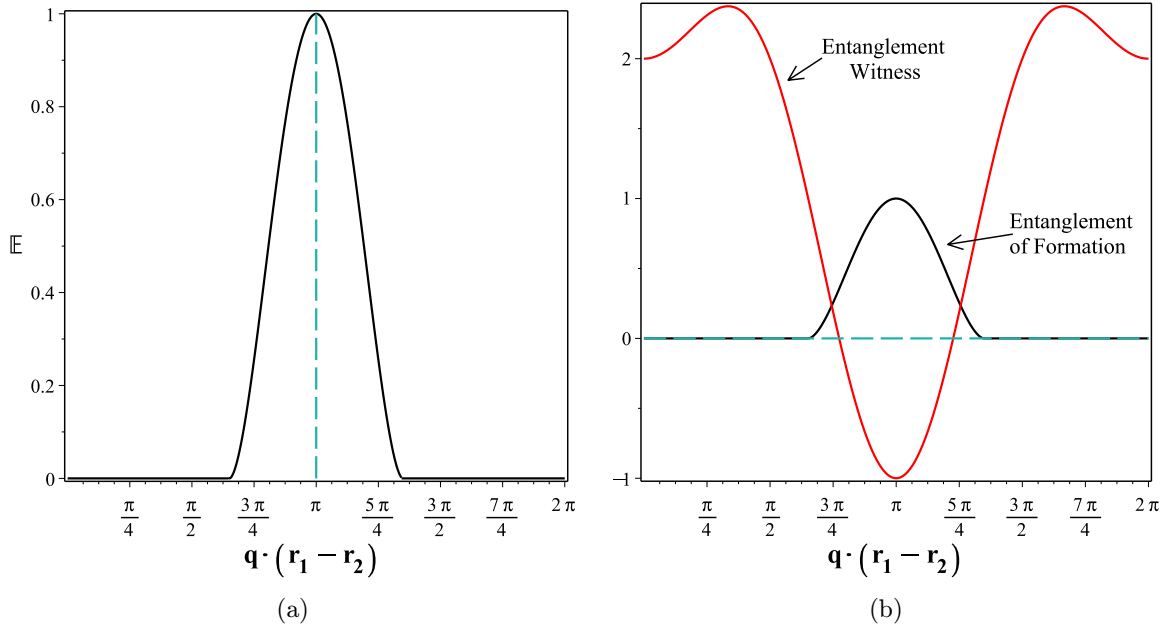
Fig. 3. (Color online) (a) Entanglement of formation as a function of $\mathbf{q} \cdot (\mathbf{r}_1 - \mathbf{r}_2)$, Eq. (18). The dashed (green) vertical line highlights the maximum of entanglement, where the system is in an antiparallel magnetic alignment with an entangled pure state. (b) We make a comparison between the entanglement of formation and the entanglement witness. The dashed (green) horizontal line separates the region where the witness has a negative expectation value, i.e. the system is in an entangled quantum state.

3.4. *Bell's inequality violation*

Bell's inequality violation[9] has an important role in the quantum information theory, as a necessary and sufficient condition for the usefulness of quantum states in the communication complexity of protocols.[43] For a Heisenberg spin-1/2 dimer, the Bell's inequality test[5,10] is related to the measurement of the Bell operator.[5]

$$\mathbb{B} = \mathbf{n}_1 \cdot \mathbf{S} \otimes (\mathbf{n}_2 \cdot \mathbf{S} - \mathbf{n}_4 \cdot \mathbf{S}) + \mathbf{n}_3 \cdot \mathbf{S} \otimes (\mathbf{n}_2 \cdot \mathbf{S} + \mathbf{n}_4 \cdot \mathbf{S}), \qquad (21)$$

where $\mathbf{n}_1 \cdot \mathbf{S}$ is the projection of the spin on the direction n.

Using the set of directions $\{\mathbf{n}_1, \mathbf{n}_2, \mathbf{n}_3, \mathbf{n}_4\} = \{(0,0,1), (-1,0,-1)/\sqrt{2}, (-1,0,0), (-1,0,1)/\sqrt{2}\}$, Eq. (21) becomes $\mathbb{B} = \sqrt{2}(S_x \otimes S_x + S_z \otimes S_z)$. Therefore

$$\begin{aligned} |\langle \mathbb{B} \rangle| &= 2\sqrt{2}|\mathcal{S}(\mathbf{q})| \\ &= 2\sqrt{2}|1 - \cos(\mathbf{q} \cdot (\mathbf{n}_1 - \mathbf{r}_2))|. \end{aligned} \qquad (22)$$

Thus, from Eq. (22), it is possible to verify whether there is a Bell's inequality violation via neutron scattering experiments.

In Fig. 4, we see the mean value of the Bell operator as a function of the scattering vector $\mathbf{q}$ times the distance between the metallic centers $\mathbf{r}_1 - \mathbf{r}_2$ of a target sample of neutron scattering, Eq. (22). As can be seen, the Bell's inequality is violated in $2.0 \lesssim \mathbf{q} \cdot (r_1 - r_2) \lesssim 4.2$, where there is a maximum violation in $r_1 - r_2 = \pi q^{-1}$, when the system is in an entangled pure state, see Fig. 3(a). It is compatible to the previous result obtained from the entanglement of formation, where we found entangled
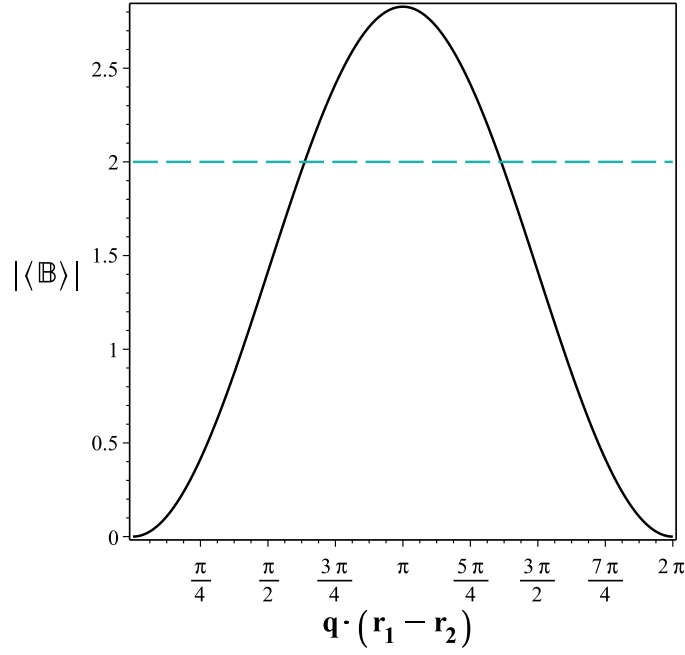
$|\langle \mathbb{B} \rangle|$

Fig. 4. (Color online) Mean value of Bell operator as a function of $\mathbf{q} \cdot (\mathbf{r}_1 - \mathbf{r}_2)$, Eq. (22). The dashed (green) horizontal line separates the region where the Heisenberg dimer violates the Bell's inequality.

quantum states at the same band. Therefore, it is possible to verify the quantum nonlocality in a Heisenberg spin dimer by diffractive properties obtained in neutron scattering experiments.

3.5. *Geometric quantum discord*

Despite quantum entanglement providing one path toward finding pure quantum correlations, it does not encompass all quantum correlations in a system. The measurement of the total amount of quantum correlations has been called *quantum discord*.[11–23]

The calculation of quantum discord is a rather complicated task, even for a two-qubit system, such as a Heisenberg spin-1/2 dimer.[17,19] This fact has stimulated alternative measurements of quantum information-theoretical quantifiers as the *geometric quantum discord*.[17] In this context, the geometric quantum discord, based on the Schatten 1-norm, is one path towards achieving a well-defined measurement of quantum correlations in a quantum system[17] and it can be defined as

$$\mathbb{Q}_G(\rho) = \min_{\omega} \|\rho - \rho_c\|, \tag{23}$$

where $\|X\| = \text{Tr}[\sqrt{X^{\dagger}X}]$ is the 1-norm, ρ is a given quantum state and ω is the set of closest classical-quantum states ρ_c,[17,19,20] whose general form is given by

$$\rho_c = \sum_{k} p_k \Pi_k^{\{1\}} \otimes \rho_k^{\{2\}}, \tag{24}$$

with $0 \leq p_k \leq 1$ and $\sum_k p_k = 1$; $\{\Pi_k^{\{1\}}\}$ denotes a set of orthogonal projectors for subsystem 1, and $\rho_k^{\{2\}}$ is a general reduced density operator for the subsystem 2.[19,20]

Thus, for a Heisenberg spin dimer, the geometric quantum discord, based on the Schatten 1-norm, is written as a function of the scalar structure factor as follows:

$$\mathbb{Q}_G(\mathcal{S}) = \left| \frac{1}{4} \mathcal{S}(\mathbf{q}) \right|$$
$$= \left| \frac{1 - \cos(\mathbf{q} \cdot (\mathbf{r}_1 - \mathbf{r}_2))}{4} \right|. \tag{25}$$

Figure 5(a) shows the geometric quantum discord as a function of the scattering vector $\mathbf{q}$ times the distance between the metallic centers $\mathbf{r}_1 - \mathbf{r}_2$ of a sample material, Eq. (25). We identify a maximum of quantum correlation at $r_1 - r_2 = \pi q^{-1}$, this is compatible to the previous results, where at this point the system is found in an entangled pure state, see Fig. 3(a). Figure 5(b) makes a comparison between the geometric quantum discord and the entanglement of formation. As can be seen, it is possible to identify the presence of quantum correlations when the entanglement is absent and even when the system is found in a parallel magnetic alignment with a separable quantum state ($0 < \mathbf{q} \cdot (r_1 - r_2) < \pi/2$ and $3\pi/2 < \mathbf{q} \cdot (r_1 - r_2) < 2\pi$), see Fig. 1; furthermore, the points of zero discord coincide with the points of zero correlation ($\pi/2$ and $3\pi/2$), indicating the absence of magnetic interaction ($J = 0$) between the magnetic ions.
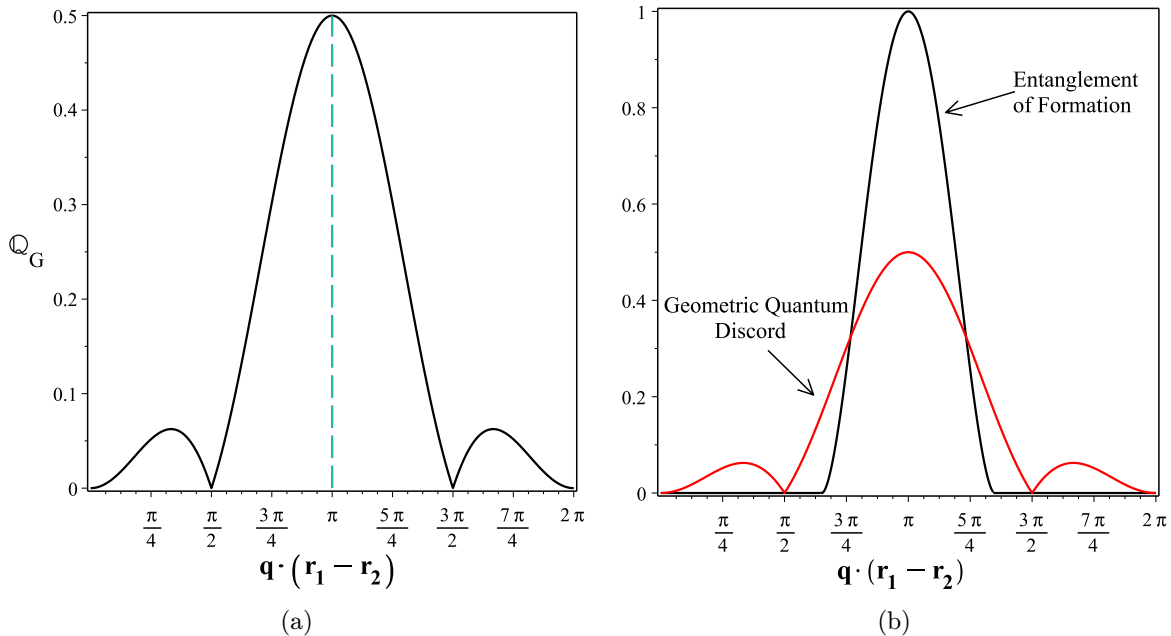

Fig. 5.   (Color online) (a) Geometric quantum discord as a function of $\mathbf{q} \cdot (\mathbf{r}_1 - \mathbf{r}_2)$. Dashed (green) vertical line highlights the point where the system is in an antiparallel magnetic alignment with an entangled pure state. (b) We make a comparison between the geometric quantum discord and the entanglement of formation; it is possible to identify the presence of quantum correlations when the entanglement is absent and even when the system is found in a parallel magnetic alignment with a separable quantum state.

Therefore, we provide one way to find the geometric quantum correlations in a Heisenberg spin dimer, by diffractive properties obtained via neutron scattering experiments, without making any assumption about their macroscopic quantities.

4. Conclusions

In summary, our main result was to provide to the literature analytical expressions for quantum information quantifiers, such as the entanglement witness, entanglement of formation, Bell's inequality violation and geometric quantum discord as a function of quantities typically obtained in neutron scattering via scalar structure factor. We provide one path towards identifying the presence of quantum correlations and quantum nonlocality in a two-qubit system such as a Heisenberg spin-1/2 dimer, using diffractive properties without making any assumption about its macroscopic properties or the external conditions under which the neutrons are scattered. We present an alternative way to describe the quantum properties of a sample material via neutron scattering experiments. Our results open doors for the detection and manipulation of quantum correlations through neutron scattering experiments in magnetic systems, such as the molecular magnets ruled by Heisenberg Hamiltonians; leading to promising applications in quantum information science, since these materials can be promising platforms in quantum information processing.

Acknowledgments

References

1. M. A. Nielsen and I. L. Chuang, *Quantum Computation and Quantum Information* (Cambridge University Press, Cambridge, 2010).
2. R. Horodecki, P. Horodecki, M. Horodecki and K. Horodecki, *Rev. Mod. Phys.* **81** (2009) 865.
3. M. Horodecki, P. Horodecki and R. Horodecki, *Phys. Lett. A* **223** (1996) 1.
4. M. Wieśniak, V. Vedral and Č. Brukner, *New J. Phys.* **7** (2005) 258.
5. A. Souza, D. Soares-Pinto, R. Sarthour, I. Oliveira, M. S. Reis, P. Brandao and A. Dos Santos, *Phys. Rev. B* **79** (2009) 054408.
6. W. K. Wootters, *Phys. Rev. Lett.* **80** (1998) 2245.
7. S. Hill and W. K. Wootters, *Phys. Rev. Lett.* **78** (1997) 5022.
8. Č. Brukner, V. Vedral and A. Zeilinger, *Phys. Rev. A* **73** (2006) 012110.
9. L. J. Landau, *Phys. Lett. A* **120** (1987) 54.
10. A Souza, A. Magalhães, J. Teles, T. Bonagamba, I. Oliveira, R. Sarthour *et al.*, *New J. Phys.* **10** (2008) 033020.
11. H. Ollivier and W. H. Zurek, *Phys. Rev. Lett.* **88** (2001) 017901.
12. V. Vedral, *Phys. Rev. Lett.* **90** (2003) 050401.

13. B.-Q. Liu, L.-A. Wu, G.-M. Zeng, J.-M. Song, W. Luo, Y. Lei, G.-A. Sun, B. Chen and S.-M. Peng, *Phys. Lett. A* **378** (2014) 3441.
14. Z. Ma, Z. Chen, F. F. Fanchini and S.-M. Fei, *Sci. Rep.* **5** (2015) 10262.
15. D. Girolami and G. Adesso, *Phys. Rev. A* **83** (2011) 052108.
16. T. Nakano, M. Piani and G. Adesso, *Phys. Rev. A* **88** (2013) 012117.
17. C. Cruz, D. O. Soares-Pinto, P. Brando, A. M. dos Santos and M. S. Reis, *Europhys. Lett.* **113** (2016) 40004.
18. M. Sarandy, *Phys. Rev. A* **80** (2009) 022108.
19. F. Paula, T. R. de Oliveira and M. Sarandy, *Phys. Rev. A* **87** (2013) 064101.
20. J. Montealegre, F. Paula, A. Saguia and M. Sarandy, *Phys. Rev. A* **87** (2013) 042115.
21. S. Luo, *Phys. Rev. A* **77** (2008) 042303.
22. A. Datta, A. Shaji and C. M. Caves, *Phys. Rev. Lett.* **100** (2008) 050502.
23. L. Henderson and V. Vedral, *J. Phys. A, Math. Gen.* **34** (2001) 6899.
24. Y. Huang, *Phys. Rev. A* **88** (2013) 014302.
25. Y. Huang, *Phys. Rev. B* **89** (2014) 054410.
26. D. Girolami, T. Tufarelli and G. Adesso, *Phys. Rev. Lett.* **110** (2013) 240402.
27. D. Girolami, A. M. Souza, V. Giovannetti, T. Tufarelli, J. G. Filgueiras, R. S. Sarthour, D. O. Soares-Pinto, I. S. Oliveira and G. Adesso, *Phys. Rev. Lett.* **112** (2014) 210401.
28. Y. Huang, *New J. Phys.* **16** (2014) 033027.
29. M. A. Yurishchev, *Phys. Rev. B* **84** (2011) 024418.
30. S. Aldoshin, E. Fel'dman and M. Yurishchev, *Low Temp. Phys.* **40** (2014) 3.
31. M. Reis, *Fundamentals of Magnetism* (Elsevier, 2013).
32. J. Haraldsen, T. Barnes and J. Musfeldt, *Phys. Rev. B* **71** (2005) 064403.
33. B. Leite Ferreira, P. Brandão, A. Dos Santos, Z. Gai, C. Cruz, M. Reis, T. Santos and V. Félix, *J. Coord. Chem.* **68** (2015) 2770.
34. D. Esteves, J. Tedesco, S. Pedro, C. Cruz, M. Reis and P. Brandao, *Mater. Chem. Phys.* **147** (2014) 611.
35. P. Krammer, H. Kampermann, D. Bruß, R. A. Bertlmann, L. C. Kwek and C. Macchiavello, *Phys. Rev. Lett.* **103** (2009) 100502.
36. D. Tennant, C. Broholm, D. Reich, S. Nagler, G. Granroth, T. Barnes, K. Damle, G. Xu, Y. Chen and B. Sales, *Phys. Rev. B* **67** (2003) 054414.
37. T. Huberman, R. Coldea, R. Cowley, D. Tennant, R. Leheny, R. J. Christianson and C. Frost, *Phys. Rev. B* **72** (2005) 014413.
38. M. Cramer, M. Plenio and H. Wunderlich, *Phys. Rev. Lett.* **106** (2011) 020401.
39. O. Marty, M. Epping, H. Kampermann, D. Bruß, M. Plenio and M. Cramer, *Phys. Rev. B* **89** (2014) 125117.
40. L. Van Hove, *Phys. Rev.* **95** (1954) 249.
41. I. A. Zaliznyak and S.-H. Lee, *Modern Techniques for Characterizing Magnetic Materials* (Springer, Heidelberg, 2005).
42. D. Soares-Pinto, A. Souza, R. Sarthour, I. Oliveira, M. Reis, P. Brandao, J. Rocha and A. Dos Santos, *Europhys. Lett.* **87** (2009) 40008.
43. Č. Brukner, M. Żukowski, J.-W. Pan and A. Zeilinger, *Phys. Rev. Lett.* **92** (2004) 127901.